THE EFFECTS OF PROCESS CONDITIONS ON THE PYROLYSIS PRODUCTS OF WASTE AND BIOMASS

By

SERPIL BESLER

B.Eng., M.Sc., S.M. Inst. E.

Under the supervision of

Dr. Paul T. Williams

B.Sc., M.Sc., Ph.D., F.G.S., C.Eng., M. Inst. E.

A thesis submitted in fulfilment of the requirements for the degree of Doctor of Philosophy

The University of Leeds

March 1993

The candidate confirms that the work submitted is her own and that appropriate credit has been given where reference had been made to the work of others.

ABSTRACT

The pyrolysis of wood, rice husks, RDF and scrap tyre has been examined in three different reactors during this research.

The fixed-bed reactor was employed to pyrolyse the waste samples at the heating rates of 5, 20, 40 and 80 C min^{-1} up to different maximum temperatures of 300, 420, 600 and 720°C. Generally, it was observed that as the heating rate and pyrolysis temperature was increased, the liquid and gas yield increased and char yield decreased. In wood pyrolysis, it was also observed that after 720°C, the liquid yield decreased as it was accompanied by an increased gas yield. The detailed gas analysis showed that from the biomass wastes wood, rice husks and RDF, the main gases evolved were hydrogen, carbon monoxide, carbon dioxide, methane, ethane, propane and propene. Scrap tyre pyrolysis showed that the main gases were hydrogen, carbon monoxide, carbon dioxide, methane, ethane, propane, propene, but butadiene was also observed. The calorific value of the gases increased as the temperature of pyrolysis was increased. The individual amounts of each gas also increased. The liquid yields from the biomass wastes consisted of oil and aqueous phases. The scrap tyre oil was of a low viscosity and negligible water content. The liquid yield reached a maximum of 53% for the biomass and 58% for the scrap tyre pyrolysis.

Examination of the fuel properties of the derived pyrolysis oils showed the biomass oils were highly oxygenated, of moderate calorific value and similar distillation range to a kerosene.

A fluidised-bed pyrolysis reactor was designed, constructed and tested to investigate the fast pyrolysis of the waste and biomass

samples. With the fluidised-bed reactor, it was shown that the liquid yield and also calorific values of the liquids increased with increased temperature of pyrolysis.

Oils from a commercial scale batch pyrolysis unit were analysed and showed similar fuel properties and compositions to those derived from the fixed-bed reactor.

A thermogravimetric analyser was employed to determine the thermaldecomposition pathways of wood, rice husks, RDF and scrap tyre. In addition, the cellulose, hemicellulose, lignin, model polysaccharide compounds as biomass components, some plastic compounds as RDF components and also natural rubber, butadiene-rubber and styrene-butadiene rubber as scrap tyre components were tested. TGA and DTG curves were used to estimate the amounts of major components of wood, rice husks, RDF and scrap tyre. The activation energies of the decomposition of wood, rice husks, RDF and scrap tyre and components were calculated assuming a first order rate of reaction and showed a decrease with increasing heating rate.

A Fourier Transform Infra-red Spectroscopy was employed to examine the functional group compositional analysis of the derived pyrolytic oils. From the FT-ir spectra it was observed that aromatic hydrocarbons increased and alkene and alkanes decreased with increased temperature of pyrolysis. Gas chromatography and gas chromatography-mass spectroscopy were performed in order to investigate the polycyclic aromatic compounds in the pyrolysis oils.

The pyrolytic oils were found to contain significant amounts of polycyclic aromatic hydrocarbons (PAH), some of which are known carcinogenic and mutagenic and consequently the oils may represent a

significant environmental and health hazard. The amount of PAH increased as the temperature was increased and it was concluded that the formation of PAH's occurred via Diels-Alder cyclisation reactions as the temperature was increased.

To my Mother and the memory of my late Father

and my sisters

Solmaz and Sonmez

With all my love as always.

"There is a straighter and more secure path for us to follow [than the one we have been]. This is to have Turkish women as partners in everything. To share our lives with them and to value them as friends and colleagues in our scientific, spiritual, social and economic life".

M. Kemal ATATURK
"31st January 1923"
(Public Speech in IZMIR)

Thanks must also be expressed to "The Institute of Energy" for awarding me "The Foxwell Memorial Award" for the year 1992.

The financial support of the Turkish Government via Anadolu University, Turkey is gratefully acknowledged.

Special thanks to Patrick Horne for help in the laboratory and Mr. Y. Akpinar and A.E. Tercan for their help during the drawings and all good, genuine friends without their support and care life would not have been enjoyable in Leeds.

Special appreciation is due for the typing of the manuscript to Michael and Sheilagh Ogden.

Lastly, I could not have survived the last four and a half years without the unconditional love of my family in Turkey.

CONTENTS

CHAPTER 1

INTRODUCTION AND LITERATURE SURVEY

Waste disposal has been a problem to mankind for a long time. Especially in recent years the decrease in space available for landfills and over pollution of the environment are forcing man to find a solution to this problem. Another important reason is that in the long term, the world will face a shortage of the traditional energy sources which are non-renewable.

Renewable energy sources are promising for the future for both the industrialized and developing countries. Although in most cases, the renewables are still unable to compete with conventional energies, it could change as a result of technological developments (1).

For the reasons above, a wide range of research has been stimulated in the area of renewable resources and disposal methods of waste materials. Achieving energy recovery from the waste in addition to disposal would provide an ideal solution to the problem.

The question of how to dispose of solid waste is followed by other sub-questions i.e. what is the solid waste? what are the methods of disposal? moreover, what are the most efficient and economic methods for converting waste into energy?

1.1 Solid Waste

In the UK, approximately 55 million tonnes of municipal, commercial and industrial waste and 29 million tonnes of forestry and crop waste is produced. The energy potential of this tonnage is

approximately equal to the energy potential of 30 million tonnes of coal or 15 million tonnes of oil (2).

The importance of solid waste has to be considered immediately, no matter what form it takes either industrial, agricultural or domestic.

In this research, solid waste materials have been investigated in three main groups.

1. Municipal solid waste/Refuse derived fuel,
2. Biomass waste,
3. Scrap automotive tyres.

1.1.1 Municipal Solid Waste/Refuse Derived Fuel

These materials are very heterogeneous with respect to the moisture content and composition of both the inorganic and organic portions which vary widely with time and location. Some approximate ranges of composition of municipal solid waste (MSW) reported in the literature are given in Table 1.1.

In general, refuse derived fuel (RDF) is produced by treatment of MSW removing non-combustible components such as metals, glass etc. As mentioned by Rampling and Hickey (7), the chemical and physical characteristics of RDF depend on both the properties of MSW feedstock and methods of RDF production.

The production of RDF can be grouped into two different methods.

(i) Pulverisation of total municipal waste feed before separation and pelletisation.

(ii) Size separation by screening to remove high moisture and ash content fines before processing.

Production of RDF is considered a better way to reutilise the waste rather than direct use of municipal solid waste. Removal of non-combustible materials makes the RDF easy to handle, especially in thermalconversion processes. Also, the separation of metals and glass contents from MSW helps recycling of those materials.

Table 1.1 Composition of Municipal Solid Waste

	Sources and dates for data				
	Tillman 1977 (3)	Kruester 1983 (4)	Agrawal 1987 (5)	Mallya & Helt 1988 (6)	Rampling & Hickey 1988 (7)
Paper	42	22-53	30-50	43	33
Glass	6	6-10	8-10	10	10
Metals	8	7-10	7-10	7	10
Plastics	1-6	1-5	1-5	5	1-5
Rubber-leather	-	1-3	1-3	-	-
Wood	2.4	1-3	1-4	-	-
Textiles	0.6	1-3	1-5	-	3-5
Food wastes	12	7-20	10-20	15	18
Yard wastes	15	5-43	5-20	10	19
Other	12.4	1-43	1-4	10	5

1.1.2 Biomass Waste

Biomass has become attractive as an energy source recently and it is one of the most important among the new and renewable sources

of energy. Energy production from biomass is also one of the most promising ways of using solar energy. The developing world and industrialised nations require new technologies to utilise efficiently the biomass resource and also biomass waste.

GrAssI (8), has reported that in the next 10 years in the E.C., biomass is predicted to provide around 10% of E.C. primary energy demand. In the long term, this could reach 300 Mtoe which is equivalent to 50% of total demand.

Biomass waste can be grouped under different types because of their different origins.

- Agricultural crop wastes:

This group addresses the residues form agricultural land use. Corn stalks, pea vines, sugar cane stalks, leaves wastes from wheat, rice and other grains constitute most of the group of waste (9).

- Forestry and wood wastes:

As reported by Strub (1), there are three sources of forest biomass wastes for energy which are existing scrub woodland, thinnings and residues from conventional forestry and also residues from joinery and harvester/chipper machines.

1.1.3 Scrap Tyres

Scrap tyre disposal has been with the rubber industry since the use of tyres became significant. As pointed out by Roy (11), each year 24 million tyres in Canada and 250 million tyres in the U.S. are disposed of. As can be seen in Table 1.2, E.C. countries are also producing quite significant amounts of scrap tyres.

Increasing numbers of worn tyres and their resistance to biodegradation cause health, safety, environmental and handling problems. In general, used tyres are dumped in rural areas or in landfills.

In the places where they are dumped, they provide an environment for vermin, rodents and the potential for fire. Burying of them is not a good solution because they eventually resurface. Also, environmental concerns prohibit the disposal of tyres by burning outdoors (11, 12).

Table 1.2. Total arisings of used tyres in different countries (12)

Country	Arising (tonne/year)
EEC	1.500,000
USA	2.300,000
Japan	579,000
Canada	220,000

1.2 Disposal Methods

The world has enormous amounts of biomass which could be converted into clean fuels and chemical feedstocks if the suitable process can be found. As Reed (13) reports, a number of biomass conversion processes were used throughout World-War II and new processes are still being developed. The same techniques of disposal may be applied to the conversion of the other waste materials such as plastics, rubber etc. either direct or with some modifications.

Disposal methods of waste and biomass to recover their energy potential are:

1. Biochemical methods
2. Thermochemical methods.

1.2.1 Biochemical Conversion Methods

Reutilization with the techniques of bioconversion such as hydrolysis, fermentation etc. These techniques are mainly applied to biomass and biomass waste (14).

In this research, because of the employment of biologically non-degradable wastes such as scrap tyres, plastics etc., biochemical conversion techniques will not be of interest.

1.2.2 Thermochemical Conversion Methods

Thermalconversion methods represent the most promising methods of disposal for a variety of wastes including biomass, plastics, tyres, MSW etc.

Thermochemical methods to reutilize biomass and/or its waste are schematised in Fig. 1.1 Those methods can also be used to convert the other types of waste materials into energy.

The characteristics of the thermalconversion technology determine the end product yield and composition. Consequently, the utilization of the end product often dictates the technology required (Table 1.3).

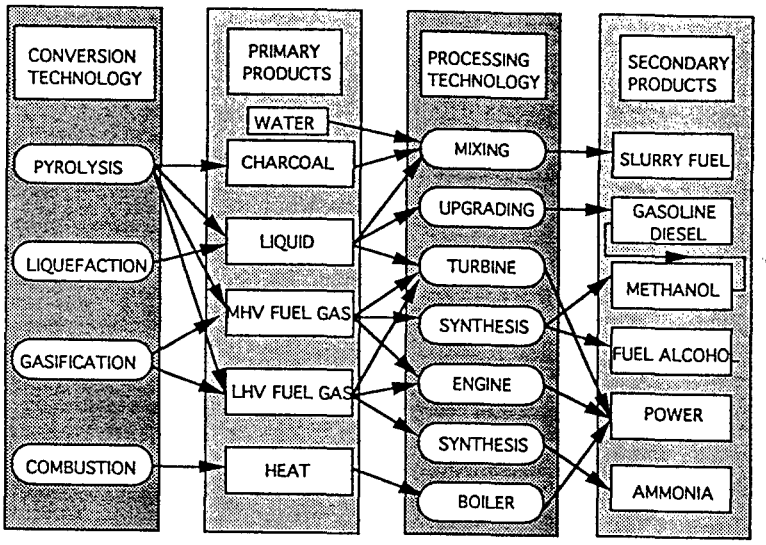

Fig. 1.1 Thermochemical conversion methods and products (15)

The liquefaction process is a catalytic process which is carried out at relatively low temperature and high pressure. The high cost of pressure reactors, the need for feed, preparation and unresolved problems of feeding slurries at high pressure as well as separation of product from solvent has reduced interest in this technology (16).

When gasification techniques are considered in the case of low heating value gas production systems are commercially available, but generally not economical. Also, medium heating value gas production is reported as an uneconomic route by Bridgewater (17).

Another method to dispose of waste is incineration/combustion. As reported by Hiraoko (19), the incineration process is excellent in the respect that perishable organic refuse can be converted to stable inert material reduced in volume and disposed under good sanitary conditions and for recovering energy from waste. On the other hand, it is inevitably apt to cause some pollution problems such as air and water pollution and concentration of heavy metals in the ash.

Table 1.3. Characteristics of thermochemical conversion technology (18)

	Pyrolysis			
Feedstock	Slow	Flash	Lique-faction	Gasifi-cation
Feedstock				
Feed size	any	small	very small	mixed, large
Moisture content	low	very low	very low	50% max
Parameters Temp. °C	400-600	450-900	250-400	1100-1500
Max. through-put dry/th	5	0.05	0.1	40
Products dry basis on dry feed				
Gas Yield	up to 40	up to 70	20	100-250
HHV mJ/kg	5-10	10-20	2-6	5-17
Liquid Yield % wt	up to 30	up to 70	up to 50	up to 3
HHV mJ/kg	23	23	30	23
Solid Yield % wt	30	up to 15	up to 25	Ash
HHV mJ/kg	30	30	30	-

On the basis of these circumstances, the need for a better solid waste disposal technique has stimulated much research. The pyrolysis technique is suitable to deal with solid wastes and biomass. In this method the energy passes into gases and oil for later use. Buekens and Schoeters (20), suggest that pyrolysis processes generate oil and limited quantities of a rather rich gas (see Table 1.4). This technique reduces the volume of wastes and air pollution (21). Also it permits recovery of the energy from waste into suitable form of usable fuel which is easy to handle i.e.

transportable, storable. Kaminsky and Sinn (22), report that pyrolysis of plastic waste and scrap tyres are suitable processes to obtain smaller molecules which can be used as an energy source or chemical materials.

This research is concentrated on pyrolysis techniques.

Table 1.4. Typical yield and calorific value of product gases (20)

Technique	Volume of refuse $m^3\ t^{-1}$	Calorific value $kg\ m^{-3}$
Pyrolysis	200-500	12500-19000
Gasification		
with O_2	600-1100	7500-15000
with air	1000-2500	3000-8000

1.2.2.1 Pyrolysis

The term of pyrolysis is applied to the heating of the sample in the absence of an oxidising agent and causing thermaldegradation of the materials (biomass, waste, coal) polymer structure into smaller molecules. This process has not been discovered recently. It has been practised for centuries.

According to Soltes (22), the older usage of pyrolysis was for describing the carbonisation process in which the principal product is a solid char. This requires relatively slow reaction at low temperatures. Today, the term pyrolysis describes processes in which liquid yields are the most preferred products (see Fig. 1.2). The change of proportions of pyrolysis yields in favour of liquid is achieved by the increasing rate of heating rate and the final

temperature. It is also important that rapid quenching of yield gases to prevent further secondary reactions which reduce the liquid yield amount.

As it is pointed out in the paper of Beenacker and Bridgwater (15), high reaction rates also minimise char formation. This is also confirmed by most researchers (23, 24).

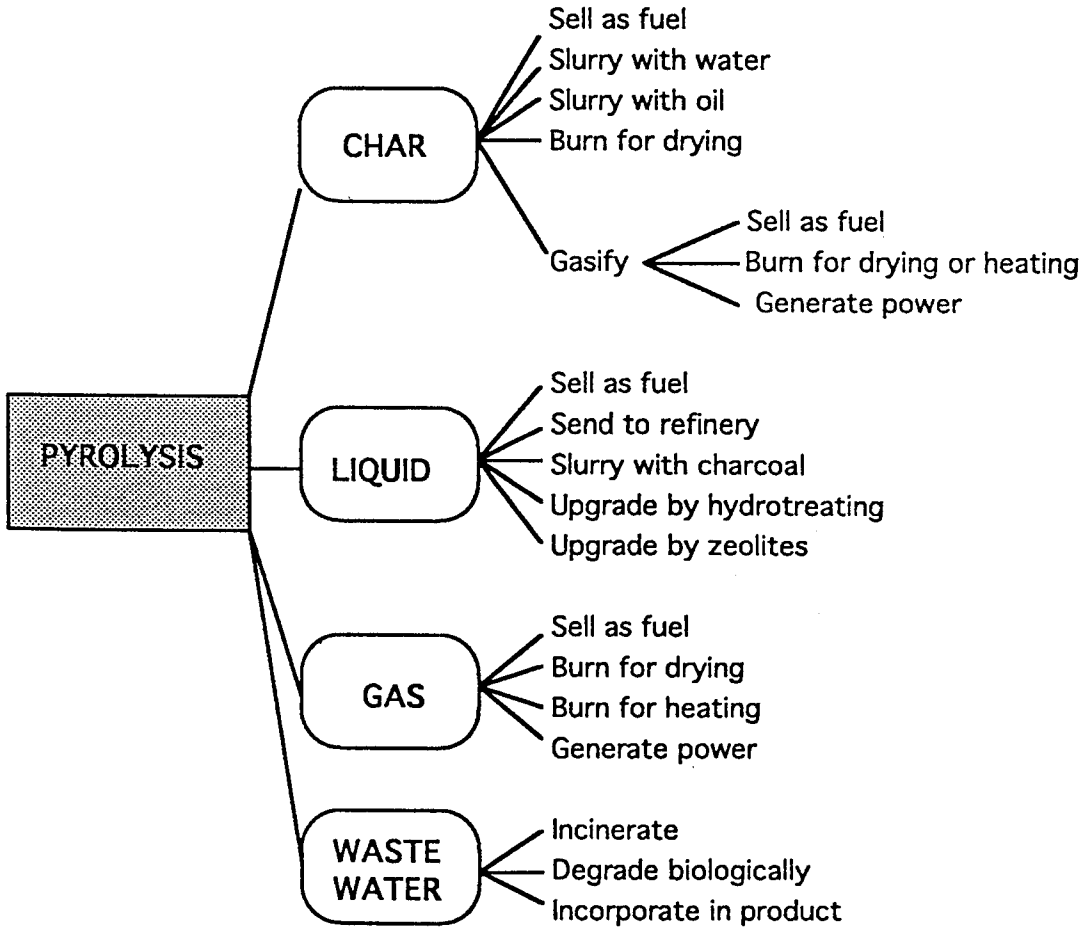

Fig. 1.2. Products from pyrolysis and applications (18)

Table 1.5. Characteristics of pyrolysis technologies (15)

	Residence Time	Heating Rate	Max Temp °C	Major Product
Slow Pyrolysis				
Carbonization	hours-days	very low	400	Charcoal
Conventional Fast Pyrolysis	5-30 min	low	600	Bio-oil, charcoal and gas
Fast	0.5-5 s	fairly high	650	Bio-oil
Flash	< 1 s	high	< 650	Bio-oil, chemicals, gas
Ultra	< 0.5 s	very high	1000	Chemicals and fuel gas
Vacuum	2.30 s	medium	400	Bio-oil
Reactive Pyrolysis				
Hydro-pyrolysis	< 10 s	high	< 500	Bio-oil and chemicals
Methano-pyrolysis	< 10 s	high	> 700	Chemicals

As mentioned before pyrolysis enables the production of solid char, liquid products and fuel gas. To increase the desired product yields especially liquid oil, different equipment and process conditions are employed. The characteristics of the main types of pyrolysis are summarised in Table 1.5.

If pyrolysis is employed to produce char, slow pyrolysis is the most suitable to obtain the maximum yield. Char yields can be optimised in different ways according to parent material i.e. biomass, scrap tyre.

Research is being undertaken to increase the liquid yield of the pyrolysis process. Flash, fast, vacuum and fluidised-bed, rotary kiln, entrained flow and moreover ablative pyrolysis are the most well known ones tested in which the desired oil yield amount can be increased depending on the reaction conditions and feedstock characteristics.

The influences of reactor design and different reaction parameters on the pyrolysis yield will be discussed later.

1.2.2.2 Pyrolysis of Biomass

The pyrolysis of biomass occurs in a complex set of chemical routes which have not been well understood. The degradation pathway is a function of heating rate, temperature, gaseous environment, pre-treatment, extent of inorganic impurities and catalysis.

Different heating rates yield tars either as the main products or as by-products in different proportions. In slow pyrolysis for example with heating rates of about 10°C min^{-1} at low temperatures (less than 500°C) and long gas and solid residence times, secondary coking and repolymerisation reactions occur. This type of pyrolysis gives tars as the by-product. In contrast, in flash pyrolysis with rapid heating rate (10-1000°C s^{-1}) at relatively higher temperatures (400-600°C) and short residence times (less than 2 s) liquid products are maximised as the major products.

In their review, Graham et al (25) underline the difference between flash pyrolysis and fast pyrolysis. Fast pyrolysis is described with extremely high heating rates (1000-10,000°C s^{-1}) at

high temperatures (greater than 600°C) and very short vapour residence time (less than 0.5 s).

Elliot (26) argues that all biomass tars are not the same and the same author (27) also considers the importance of dealing with not only the quantity of tar but also the quality of tar. The comparison of tar which is either the major product or the by-product, is dependent on the formation conditions. This is also confirmed by Graham et al (25).

As schematized in Fig. 1.4, biomass pyrolysis gives different yields with different treatment conditions (28). In 1986, another global pyrolysis mechanism was proposed by Evans and Milne (29) (see Fig. 1.5). In this mechanism, a more complete series of pyrolysis pathways were presented.

Also, Elliot (27) identified the progression of chemicals derived from biomass pyrolysis in relation to pyrolysis temperature which are reported below.

Mixed Oxygenates	→ Phenolic Ethers	→ Alkyl Phenolics	→ Heterocyclic Ethers	→ PAH	→ Larger PAH
400°C	500°C	600°C	700°C	800°C	900°C

The reactions of primary pyrolysis can be classified either as depolymerisation or dehydration reactions. Dehydration is favoured by low temperatures. It involves a reduction of molecular weight the evolution of CO, CO_2 and water and also the formation of char.

Depolymerisation involves higher temperatures. These higher temperature reactions are much more the subject of flash or fast

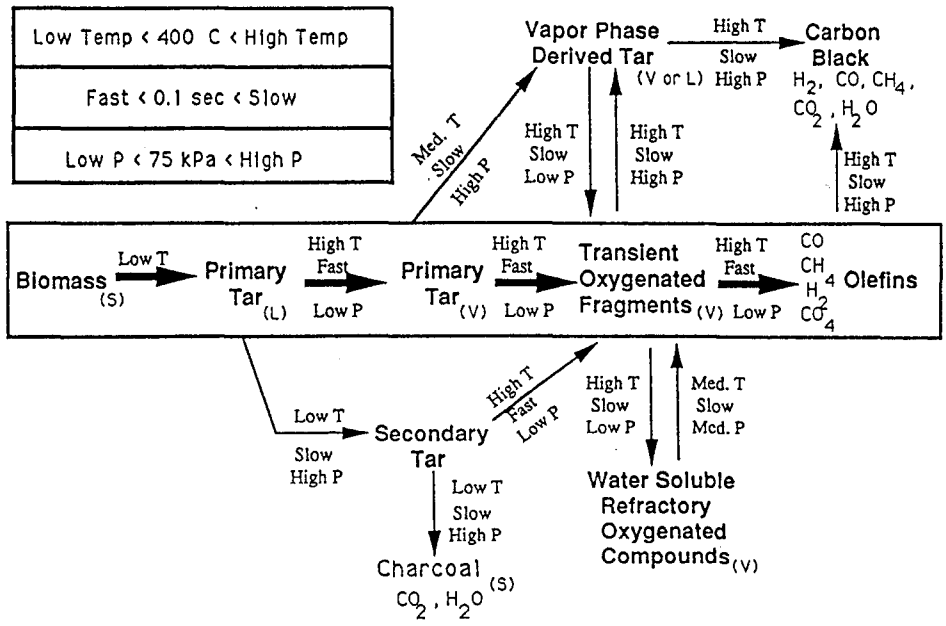

Fig. 1.4. Biomass pyrolysis global mechanism circa 1980 (28)

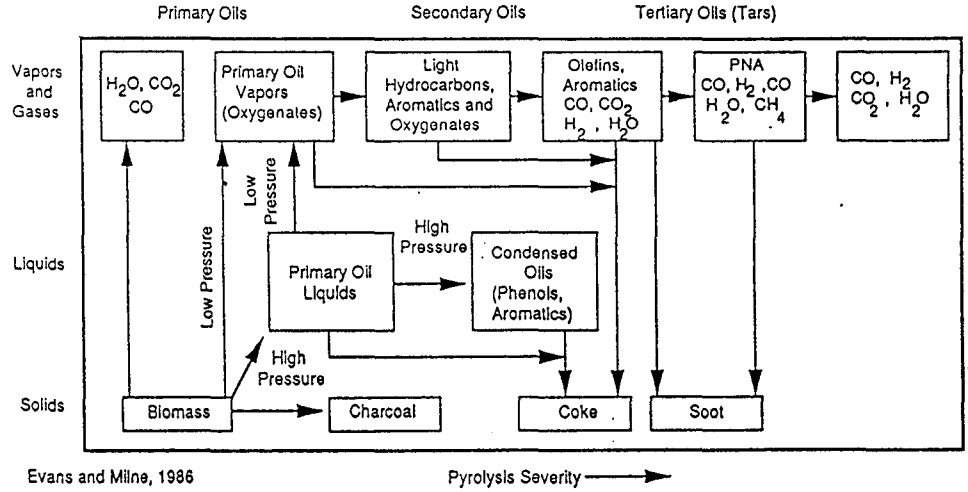

Fig. 1.5. Biomass pyrolysis global mechanism circa 1986 (29)

pyrolysis processes. It is clearly seen from the pyrolysis pathways proposed once the liquid primary tar is formed on the biomass surface. High temperatures, high heating rates and low vapour partial pressures will promote olefin formation by the reaction sequence below (25).

1. Primary tars are vaporised from the liquid tar surface. This prevents occurrence of secondary repolymerisation reactions.
2. The vaporised primary tars are cracked to produce transient oxygenated fragments.
3. The transient oxygenated fragments are thermally cracked and reformed to yield olefins, other hydrocarbons, carbon oxides and hydrogen.

Also, extended reaction times cause olefins to react to produce particulate carbon. Therefore, this pyrolytic pathway can be stopped by rapid quenching in order to preserve the olefins.

It is necessary to know about chemical structure and composition of biomass (in this work mainly wood and rice husks) in order to understand the reactions which take place during the thermal processing. Also, as it is reported by Graham et al (25) that the pyrolysis of a given biomass material was simply the sum of the pyrolytic properties of its individual components.

1.3 The Structure And Chemistry Of Biomass

Biomass has a hierarchical organisation. Even though the tree is used as an illustration, each type of biomass has a similar morphology (Fig. 1.6).

It is clear that understanding of the pyrolysis of biomass components such as cellulose, hemicellulose and lignin will help to predict the behaviour of a given biomass material's known lignocellulosic composition (30).

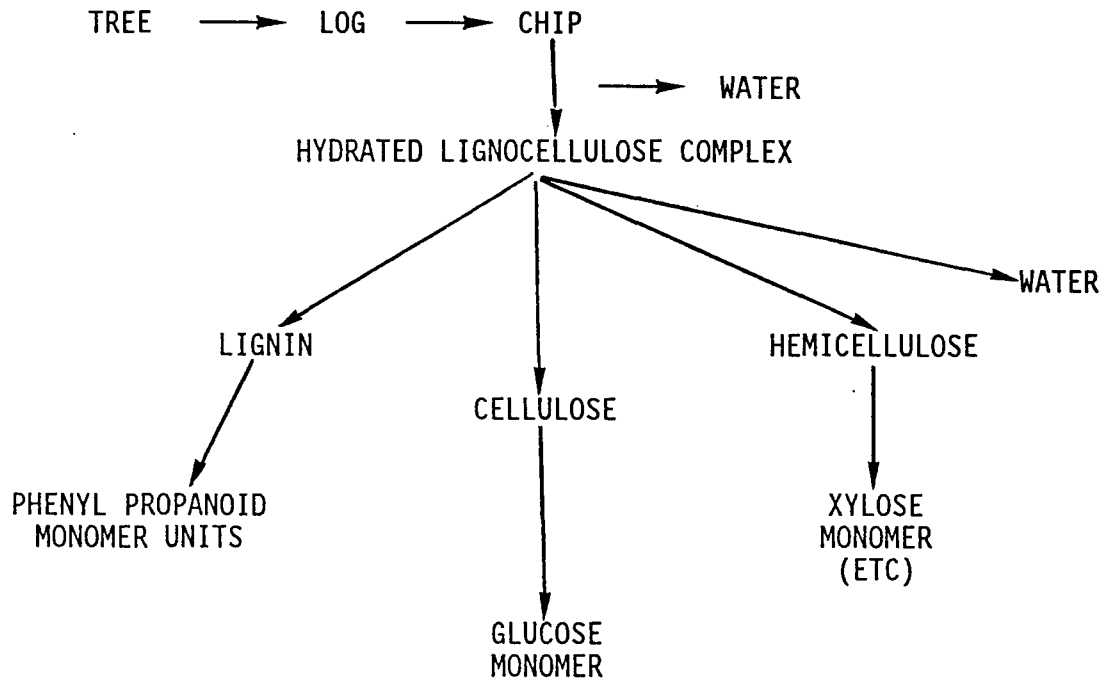

Fig. 1.6. Hierarchical organisation of biomass (31).

1.3.1 Structure of Wood

Wood has been the most common material used by mankind for its energy requirements. Usage of wood was abandoned after the widespread use of coal in the 19th century and particularly of petroleum in the 20th century (32). After the oil shortage (early seventies) and the increasing awareness about the hazards of solid fuels usage on the health and environment, wood (and the other biomasses) have again become attractive as a clean energy source. This is because of its low ash and sulphur content, renewability and also the ability to keep in balance the CO_2 level of the atmosphere.

It is still to be found playing an important part in energy economics (21). Wood and other lignocellulosic materials represents more than two thirds of all renewable matters produced on land (33).

Wood is described as a name given to the main tissue of the stems, roots and branches of the so called 'woody plants' by Kanury and Blachshear (34).

It is composed of elongated cells, most of which are oriented in the longitudinal direction of the stem (Fig. 1.7). Some of the cells (prosenchyma) are vessels tracheids and libliform fibres for transport of water and air for giving mechanical strength (35). The cell diameters of prosenchymas are given in the range of 0.02 to 0.5 millimetres.

Other cells (parenchyma) contain living protoplasm cell nuclei, metabolitas and reserve food such as starch, fats, dye-stuffs and resins. These cell fibres range in length from 0.5 to 1.5 mm and in width from 0.07 to 0.1 mn (34).

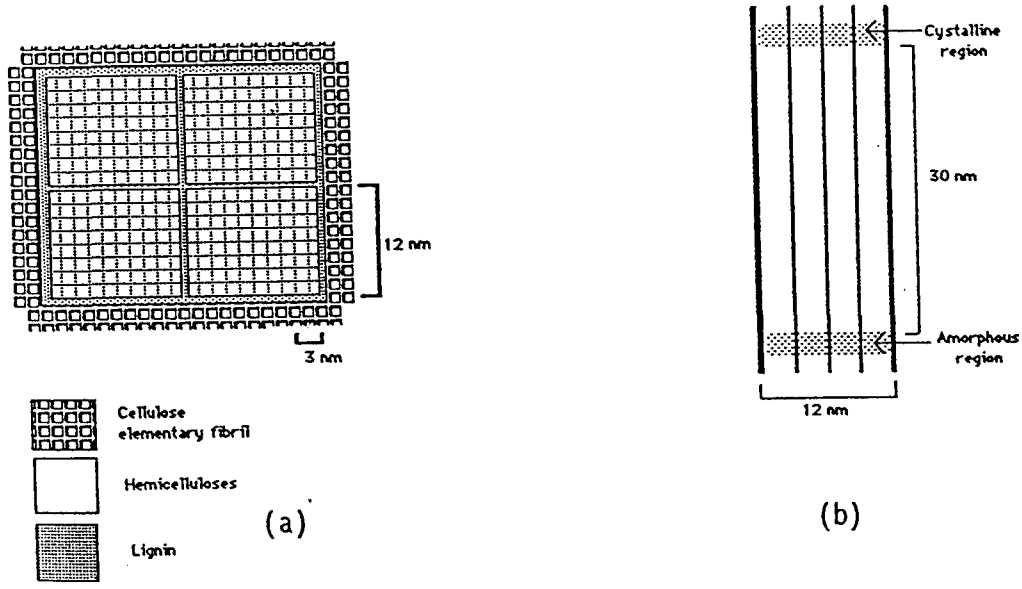

Fig. 1.7. Model of the ultrastructural organisation of a microfibril in wood, (a) cross-section, (b) longitudinal section (37)

The cell wall is made up of a twisted skin of cellulose molecules bunched into elementary fibrils and ordered into microfibrils which are embedded in a matrix of hemicelluloses and lignins.

Young and Davis (36) classify the wood polymers as follows: Hemicelluloses are amorphous polysaccharides with susceptible glycosidic bonds, cellulose is a crystalline polysaccharide with susceptible but less accessible glycosidic bonds and lignin in an amorphous cross-linked aromatic polymer with some resistant carbon to carbon bonds and greater heat stability.

The space-percentage map of the distribution of the principal chemical constituents of the cell wall is shown in Fig. 1.8.

In addition to the major components given above, the wood cell is also comprised of minor components including extractive and inorganic materials. The extracts include invariable quantities from 4 to 15% namely terpenes, resins, fatty acids, tannins, pigments and carbohydrates (32).

1.3.2 Rice Husks

Rice crop residues are one of the biomass wastes which are a major environmental disposal problem. The disposal of the residues is becoming much more difficult as the grain yield is increased by technology (38). Rice residues with energy contents of approximately 16 MJ/kg and lower lignin content are suitable as renewable energy source (39). The main characteristics of rice biomasses are illustrated in Table 1.6.

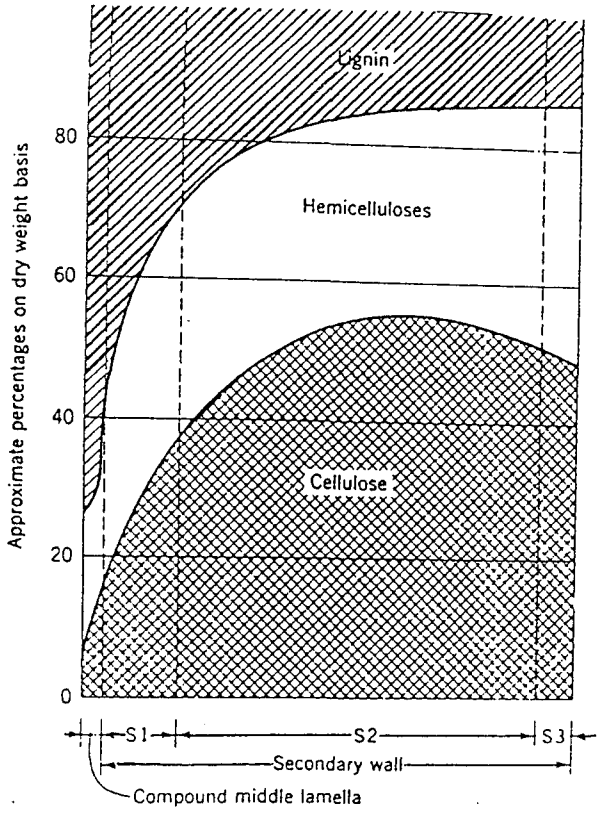

Fig. 1.8. Distribution of the principal chemical constituents within the various layers of the cell wall in conifers (37)

Table 6. Main characteristics of rice biomasses

	Density Kg/m^3	Calorific value Mj/Kg
Rice Husks	110	3300
Rice Straw	300	3350

The lignin content of rice husks and rice straw are reported as 19.2% and 21.5% by weight respectively. Cellulose content of rice straw 40.1% and 34.4% for rice husks were calculated by Grassi et al (40).

Elemental compositions and compounds of rice biomasses are given in Table 1.7.

Over the years, rice biomasses were disposed of by burning, but increasing awareness of environmental issues and growth in public opposition may bring legal regulations on disposal.

Thermaldegradation, which is one of the methods of disposing of waste and biomass, could be better applied to rice biomasses than the traditional way of burning. As is pointed out by Lipska-Quinn et al (38), thermaldegradation of rice biomasses has not been examined extensively, although cellulose, which is one of the components of rice biomasses, has been studied by numerous researchers for years.

In Italy, rice biomasses are used in order to produce electrical power and low temperature heat energy to be used to heat greenhouses (40). Also, some research has been undertaken with a small single cylinder spark ignited internal combustion engine to be operated with gas generated from a static bed rice hull gasifier (41).

Some rice biomass gasification experiments have been practised in Indonesia. One of the projects involves a pilot scale fluidised-bed gasifier, employing rice husks. Since gasification of rice husks is comparatively difficult due to high ash content and the particularly high silica content of the ash. Hartiniati et al (42) tried to optimise reactor conditions. In another project, rice husks were employed to produce rural electricity (43).

Also, Manurung (44) developed a mathematical reaction engineering model for rice husk gasification in order to get an optimal design for an open core rice husk gasifier.

Table 1.7. Elementary compositions and compounds of rice biomasses (40)

	Rice Straw	Rice Husk
Elemental Composition		
Moisture	11.15	9.95
Ash	10.17	14.17
S	0.12	0.06
H	4.31	4.88
N	0.94	not reported
C	35.48	36.62
O	37.83	34.32
Compounds		
Moisture	10.50 ÷ 11.80%	2.4 ÷ 11.3%
Ashes	12.90 ÷ 14.50%	13.2 ÷ 29.0%
Silica	7.40 ÷ 12.40%	not reported
Fats	1.5 ÷ 6.60%	0.3 ÷ 3.0%
Cellulose	40.1 ÷ 47.7 %	34.4 ÷ 43.8%
Lignin	21.5 ÷ 27.5 %	19.2 ÷ 47.0%
Pentolan	12.2 ÷ 21.3 %	16.9 ÷ 22.0%
Insoluble		13.7 ÷ 20.8%

1.3.3 Cellulose

Cellulose is the main constituent of wood. It is the most abundant renewable organic molecule in nature. It is also of prime importance in this work since rice husks contain 40-48% cellulose and RDF contains in the range of 20-50% paper which is 85-95% cellulose and other cellulosics.

Shafizadeh (30) presented cellulose compositions for soft and hard wood as 41% and 39% respectively. Cellulose composition is presented in the range of 40-45% for most wood species by Sjostrom

(35). Also, Maniatis and Buekens (45) with 44.8% and Stiles (21) with 40% give similar cellulose compositions.

Cellulose is a range of polymer chains comprised of up to 10-10,000 β-1.4 linked D-glucopyronase units with the elementary chemical formula $(C_6H_{10}O_5)_n$ and it is predominantly located in the secondary cell wall (Fig. 1.9) (46).

Each monomer unit of cellulose contains 4 C-O bonds which are slightly weaker than the C-H or C-OH bonds. Cellulose molecules are completely linear and have a strong tendency to form intra and intermolecular hydrogen bonds. The functional groups present in the cellulose molecule have a significant effect on its chemical and physical properties. The principal functional groups in pure cellulose are the hydroxyl groups, thus, cellulose behaves as a polyalcohol when undergoing oxidation (47).

The degree of polymerisation which is the number of glucose units placed within one chain, varies from 7000 for the lower plant celluloses, to 15000 for the higher plant celluloses. Cellulose can form both crystalline and non-crystalline (amorphous) areas when microfibrils associate (21).

As it will be discussed later, the degree of crystallinity and the degree of polymerisation have significant effects on the decomposition of the cellulose.

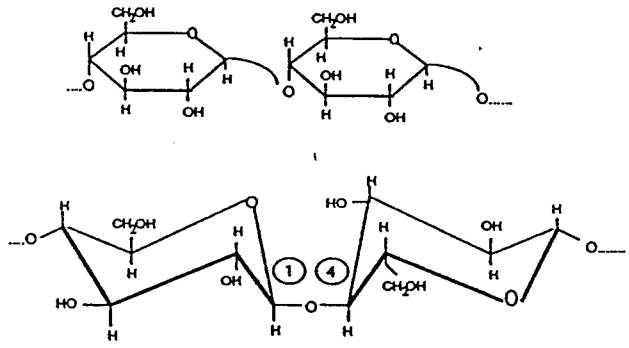

Fig. 1.9. Structure of cellulose

1.3.4 Hemicellulose

Hemicelluloses are the second most important constituent of biomass. They are known as a group of heterogeneous polysaccharides which are formed through biosynthetic routes different from that of cellulose although they previously were believed to be intermediates in the biosynthesis of cellulose (3)].

Antal (47) describes all noncellulosic polysaccharides and related substances as hemicelluloses. Shafizadeh (48) emphasised that the hemicelluloses were amorphous, have a lower degree of polymerisation (100-200 units) and could be preferentially hydrolysed under relatively mild conditions.

The hemicellulose content of wood was reported as 28% and 35% for softwood and hardwood respectively by Shafizadeh (49). Those figures are confirmed with the identical amounts by Mitchell and Pierce (50). Various authors also report hemicellulose content in the same range above (21, 45).

Softwood hemicelluloses and hardwood hemicelluloses have different structures and natures. Galactoglucomannans are the

principal hemicelluloses in softwood (Fig. 1.10A). They have a backbone of 1,4-β-linked D-glucopyranose and D-mannopyranose sugar units to which are linked single α-D-galactopyranose units at some of the C-6 positions. Also, less amounts of arabinoglucionoxylans and arabinogalactans are included in the softwood hemicelluloses. Antal (47) describes all softwood hemicelluloses as mannose, while Shafizadeh (49) named them as mannans.

In hardwood polysaccharides glucuronoxylan is the main hemicellulose component. Depending on hardwood species, the xylan content varies (15-30%). The backbone of xylan consists β-D-xylopyranose units linked by (1-4)-bonds (Figs. 1.10B) and most of the xylose residues contain an acetyl group at C-2 and at C-3 positions.

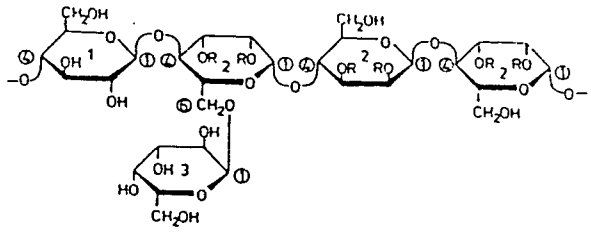

A

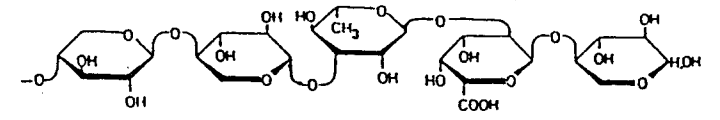

-β-D-Xyl p-1→4-β-D-Xyl p-1→3-α-L-Rha p-1→2-α-D-Gal pA-1→4-D-Xyl p

B

Fig. 1.10. Hemicellulose structure

1.3.5 Lignin

Lignin is a high molecular weight and complex three dimensional phenolic copolymer, derived from woody plants and provides mechanical support to plants and seals water conducting systems which link roots with leaves (51, 52).

The abundance of lignin depends on species, age, juvenile or mature wood. Lignin contents of wood are reported by a number of researchers in the range of 25-40% (30, 32, 35, 45, 52, 53, 54).

Lignin is the polymeric wall component of wood cell with the highest energy content and consists of approximately 60% carbon and 30% oxygen in contrast to hemicellulose and cellulose in which contents of carbon and oxygen contents are less than 50% and nearly 50% respectively (52). Furthermore, Shafizadeh (48) speculated that lignin is more abundant and polymeric in softwood than in hardwoods and the softwood lignin contains guaiacyl propane units, while hardwood lignins contain syringyl propane units. Antal (47) also underlines that agricultural materials have less lignin content than most woods.

The residues of industrial pulping processes which are light lignins and milled wood lignin prepared in a laboratory, differ by way of structure. Train and Klein (51) conclude that lignin structures and properties are dependent on both the parent wood types and molecular weight. This is confirmed by Glasser (52) who summarises that the ratio between the precursors of lignin (Fig. 1.11A) which are *p*-coumaryl alcohol, coniferyl alcohol and sinapyl alcohol, depends on genetic factors, environmental conditions and the

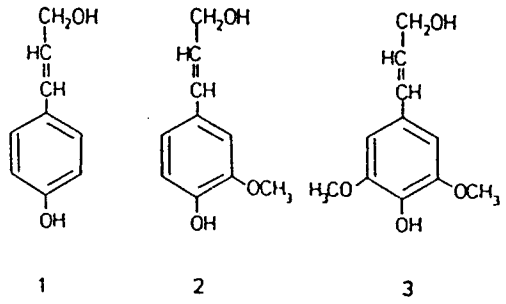

1, *p*-Coumaryl alcohol, 2, coniferyl alcohol; 3, sinapyl alcohol.

(a)

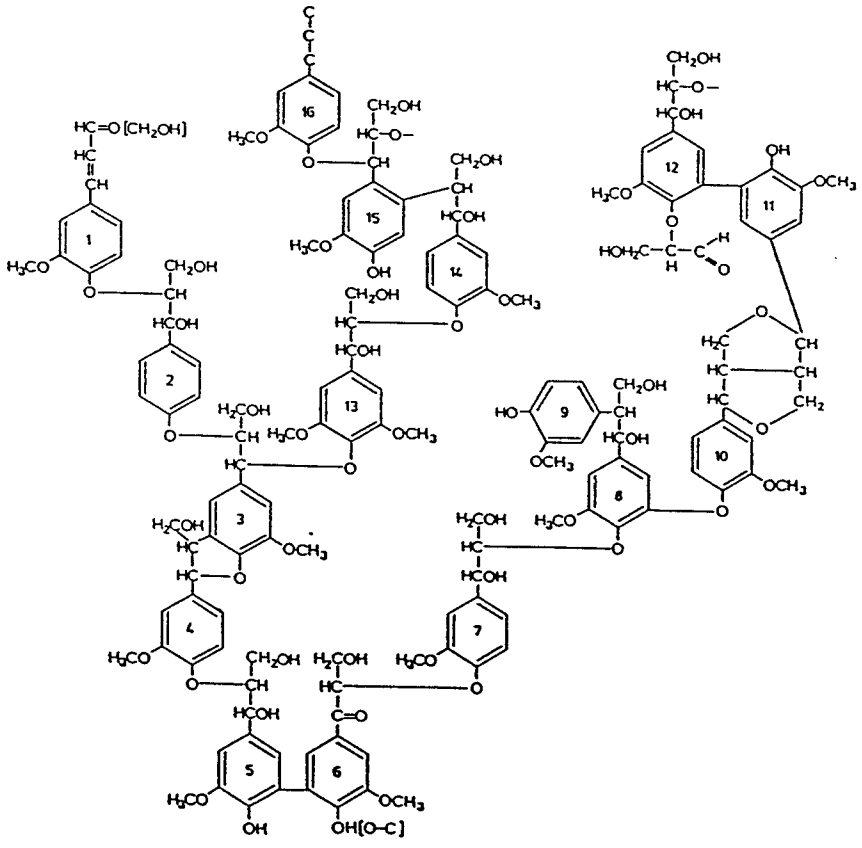

(b)

Fig. 1.11 Lignin, (a) precursors, (b) structure

particular physiological situation of the growing plant, all at the time of lignification.

It is also reported by Sjostrom (35) that covalent linkages exist between lignin and wood polysaccharides (Fig. 1.12).

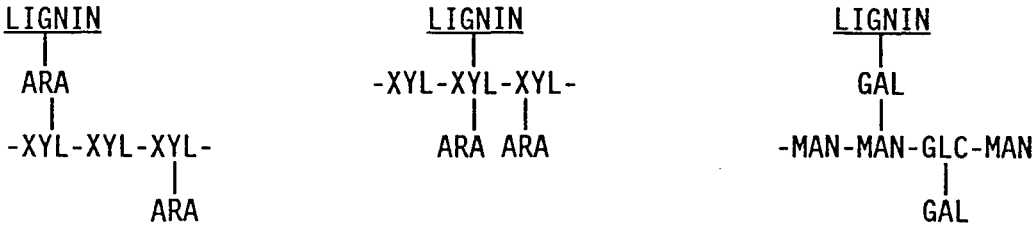

ARA = Arabinose GAL = Galactose GLC = Glucose

XYL = Xylose MAN = Mannose

Fig. 1.12 Some examples of linkages between lignin and hemicellulose.

Lignin may be converted into high quality metallurgical coke used in the production of plywood, adhesives, dispersants and surfactants. Since it was three-dimensional, polymer transformation of lignin into higher value products is more difficult (55). As it will be discussed later, thermaldegradation of lignin appears one of the best solutions to utilise it, Avni et al (56).

1.4 Pyrolysis Of Cellulose, Hemicellulose And Lignin

1.4.1 Cellulose Thermaldecomposition Reactions

Since the cellulose is the most important component of wood and other biomass species, cellulose thermaldegradation reactions have been studied in order to determine the pyrolytic behaviour of cellulosic materials.

Various investigations of cellulose pyrolysis experimentation give a large number of theories and considerable discussions about kinetic models and mechanisms of the pyrolytic reactions.

The rates of the reactions and the overall decomposition process are highly dependent on the ambient atmosphere. When the degree of polymerisation is considered, it is found that the degree of polymerisation of cotton heated in air decreased more rapidly than in nitrogen (57). After pyrolysing of cellulose under vacuum at 251°C, Basch and Lewin (58) found a sharp drop in the degree of polymerisation. At the end of pyrolysis, the degree of polymerisation of various cellulosic samples were found around 200.

The same research group carried out pyrolysis experiments only changing the pyrolysis environment from vacuum to air and they found degrees of polymerisation less in air than in vacuum for the same cellulose samples (59) (Table 1.8).

Antal (47) states in his review that below 250°C volatilisation of the cellulose polymer is slow and its pyrolysis behaviour is effected by the substrate's fine structure.

Patai and Halpern (60), after heating samples which have different crystallinity at 250°C for 2 and 4 hours, came to the same conclusions as Antal (47), that crystallinity considerably affects the pyrolytic behaviour of the different samples, whereas, the samples with a bigger crystallinity index give less yield than the ones with less crystallinity index (Table 1.9).

Weinstein and Broido (61) agree with Patai and Halpern (60). In their work, after swelling cellulose in liquid ammonia, careful

removal of the ammonia can provide an uncontaminated decrystallysed sample which shows significant reduction in char formation on pyrolysis.

Table 1.8. Comparison of degree of polymerisation (DP) in various environments (59)

Sample	DP (Natural)	DP (After pyrolysis in vacuum)	DP (After pyrolysis in air)
Cotton fabric	3083	213	198
Cotton fabric mercerized	2870	185	135
Cotton fabric Pima.	3082	235	190

Table 1.9. Influence of crystallinity on the yields (60)

			Tarry Fraction (mg)	
Sample	CrI (Natural)	DP	2hr pyrolysis	4hr pyrolysis
Whatman filter paper No. 544	82	1800	1.3	28
Fine powder of Whatman filter paper No. 544	81	1062	33	40
Microcrystalline cellulose	74	144	64	65
Ball milled Whatman filter paper No. 544	0	170	115	267

Also, the degree of polymerisation effects pyrolysis yields as seen in Table 1.9. The samples with a higher degree of polymerisation give less yield than with a lower degree of polymerisation.

Earlier in 1968, Shafizadeh (62) proposed two general pathways for degradation of cellulosic materials: One a gradual degradation decomposition and charring on heating at the lower temperatures and a

rapid volatilisation accompanied by the formation of levoglucosan on pyrolysis at the higher temperatures (Fig. 1.13). Also, he speculated that these two pathways compete to predominate at the expense of the other. Heating at the higher temperatures favours the generation of combustible volatiles as in reaction 3 (Fig. 1.13).

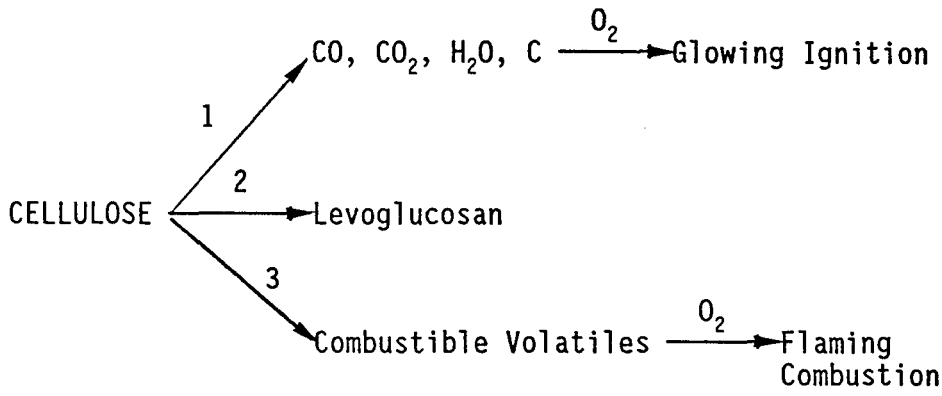

Fig. 1.13. Model for cellulose pyrolysis (62)

As it was stated by Shafizadeh et al (57), cellulose degrades slowly at lower temperatures and when it is heated above 250°C undergoes rapid decomposition to produce levoglucosan.

Basch and Lewin (58) examined the tars produced at 251°C and did not observe any measurable amounts of levoglucosan and they concluded that the crystalline regions were not decomposed. Patai and Halpern (60) also agree with this conclusion.

Ramiah (63) after heating avicell cellulose at a rate of 4°C min^{-1} found that the initial temperature for the pyrolysis was 295°C.

Kosiewicz (64) speculates that it is possible to observe thermaldecomposition of cellulose starting at 70°C with more sensitive tests than thermogravimetry. It is also reported by the

same author that the gas generated at this stage was composed of 90-95% CO_2 and 5-10% H_2.

The mechanism of cellulose pyrolysis at low pressure (1.5 Torr) can be described by a three reaction model. In this model (Fig. 1.14), Bradbury et al (65) assume that an initiation reaction leads to formation of an active cellulose which further decomposes by competitive first order reactions. One yielding volatiles and the other char and gaseous fractions.

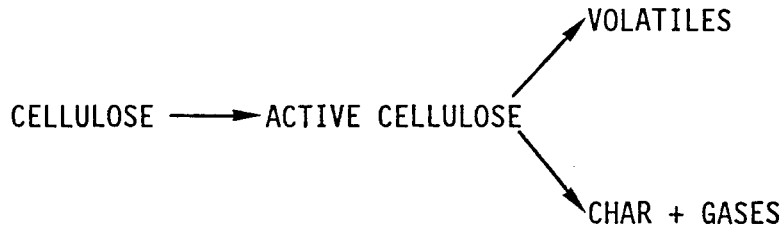

Fig. 1.14. Bradbury model for cellulose decomposition

Another scheme for the low temperature pyrolysis of cellulose was proposed by Kilzer and Broido (66). According to their model (Fig. 1.15), dehydration occurs about 220°C and pure cellulose looses water to yield dehydrocellulose. Depolymerisation, which competes with the dehydration, takes place about 280°C. The last reaction step proposed is the decomposition of dehydrocellulose into gaseous products and char.

The mechanism of cellulose pyrolysis, which consists of two competitive reactions proposed by Kilzer and Broido, has also been intensively investigated by many researchers (67, 68, 69).

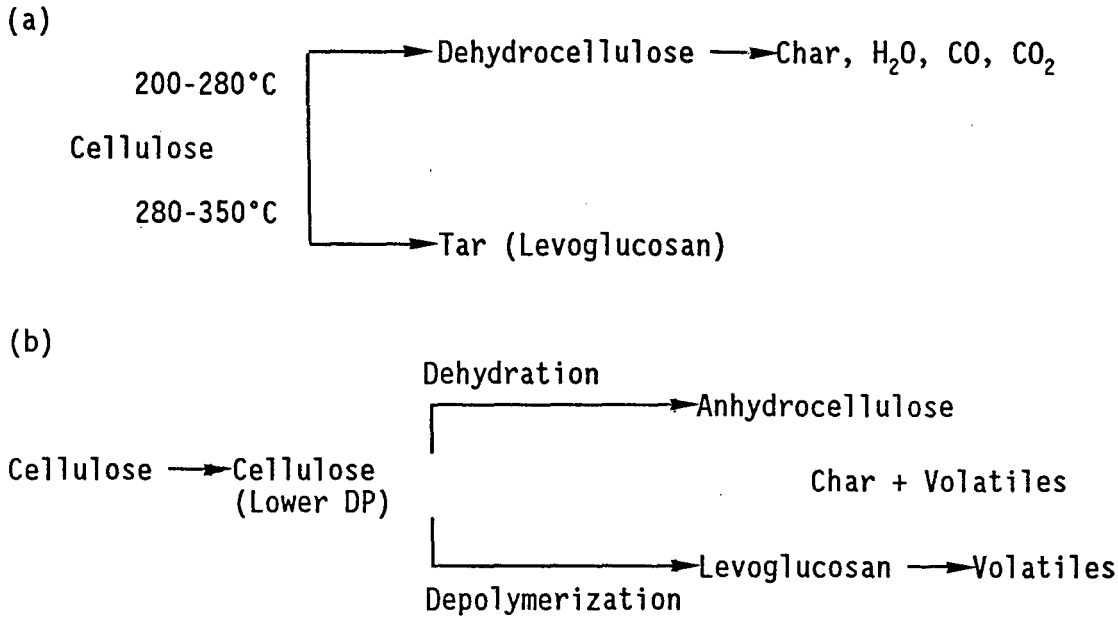

Fig. 1.15. Kilzer-Broido model

Another possible mechanism (Fig. 1.15.b) represents a consensus of the literature. The first step is a decrease in the degree of polymerisation (DP) to about 200 with no detectable weight loss. After reaching lower DP, pyrolysis mechanism starts to appear with two competitive reactions. It is reported by Arsenau (68) that dehydration reaction causes increasing of C=O and C=C bond activity. The anhydrocellulose later react to produce char and some volatiles.

Agrawal (70, 71) compares two different reaction schemes, one is a three reaction model the other is the Kilzer-Broido model modified by him (Fig. 1.16).

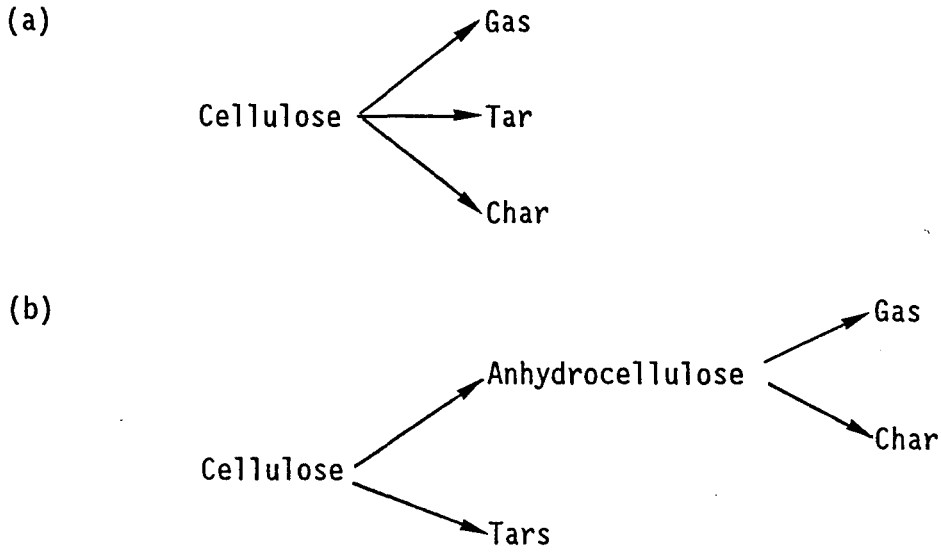

Fig. 1.16. (a) Three reaction model, (b) Modified Kilzer-Broido model

The three reaction model predicts that the chars and gases are evolved from two competitive first order reactions. It is also assumed in the modified Kilzer-Broido model that the formation of chars and gases are not linked. Shafizadeh et al (72) report that the ratio of gas to char yields increases from less than 1 below 300°C to 4 above 400°C. This also supports the assumption of the modified Kilzer-Broido model.

In their intensive work, Alves and Figueiredo (73), listed possible reaction schemes proposed over the years (Fig. 1.17). Using an isothermal thermogravimetric method, they tried to plot "DMM" curves namely as dm^1/dt versus M^1 where M^1 is dimensionless mass and t is time. Among the schemes listed, they found that the scheme 4 which consists of three (first-order) reactions in series was the simplest reaction scheme which generates DMM curves for cellulose pyrolysis. Also, they (74) reported that the mechanism proposed is consistent with the mechanism of the Kilzer-Broido model proposed earlier. The dehydration path is the dominant at lower temperatures

(~220°C). The depolymerisation path is quicker at temperatures above 280°C.

As reported earlier, flash pyrolysis and fast pyrolysis processes are employed at relatively much higher temperatures and faster heating rates than slow pyrolysis. The particle size effect is also of more significance than in slow pyrolysis.

Fast pyrolysis is one of the possible methods used for thermaldegradation of cellulose materials. It is a rapid heating rate process occurring at moderate temperatures (400-600°C).

ONE REACTION

$$Ce \xrightarrow{k_1} a_1 S_1 + (1 - a_1)G \qquad \text{Scheme 1}$$

TWO REACTIONS

Series

$$Ce \xrightarrow{k_1} a_1 S_1 + (1 - a_1)G \qquad \text{Scheme 2}$$
$$S_1 \xrightarrow{k_2} a_2 S_2 + (1 - a_2)G$$

Parallel

$$Ce \xrightarrow{k_1} a_1 S_1 + (1 - a_1)G \qquad \text{Scheme 3}$$
$$Ce \xrightarrow{k_2} a_2 S_2 + (1 - a_2)G$$

THREE REACTIONS

Series

$$Ce \xrightarrow{k_1} a_1 S_1 + (1 - a_1)G \qquad \text{Scheme 4}$$
$$S_1 \xrightarrow{k_2} a_2 S_2 + (1 - a_2)G$$
$$S_2 \xrightarrow{k_3} a_3 S_3 + (1 - a_3)G$$

Parallel

$$Ce \xrightarrow{k_1} a_1 S_1 + (1 - a_1)G \qquad \text{Scheme 5}$$
$$Ce \xrightarrow{k_2} a_2 S_2 + (1 - a_2)G$$
$$Ce \xrightarrow{k_3} a_3 S_3 + (1 - a_3)G$$

Series-Parallel

$$Ce \xrightarrow{k_1} a_1 S_1 + (1 - a_1)G$$
$$S_1 \xrightarrow{k_2} a_2 S_2 + (1 - a_2)G$$
$$S_1 \xrightarrow{k_3} a_3 S_3 + (1 - a_3)G$$

Parallel-Series

$$Ce \xrightarrow{k_1} a_1 S_1 + (1 - a_1)G$$
$$Ce \xrightarrow{k_2} a_2 S_2 + (1 - a_2)G$$
$$S_2 \xrightarrow{k_3} a_3 S_3 + (1 - a_3)G$$

Fig. 1.17 Possible cellulose decomposition reaction

Liden et al (75), proposed a reaction mechanism assuming the cellulosic material decomposes according to a two parallel reaction. One yielding tar and the other char and gas (Fig. 1.18). It was also assumed that the tar undergoes further secondary reactions giving mainly gas as a product. This model showed that this mechanism was suitable for flash pyrolysis of cellulosic materials having particle size less than 2 mm.

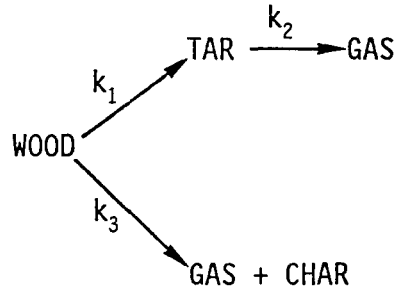

Fig. 1.18. The flash pyrolysis reaction mechanism proposed by Liden et al (75)

Fast pyrolysis is differentiated from flash pyrolysis in the biomass with extremely high heating rates (1000-10,000°C s^{-1}) high temperatures (greater than 600°C) and short vapour residence times (less than 0.5 s).

In their earlier work, Piskorz et al (76) were pointing out that if fast pyrolysis was employed, hydroxy-acetaldehyde would be one of the principal products, but lately they (77, 78) proposed that levoglucosan and hydroxy-acetaldehyde are produced in parallel reactions (Fig. 1.19).

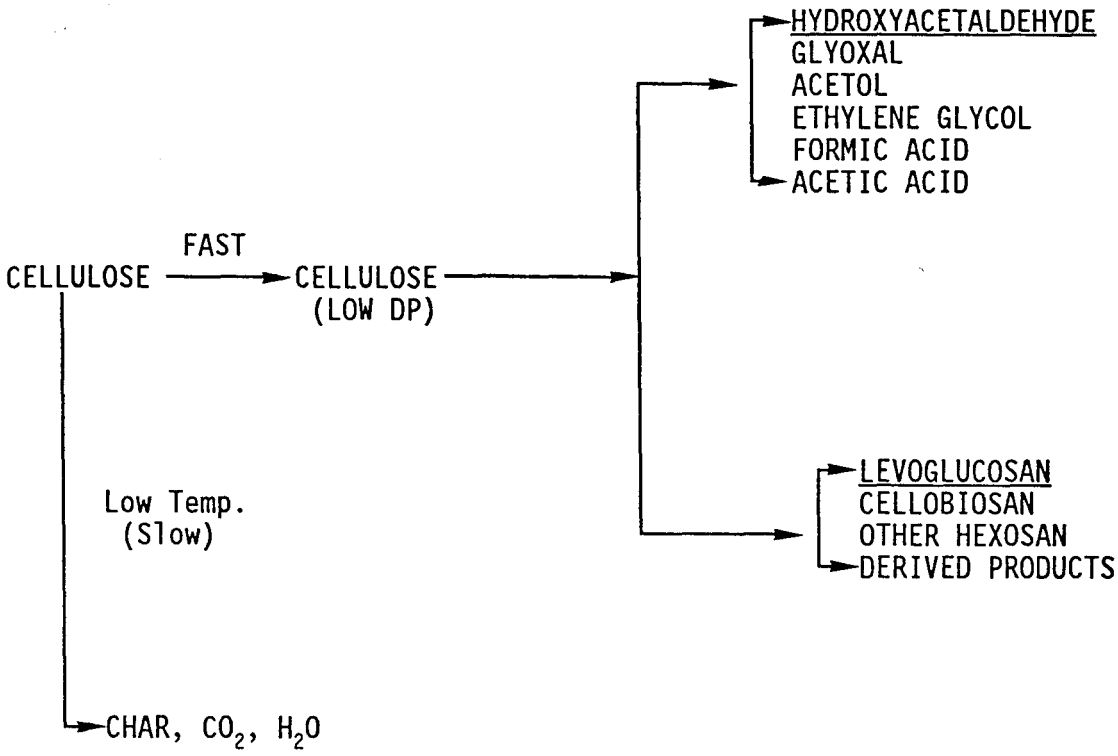

Fig. 1.19. Cellulose decomposition mechanisms in fast pyrolysis Waterloo Model

In their recent work, Radlein et al (79), suggest that pre-heating and lower temperatures favour the production of the monomer levoglucosan. Higher temperatures and addition of inorganic salts favour the latter pathway to yield hydroacetaldehyde.

The influences of particle size on the pyrolysis of cellulosic material are significant, particularly with low temperature pyrolysis. Maa and Bailie (80) proposed two assumptions:

(i) Reaction is controlled by chemical kinetics

(ii) Reaction is controlled by heat transfer.

In his detailed paper, Shafizadeh (62) argued that lower temperatures favours the dehydration and charring reaction (reaction 1) and the temperatures above 250°C reactions are controlled by heat transfer (reaction 2).

The space-time map diagram proposed by Kanury and Blackshear (34) shows four zones virgin solid, pyrolysing solid, char with gas flow and no gas flow (Fig. 1.20).

It is reported that (80) chemical reaction control has more influence than heat transfer control on the sample with radius less than 0.1 cm. In contrast, heat transfer control has more influence on samples having radius bigger than 3 cm. This is confirmed by Liden et al (75).

The wall temperature also has a large effect on the pyrolysis reaction for the particles of all sizes, but it has stronger effects on a small size particle than on a larger size particle. Effective thermal conductivity and solid density have importance on the larger particle size. While activation energy and frequency factor have importance on the smaller particle size.

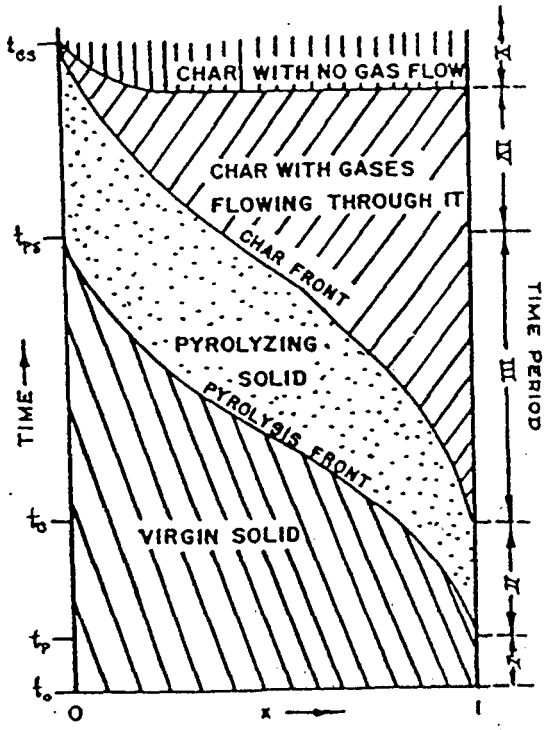

Fig. 1.20. A qualitative diagram showing the zones of a space-time map in a pyrolysing solid.

1.4.2 Hemicellulose Thermaldecomposition Reactions

Hemicellulose is another constituent of biomass which thermally decomposes earlier than the other components of biomass. Hemicellulose thermaldecomposition occurs between 190-230°C in slow pyrolysis (81).

According to Graham and Bergougnou (25), hemicellulose decomposition is initiated as low as 120°C and completed by 325°C.

Ramiah (63) gives the range as 195-325°C for decomposition of potassium xylan. Jonsson (82) is also agreed that by 320°C most of the hemicellulose component of wood is pyrolysed.

The thermaldecomposition pathway is similar to cellulose decomposition in that dehydration reactions are important at temperatures less than 280°C and when the temperature increased, rapid depolymerisation takes place (81). Soltes and Elder (83) report that pyrolysis of hemicellulose produce more gas and less tar than for cellulose pyrolysis and about the same amount of aqueous distillate but no levoglucosan.

During dehydration, random cleavage of the C-O bonds produce branched-chain anhydride fragments, water soluble acids, char and light gases.

It is suggested that hemicellulose degradation occurs in two steps. Firstly, decomposition of the polymer into water soluble fragments and secondly conversion to very short or monomeric units that decompose into volatiles (83).

It is suggested that pyrolysis of hemicellulose produces a substantial amount of acetic acid, although Lipska-Quinn (38) did not observe any in their work with hemicellulose isolated from rice straw. Also, 2-furaldehyde and formaldehyde have been identified in the pyrolysate oil of hemicellulose (83).

1.4.3 Lignin Thermaldecomposition Reactions

The thermaldecomposition of lignin is the least well understood compared with the other components of biomass and also, as reported earlier, lignin is the most refractory and thermally stable of the biomass components.

The mechanism of lignin pyrolysis is virtually unknown. The lack of clear understanding could be related to the complex structure of lignin, which varies as a function of species and also method of preparation (84).

The work carried out by Ramiah (63) with two different lignin, Klason lignin and periodate lignin, showed that Klason lignin was more thermally stable than periodate lignin (Table 1.10). And it was suggested that the difference in the stability of the two lignins could be due to the difference in their preparation. Also it is reported that lignins isolated from softwood are more stable than those from hardwood.

Antal (47), reports that lignin isolation is known to affect its pyrolysis behaviour, however, the method of lignin isolation influences the distribution of products formed in the 100 to 200°C temperature range. Products formed at 300°C were identical for all types of lignin studied.

Lignin pyrolysis yields more char and higher fraction of aromatics in the liquid product than cellulose and hemicellulose (85).

Table 1.10. Dynamic thermogravimetric analysis of lignins (63)

	Temperature of active pyrolysis °C			Volatilisation (%)			
Sample	Initial	Maximum	Final	250°C	300°C	350°C	400°C
Periodate Lignin	230	295	390	9	21	32	40
Klason Lignin	320	375	440	3	5	12	30

Antal (47) has reviewed lignin pyrolysis in three temperature regimes, low, modest, high temperature (Fig. 1.21).

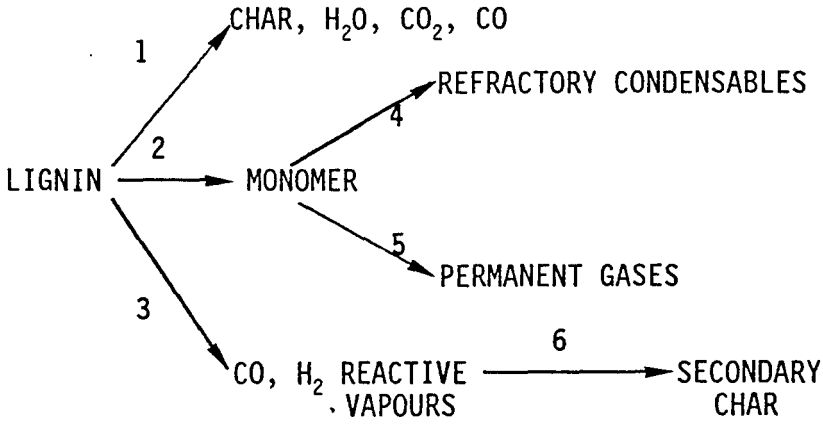

Fig. 1.21. The concurrent and consecutive pathways of lignin pyrolysis.

In low temperature studies (pathway 1), lignin pyrolysis yields char, H_2O, CO_2 and CO. At moderate temperatures, the occurrence of lignin monomers takes place via pathway 2, also, high heating rates and low pressures favour the formation of tar via pathway 2.

At the temperatures above 500°C, monomeric species evolved from pathway 2 start to undergo degradation by the vapour phase thermolysis reaction (pathways 4 and 5).

At very high heating rates, lignin thermolysis occurs without producing char. Char formation was observed to occur by the condensation of vapour-phase species (pathway 3 and 6).

Avni et al (56), confirms that at higher temperatures (>500°C), the aromatic rings are thought to rearrange and condense, releasing hydrogen, also, at higher temperatures there is a rising probability of CO from ether linkages.

It is reported that alkyl-substituted phenols, cresols, guaiacals, catechols and dimethoxyphenols are found in lignin pyrolysis products. Numerous researchers identified over 30 different phenols from lignin pyrolysis (86).

Hurf and Klein (86) also suggest that thermochemical conversion of lignin can be controlled and modified by catalytic hydrodeoxygenation, which results in higher yields of less complex phenol product spectra.

The work carried out by Sada et al (87), with two kinds of lignins i.e. Kraft and Solvolysis lignin pyrolysed using mixtures of molten $ZnCl_2$ and KCl led to a proposed reaction mechanism (Fig. 1.22).

Many researchers make an approximation of the lignin pyrolysis reaction as a combination of many parallel reactions of first order with distributed activation energies.

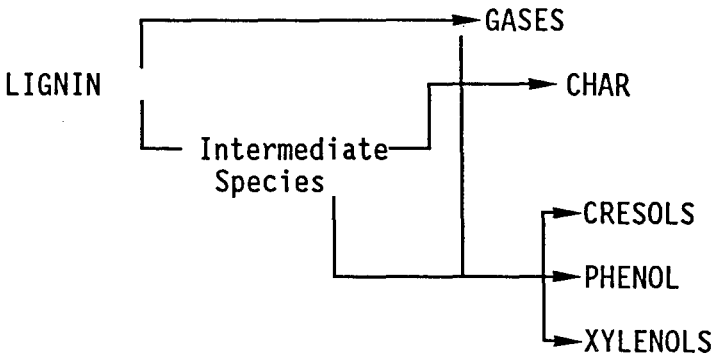

Fig. 1.22. Mechanism for reaction path of lignin pyrolysis in mixed molten $ZnCl_2$ and KCl.

Avni et al (84) concluded after experiments on the flash pyrolysis of lignin, that lignin pyrolysis kinetics were insensitive to lignin source or extraction process and the lignin parameters of the model were related to the functional group composition of the lignin.

Pakdel et al (88) applied vacuum pyrolysis to lignin derived from wood and they observed 42.7% oil, 38% charcoal, 10% gas and 9.3% pyrolytic water at 465°C and below 2 t Pa absolute pressure. When pyrolysis oil was fractioned into 8 fractions after it was found that the fractions 3 to 7 were mainly mono and diphenols.

Vasalos et al (89) also pyrolysed forest biomass with a high content of lignin and they reported that phenols are produced from the decomposition of lignin and maximum yield of phenols appears at nearly 500°C.

Chua, and Wayman, (90) found that extracted autohydrolysis lignin was higher in carbon but lower in hydrogen and oxygen content that aspen milled wood lignin.

1.5 Refuse Derived Fuel (RDF)

1.5.1 Contents of RDF

Refuse derived fuel is highly variable changing in composition and morphology depending on the processing and mixing, source, season and daily fluctuation and it can be defined as the form of municipal solid waste after separating the non-combustible materials i.e. metals, glass. Jaradat et al (91) also defines RDF as a combustible fraction of about 83% municipal solid waste.

Evans and Milne (92) report that, refuse derived fuel be considered a biomass matrix, which is enriched in cellulose due to the presence of higher grades of paper and contains up to 10% of synthetic plastics and other unidentified material and has a higher ash content than biomass.

Pyrolysis capillary gas chromatography was used to characterise RDF by Jaradat et al (91) and eight oxygenated and hydrocarbon compounds were identified (Table 1.11).

Table 1.11. Chemical compounds identified from RDF

Peak No.	Compound
1	2-Cyclohexen-1-ol
2	2.6.10-Trimethyldodecane
3	2.6.10-Trimethyltetradecane
4	2.6-Di-tert-butyl-1.4-benzoquinonene
5	2.6-Di-tert-butyl-4-methylphenol
6	1-Heptadecene
7	2-Phenyl-4.4-dimethyldecane
8	Phenylbi-s-1.1-(3.3-dimethyl-1-butenylidene

Cellulosic materials including paper, newsprint, packaging materials, wood wastes and yard clipping comprise over 50% of MSW structure and pyrolysis of cellulosic materials and lignin were discussed previously.

Plastic wastes can be divided into two main groups as industrial wastes and city rubbish. Industrial wastes have a much higher plastic concentration such as by product and substandard polymers from synthetic resin plants. Scrap from plastics converting plants, milk containers, soft drink bottles, carrier bags and packaging materials are the main source of polyethylene and polystyrene in city rubbish, while electric cable covers and pipe materials are the source of polyvinylchloride in RDF (93, 94).

1.5.1.1 Polypropylene

Polypropylene is a linear hydrocarbon polymer (Fig. 1.23a), containing little or no unsaturation. It is therefore that polypropylene and polyethylene have many similarities in their properties, particularly in their electrical properties. The most significant influence of the methyl group is that it can lead to products of different tacticity.

1.5.1.2 Polyethylene

Polyethylene is a wax-like thermo-plastic softening at about 80-130°C, with a density less than that of water. It has the simplest basic structure (Fig. 1.23b) of any polymer. The main attractive features of polyethylene in addition to its low price are, very good chemical resistance, good processability, toughness, transparency in thin films.

1.5.1.3 Polystyrene

Polystyrene has the simple repeating structure shown in Fig. 1.23c and as might be expected from such a substantially linear polymer, it is thermo-plastic.

Polystyrene is a hard, rigid, transparent thermo-plastic. Because of its low cost, good mouldability, low moisture absorption, good dimensional stability it is widely used.

1.5.1.4 Polyvinylchloride

Polyvinylchloride is a linear polymer and substantially thermo-plastic shown in Fig. 1.23d. The presence of the chloride atom, causes an increase in the inter-chain attraction and hence an increase in the hardness and stiffness of the polymer (95, 96, 97).

1.5.2 Thermaldecomposition of RDF

Individual plastics will generally be present in RDF. The products of pyrolysis of each plastic may be difficult to identify from small scale RDF experiments because of their low proportions in the RDF. Therefore, a knowledge of the mechanism of thermaldegradation of the individual plastics may help to explain the thermaldegradation of RDF (98).

Thermaldegradation of plastics occur in several stages depending on temperature. Around 200°C, many plastics undergo weight reduction, but at 400-500°C, most thermaldegradation occurs with gas evolution (Fig. 1.24) (99). Daborn and Rampling (98) suggest that at higher temperatures, more hydrocarbons are produced as the solid

residues decompose. Then secondary pyrolysis yields hydrogen and the heating value of the product gas falls.

1.5.2.1 Thermaldecomposition of Polypropylene

Only traces of monomer are produced when this polymer is pyrolysed (98).

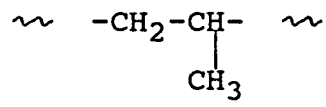

(a) polypropylene

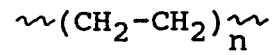

(b) polyethylene

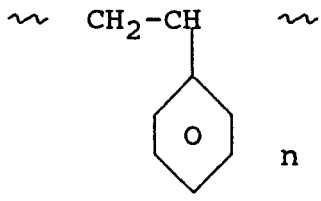

(c) polystyrene

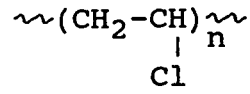

(d) polyvinyl chloride

Fig. 1.23. Formulations of some plastic materials

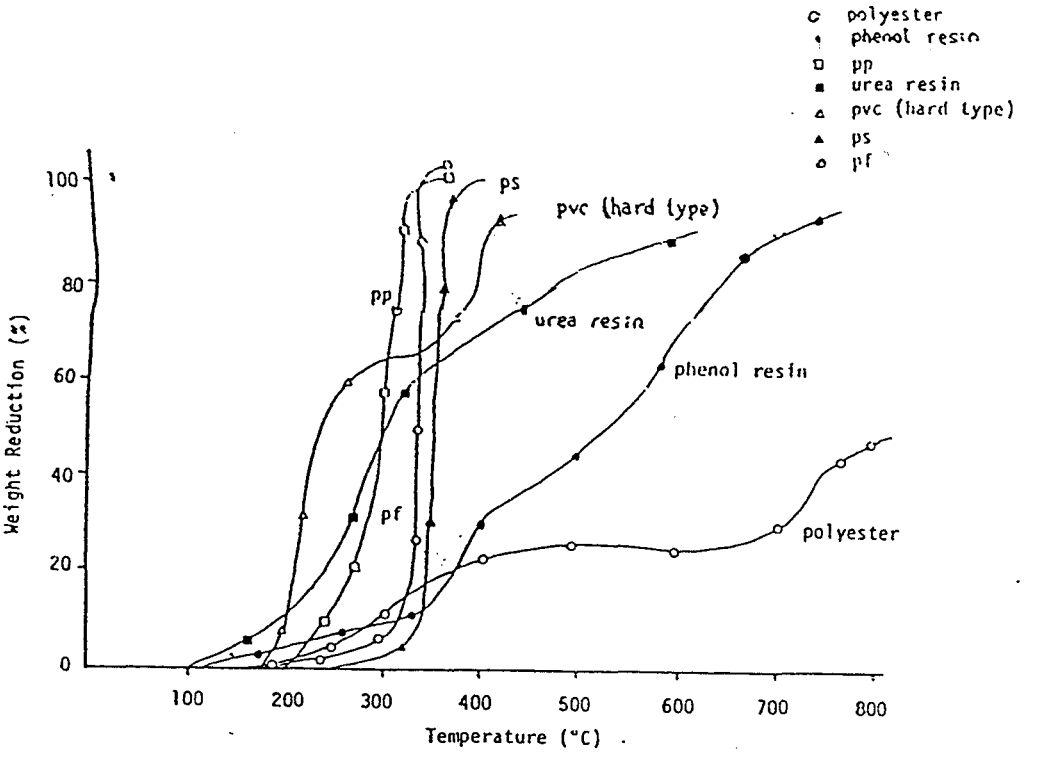

Fig. 1.24. Thermaldecomposition characteristics of some plastic materials (99).

1.5.2.2 Thermaldecomposition of Polyethylene

As it has been earlier investigated by Tsuchiya and Sumi (100), during thermaldecomposition of polyethylene, the predominant process for the formation of volatiles appears to be intramolecular transfer of radicals. The thermaldecomposition products of polyethylene found in volatile fraction are presented in Fig. 1.25.

Kiran and Gillham (101) are agreed that the formation of a homologous series of volatile products corresponding to alkanes and alkenes is interpreted in terms of an intermolecular radical transfer process in the primary macro radicals to the 5th, 9th, 13th and 17th carbon atoms of the chain.

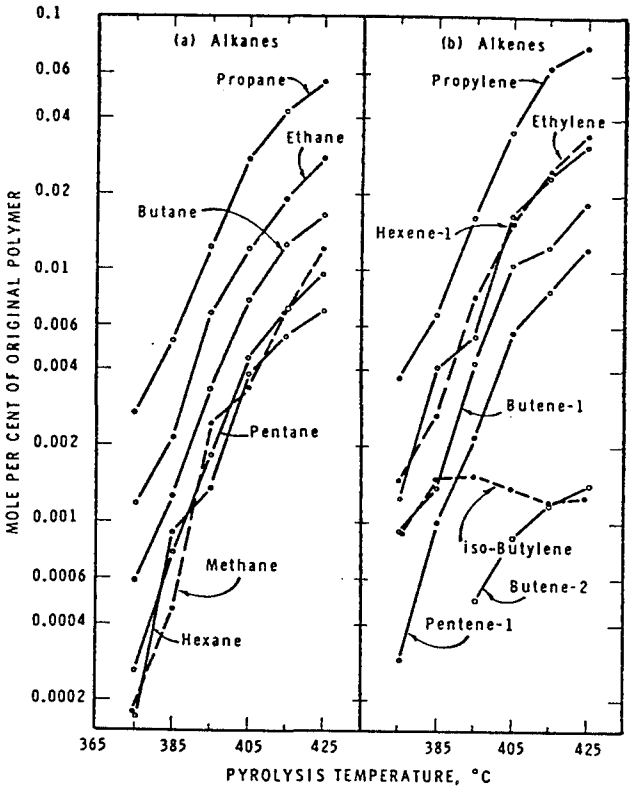

Fig. 1.25. Decomposition products of ethylene (100)

1.5.2.3 Thermaldecomposition of Polystyrene

Only three major compounds which are styrene monomer, a linear dimer and a linear trimer with an ethylene-end group (Fig. 1.26) have been characterised in thermaldegradation products of commercial polystyrene by Daust et al (102) using gel permeation chromatography.

Styrene monomer appears during the degradation from unzipping at 350-370°C temperature. Kamisky et al (103) confirm and they state that a high yield of monomer styrene is only possible at relatively low temperatures.

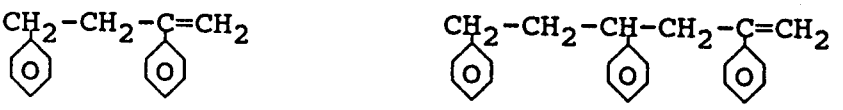

(a) (b)

Fig. 1.26. Styrene (a) dimer and (b) trimer

According to Schoeters and Buekens (104), recovery of styrene from polystyrene waste is attractive because of the high value of styrene monomer. Moreover, they underline that polystyrene is one of the most frequently used types of plastic. It is also reported that polystyrene pyrolysis yielded an oil with a high content of styrene monomer (105). When they optimised the reaction conditions maximum yield of styrene, 76% was obtained.

Pyrolysis of polystyrene chips has been experimented in fluidised-bed reactor by Nishizaki et al (106) and it is reported that polystyrene was mostly decomposed to styrene monomer and conversions of more than 50% to oil were obtained.

The thermaldecomposition of polystyrene in a fluidised-bed was proposed as below.

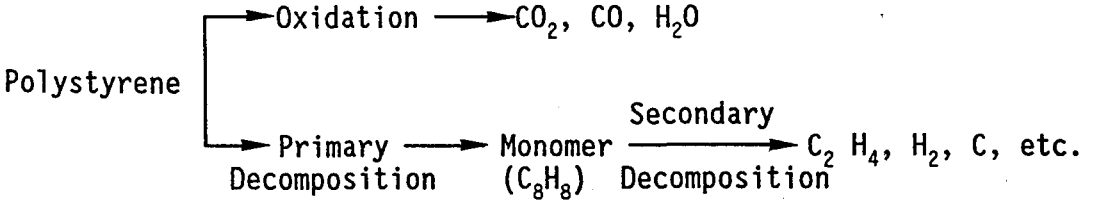

Fig. 1.27. Polystyrene thermaldecomposition mechanism.

Koo et al (107) pyrolysed polystyrene (PS) and polyethylene (PE) and concluded that:

- The pyrolysis time for the maximum oil production from PE-PS mixtures is shorter than for PE alone and approaches that of PS alone.

- The maximum recovery of toluene, xylene, styrene and I-propenyl benzene was 8.6, 8.9, 51.0 and 7.4 percentage of feed respectively for the pyrolysis of PS at 300°C. In addition, naphthalene was 1.3 wt % of feed at 300°C when pyrolysing a 1÷1 mixture of PT and PS.

1.5.2.4 Thermaldecomposition of Polyvinyl Chloride (PVC)

Wilkins and Wilkins (99) underline that when PVC was pyrolysed at about 300°C, most of the chlorine is produced and cracking steps occur about 400-500°C depending on the exact nature of the feed.

According to Kamisky et al (103), the weight percentage of the PVC products is very low because of the high HCl content of PVC.

Levie et al (93) studied slow pyrolysis of RDF pellets with a single-particle reactor and they summarised that the char yield could be correlated with temperature, polystyrene, PVC polyester and polyethylene. It is also shown that different composition of feed and reactor conditions have to be known when designing the reactor.

Fast pyrolysis of RDF in a vortex reactor examined by Diebold et al (108) showed that polyethylene pyrolysis products were dominated by alkyl and dialkyl fragment ion series while polystyrene yielded styrene. Also, polyethylene terephtalate (PET) pyrolysis products are most likely to be terephatalic acid.

The vacuum pyrolysis of RDF has been tested by Roy et al (109). According to their experimental results, pyrolysis oil accounts for more than 50% of the products and mainly oxygenated in nature and is believed to have a low molecular weight distribution range.

Pober and Bauer (110) suggested that the pyrolytic oils derived from solid waste may be fundamentally similar to pyrolysed cellulose and non-cellulose materials (degraded plastic, ash, metals etc.) in solid waste may either catalyse or suppress competing reactions.

1.6 Scrap Tyres

1.6.1 Contents of Scrap Tyres

The disposal of scrap tyres has been an important problem to be solved since the use of tyres became significant. Earlier scrap tyres used to be reclaimed by the rubber industry. By the time of World War II, scrap tyres and all other scrap rubber contained only natural rubber. Approximately 30% of scrap tyres used to be accepted in compounding of new tyres (111).

Since styrene-butadiene rubber (SBR) replaced natural rubber in the production of tyres, reclaiming technology had to change because of the big difference in the structure of SBR and natural rubber.

The pyrolytic technique used to be applied in the early 19th century for studying the structure of natural rubber. Dipentene was isolated by Faraday in 1826 from pyrolysis oil obtained from the destructive distillation of rubber.

Rubber tyre is a blend of styrene-butadien rubber (SB), carbon black and other additives (Table 1.12). Depending on the product,

natural rubber (NR) and butadiene rubber (BR) are also used in the tyre production processes.

Table 1.12. Rubber compounding composition

COMPONENT	WEIGHT %
SBR	62.1
Carbon Black	31.0
Extender Oil	1.9
Zinc Oxide	1.9
Stearic Acid	1.2
Sulphur	1.1
Accelerator	0.7
TOTAL	99.9

1.6.1.1 Natural Rubber (NR)

Natural rubber is a high molecular weight polymer of isoprene (Fig. 1.28). It can be obtained from nearly five hundred different species of plants. The most common name for the source is Hevea rubber.

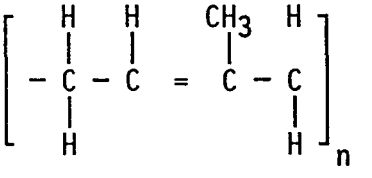

Fig. 1.28. Structure of natural rubber molecule.

Natural rubber has a number of features that styrene butadiene rubber (SBR) does not have:

(a) its mastication behaviour,

(b) its ability to crystalise,

(c) its high resilience,

(d) its reactivity with oxygen and sulphur (95)

Commercial raw material rubber has a small but highly important content of non-rubber constituents.

Table 1.13. Analysis of representative natural rubber.

Ingredient	Average %	Range %
Moisture	0.5	0.3 - 1.0
Acetone extract	2.5	1.5 - 4.5
Protein	2.5	2.0 - 3.0
Ash	0.3	0.2 - 0.5
Rubber Hydrocarbon	94.2	-
TOTAL	100.0	

1.6.1.2 Styrene-Butadiene Rubber (SBR)

The most important and widely used rubber in the entire world is SBR, a copolymer of styrene and butadiene which are the chief raw materials necessary to manufacture SBR (Fig. 1.29).

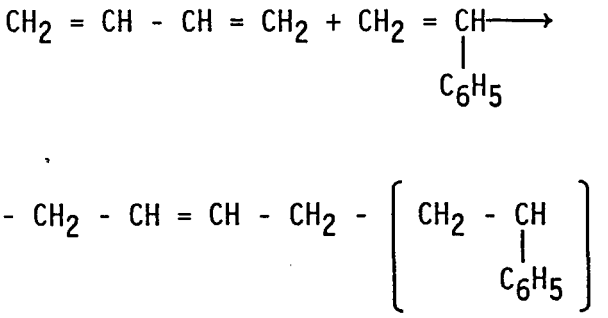

Fig. 1.29. Polymerisation and structure of SBR

SBR was first developed and manufactured in Germany during the period 1930 - 1935 and was called Buna. Its molecular weight is dependent on the styrene/butadiene ratio.

According to Brydson (95), in many respects SBR is not a particularly good rubber, but it has a large commercial market for the reasons below:

(a) its low costs,

(b) its suitability for passenger car tyres,

(c) a higher level of product uniformity than can be achieved with natural rubber

SBR made in emulsion, usually contains about 23% styrene with butadiene in the polymer chains for different styrene/butadiene ratios it is also used producing different products such as jacketing for wire and cable, mechanical goods, footwear and shoe, hose, tubing, sponge, adhesive, belts besides car tyre.

1.6.1.3 Polybutadiene Rubber (BR)

The structure of Cis - 1,4-polybutadiene is very similar to that of the natural rubber molecule (Fig. 1.30).

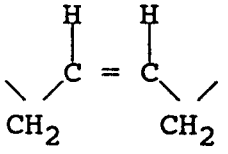

Fig. 1.30. Structure of BR.

The polybutadiene rubbers have a lower heat build-up and this is important in tyre applications. On the other hand, these rubbers have poor tear resistance, poor tack and poor tensile strength. For this reason the polybutadiene rubbers are seldom used on their own. They are blended with natural rubber in the manufacture of truck tyres and widely with SBR in the manufacture of passenger car tyres.

1.6.1.4 Carbon Black and Other Additives

The carbon black acts to strengthen and impart abrasion resistance to the rubber. It is defined as a black pigment produced by the incomplete burning of natural gas or oil (96) followed by separation from combustion products by electrostatic precipitation and cyclones. Carbon black is widely used particularly in the rubber industry.

The recovery of carbon black from scrap tyres is one of the reasons for thermaldegradation of scrap tyres, its surface area particle shape, purity etc. influence marketability as an ingredient in tyre production.

The extender oil is a mixture of hydrocarbons and its main job is to soften the rubber to make it more workable.

The sulphur reacts with the double bonds in adjacent polymer chains to cause cross-linking which hardens the rubber and prevents deformation at higher temperatures.

The accelerator acts as a catalyst for the vulcanisation process. The addition of zinc oxide and stearic acid are for improving the physical properties of the rubber.

1.6.2 Thermaldecomposition of Scrap Tyres

By thermaldecomposition, scrap tyres represent a source of energy and chemicals. Much research has been carried out to pyrolyse scrap tyres and maintain the valuable C-H bonding of the macromolecules to obtain smaller molecules which can be used as energy resources or raw chemical materials.

Kaminsky and Sinn (112) argue that during pyrolysis, even heat transfer is necessary for preventing the uneven decomposition caused by the uneven heat transfer and they add, using quartz sand or carbon black fluidised-bed reactors are useful to supply uniform conditions for proper decomposition.

Vacuum pyrolysis of scrap tyres has been experimented by Roy and Unsworth (113), vacuum conditions were used in order to minimise the extent of secondary reactions such as thermal cracking, re-polymerisation and re-condensation reactions, gas phase collision catalytic cracking and reduction and oxidation reactions. They report that with the vacuum pyrolysis reactor, oil yield increases with the increasing temperature up to 500°C, while carbon black yield decreased. Mirmiran et al (114) with the same group of Roy and Unsworth (113) suggest that thermal destruction of scrap tyres under vacuum yielded 61% pyrolysis oils, 26% pyrolytic carbon black and 13% gas.

Bouvier et al (115) tried to make a material balance of scrap tyre pyrolysis using batch pyrolysis in a pilot-scale unit. In their work, steel cords were not separated from the scrap tyre feed. They present 37.6% char, 12.4% iron steel, 34.7% oil 3.4% water and 5.8% gas yield. The yield of pyrolysis products from tyre waste was summarised as char 30.5%, oil 61.9%, water 2% and gas 5.6% by Nag et al (116) using a silica tube containing sand soaked in tyre oil.

Thermaldecomposition of rubber tyre is an extremely complicated process. It is generally conducted at a relatively high temperature. Beckman et al (111) report that, without a catalyst the reaction products are probably thermodynamically controlled and they also add

that kinetic control is a probability because of the organic salts derived from vulcanisation. Bouvier et al (115) showed that pyrolysis time decreases sharply at temperatures below 500°C and above 500°C decreases less sharply and becomes linear. They showed that at higher temperatures, pyrolysis rate is limited by conductive heat transfer and for lower temperatures, pyrolysis is controlled by kinetics of thermaldegradation.

According to Bouvier et al (117), the SBR co-polymers molecular weight is close to 500,000 and these huge macromolecules are tied together after vulcanisation by sulphur bonds. When the temperature is increased, the polymer passes from the solid state to the liquid state, it swells, softens and dissolves. Scission of sulphur bonds and dissolution occurs. After this stage, three steps are considered to take place:

(a) Below 260°C. NO breakage of C-C bonds and dissolution occurs.

(b) Temperatures above 340°C. The rate of degradation is limited by kinetics of the scission of the C-C bonds and total disappearance happens in a few minutes.

(c) Temperatures between 260°C and 340°C. This is the most difficult step. Two competitive reactions take place which are a radical scission of C-C bonds either dissolution.

In their later work, Bouvier et al (115) report that thermaldegradation of tyre rubber proceed in two steps. The polybutadiene part cracked at lower temperature than the polystyrene part. Also, the predominant monomers in worn tyres are found in the liquid product of pyrolysis (118).

Formation of benzene and toluene are expected through reactions involving the styrene monomer, along with a wide range of higher aromatics and condensed ring compounds.

The temperature and residence time of pyrolysis have important influences on the yield. Higher pyrolysis temperatures and longer vapour residence times promote gas production at the expense of the liquid fraction.

Bouvier et al (115) have shown that pyrolysis time appears relatively short and treatment of whole tyres seems possible because of a high gas-solid contact area.

Grinding of tyres would not increase this contact area notably also it is inexpensive. Roy et al (119) also agree with this conclusion.

To enlighten the pyrolytic pathway of the scrap tyre decomposition. Mocaione et al (120) tried to use a thermogravimetric analyser employing scrap tyres with different blends. They obtained thermaldecomposition curves (TGA) and differential weight loss curves (DTG). As seen in Fig. 1.30, DTG curve of SBR-BR blend has a significant shoulder above 500°C the one which was a blend of SBR-BR-NR has got two peaks, one is just above 400°C probably 415° - 420°C and the other one appears at the same temperature with SBR-BR blend.

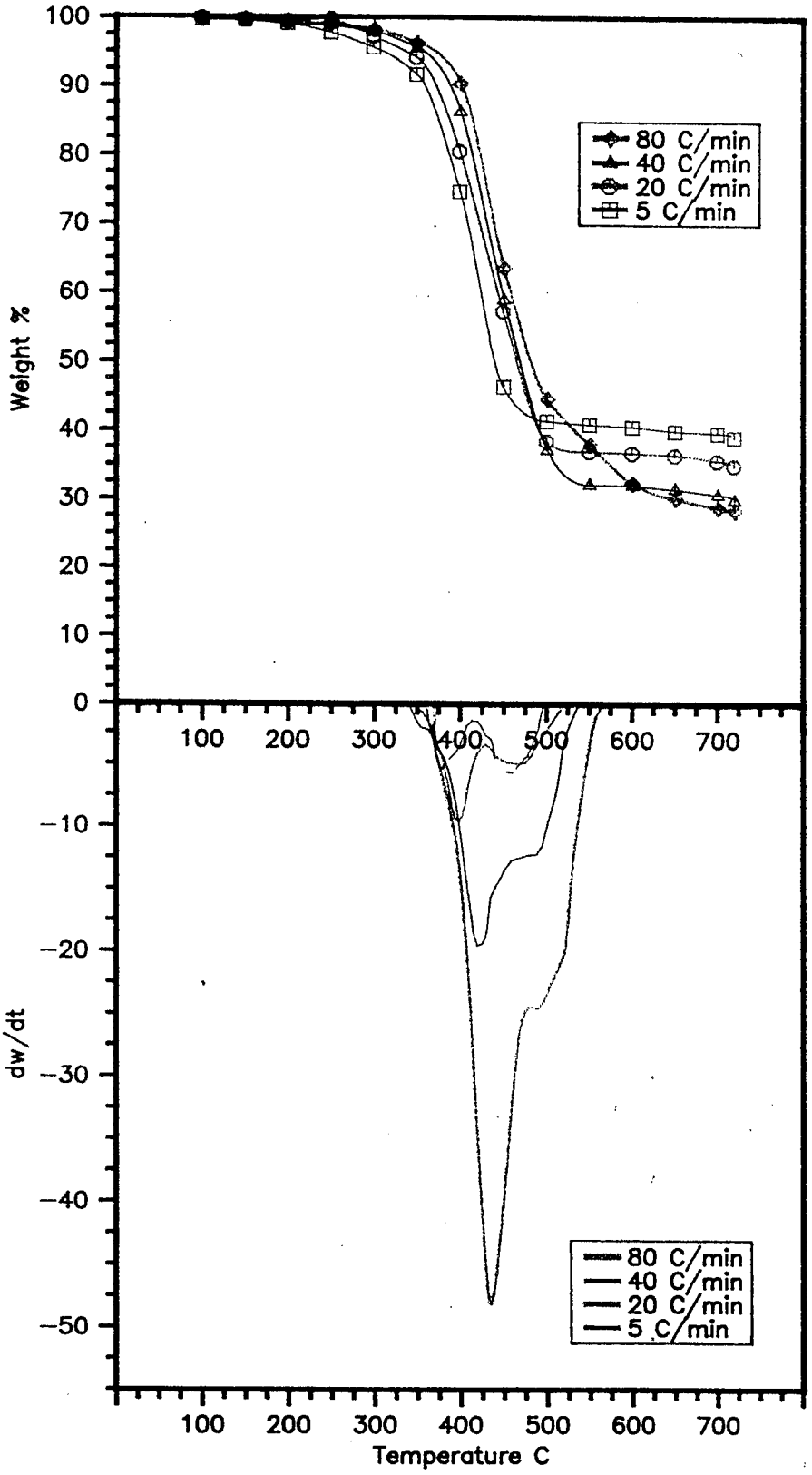

Fig. 1.31. Thermogravimetric analysis of some tyre samples.

1.6.3 Re-utilisation of Chars

The pyrolysis char derived from waste tyres has a high content of carbon and low content of ash and thus it is very suitable as:

- Carbon black to enrich low and medium rubber qualities.
- A colour pigment in printing ink, colour and plastic industry.
- Activated carbon for waste water purification (121).

Pyrolysis of scrap tyres gives a char yield in the range of 36%-38% of weight (122). Char production is reported by Cypres and Bettens (123) in the range of 35%-40% weight depending on the reaction conditions. Roy (124) found char yields of 34.8% employing vacuum pyrolysis.

Cypres and Bettens (123) studied the adsorption properties of various types of residual carbon obtained from tyre pyrolysis after they had been activated by steam and so converted into active carbon. They report that it is an excellent adsorbent and is well known on the market as a purification medium.

Roy (124) determined the physical properties of carbon black and he suggests that the re-cycled carbon blacks have numerous potential uses including reinforcement or semi-reinforcement for bicycle tyres, shoes, auto flaps, footwear, conveyor belts and dock fenders.

Kawakami et al (125) has outlined the process flow from crushing and pyrolysis of the scrap tyres to refining of char into carbon black. They report that the main products are char and oil

which amount to approximately one third and one half of the total products respectively. It is also suggested that the pyrolysis temperature has to be kept under 600°C in order to get the char from which high quality carbon black can be produced, although the rate of pyrolysis increases at higher temperatures.

Kawakami et al (125) also compared the properties of carbon black recovered with the commercial carbon black. It is found that the reinforcing properties of the recovered carbon black are higher than the commercial one.

1.6.4 Pyrolysis Oil From Scrap Tyre Pyrolysis

Pyrolysis oils of scrap tyres have been analysed by Cypres and Bettens (123). They identified the constituents reported in Table 1.14.

Table 1.14. Percentage weight of the constituents of the liquid phase

	wt %
Octane + lights	1.04
Benzene	36.41
Toluene	16.78
M + p-xylenes	4.83
Styrene	4.58
Indane	1.68
Indene	2.47
Naphthalene	9.15
2-Methylnaphthalene	2.42
1-Methylnaphthalene	4.06
Acenaphthene	4.35
Phenanthrene	3.19
Heavy fraction	7.68

Pakdel et al (126) identified the naphtha fraction of vacuum pyrolysis oils of scrap tyres. The benzene, toluene and xylene

content of this naphtha fractions are reported remarkably high (Table 1.15).

Table 1.15. Major compounds identified in Naphtha fractions (126).

Compound	(wt % in Naphtha) Hearth (1-VI)
Methylpentane	1.44
Dimethylpentane	1.04
Benzene	2.54
2,4.4-trimethyl-1-pentane	1.43
Dimethylcyclopentadiene	1.58
Toluene	6.95
Trimethylpentadiene	0.46
Ethylhexadiene	0.83
4-vinyl-1-cyclohexene	1.66
3-methyl-1,4-hexadene	0.41
p-xylene	2.78
m-xylene	2.43
o-xylene	0.91
Isopropylbenzene	0.97
Dipentene	14.92

They also identified limonene (dipentene) at 15% by weight in naphtha fraction.

Limonene has an extremely fast growing, wide industrial application. It is used in formulation of industrial solvents, resins and adhesives and as a dispersing agent for pigments. It is also used as feedstock for the production of various kinds of terpenoid alcohol fragrances, for example l-Carvon is synthesized from limonene and is used in the manufacture of synthetic spearmint flavouring in toothpastes and mouthwashes.

They conclude that the presence of large amounts of dipentene and other useful chemicals in the light fraction of the used tyre

vacuum pyrolysis oils positively influences the economics and feasibility of the thermaldecomposition process.

1.7 Polycyclic Aromatic Hydrocarbons

1.7.1 Introduction

The production of a liquid hydrocarbon product from biomass and waste by pyrolysis seems a better way than other thermaldecomposition methods. Although, the oils have high calorific value, similar to a medium heating oil and may be used directly as fuel or added to petroleum refinery feed stocks, the use of the oils derived from plastics, tyre and biomass as oils may be restricted since they have been reported to contain high concentrations of certain aromatic hydrocarbons (112, 206).

1.7.2 Sources of Polycyclic Aromatic Hydrocarbons

Polycyclic aromatic hydrocarbons (PAH) are released to the atmosphere from a variety of natural and anthropogenic activities (192). Anthropogenic outputs far outweigh those from natural means.

1.7.2.1 Natural (non-technological) Source of PAH

Uncontrolled combustion, such as that in forest fires and volcanic activity are the major sources of atmospheric PAH (233, 234). Although, the requirements for appreciable PAH formation can be met by these natural sources, the data on actual emission rates is lacking (233).

1.7.2.2 Anthropogenic Sources of PAH

Man-made PAH emissions can be broadly separated into transportational (mobile) sources and stationary sources. Mobile sources are both petrol and diesel engines which contributes to the overall PAH burden (233), while the stationary sources may be

conveniently divided into heating and power generating, refuse incineration and due to the industrial processes. Standardised PAH profiles for several of the above sources showing the many individual components present have been presented by Grimmer (235).

1.7.3 Distribution of PAH

Until the beginning of this century, a natural balance between the production and natural degradation of PAH is believed to have existed, which kept the background concentration low and fixed (236). However, with increasing industrial development throughout the world, the natural balance has been disturbed and the production and accumulation rates of PAH are constantly rising (236).

PAH in the atmosphere are always associated with aerosols arising from either natural sources (forest fire, volcanic and meteoric dusts) or man-made (incomplete combustion of fossil fuels leading to carbonaceous particles) sources.

Numerous studies have taken place to measure airborne PAH with respect to geographical location, point sources, seasonal variation and meteorological conditions (237, 238).

1.7.4. Toxicology and Metabolism of PAH

PAH have been linked with chemical carcinogenesis for over two centuries. In 1775, Sir Percival Pott observed that the high incidence of cancer in chimney sweeps was probably caused by some agent in coal soot (now known to be rich in PAH) (239). As a result of Pott's discovery, a number of biological studies of coal tar were carried out with little success. However, in 1918, Kamagiwa and Ichikawa (240) successfully induced tumours on rabbits ears by

repeated skin application of a coal extract. This marked the beginning of the search for the identification of the active carcinogenic substance in soot which culminated in the isolation of dibenz (a,h) anthracene by Kenneway (241) in 1930 and benzo(a)pyrene by Cook et al (242) in 1933. During the next quarter century, the major emphasis was on the synthesis of PAH compounds and assessment of their invivo carcinogenic potential in a variety of rodents and primates (243). Generally, PAH were found to act locally and induce tumour genesis at the site of administration of the compound. Although, the development of tumours could be initiated by a single administration of a carcinogen, repeated doses were generally considered to be more efficient. PAH can act as co-carcinogens. Hoffmann and Wynder (244) demonstrated this phenomenon by applying mixtures of carcinogen and non-carcinogen as a mixture, always increase the expect tumour incidence. Other organic compounds such as solvents and inorganic metals have also been indicated as co-factors in PAH carcinogenesis.

CHAPTER 2

EXPERIMENTAL TECHNIQUES

2.1 Introduction

The nature and composition of the waste materials used in this work were complex and variable, for example, municipal solid waste is highly variable by both season and location, scrap tyre which is a complex mixture of polymer, carbon black or mineral filler, curatives, plasticisers and other ingredients and agricultural and forestry residues which are a mixture of mainly cellulose, lignin and hemicellulose.

The experimental techniques may be described in terms of

(1) The pyrolysis apparatus

(2) The analytical techniques

1. Pyrolysis apparatus

In this research, fixed-bed and fluidised-bed pyrolysis reactors were used in order to investigate the influences of process conditions on the yields, compositions and fuel properties of the derived products.

In addition, pyrolytic oils derived from a commercial scale batch reactor for scrap tyre pyrolysis were examined to correlate data from this work with the commercial scale. Consequently, this apparatus will also be described. The apparatus was sited at Harwell, Oxfordshire.

2. Analytical Techniques

In this research, the following techniques were used:

- A thermogravimetric pyrolyser was employed at identical conditions to those of the fixed-bed reactor to determine the thermaldegradation pathways of the waste and biomass materials studied in this research.

- Fourier Transform Infrared Spectroscopy (FTIR) was used to identify the functional groups in the oil yields.

- Capillary Column Gas Chromatography and Gas chromatography Mass Spectroscopy (GS-MS): to characterise polycyclic aromatic hydrocarbons in the benzene fractions of oils.

- Packed Column Gas Chromatography was used to determine the compositions and yields of the gases produced throughout the pyrolysis.

- The surface areas of chars obtained from the experiments were determined by the nitrogen absorption method of Brunaer, Emmett and Teller (BET) (149), using a technique developed by Nelson and Eggertsen (150). The method was extended to examine the pore-size distributions of chars from scrap tyre pyrolysis.

- Calorific values and elemental analysis of the pyrolysis chars were compared. The condensed oils were analysed for their properties as potential fuels and compared.

2.2 Description of the Reactors

2.2.1 Fixed-Bed Reactor

The pyrolytic reactor consisted of a 200 cm^3 stainless steel fixed-bed reactor externally heated by an electric ring furnace. The different heating rates and maximum temperatures were supplied by the furnace and controlled automatically.

The control panel of the furnace had two temperature displays, one was for displaying of the main furnace temperature, the other was for the inside temperature of the main rig. During the experiments, the inside temperature of the rig and the furnace temperature were continuously recorded by means of thermocouples.

The liquid condenser consisted of a glass liner contained within a cold trap, maintained at 0°C and connected to the reactor outlet. The gases were sampled via a glass sampling tube placed down stream of the condenser. Sampling syringes were used to obtain gas samples via a rubber septum from the sampling tube.

A bubbler was placed after the gas sampling tube to check the flow before releasing the off gases to the atmosphere. Nitrogen was used as the carrier gas at a fixed metered flow rate for all experiments. The nitrogen carrier gas reduced the extent of secondary reactions such as thermal cracking, i.e. polymerisation and recondensation.

Figure 2.1. Shows the schematic diagram of the fixed-bed apparatus.

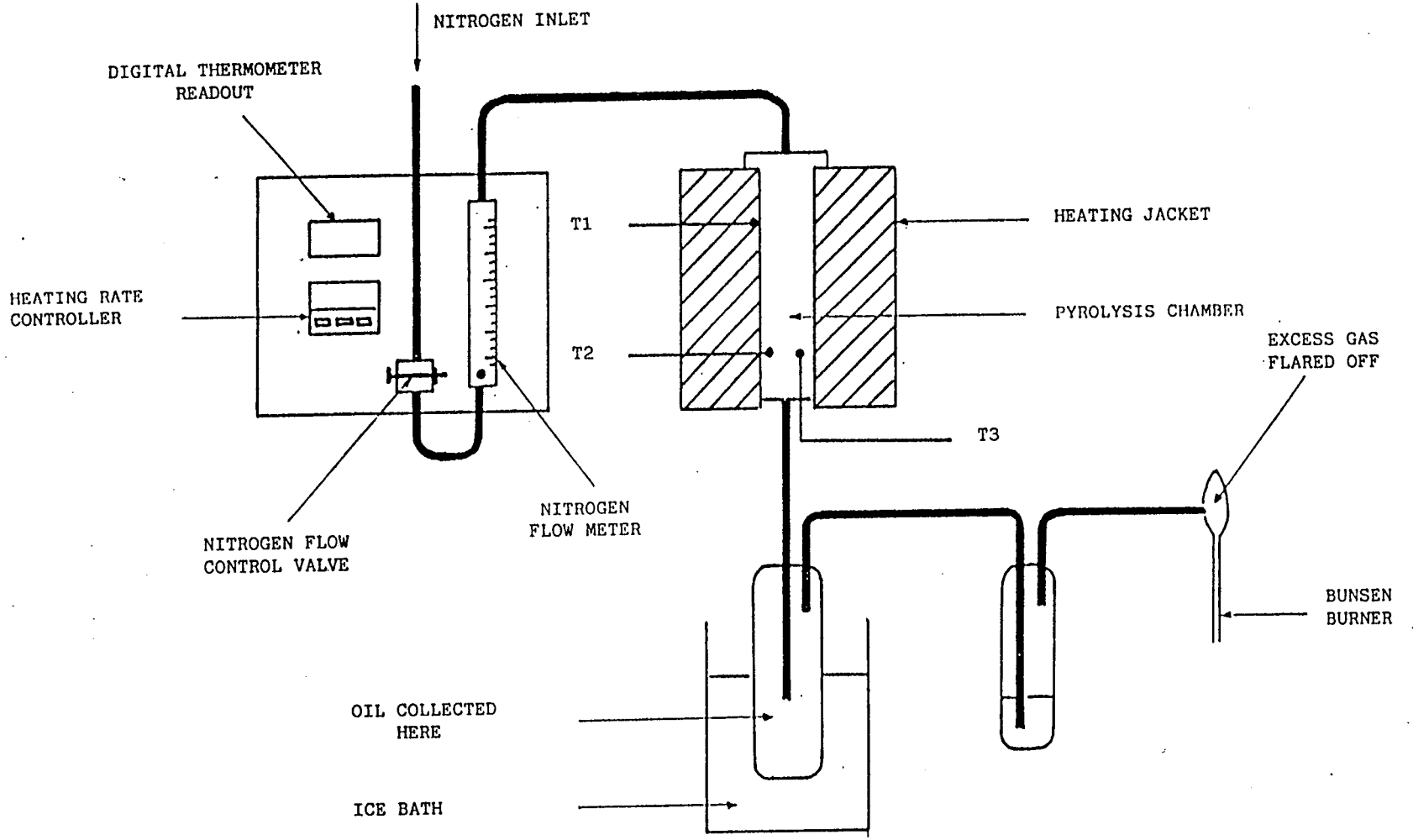

Fig.2.1 The schematic diagram of the fixed-bed pyrolyser.

2.2.1.1 Experimental Procedure

Two different experimental methods were carried out throughout the pyrolysis experiments with fixed-bed reactors for all samples.

After placing the samples in the reactor, they were heated to 150°C at 10 min^{-1} heating rate and held at that temperature for 1 hour to make sure that the samples were dry (Fig. 2a).

The temperature was then raised at either heating rates of 5, 20, 40 or 80 C min^{-1} to a final temperature of 300, 420, 600 and 720°C and held at that temperature for a minimum of 2 hours or until no further significant release of gas was observed.

In separate experiments, samples were heated up to 720°C at 5, 20, 40 and 80 C min^{-1} and held at 720°C for 2 hours as before, however, these separate experiments allowed the sampling of the oil throughout the pyrolysis experiment. The oil yields were collected at each interval of temperatures 300, 420 and 600°C as the pyrolysis heating was carried out (Fig.2.2b).

The liquid phase was trapped in a glass liner inside a cold trap and the samples of the liquid phase were collected throughout each experiment and consisted of an aqueous phase and oil phase which were separated by centrifuge, removed by pipette, weighed separately and stored in a refrigerator under nitrogen before analysis.

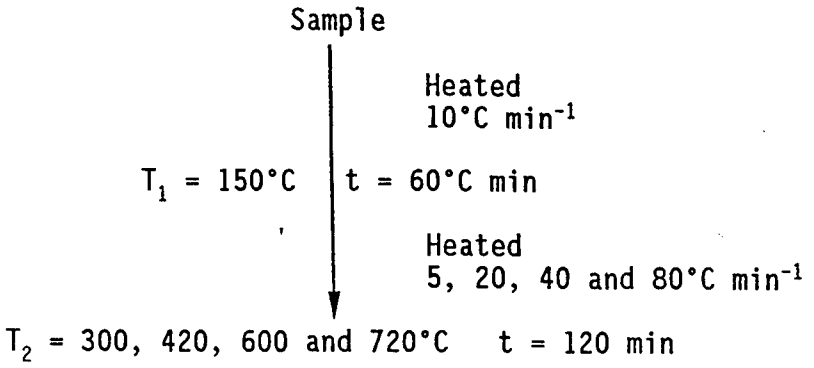

(A)

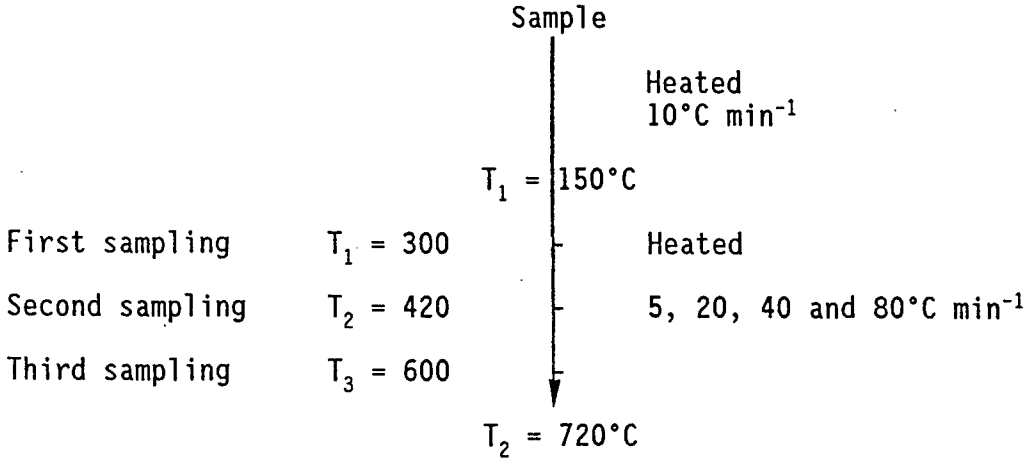

(B)

Fig. 2.2. Experimental procedures carried out with the fixed-bed reactor.

2.2.2 Fluidised-Bed Reactor

The fluidised-bed pyrolysis reactor has been designed and constructed by the author in order to investigate the fast pyrolysis of waste materials while they are fed from room temperature to high temperatures.

The considerations for the use of fluidised-beds for pyrolysis of waste and biomass include better heat transfer, the easiness of

changing the residence time with the changing of fluidisation velocity and changing free board height with changing bed depth.

The fluidised-bed reactor consists of three main parts which are

- The main reactor body including bed and free board
- The external parts of main body which are the hopper feeder, cyclone and set of condensers
- The heating system and control unit.

A schematic diagram of the system is shown in Fig. 2.3.

2.2.2.1 Main Reactor Body

The main body was constructed of stainless steel with a total height of 700 mm. The bed and free board consisted of a 100 mm diameter tube with a 200 mm expander section at the top of the free board to reduce gas velocity and minimise elutriation of bed material. Thermocouples were placed throughout the bed and free board sections to monitor temperature (Fig. 2.4).

The distribution plates were made of stainless steel (Fig. 2.5a). Each of them has 100 holes with 0.1 cm diameter in order to supply proper fluidisation for the bed. Two separate sections which were 100 mm ID x 80 mm long were connected to the bottom side of the rig.

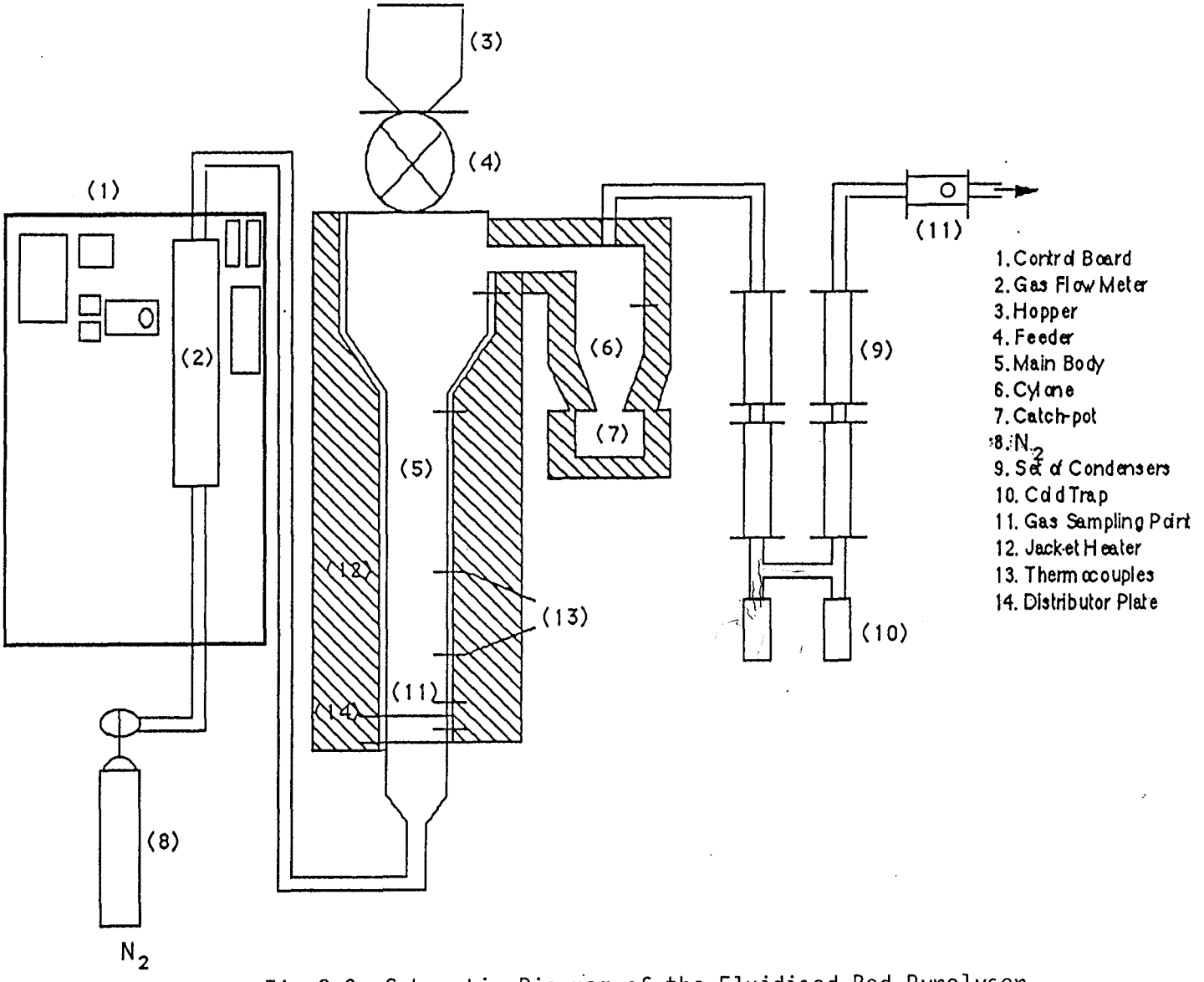

Fig.2.3 Schematic Diagram of the Fluidised-Bed Pyrolyser

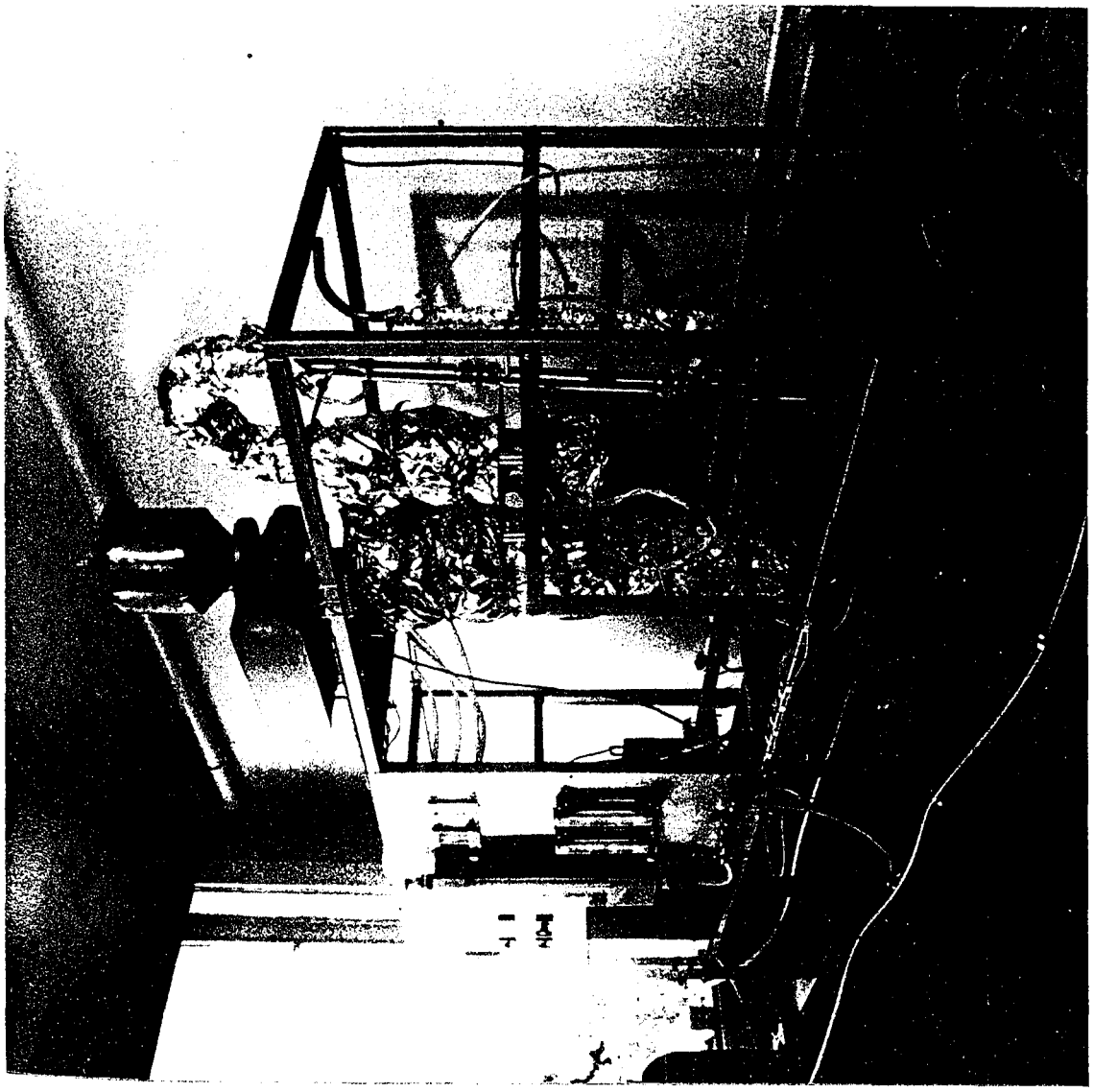

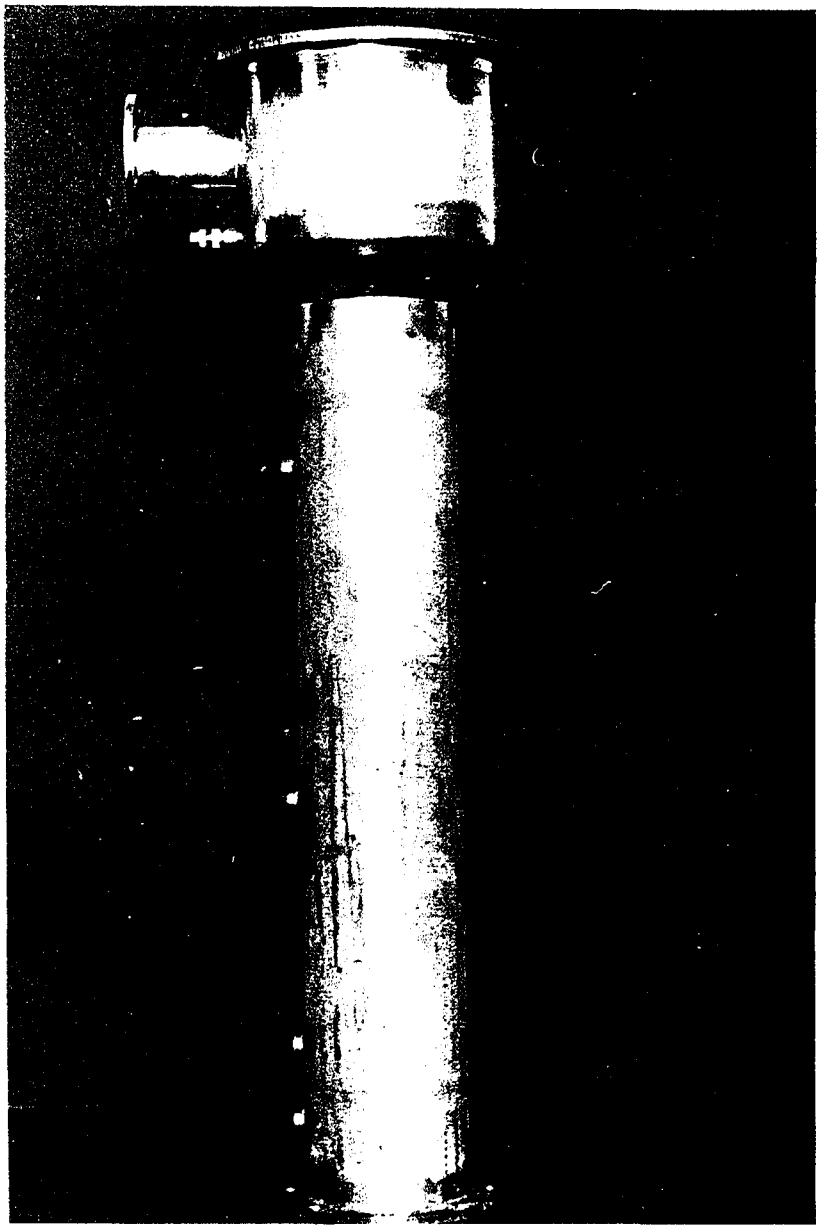

Fig. 2.4. The main reactor body

The lower section was for pre-heating of fluidisation gas to prevent the temperature drop in the rig caused by the nitrogen fluidising gas coming from a gas cylinder at room temperature. This section was filled with copper rings in order to increase surface area between hot copper rings and gas (Fig. 2.5b).

The upper section was designed for future experiments with steam. It has a thermocouple to measure the temperature of pre-heated gas just before entering the main part of the reactor (Fig. 2.5c).

Sand was employed (300 mesh) as the bed material in order to carry the heat from the reactor walls to the sample to be pyrolysed. A 10 cm of bed height was chosen during the design work.

Nitrogen was used as a fluidisation gas at the minimum fluidisation rate of 20 lt min^{-1} at all experiments. It also helped to sweep the volatiles produced during the experiments from the reaction zone to the condensers through the cyclone.

2.2.2.2 External Parts

2.2.2.2.1 Hopper

The hopper constructed of stainless steel with 5800 cm^3 volume, was placed at the top of the reactor. Before the experimentations it was filled up with the material to be pyrolysed. The hopper's temperature was also monitored in case of overheating. The hopper was continuously purged with nitrogen to prevent air contamination (Fig. 2.6a).

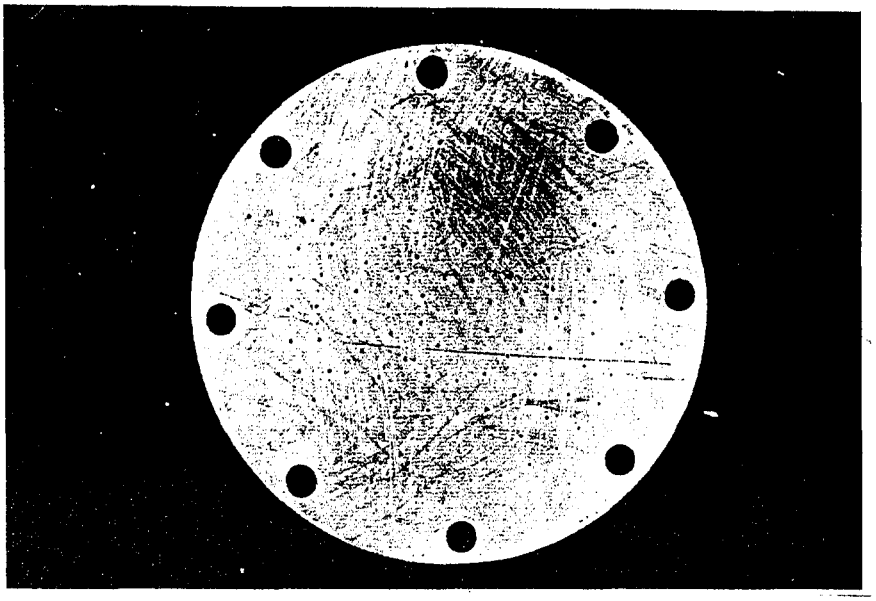

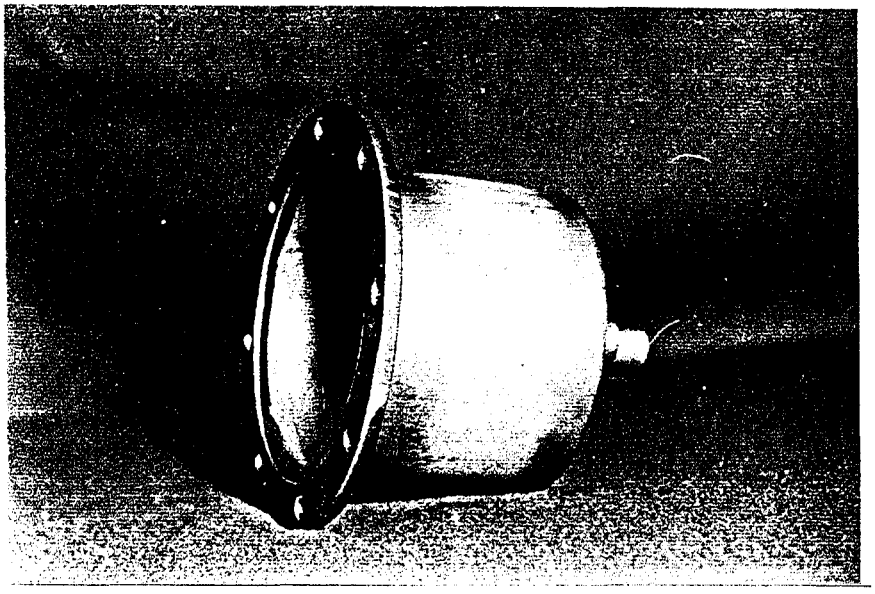

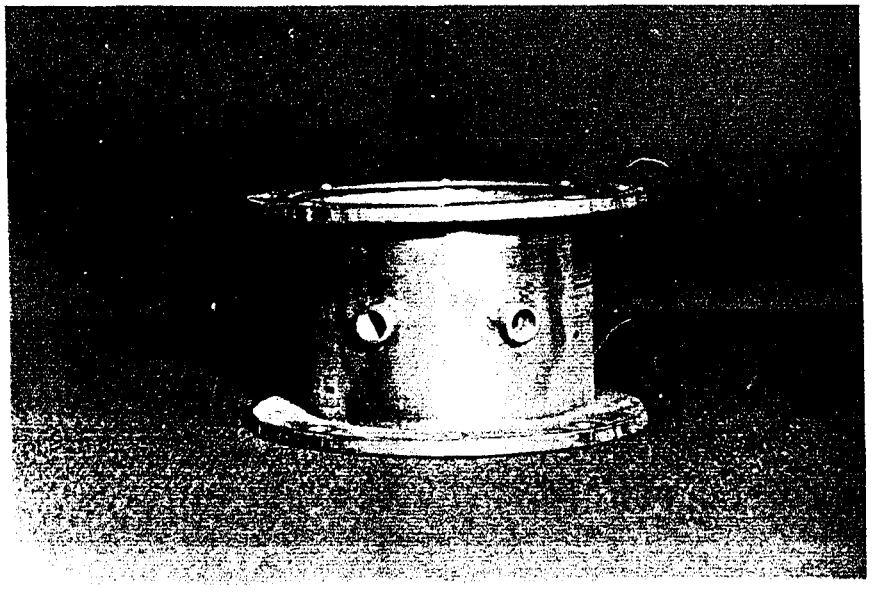

Fig. 2.5 (a) The distribution plate

(b) Pre-gas heating port (c) Steam production port

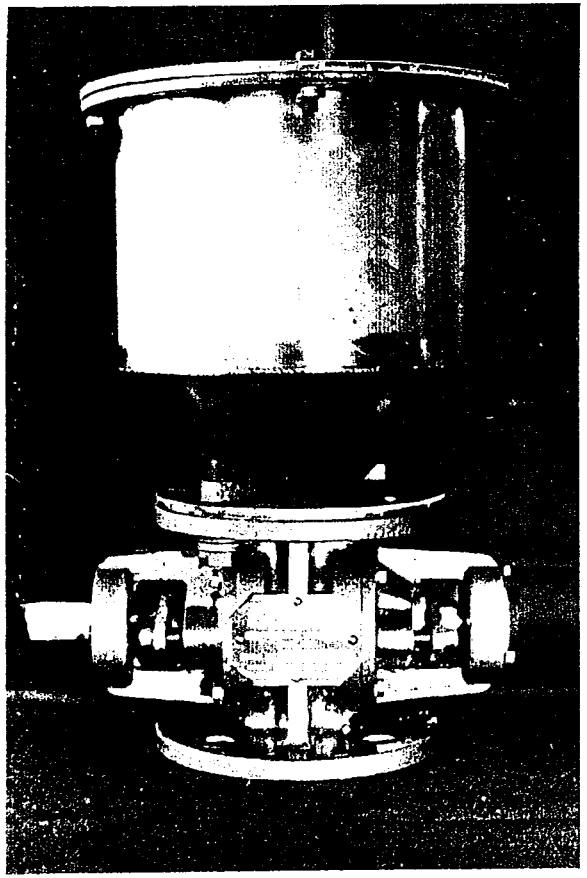

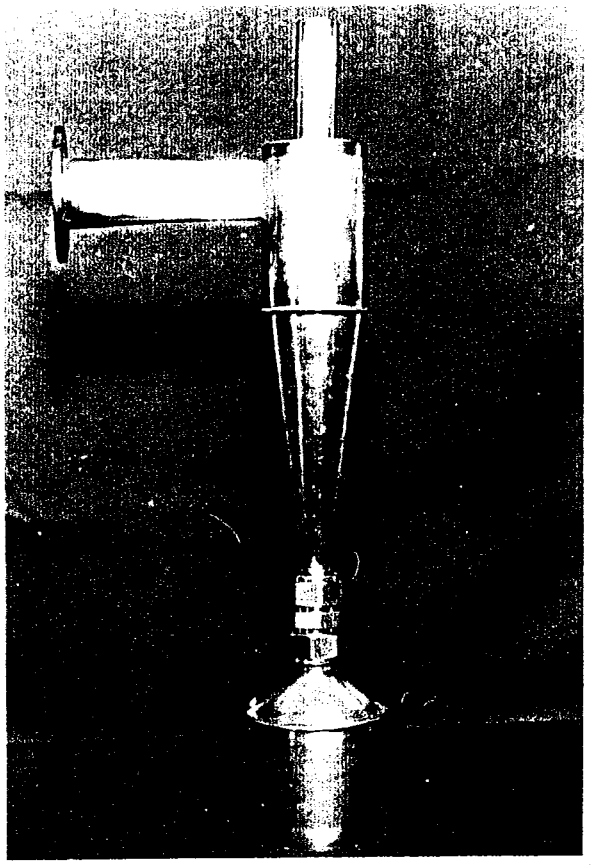

Fig. 2.6 (a) Hopper and feeder (b) Cyclone (c) Condenser section

2.2.2.2.2 Feeder

The automatically controlled feeder was placed between the hopper and the main rig. A nitrogen purge was used between hopper and feeder in order to keep samples in an inert atmosphere just before feeding them into the rig and prevent leakage of pyrolysis gases to the hopper. There were also two pressure check valves for the purpose of safety to prevent any explosion caused by over-pressurising (Fig. 2.6a).

2.2.2.2.3 Cyclone

The cyclone was made of stainless steel consisting of the separation section and catch pot. It was connected to the main rig in order to separate char and elutriated bed material from volatiles. The char particulates travelling with volatiles were captured in the separation section and collected in the catch pot. The separating section and catch pot were externally heated to prevent condensing of volatiles. The temperature of cyclone and catch pot was kept at 150-200°C to prevent secondary reactions also condensing of volatiles before reaching to the condensers.

There were two thermocouples attached to the separation section and catch pot to control the temperature throughout the experiments (Fig. 2.6b).

2.2.2.2.4 Set of Condensers

During the design work, condensers were designed as two stainless steel tubes 1 inch ID x 22 cm long, wrapped with copper cooling coils carrying cold water. After starting the initial test runs, it was seen that they were not efficient to condense all the

volatiles properly. Two more condensing parts were later added to improve the efficiency.

The latter ones were designed 30 cm long x $1\frac{1}{4}$ inch ID stainless steel tube having cooling coils also inside of the tube in order to increase the surface area between hot gas and cooling coils. Even with the re-designed condensers 100% condensing efficiency was not obtained.

At the end of each condenser set there was a cold trap connected to the condenser outlet. The pyrolysis oils were collected in a glass liner contained in the trap immersed in a solid CO_2 bath. At the end of each run, all parts of the condenser set were removed and rinsed out with acetone in order to prevent contamination between different samples (Fig. 2.6c).

2.2.2.2.5 Gas Sampling Tube

After the condensing section, non-condensible gases were sampled using sampling syringes at chosen intervals. The gas sampling section consisted of a glass gas sampling tube sealed with a rubber septum seal immediately after gas sampling off gases were sent to atmosphere via a fume cupboard in the laboratory.

2.2.2.3 Heating System and Control Unit

The heating of the main rig and cyclone were supplied by electrothermal flexible ceramic mat heaters. For the main rig furnace, the temperature was controlled by a variac Cyclone heater, catch pot heated and pre-gas heater had separate controls for the purpose of safety. For each control there was a display on the control board. Also, all thermocouples (K type chrome alumel)

attached to different parts of the rig had temperature displayed on the control board.

2.2.2.4 Experimental Procedures

The experimental procedure below was followed for each separate experimental run.

- The hopper was filled with the material to be pyrolysed.
- The sand-bed was fluidised with the fluidisation gas stream.
- Temperatures desired for the main rig, pre-gas heater, cyclone and cyclone catch pot were set.
- After reaching the desired temperatures, the material to be pyrolysed was fed to the reactor through the feeder.
- Gas sampling was carried out at chosen intervals.
- After each run, when the reactor had cooled down, the char in the catch pot and liquid collected in the glass liner were removed.
- Gas samples were determined using gas chromatography.
- The condensed liquid was centrifuged in order to separate the aqueous part from the oil and were stored in the fridge.

- Char samples were weighed and stored in the laboratory for further tests.

2.2.3 Commercial Scale Pyrolysis

The commercial scale pyrolyser was sited at Harwell, Oxfordshire and was used to pyrolyse up to 2 tonnes a day of scrap tyres. The units are manufactured by AEA-BEVEN (Atomic Energy Authority and a private company H. Beven Ltd.). The unit is described as a multipurpose disposer (Fig. 2.7).

The multipurpose disposer is the application of pyrolysis of waste on an industrial scale. The system safely recycles wastes in a sealed system and can produce useful and valuable by products from its operation.

The advantages of the equipment can be listed as:

- It does not cause any pollution - odourless and smokeless.
- Negligible fuel costs.
- Easy to operate.
- Easy maintenance.
- Feedstocks do not have to be processed before being placed into the reactor.

The principal items of the AEA-BEVEN 7P2000 tyre recycler are shown in Fig. 2.8. They include the following.

2 Oil Burners

2 Gas Burners

1 Furnace and Stack

1 Outer Retort

2 Inner Retorts

1 Pre-Condenser

1 Shell and tube heat exchanger

1 Post-Condenser

1 Scrubber

1 Flare Stack

1 Control Pane.

The pyrolysis unit has an inner kiln with the capacity of 4.3 m^3. It is loaded with the whole tyres and the capacity is approximately one tonne of tyre per 12 hours batch run.

The inner kiln loaded with tyre is placed into an outer one which consists of a ceramic lined vessel fitted with a gas tight lid. The system is purged with nitrogen to eliminate any oxygen. The inner kiln is heated initially by natural gas, is replaced by the gas derived from the tyre pyrolysis. The evolved pyrolysis vapours and gases pass through a heat exchanger to condense the vapours. The non-condensed gases then pass to a scrubbing unit to clean the gases, before passing to the burner or to storage. The oil from the condensing tank is pumped to storage or can also be used to provide auxiliary fuel for the burners.

The pyrolyser is operated in automatic mode and requires little operator involvement in the running of the plant when processing tyres. The system can also be operated in manual mode if required.

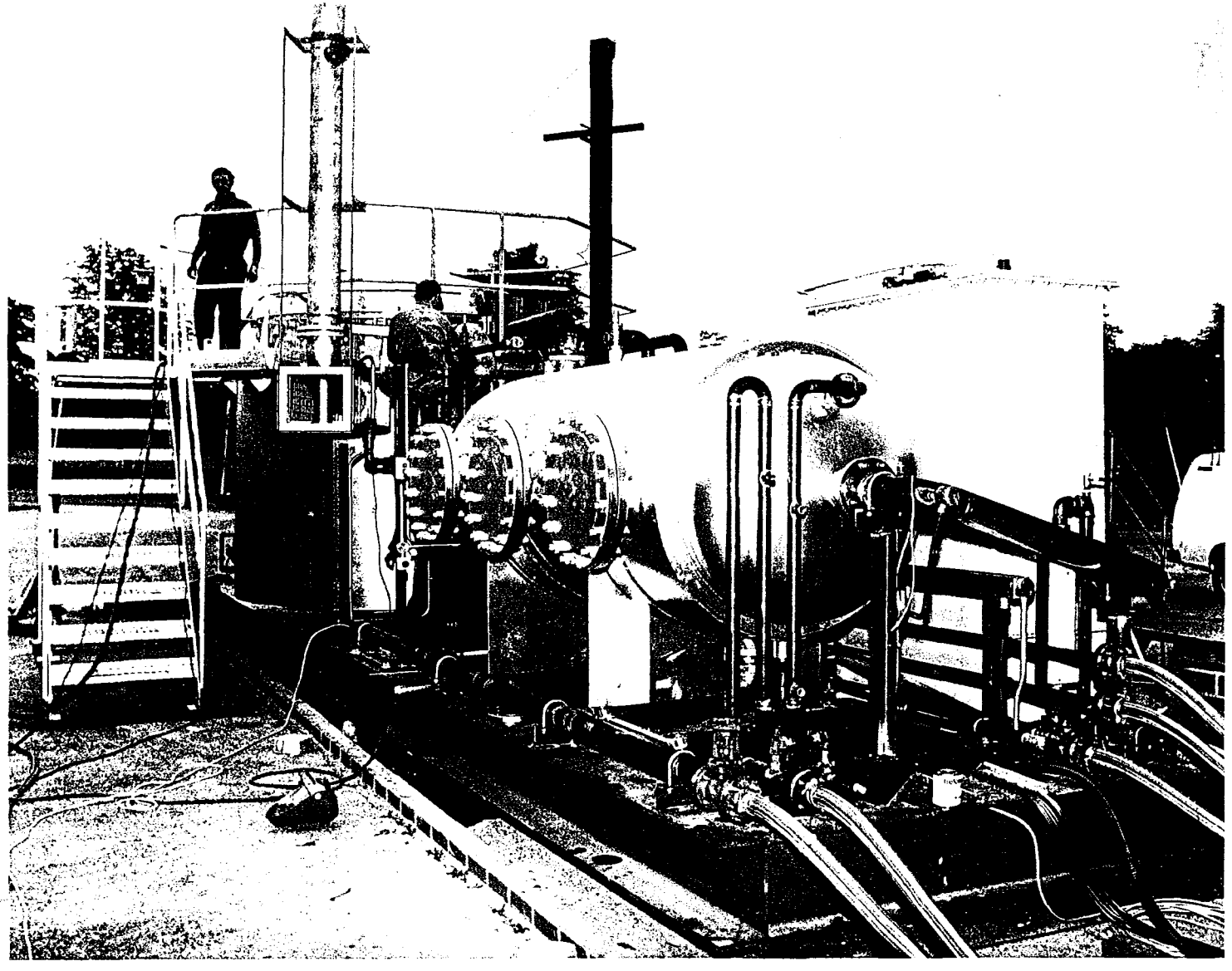

TP2000 Tyre Recycler

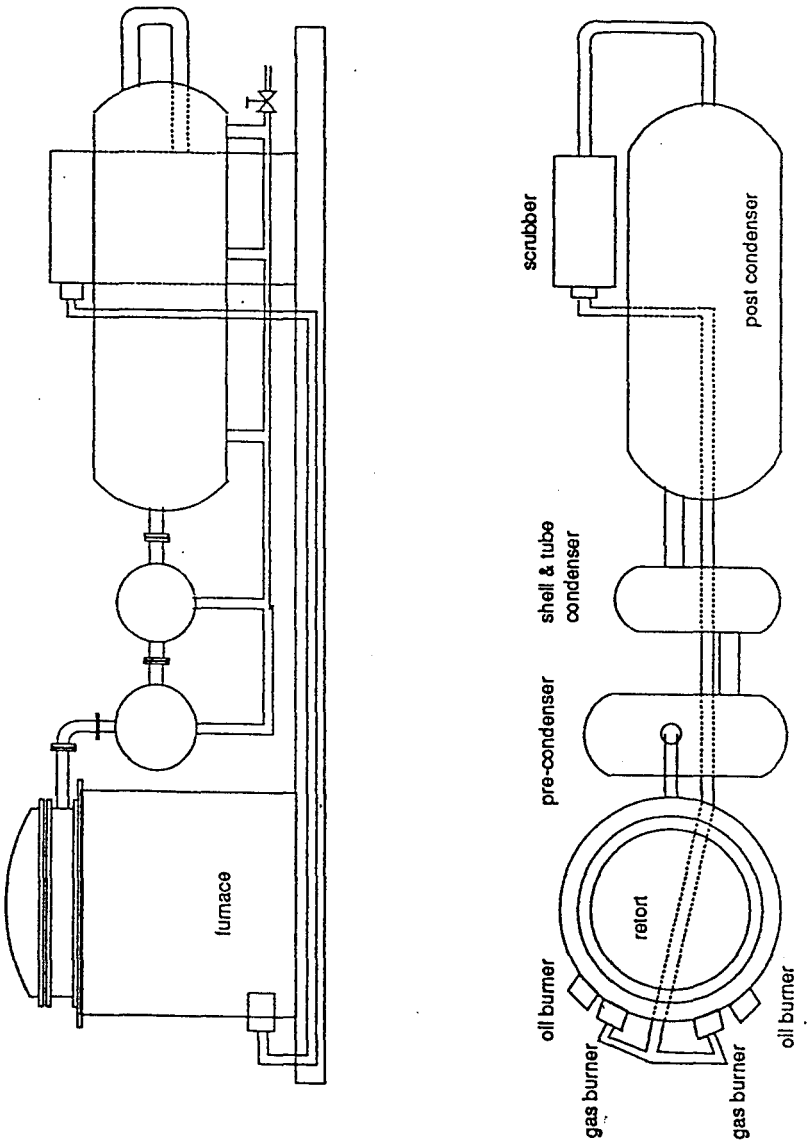

Fig. 2.8 TP2000 Tyre Recycler

2.3 Descriptions of the Sample Preparations

In this research, four different samples which are wood and rice husks as biomass, refuse derived fuel (mainly cellulosics and plastics) and scrap tyres (complex polymers) were pyrolysed in different reactors in order to investigate the influences of the reactor types on the thermal decomposition characteristics of the wastes and yields produced.

The pyrolysis of biomass and waste materials namely, wood, rice husks, RDF and scrap tyre were carried out in both the fixed-bed and fluidised-bed reactor. But for the commercial scale pyrolysis unit, only tyre samples were employed.

Since the technical characteristics of both the fixed-bed and the fluidised-bed reactors were different, the sample preparation differed, although the main aim of using both reactors was the same, to pyrolyse waste and biomass materials.

Consequently, for each sample the preparation is described depending on pyrolysis reactor.

2.3.1 Sample Preparation For Fixed-Bed Reactor

2.3.1.1 Wood

Wood samples were obtained from the University of Leeds joinery workshop. The pine wood sticks were cut into 1 x 1 x 1 cm cubes and stored in the laboratory under dry conditions. Wood chips were sieved and 1 cm long thin ones were separated for the investigation of the effects of particle size on the yields. 25 g of wood cubes/chips were pyrolysed during each pyrolysis experiment.

2.3.1.2 Rice Husks

The rice husks, obtained from Nigeria, were sieved to less than 1 mm and stored in the laboratory under dry conditions. 20 g of rice husks were pyrolysed for each run.

2.3.1.3 R.D.F.

The refuse derived fuel samples used throughout this research were obtained from the Byker RDF plant, U.K. The samples were in the form of refuse derived fuel pellets. The pellets were shredded from an initial size of 16 mm diameter by up to 100 mm length to produce sample size of approximately 2 mm to 5 mm to minimise heat transfer problems during pyrolysis.

The use of RDF as opposed to unsorted and unshredded municipal solid waste reduces considerably the problems of inhomogenity of the waste material. After shredding, the pieces of RDF were stored in the laboratory and 10 g of samples were pyrolysed for each run.

2.3.1.4 Scrap Tyre

The automotive scrap tyres used represented a mixture of light and heavy duty tyres and were shredded including the metal core to 2-5 cm^2 pieces. The tyre pieces were stored in the laboratory under dry conditions. The weight of the tyre pieces was 25 g for each separate run.

2.3.2 Sample Preparation For Fluidised-Bed Reactor

2.3.2.1 Wood

The wood chips obtained from the joinery workshop were sieved between 0.1 - 0.3 cm and kept in a dry place in the laboratory. When the initial test runs were started, it was seen that the wood samples were not heavy enough to drop through the feeders blades from the hopper. In order to give them enough weight, wood samples were mixed up with sand which was fluidised-bed material and its amount was not enough to cause any temperature drop throughout the free board and bed. 75 g of sample was employed for each run of pyrolysis with the fluidised-bed.

2.3.2.2 Rice Husks

The Nigerian rice husks were sieved to < 0.4 cm and kept in the laboratory under dry conditions. Sample feeding problems with wood chips were observed during the initial test runs and rice husk samples were also mixed up with sand. 75 g of sample was employed for each single run.

2.3.2.3 R.D.F.

The refuse derived fuel samples were chopped into 1-2 cm small pieces. During the initial tests, feeding was not successful, in fact some more blocking problems appeared because of the plastic content of the RDF. The samples stayed between the feeders blades and caused severe blockages.

There was no equipment available for the author to chop them into 1-2 mm size. A coffee grinder was tested to grind them, but the

sample obtained from the coffee grinder was dust like and there again were blockage and feeding problems. Finally, the RDF pellets were kept in a flask filled with liquid nitrogen for half an hour and then the samples were smashed and ground with a hammer. The size of 1-2 mm RDF samples were fed successfully. 50 g of sample was pyrolysed for each single run.

2.3.2.4 Scrap Tyre

The scrap tyre pieces (1-2 cm size), caused feeding problems similar to RDF. It was extremely difficult to chop them into 1-2 mm pieces by use of a hand cutter.

The cryogenic method applied to RDF was also very efficient for chopping the scrap tyre samples into desired samples. The tyre pieces (2-5 cm^2) were kept in liquid nitrogen and there after they were smashed by hammer. The steel cords were removed and 50 g of samples were introduced to the pyrolysing system for each run.

2.3.3 Sample Preparation For Commercial Scale Reactor

The commercial scale pyrolysis unit did not require any certain size of sample in fact, it was one of its features that scrap tyres could be pyrolysed without any pre-treatment. Consequently, employing whole tyres for pyrolysis did not incur any shredding cost.

It is also confirmed by Roy et al (119) after examining the scrap tyre pyrolysis plants that the most successful recycling process is the one that uses whole tyres as feedstock. Shredding tyres is expensive and results in materials that are difficult to handle inside the reactor, eventually giving rise to the so called ball milling problem.

2.3.4 Sample Preparation For TGA

The thermogravimetric analyser was employed to determine the thermaldecomposition characteristics of biomass and waste materials (to be discussed later). The experiments were carried out under the identical conditions to that of the fixed-bed reactor. Besides main samples, which were wood, rice husks RDF and scrap tyre, components of these wastes were also examined.

2.3.4.1 Wood

Wood samples were chopped into small pieces, to less than 0.5 cm and stored in the laboratory under dry conditions. The sample amount studied for each run was between 15-19 mg. The main components of wood, cellulose, hemicellulose and lignin were also studied.

2.3.4.1.1 Lignin

Lignin was extracted from wood using the standard test method (ASTM D 1106-84) (151) for acid-insoluble lignin as follows: 1 g of sample is extracted with 95% alcohol in a soxhlet-extraction apparatus for four hours. Then the specimen is extracted with alcohol-benzene solution (mixed 1 volume of ethyl alcohol and 2 volumes of pure benzene). The specimen is transferred to a beaker and digested with 400 ml of hot water. After filtering, the specimen is left to dry in the air. The air-dried test specimen is transferred to a glass-stoppered bottle and 15 ml of cold H_2SO_4 is added. The specimen is mixed with the acid by stirring constantly and then is washed into a 1 l flask. The acid solution concentration is made up to 3% and with the specimen is boiled for 4 hours under a

flux. The specimen is finally washed with water and allowed to dry in an oven for 2 hours at 100°C.

2.3.4.1.2 Hemicellulose

The hemicellulose in the form of xylan was obtained commercially and used without any pre-treatment.

2.3.4.1.3 Cellulose

The microcrystalline cellulose was obtained commercially and used without any pre-treatment. Also, cellulose in fibrous form as ashless Whatman filter paper No. 1 was studied.

2.3.4.2 Rice Husk

The rice husks were sieved to less than 1 mm and stored in the laboratory under dry conditions. For the investigation of the thermaldegradation the components of rice husks, besides microcrystalline cellulose and hemicellulose, lignin was also extracted from rice husk (same method as with wood lignin) and were examined using the thermogravimetric analyser.

2.3.4.3 Model Saccharides

Model carbohydrates were also examined in order to understand thermaldegradation of biomass components. The monosaccharides, hexose (glucose) and pentose (xylose), disaccharide (maltose), trisaccharide (melezitose) and tetrasaccharide (stachyose) were obtained commercially and separately pyrolysed in the thermogravimetric analyser.

2.3.4.4 R.D.F.

The RDF sample was prepared from several pellets, which were shredded further and mixed to obtain a sample, several determinations of the thermogravimetric analysis were carried out. Between 15-20 mg of sample was pyrolysed in the thermogravimetric analyser at the 5, 20, 40 and 80 C min^{-1} heating rates up to 720°C.

2.3.4.4.1 R.D.F. Components

The components of municipal solid waste which were PVC cardboard, waxed cardboard, cotton, polyethylene, newsprint, fast food pack and carpet were collected as separate waste and pyrolysed in the thermogravimetric pyrolyser at the identical experimental conditions to that of RDF in order to understand the thermaldecomposition of RDF.

2.3.4.5 Scrap Tyre

The scrap tyre samples were ground into small pieces less than 0.3 cm. Before thermal analysis, textile and steel cords were finely separated from the rubber parts to investigate the thermaldecomposition of scrap tyres accurately. The samples were kept in a laboratory under dry conditions. Thermaldecomposition experimental conditions were identical to those of the fixed-bed pyrolysis experiments.

2.3.4.5.1 Scrap Tyre Components

The components of scrap tyre which are SBR, NR and BR were obtained from tyre manufacturers were pyrolysed and also three different tyre samples of known composition consisting of SBR, NR, BR

and other additives in different percentages were obtained from manufacturers and pyrolysed in the thermogravimetric pyrolyser to compare with scrap tyre whose composition was unknown.

2.4 Analytical Techniques

2.4.1 Gas Chromatography

The gas samples taken during the experimental runs were analysed by off line gas chromatography.

Gas chromatography is a method of separating and analysing mixtures of gases or volatile compounds. The sample is injected into a moving inert carrier gas which passes through a heated column packed with a granular solid of large surface area. A sample gas moves through the column at a rate dependent on its adsorption coefficient, on the nature of the packing material and on the carrier gas velocity. Consequently, mixtures of gases are separated out and then concentration can be measured. With a suitable column and detector, several gases can be determined in a single run. Two detecting systems were used depending on the gas to be measured. The flame ionisation for hydrocarbons and thermal conductivity for H_2, CO, CO_2 and O_2 were employed.

2.4.1.1 Flame Ionisation

In a flame ionisation gas detector, the sample is burned in a small H_2 flame, H_2 being the carrier gas. Upon combustion of the sample, additional charged species are formed in the flame and are collected by an electrode. The signal from the electrode is in proportion to the concentration of gas being measured. This method

is very sensitive and has a large linear dynamic range, but cannot detect CO_2, CO, H_2O O_2 and H_2. An n-octane porasil-C column was used.

2.4.1.2 Thermal Conductivity

Two columns, silica gel to determine CO_2 and a molecular sieve to determine N_2, O_2 and CO were used.

The analytical filament is heated by an electric current and positioned at the end of the column. The carrier gas is Helium which has a very large thermal conductivity. The gases with a smaller thermal conductivity pass the thermistor, the temperature increases as heat is conducted away less rapidly. The change in resistance of the filament is then measured and is in proportion to the concentration of the species being measured. This method is sensitive to all compounds except the carrier gas, it is non-destructive and has a large linear dynamic range, but it is not as accurate as flame ionisation.

2.4.2 Thermogravimetric Analysis

Thermogravimetric analysis experiments were carried out using a Stanton Redcroft 280 Series thermogravimetric analyser, with samples weighing between 15-20 mg. The temperature profile of the sample placed in a small platinum crucible is monitored by a thermocouple which also supports the crucible.

The weight loss of the sample as a percentage of initial weight and temperature was recorded as a function of time at heating rates of 5, 20, 40 and 80 C min^{-1} up to 720°C, which also was the maximum temperature of the pyrolysis experiments in fixed-bed rigs.

Experiments were carried out in a nitrogen atmosphere at constant flow rate. After reaching maximum temperature in the nitrogen atmosphere and observing no more weight loss of the sample, the nitrogen flow was changed into air to burn the sample out and to observe the percentage of combustible materials in the sample.

Fig. 2.9 shows a typical thermogram and the schematic of thermal analysis system is shown in Fig. 2.10.

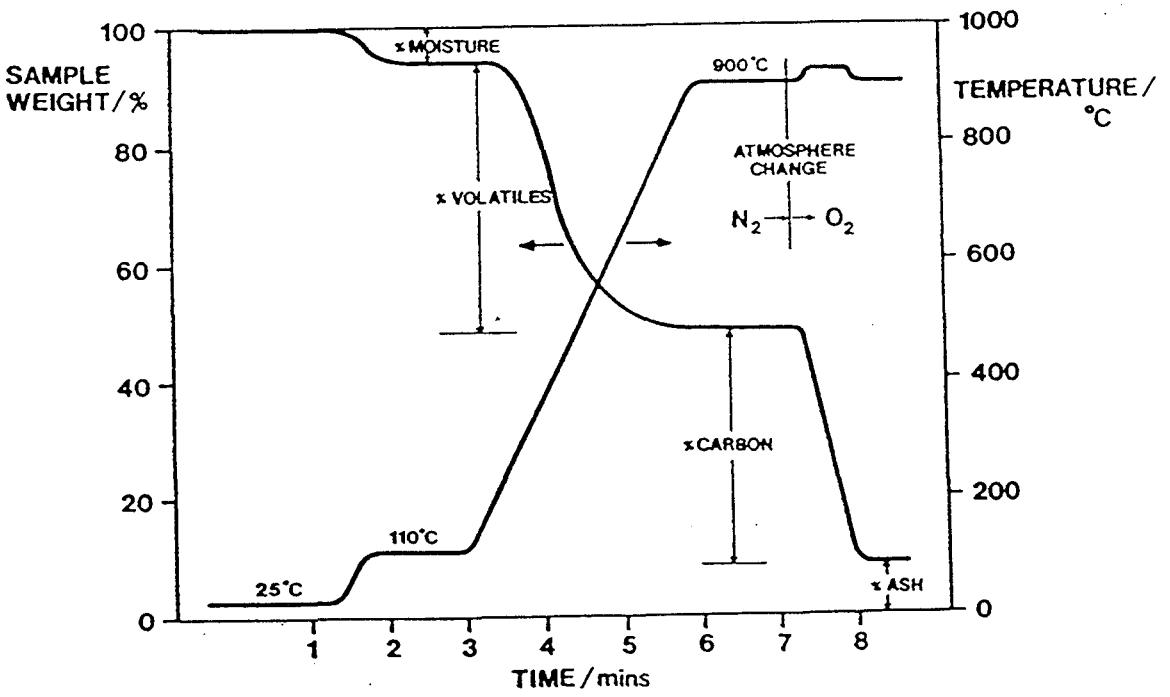

Fig. 2.9 Typical thermogram obtained.

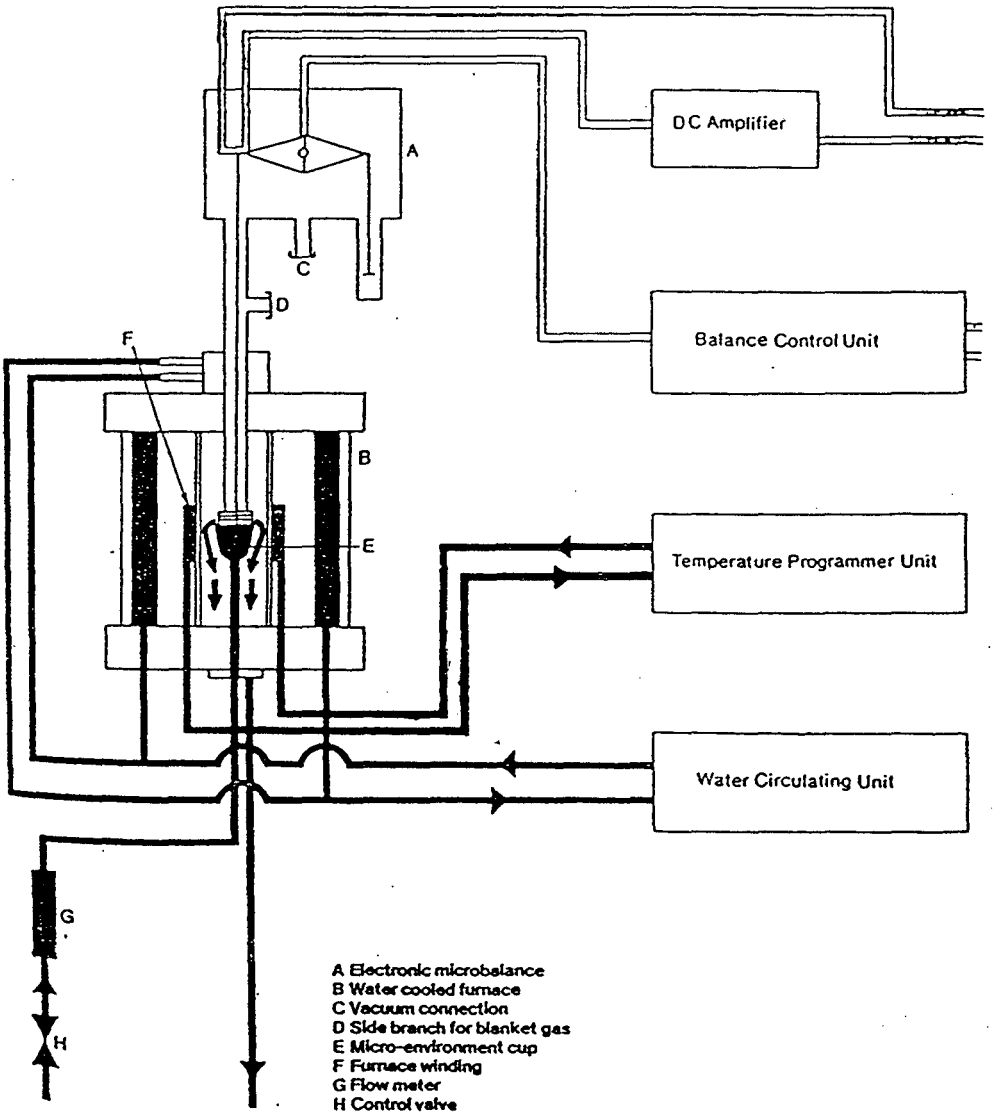

Fig. 2.10 Schematic of thermal analysis system.

2.4.3 Determination of Fuel Properties

The pyrolytic oils obtained from commercial scale pyrolysis plant were analysed for their fuel properties according to Standard Institute of Petroleum (IP) or American Society for Testing and Materials (ASTM) tests. The analyses carried out were: (152)

- Carbon residue (IP14, ASTM D524)
- Relative density and API gravity (IP160, ASTM D1298)
- Viscosity (IP71, ASTM D445)
- Flash point (IP34, ASTM D93)
- Cetane index (IP218 ASTM D976)
- Calorific value and sulphur content (IP12)
- Distillation range (IP123, ASTM 86).

2.4.3.1 Carbon Residue (IP14, ASTM D524)

This method covers the procedure for determining the amount of carbon residue left after evaporation and pyrolysis of an oil and is intended to provide some indication of relative coke forming propensity. The method is generally applicable to relatively non-volatile petroleum products which partially decompose on distillation at atmospheric pressure.

The sample, after being weighed into a special glass bulb having a capillary opening, is placed in a furnace at 550°C. The sample is quickly heated to the point at which all volatile matter is

evaporated out of the bulb with or without decomposition, while the heavier residue remaining in the bulb undergoes cracking and coking reactions. After a specified heating period, the bulb is removed and cooled in a desiccator and again weighed. The residue remaining is calculated as a percentage of the original sample and reported as the Ramsbottom carbon residue.

2.4.3.2 Relative Density and API Gravity (IP160, ASTM D1298)

This method covers the laboratory determination, using a glass hydrometer of the density, specific gravity or API gravity of crude petroleum. The density, specific gravity or API gravity by the hydrometer is most accurate at or near the reference temperature of 15°C or 60°F.

After adjusting the temperature of the sample to the temperature desired, the sample is transferred to a hydrometer cylinder. The hydrometer is lowered into the sample and depressed about two scale divisions into the liquid and then released. When the hydrometer is come to rest, the hydrometer scale reading is estimated to the nearest 0.0001 specific gravity or density or 0.05 deg API.

The relevant corrections are applied to the observed thermometer reading. In this work, a density scaled hydrometer was employed and Table 53 (Petroleum Measurement Tables) were used to obtain density at 15°C.

2.4.3.3 Viscosity (IP71, ASTM D445)

This method describes a procedure for the determination of the kinematic viscosity of liquid petroleum products, both transparent

and opaque, by measuring the time for a volume of liquid to flow under gravity through a calibrated glass capillary viscometer. The dynamic viscosity can be obtained by multiplying the measured kinematic viscosity by the density of the liquid.

2.4.3.4 Flash Point (IP34, ASTM D93)

This method covers the determination of the flash point by Pensky-Martens closed tester of fuel oils, lubricating oils, suspensions of solids, liquids that tend to form a surface film under test conditions and other liquids.

The sample is poured into a cup to the level indicated by the filling mark. The lid of the cup is placed and the test flame is lighted. The heat is supplied at 5°C min^{-1} and also the stirrer is set at a downward direction. The test flame is applied by operating the mechanism on the cover, which controls the shutter and test flame burner. The test flame is lowered into the vapour space of the cup of 0.5 sec and it is left in that position for 1 second and quickly raised to the high position. When the test flame application causes distinct flashes, the temperature is recorded at the flash point.

2.4.3.5 Cetane Index (IP218, ASTM D976)

The calculated cetane index formula represents a means for directly estimating the ASTM cetane number of distillate fuels from API gravity and mid-boiling point.

$$\text{Calculated Cetane Index} = 0.49083 + 1.06577(x) - 0.0010552\ (x)^2$$

where

$n = 97.833$ (log mid-boiling point F)^2 + 22088 (API) (log mid-boiling point deg F) + 0.01247 (API)^2 - 423.51 (log mid-boiling point deg F) - 4.7808 (API) + 419.59.

2.4.3.6 Distillation Range (IP123, ASTM 86)

The distillation range of the pyrolytic oils were determined by the aromatic distillation apparatus (ISC INS. Ltd.).

This method of test covers the distillation of motor gasolines, aviation gasolines, aviation turbine fuels, gas oils, distillate fuel oils and similar petroleum products.

A 100 ml sample is distilled. Systematic observations of thermometer readings and volumes of condensate are made.

2.4.3.7 Calorific Value and Sulphur Content

This method provides for the determination of the gross heat of combustion of liquid fuels.

A weighed quantity of the sample is burned in oxygen in a bomb calorimeter under controlled conditions. The heat of combustion is calculated from the weight of the sample and rise in temperature, with proper allowance for heat transfer and for the formation of nitric and sulphuric acid in the bomb. The values obtained are the gross heat of combustion at constant volume.

2.4.3.8 Hydrogen Content

The hydrogen content of pyrolytic oils were determined by low resolution nuclear magnetic resonance spectrometry (Newport Fuel Analyser, Oxford Analytical Instruments).

A sample of the material is compared in a continuous-wave low resolution nuclear magnetic resonance spectrometer, with a reference standard sample of a pure hydrocarbon. The results from the integrator on the instrument are used as a means of comparing the theoretical hydrogen content of the standard with that of the sample, the result being expressed as the hydrogen (% m basis) in the sample.

2.4.4 Elemental Analysis

In this part of the work, a Model 240C Perkin-Elmer Elemental analyser was employed.

The equipment is based upon the proven combustion design of the classical methods of Pregland Dumas and the original work of Professor Simon and co-workers. The sample is oxidised under static conditions in a pure oxygen environment, for two to six minutes. The process concludes with a dynamic combustion procedure. The resulting combustion products are swept into a mixing chamber, where they are controlled to a constant pressure, temperature and volume. The temperature is thermo-stated at 75°C, the volume fixed at 300 cc and the pressure of 2 atmospheres absolute. The homogeneous mixture is then analysed by passage through a series of three high precision thermal conductivity detectors. As the gas passes through, water is removed from the stream. The differential signal obtained before and after the trap, as lead on a potentiometric recorder or a digital readout system, reflects the water concentration and therefore, the amount of hydrogen in the original sample.

A similar measurement is made of the signal output of a second pair of conductivity cells, between which is a trap which removes carbon dioxide. The remaining gas now consists of helium and

nitrogen. This gas passes through a conductivity cell, the output of which is compared to that of a reference cell where pure helium flows to give the nitrogen concentration.

For oxygen analysis, the sample is pyrolysed in a helium environment. The products are swept through heated platinised carbon to convert oxygen products of reaction to carbon monoxide. The carbon monoxide is then oxidised by copper oxide to carbon dioxide, which is detected and measured in the same manner and sequence as carbon the CHN mode.

The flow schematic of elemental analyser is shown in Fig. 2.11.

2.4.5 Fourier Transform Infrared Spectroscopy (FTIR)

FTir spectroscopy was used to analyse the pyrolysis oils.

An FTir spectrometer basically consists of two parts:

(1) an optical system which uses an interferometer

(2) a dedicated computer.

The computer controls optical components, collects and stores data, performs computations on data and displays spectra. A schematic diagram of the essential components of a rapid scanning Fourier transform spectrometer is given in Fig. 2.12. The light form an infrared source is collimated and sent to the beam splitter of a Michelson interferometer. The beam is divided, part going to the moving mirror and part to the fixed mirror. The return beams recombine at the beam splitter undergoing interference. The reconstructed beam is then directed through the sample and focused onto the detector. A laser beam undergoing the same change of

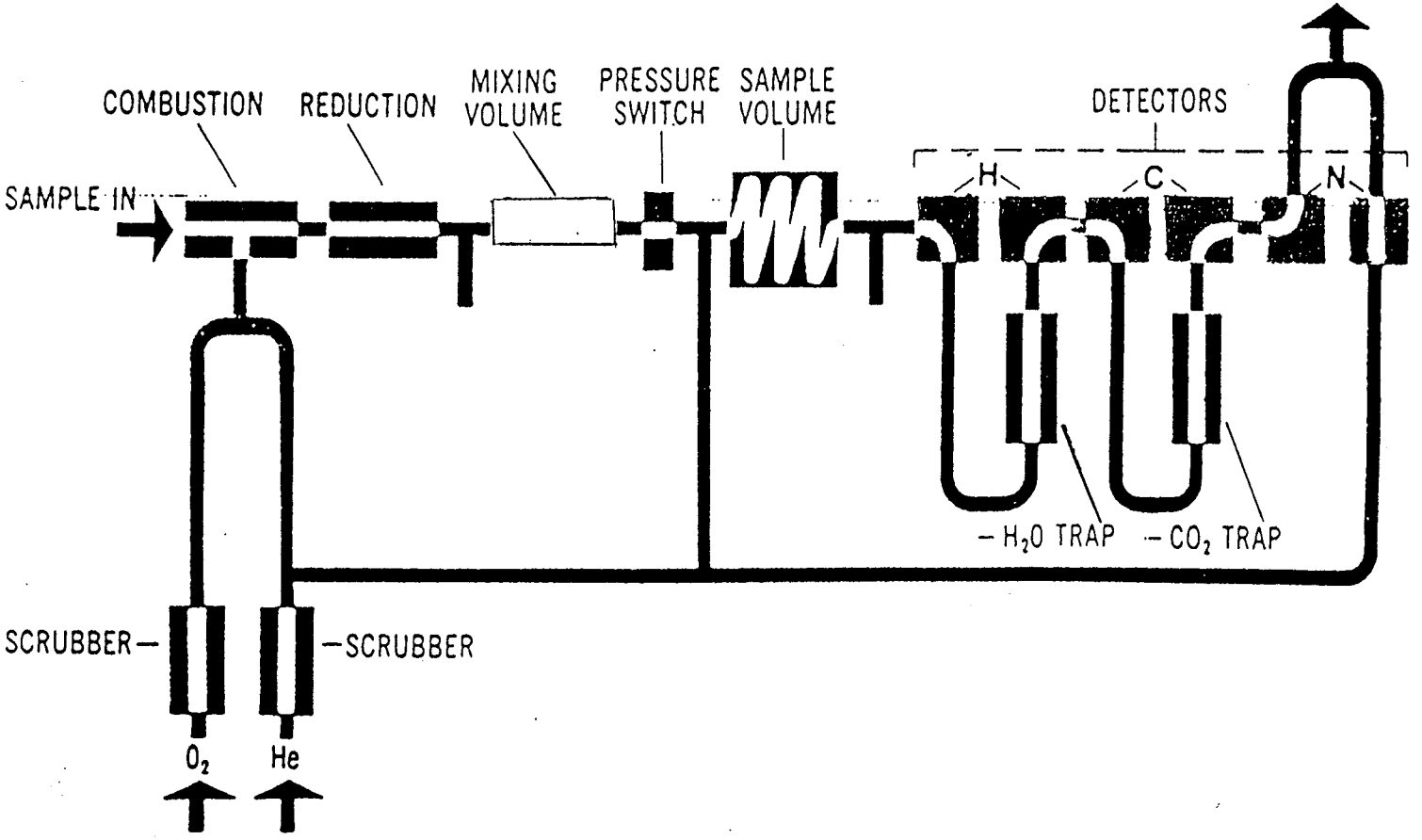

Fig. 2.11. Flow schematic of the elemental analyser.

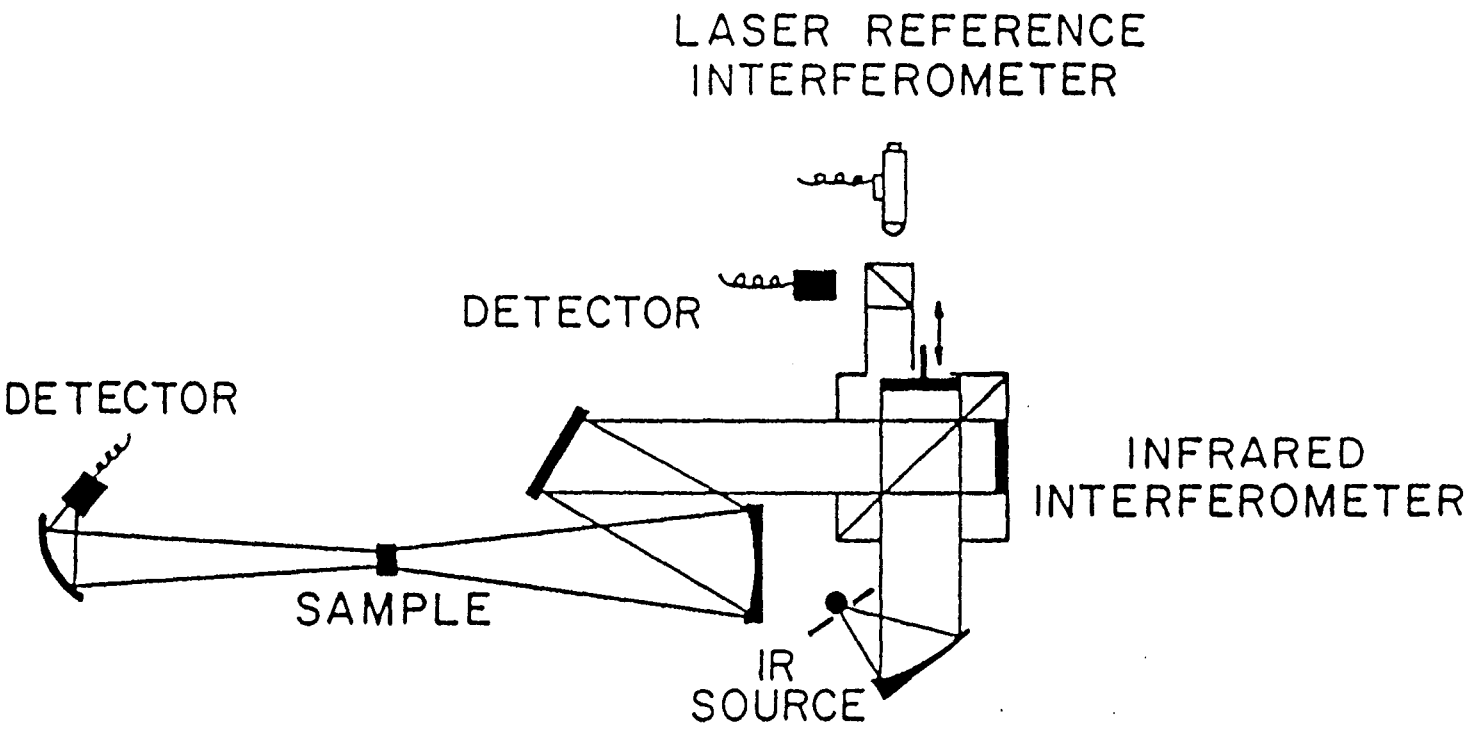

Fig.2.12 Diagram of the optical system of a Fourier Transform Infrared Spectrometer.

optical path as the infrared beam, serves to reference the position of the mirror during the scan and initiates the collection of data points from the signal by the infrared detector at uniform intervals of mirror travel.

Fourier transform infrared spectroscopy offers potential advantages, namely (153) higher signal-to-noise ratios for spectro obtained under conditions of equal measurement time (2) higher accuracy in frequency for spectra taken over a wide range of frequencies.

Functional group, compositional analysis of the derived oils was performed using Fourier transform infrared spectroscopy. A thin uniform layer of the oil was placed on a KBr sample cell and peak heights were normalised to the major C-H peak.

2.4.6 Surface Area Measurements

The Quantasorb (Quantachrome) was employed to determine the surface areas of the pyrolysis chars.

The Quantasorb determines the surface area of the sample by employing the techniques of adsorbing the adsorbate gas from a flowing mixture of adsorbate and an inert non-adsorbable carrier gas.

The process of adsorption and desorption is monitored by measuring the change in the thermal conductivity of the gas mixture. Fig. 2.14 shows a typical adsorption-desorption cycle.

The pre-weighed dry sample cell is filled by the sample as possible as while still allowing adequate passageway for the unimpeded flow of gas above the sample surface. The cell is immersed in a liquid nitrogen filled dewar.

Adsorption is started at point A by immersing the sample contained in a glass cell in an appropriate coolant. Liquid nitrogen is used as the coolant when nitrogen is the adsorbate in a helium carrier.

The adsorption peak is produced by the change in the thermal conductivity of the gas mixture, resulting from the decrease in adsorbate concentration due to adsorption on the powder surface. Adsorption is completed when there is no longer any difference in the thermal conductivities of the gas entering and leaving the sample cell.

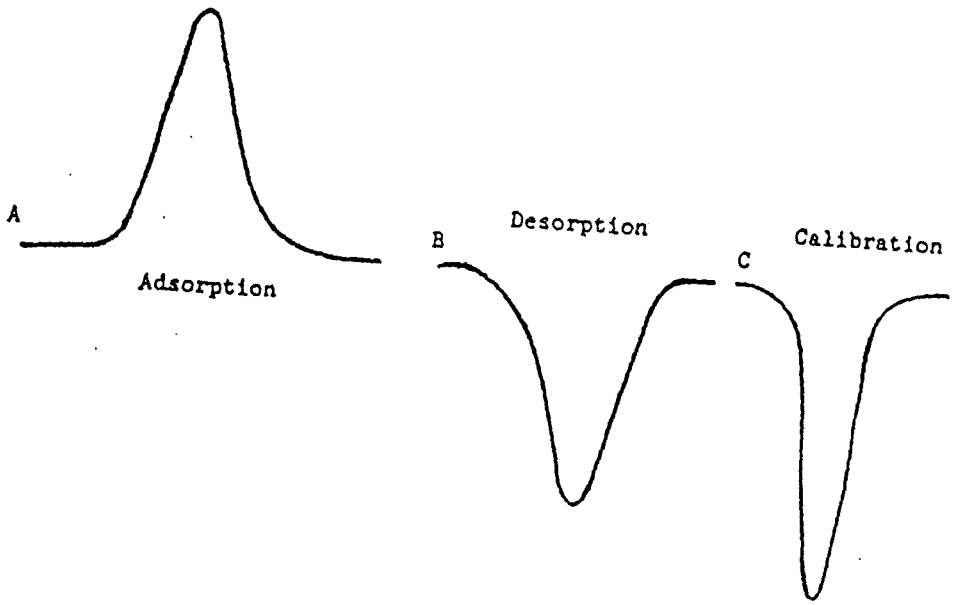

Fig. 2.13 Typical Adsorption-Desorption Cycle.

Desorption is initiated at point B by removal of the sample cell from the coolant. During the desorption process, the gas leaving the sample cell is richer in adsorbate.

At C, a known amount of adsorbate is introduced into the flow stream in order to calibrate the desorption signal.

The three point B.E.T (Bruanauer, Emmett and Teller) theory is used to determine the surface areas of chars. Also, the pore size distributions of the scrap tyre chars were calculated [154].

2.4.7 Polycyclic Aromatic Hydrocarbon Analysis

2.4.7.1 Liquid Chromatography

The oils obtained from the fixed-bed and fluidised-bed reactors were fractioned by liquid chromatography in order to investigate the contents of the polycyclic aromatic hydrocarbons (PAH), which are considered a potential health hazard.

The aliphatic and aromatic fractions were separated using silica-gel mini-columns. One of the reasons for separation was that the oils are chemically very complex and consequently require separation into various fractions. The second reason was that for the gas chromatography/mass spectrometry analysis at certain retention times, the aliphatic breakdown species give mass fragments in the region of aromatic fragments.

A glass mini-column packed with silica, Bodesil (sepralyte) sorbent was pre-activated at 105°C for two hours prior to use. Before loading the sample, the column was rinsed with n-pentane and

the oil was mixed with chromosorb G/AW/DMCS 60-80 support in order to prevent the formation of a solid phase and to improve solvent contacting with the oil.

The sample was then loaded onto the column and the column was sequentially eluted under vacuum with pentane, benzene, ethyl acetate and methanol to produce aliphatic, aromatic, ester and polar fractions respectively. After removing the solvents by nitrogen blow down, the vials were re-weighed in order to determine chemical class mass composition. From those, the benzene fractions of the pyrolysis oils were analysed by gas chromatography with a flame ionisation detector to determine the content of polycyclic aromatic hydrocarbons (PAH). Identification was performed using a standard mixture of PAH and retention time with the use of the Lee Relative Retention Index. The benzene fractions were also analysed by gas chromatography with a mass spectrometric detector for confirmation of identities.

2.4.7.2 Gas Chromatography

Gas chromatography analyses were carried out with a Carlo Erba gas chromatogram. The standard mixture of PAH consisted of naphthalene, phenanthrene, chrysene, perylene and picene. Before injecting the benzene fractions, the standard PAH mixture was injected and the retention index was used in the identification and quantitation of PAH compounds.

2.4.7.3 Gas Chromatography/Mass Spectroscopy (GC/MS)

The aromatic compounds of pyrolysis oils were analysed by gas chromatography mass spectrometry using a GC/MS Carlo Erba Vega series 2 GC 6000 and a Finnigan Mat Ion Trap Detector. The column was an

SGE 25QC3/BP5-0.25 part number 054180, with GC temperature program, 60°C for 5 minutes and then 5°C min^{-1} to 280°C and hold 20 minutes.

The mass spectra of the separated components were compared with standard spectra in an NBS/EPA/NIH (with 42222 entries) library.

Single Ion Monitoring

The expected compounds were identified by introducing their molecular weight to software for a fragment of a single mass e.g 178 found phenanthrene.

CHAPTER 3

FIXED-BED REACTOR PYROLYSIS

3.1 Pyrolysis of Biomass

3.1.1 Wood

3.1.1.1 Introduction

The breakdown of the complex polymer structure of wood leads to a large number of products.

According to Roberts (127), a fully developed pyrolysis wave advancing into a block of wood can be subdivided into the following regions (in order of increasing temperature):

- A region in which the wood structure is virtually intact and autocatalysis of the pyrolysis of the most reactive constituents is occurring.

- A region in which failure of wood structure has occurred. The effects of autocatalysis are reduced and pyrolysis of the most reactive constituents is occurring.

- A region in which the pyrolysis of cellulose and hemicellulose is complete and the pyrolysis or lignin is dominant.

- A region in which all wood has been pyrolysed to char. Secondary reactions between volatiles generated further into the wood and the char residue may be occurring.

The complexity of thermal decomposition reactions is reflected by the number of variables involved. This includes temperature, heat pre-treatment, heating rate, contact time of reactives and products

in the reactor gaseous atmosphere, pressure, particle size and extent of secondary reactions. Some of these parameters have interaction effects one with the other (128). Also, the role of wood components in thermal decomposition is quite significant.

In this part of the research, wood chips were pyrolysed in a fixed-bed reactor at different heating rates up to different maximum temperatures. Also, two different sizes of samples were pyrolysed in order to investigate the effects of particle size on the pyrolysis yields.

3.1.1.2 Results and Discussions

The pine wood samples (1 x 1 x 1 cm cubes) whose properties are shown in Table 3.1, were pyrolysed at the heating rates of 5, 20, 40 and 80°C min^{-1} up to a maximum temperature of either 300, 420, 600 and 720°C. The yields are shown in Table 3.2.

Table 3.1. Properties of the raw pine wood sample (as received)

Elemental Analysis		
	(% wt)	CV (MJ kg^{-1})
C	48.21	17.69
H	5.87	
N	0.18	
O	44.76	
S	0.03	
Ash	0.75	

In this research, as indicated in Chapter 2, oil sampling was performed by two different procedures:

(a) Sampling of the liquid at the end of the experiments

(b) Sampling of the liquid at different intervals throughout the experiments.

3.1.1.2 a Sampling of the Liquid at the End of the Experiment

As seen in Table 3.2, when the wood chips are pyrolysed in the fixed-bed reactor, char yield decreased as the maximum temperature of experiments increased for all the heating rates. Conversely, for each run, liquid and gaseous yields increased with increasing maximum temperature.

When the char yields of each maximum temperature are compared with their counterparts at different heating rates, it is seen that for the maximum temperatures of 420, 600 and 720°C, char yields decrease as the heating rate increased.

Only for the maximum temperature of 300°C char yields increased as the heating rate increased.

Also, it is seen that liquid and gaseous yields of each different maximum temperature runs increase as the heating rate increase. Only for the maximum temperature of 300°C liquid and gaseous yields decrease with the increasing maximum temperature.

From these, it can be concluded that, for the maximum temperatures of 420, 600 and 720°C, increasing heating rates influence reactions in favour of liquid and gaseous yield. For the

maximum temperature of 300°C, especially for rapid heating rates, devolatilisation reactions stay uncompleted.

Table 3.2. Yield of wood pyrolysis products.

	Char % wt	Liquid (oil + aqueous) % wt		Gas % wt
5°C min^{-1} T max				
300	53.76	31.6	(10.6 + 21)	14.64
420	29.7	48.31	(12.4 + 35.9)	21.5
600	24.4	49.2	(12.4 + 36.6)	26.4
720	23.2	50.0	(13.0 + 37)	26.8
20°C min^{-1} T max				
300	55.6	30.6	(10.1 + 20.5)	14.0
420	27.2	49.6	(12.2 + 37.4)	23.0
600	22.6	50.4	(12.8 + 37.6)	27.0
720	19.6	51.6	(14.1 + 37.5)	28.8
40°C min^{-1} T max				
300	58.0	28.4	(6.7 + 21.7)	13.6
420	26.4	46.0	(11.8 + 34.2)	27.6
600	20.4	50.8	(13.2 + 37.6)	28.8
720	18.4	52.0	(14.3 + 37.7)	29.6
80°C min^{-1} T max				
300	60.8	28	(6.4 + 21.6)	11.2
420	25.2	48.8	(11.9 + 36.9)	26.0
600	18.7	52.4	(14.6 + 37.8)	29.1
720	16.2	53.6	(15.9 + 37.7)	30.2

This is confirmed by Nunn et al (129). They had investigated time-temperature history of the rapid pyrolysis of sweet gum hardwood and reported that the decomposition of the wood is first observed at about 327°C.

Graham et al (130), who investigated the fast pyrolysis of biomass are also agreed that dehydration is dominant at lower

temperatures (below 300°C) and fragmentation predominates at higher temperatures.

Table 3.2 shows that total liquid amount increased with the heating rate and also maximum temperature except for the maximum temperature of 300°C as mentioned above.

If the 720°C final temperature results are considered, it is seen that total liquid yield increased from 50.0% to 53.6%. Also, it is seen that the aqueous content of the total liquid increased from 37% to 37.7%, while oil content increased from 13% to 15.9% wt. From these figures, it can be said that the oil part of liquid yield increases as the heating rate increases.

Roy et al (128) have reported that the increased rate of heating effects the yield amount of vacuum pyrolysis of aspen wood in favour of oil yield.

Shafizadeh (48) has shown that at higher temperatures, the tar forming reactions accelerate rapidly and overshadow the production of char and gases. It was also shown by Shafizadeh (49) that pyrolysis of hemicellulose in the form of xylan at 500°C produced mostly tar together with CO_2 water char and other hydrocarbons.

Deglise et al (32) and Mezerette and Girard (131), reported that rapid heating and quick removing of the products from the reaction zone makes it possible to obtain a high content of oils compared to char and gas.

Table 3.3 shows elemental analysis and calorific values of wood pyrolysis oils for the heating rates of 5, 20, 40 and 80°C min^{-1}. It is seen that increased heating rate does not effect significantly oil

in terms of ultimate analysis. There is a small increase in the calorific values.

Roy et al (132) report the calorific value of wood pyrolysis oil as 22.5 MJ kg^{-1}, similar to that of this research.

For the heating rates of 40 and 80°C min^{-1}, the maximum temperature of 780°C was also investigated at low N_2 flow rate in order to observe the peak temperature for the maximum liquid yield. For 780°C, it was observed that the char yield remained constant, but liquid yield decreased (Table 3.3). From this information, it was believed that secondary cracking reactions occurred after 720°C. This is also confirmed by Nunn et al (129).

Table 3.3. Maximum temperature effect on the yields of wood pyrolysis

Heating Rate (C min^{-1})	Max Temp	Char	Liquid	Gaseous % wt
40	780	18.6	48	32.4
80	780	16.0	50.7	32.3
1000 K s^{-1} (129)	780	9.3	50.7	40.0
20 (C min^{-1}) (45)	600	23	45	32

Maniatis and Buekens (45) for the pyrolysis of biomass, have reported for the heating rate of 20°C min^{-1} and a final temperature of 600°C tar, gas and char yields as 45, 32 and 23% respectively. For 700°C, there was also an increase in tar and gas yield. They observed for the final pyrolysis temperature of 800°C a decrease in tar amount, increase in gas and also a decrease in char yield.

Stiles and Kandiyoti (133) have also observed that the tar yield above 450°C was decreased in their work concerning the pyrolysis of silver birch in a fluidised-bed reactor.

3.1.1.2 a (i) Effect of Particle Size

Two different sizes of wood chips (1 x 1 x 1 cm cubes and 1 x 1 cm chips) were pyrolysed in order to investigate the particle size effects on the yield of wood pyrolysis. It can be seen Fig. 3.1 for the heating rate of 5°C min^{-1}, the yields of gas, liquid and char amounts are similar for both particle sizes. When the heating rate increased, the small particles give more liquid and gas and less char than the bigger size.

Roy et al (128) observed the same effect, that is, a decrease in size of the particles enhanced very significantly the formation of pyrolytic oils, correspondingly there was a decrease in yield of charcoal.

Figueiredo et al (134) have reported the liquid yield of pyrolysis of holm-oak wood as 46.1 and 45.0% for the particle sizes of 0.4 mm and 1.6 mm respectively.

Table 3.4. Effect of heating rate on the product composition of wood pyrolysis oils (%)

	5°C min^{-1}	20°C min^{-1}	40°C min^{-1}	80°C min^{-1}
C	58.75	59.50	59.92	59.24
H	7.55	7.40	7.82	7.7
N	0.072	0.08	0.08	0.06
O	33.2	32.99	31.81	32.59
S	0.42	0.03	0.37	0.41
CV MJ kg^{-1}	22.801	23.049	23.21	23.07

Beaumont and Schwob (139) have also shown that coarser particles yield more char and gas and less oil. With slow pyrolysis, particle size did not show any influence, similar to this research. They summarised that with slow pyrolysis, particle size did not show any influence.

3.1.1.2 b Sampling Of Liquid Yield At Different Intervals

In this procedure, sampling was performed for the maximum temperature of 720°C. As the heating continued, the cold trap of the fixed-bed reactor was opened at the intervals of 300, 420, and 600°C and at the end of the run for each heating rate. Fig. 3.2 shows the liquid yield of intervals for each heating rate.

The yield of liquid shows a lateral shift to higher temperatures for the initiation of pyrolysis and also peak liquid yield increased as the heating rate increased. This lateral shift was also seen in the thermogravimetric analysis of wood (this will be discussed later).

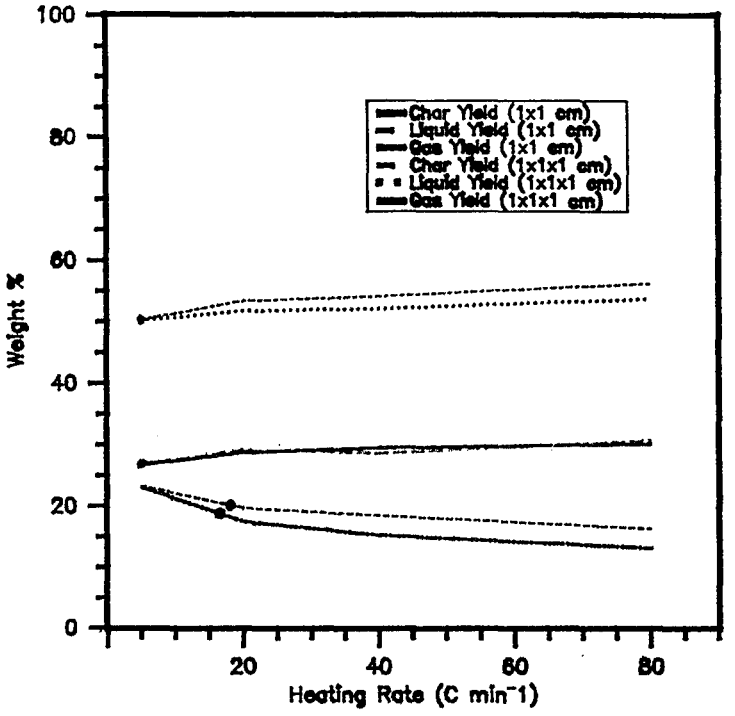

Fig. 3.1. Effects of particle size on the yields of wood pyrolysis.

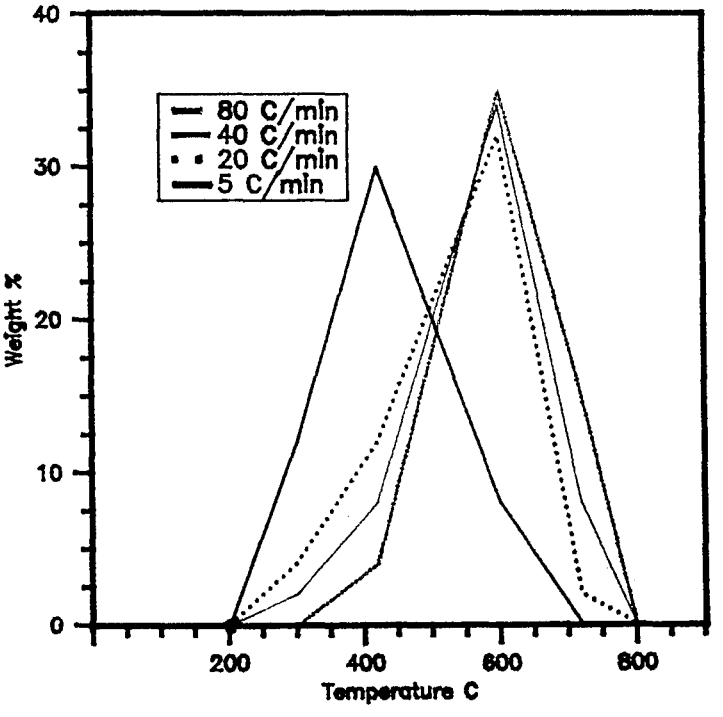

Fig. 3.2. Liquid yields at different intervals for the pyrolysis of wood.

The increased heating rate had a similar effect on the gas yield, as it had on the liquid yields. For the maximum temperature of 720°C, the total gas yields are 26.8%, 28.8%, 29.6% and 30.2% for the heating rates of 5, 20, 40 and 80°C min^{-1} respectively.

Figure 3.3 shows total gas yields of pyrolysis for each heating rate. Detailed analysis of the gas composition from the pyrolysis of wood revealed the main gases were hydrogen, carbon dioxide, carbon monoxide, methane, ethane, propane and propene, with lower concentrations of butane and butadiene. The maximum evolution of each gas was dependent on temperature and heating rate. Fig. 3.4 shows the data for the highest concentration gases.

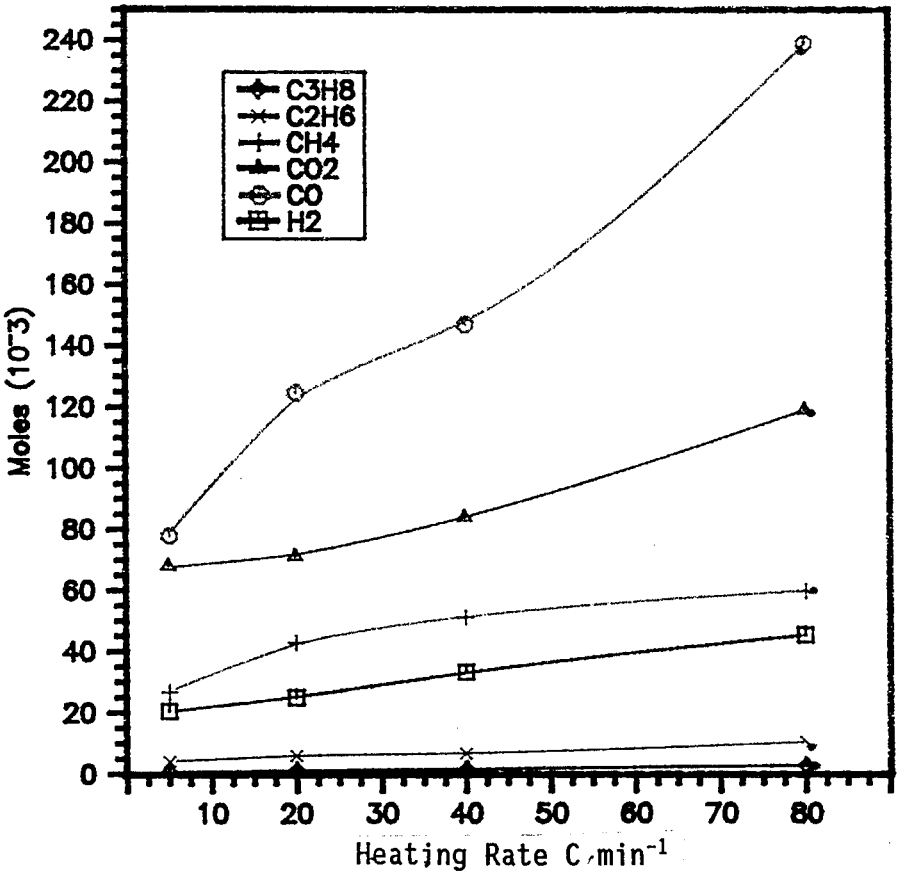

Fig. 3.3. Gas yields of pyrolysis of wood.

The main gas evolution also shifts to higher temperature levels as the heating rate is increased.

The evolution of gases is the result of the collapsing main polymer structure, with bond scission reactions followed by decarbonylation and decarboxylation reactions.

Since one of the most important contents of wood, cellulose decomposition significantly characterises the thermaldecomposition history of wood as well as hemicellulose and lignin.

The pyrolysis of cellulose pathways leading to production of char as well as gaseous and volatile products is shown in Fig. 3.5.

The appearance of gaseous yields at lower temperatures gives information about general decomposition pathways. For lower temperatures and low heating rates, the molecular weight reduction or decrease in degree of polymerisation or in other words saying bond scission occurs resulting in free radicals, elimination of water and formation of carbonyl and carboxyl groups.

The appearance of carbon dioxide and carbon monoxide are the results of decarboxylation and decarbonylation reactions.

As it will be discussed later (chapter 6), the hemicellulose content of wood plays an important role in the overall thermaldegradation of wood. Hemicellulose decomposition generally occurs between 250-318°C, but it is seen that with the increased heating rate it also shows a lateral shift. During the thermaldecomposition of hemicellulose, the dehydration reactions are characterised by random cleavage of the C-O bonds, producing water soluble acids, char and light gases.

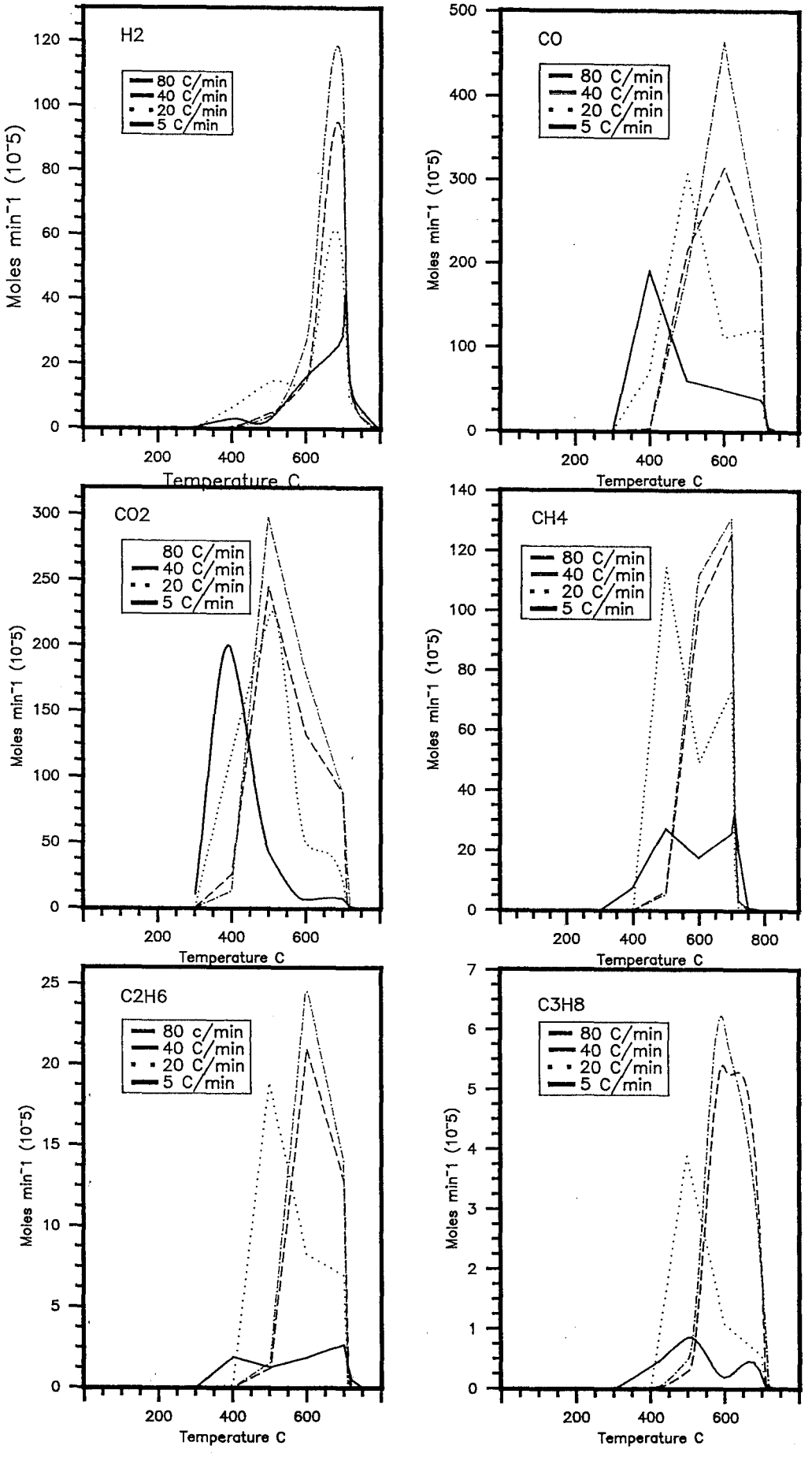

Fig.3.4 Gas evolution versus temperature for the highest concentration gases from wood pyrolysis

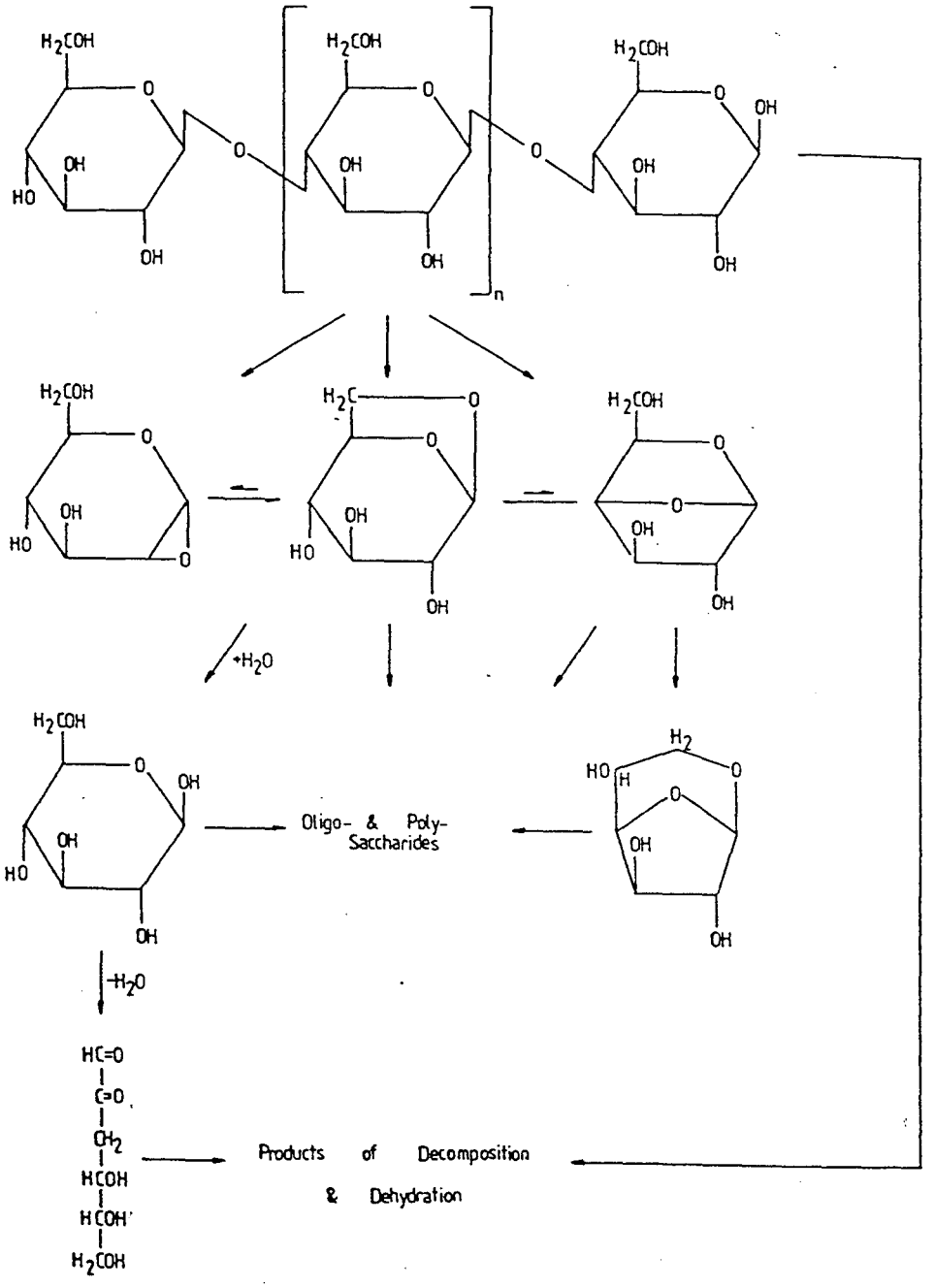

Fig. 3.5. Pyrolysis of cellulose.

The third component of lignin decomposes differently than cellulose and hemicellulose. Thermaldegradation occurs with cleavage of the straight carbon chains, which connect the aromatic rings. Further decomposition gives carbon oxides, hydrocarbons and char.

From these data it can be concluded that the thermaldecomposition of wood proceeds as follows:

- Drying area under 250°C loosing water.
- 250-300°C. The wood pieces become roasted with dark brown colour without releasing any significant gases.
- 320-475°C. Pyrolysis area. Main pyrolysis reactions occur.
- Over 500°C. Gasification area. Gas yield grows rapidly.

The calorific values of the gases were calculated from total gas yields. The gas yields have significant calorific values (Table 3.5), illustrating their potential to provide the energy requirements for the process heating.

Table 3.5. Calorific values of total gas yields of wood pyrolysis.

Heating Rate ($C\ min^{-1}$)	Calorific Value ($MJ\ m^{-3}$)
5	13.6
20	15.7
40	15.7
80	15.8

Char yields decreased as the heating rate increased in the wood pyrolysis reactions. The final temperature of reaction also effects the char yields producing a decrease in yield.

General characteristics of char yields of wood pyrolysis are shown in Table 3.6.

Table 3.6. General characteristics of wood pyrolysis chars.

Heating Rate °C min^{-1}	5	20	40	80
Calorific Value (MJ kg^{-1})	33.51	32.10	33.04	29.0
C	90.9	90.5	89.7	90.1
H	1.86	2.02	2.17	2.21
N	0.08	0.06	0.04	0.03
O	0.25	0.18	0.21	0.17
S	6.3	6.72	6.47	6.31
Ash	0.61	0.52	0.50	0.53

The calorific values of wood char decreased with the increasing maximum temperature. Also, surface area of the chars increased as the heating rate increased (Fig. 3.6).

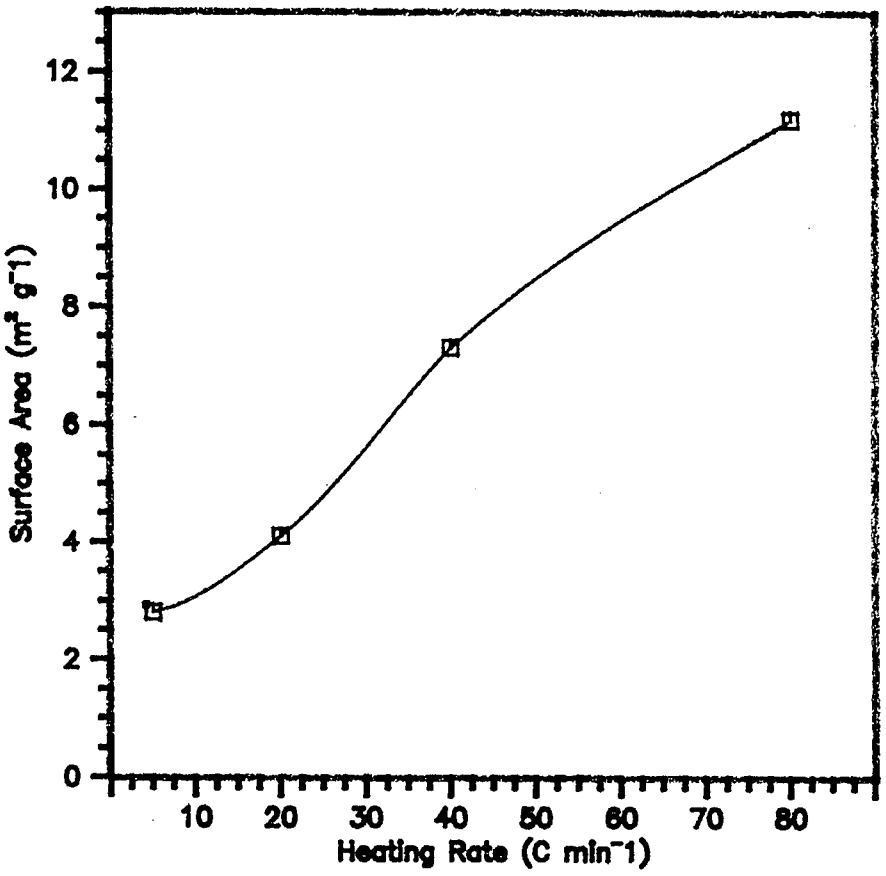

Fig. 3.6. Surface areas of wood chars.

Zanzi et al (143) calculated the surface area of wood pyrolysis chars for the heating rate of 20°C min^{-1} and maximum temperature of 850°C as 28.3 m^2 g^{-1}. The charcoal obtained from pyrolysis of wood and other biomass materials has a potential as activated carbon. Keirsse et al (156) obtained activated carbon using partial gasification and reported that it was possible to produce different brands of adsorbents which could either be applied in drinking water production or waste water treatment.

Also, charcoal based slurries with water or oil provide an alternative liquid fuel that has some advantages over bio-oil. Esnouf (157) describes several char water slurry and ternary slurry manufacturing processes and she concludes that these are currently

limited opportunities for implementation, but research and development in well defined areas could improve the economic viability of these products.

3.1.2 Rice Husks

3.1.2.1 Introduction

Rice husks are a form of biomass waste generated in large quantities. It is estimated that over 100 million tonnes per year are generated with 90% accounted for by developing countries (158).

In this part of the research, the second biomass sample employed was rice husk, which is a by-product of the rice milling industry and thought to be a potential fuel for energy.

As for the wood chips, rice husks were pyrolysed in the fixed-bed reactor up to maximum temperatures of 300, 420, 600 and 720°C at the heating rates of 5, 20, 40 and 80°C min^{-1}.

The pyrolysis oil sampling procedures were also identical to that of the wood pyrolysis oil sampling.

In this part of the research, the effect of heating rate and maximum reaction temperature on the rice husks pyrolysis yields were investigated.

3.1.2.2 Results And Discussion

The rice husks (1.2 mm), whose properties are shown in Table 3.7 were stored in the laboratory under dry conditions before pyrolysis. The pyrolysis yields are summarised in Table 3.8.

Table 3.7. Properties of the rice husks sample (as received).

	Elemental Analysis wt %	Calorific Value (MJ kg^{-1})
C	44.22	15.25
H	5.06	
N	0.5	
O	41.81	
S	0.5	
Ash	10.91	

Table 3.8. Rice husks pyrolysis yields.

	Char % wt	Liquid (oil + aqueous) % wt	(% wt % wt)	Gaseous % wt
5°C min^{-1}				
300	70.5	18.5	(0.25 + 18.25)	11
420	41.8	36	(4 + 32)	22.2
600	36.3	39	(7 + 32)	24.7
720	35.2	40	(7.5 + 32.5)	24.8
20°C min^{-1}				
300	73	16	(0.5 + 17.5)	11
420	40	36	(4.5 + 31.5)	24
600	35.6	39	(5 + 34)	25.4
720	33.4	41.5	(9 + 32.5)	25.1
40°C min^{-1}				
300	69.5	18	(1 + 17)	12.5
420	42	34.5	(4.5 + 30)	23.5
600	37	41	(8 + 33)	22
720	32.5	42	(9.5 + 32.5)	25.5
80°C min^{-1}				
300	69	18	(1 + 17)	13
420	42	36	(4 + 32)	22
600	35.6	42.3	(9.8 + 32.5)	22.1
720	31.4	43	(10.5 + 32.5)	25.6

Table 3.8 shows that increased maximum temperature effects percentage mass yields in favour of liquid and gaseous yields. Conversely, char yields decreased as the maximum temperature increased. The char yields are also in close agreement with the char yields obtained from TGA (chapter 6).

In addition, cellulose as Whatman filter paper No. 1 was pyrolysed in the gas purged fixed-bed reactor and char yield results obtained were very similar to those of Shafizadeh et al (57) for the pyrolysis of small samples of Whatman filter No. 1 under vacuum conditions.

Consequently, char formation by secondary repolymerisation or tar cracking reactions was deemed to be minimised in the gas-purged fixed-bed reactor.

The yields of rice husks pyrolysis are effected by the increased heating rate as well as by the maximum temperature.

The liquid yields and the oil contents of the liquid yield also increased as the maximum temperature and the heating rate increased. It is believed that increased heating rate and high temperatures with rapid quenching, yield more liquid (128).

Eklund and Wanzl (135) investigated the influence of heating rate on pyrolysis and hydropyrolysis of peat. 500 K s^{-1} and 10000 K s^{-1} heating rates were tested and they observed a decrease in char yield and increase in gas yields. It was also observed that there was no change in liquid yields in a N_2 environment. In hydropyrolysis experiments, they also observed an increase in liquid yields as the heating rate increased.

The properties of rice husk pyrolysis oils are shown in Table 3.9. Calorific values of oils are not affected by the increased heating rate, although yields are affected by heating rate. In addition, Table 3.9 shows that the elemental analysis of the oils derived from the rice husks at different heating rates, do not differ significantly.

Table 3.9. The properties of rice husks pyrolysis oils.

	Heating Rate			
	5°C min^{-1}	20°C min^{-1}	40°C min^{-1}	80°C min^{-1}
C	59.3	57.95	55.8	55.4
H	7.5	8.0	7.8	8.25
N	2.3	1.45	1.15	1.65
O	30.5	32.33	34.77	34.28
S	0.40	0.37	0.48	0.42
CV (MJ kg^{-1})	24.3	22.3	24.5	24.5

Gas Composition

The composition of total gas yield of the gases evolved with increasing rate is shown in Fig. 3.7. As the heating rate increased, the yields of CO, CO_2, H_2, CH_4 and C_2H_6 increased. There were also lower concentrations of propane, propene, butane and butene, which also showed an increase in yield with heating rate.

Total calorific values calculated from gas analysis data for the rice husk samples are shown in Table 3.10.

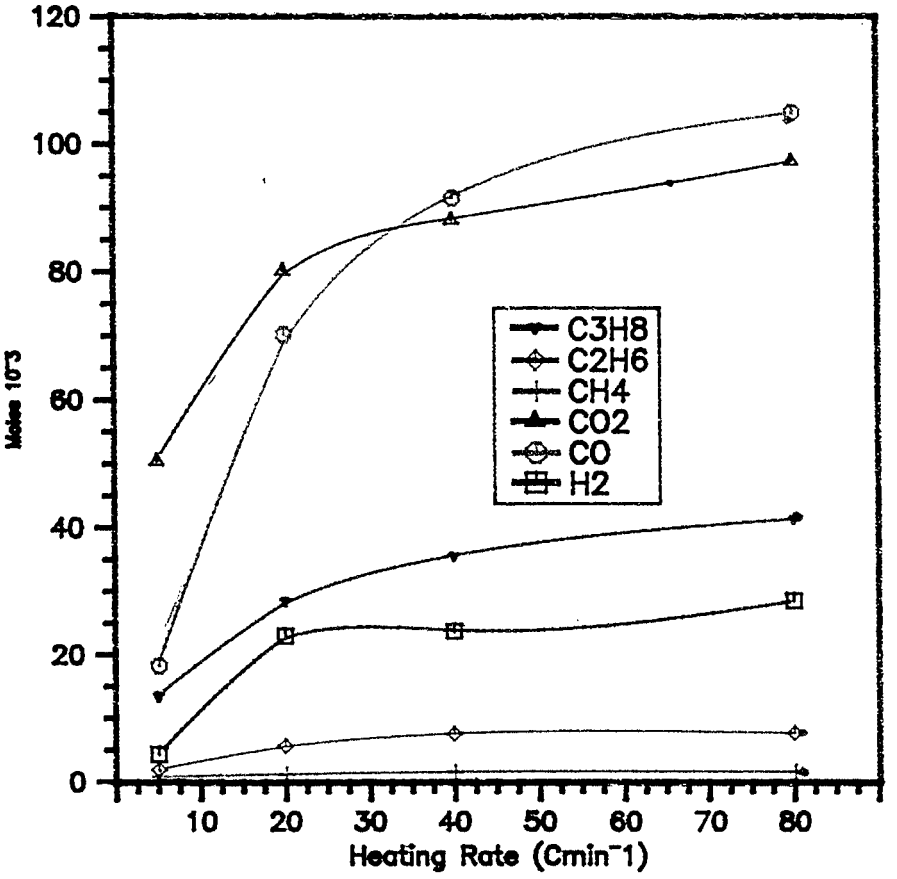

Fig. 3.7. Total gas yield from rice husks pyrolysis.

Table 3.10. Total calorific values of gases evolved from rice husks pyrolysis.

Heating Rate C° min^{-1}	Calorific Value MJ m^{-3}
5	12.18
20	14.39
40	15.45
80	15.60

Rice husks have a high cellulose and silica content. The silica contents were reported as 18-22.3% and 15-21% by Boateng et al (136) and Ganesh et al (137) respectively for rice husks. Both research groups agreed that the silica content of ash as 95% wt.

In this research, the ash content of rice husks was determined as 10.9% wt (Table 3.7). The high silica content and unique physico-chemical structure of the rice husk impart specific devolatilisation. The reactivity of the charcoal derived from rice husks can be related to its structural developments (136).

The properties of charcoal derived from rice husks at different heating rates are shown in Table 3.11.

Table 3.11. General characteristics of rice husks pyrolysis chars.

Heating Rate (C min^{-1})				
	5	20	40	80
C V (MJ kg^{-1})	19.57	21.12	20.4	20.6
C	56.7	56.44	55.2	54.4
H	1.27	1.34	1.38	1.21
N	1.12	1.38	1.28	1.34
O	0.75	0.71	0.72	0.75
S	8.46	7.4	7.57	7.51
Ash	31.7	32.91	32.23	32.8

The results illustrate that the carbon content of the char decreased with the increased heating rate. The sulphur and ash contents of the char were high and imply that the chars would not be suitable as solid fuel.

When the chars obtained at maximum temperature of 420°C are examined, it is seen that there is small increase in surface areas as the heating rate increased. For the maximum temperature of 720°C, surface areas of chars increased significantly as the heating rate increased.

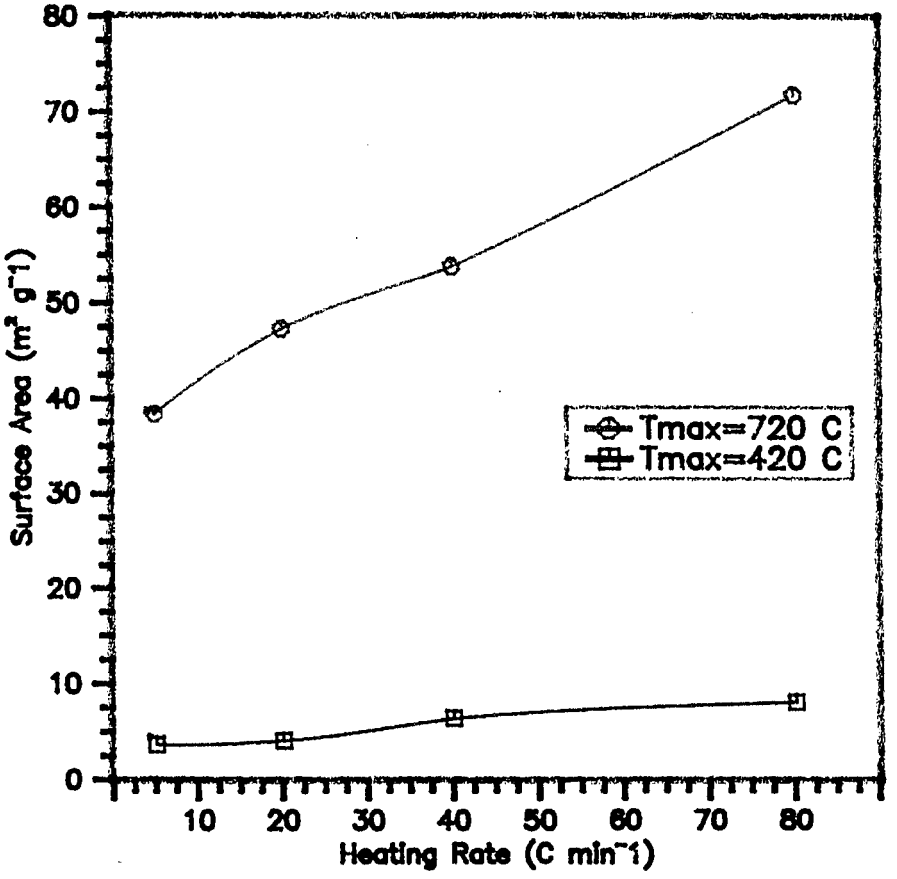

Fig. 3.8. Surface areas of char for rice husk sample pyrolysed.

The changes in surface areas of coal particles with the extent of conversion was investigated by Jiang et al (138). They reported that specific surface areas increased with increasing

devolatilisation temperature up to 873-973°C and decreased thereafter because of reaccumulation caused by repolymerisation.

3.1.3 Conclusions

After pyrolysis of the two biomass samples, which were wood and rice husks, it can be concluded that pyrolysis of biomass waste is a promising technique in the reutilisation of waste biomass. The yield of oil, gas and char has quite significant properties which could be improved by various techniques. According to the requirements of an oil or char end product, both can be increased or decreased. The oil produced from biomass pyrolysis have a significant calorific value and could be used directly as fuels. The production of liquid fuels from biomass has a number of advantages over other energy recovery systems from biomass in that since the fuel is liquid, it can be stored and transported and hence does not have to be used at or near the recycling plant.

The char produced by pyrolysis from biomass can be used as a solid fuel or as char/water or char/oil slurry liquid fuels.

Also, the gas has a high calorific value with the potential to be used to provide the energy requirements of the pyrolysis plant.

3.2 Pyrolysis of RDF

3.2.1 Introduction

Disposal of municipal solid waste has centred on thermal degradation methods because of the resistance of plastic contents to biodegradation.

Pyrolysis has certain advantages over other forms of waste disposal in that potentially all the products of pyrolysis, the gases, pyrolysis oils and char can be used as fuels to offset the costs of disposal.

Although, refuse derived fuel contains a high percentage of paper and other cellulosic materials, thermaldegradation of RDF proceeds differently than biomass because of its plastic contents.

The optimisation of the thermalconversion of RDF is desirable in order to produce desired products in the form of either gaseous liquid or solid.

Evans and Milne (92) showed that the control of the feedstock moisture content and particle size and temperature of pyrolysis could significantly affect the chemical composition and yield of the products.

In this part of the research, municipal solid waste pellets in the form of refuse derived fuel were pyrolysed in a fixed-bed reactor at different heating rates up to different maximum temperatures.

The reasons for using RDF pellets instead of municipal solid waste were to keep the sample as homogeneous as possible and remove

all non-combustibles i.e. metals and glass to prevent further handling complications.

3.2.2 Results and Discussion

The shredded refuse derived pellets (2-5 mm), whose properties are shown in Table 3.12, were pyrolysed in a fixed-bed reactor at the heating rates of 5, 20 40 and 80°C min^{-1} up to a maximum temperature of either 300, 420, 600 and 720°C. The nitrogen was used to sweep the evolved gases from the reaction zone to reduce the extent of secondary reactions. Mallya and Helt (6) and Beaumont and Schwob (139) all agree that secondary degradation of the evolved volatiles are minimised when a purge gas is used to carry the evolved gases from the reaction zone.

Table 3.12. Properties Of The Refuse Derived Fuel (as received).

	Elemental Analysis (% wt)	CV (MJ kg^{-1})
C	41.22	
H	5.06	19.25
N	0.5	
O	0.5	
S	41.81	
Ash	10.91	

During the ultimate analysis tests, the chloride content of RDF could not be determined with the available equipment. However, Barton (140) reported the chloride content of Byker RDF as 0.9% wt. Table 3.13 shows the mass yield results for the RDF samples. The yield of char decreased and the yield of oil increased as the

temperature was increased. There was a corresponding increase in gas yield from 300°C to 420°C. However, above 420°C, the gas yield remained essentially constant with approximately 18-22% depending on heating rate. Consequently, the increased yield of liquid, as the pyrolysis temperature was increased from 420°C to 720°C, was mainly derived from the char decomposition.

Table 3.13. Product yield from the pyrolysis of RDF.

Heating Rate °C min^{-1}	Char Yield (% wt)	Liquid (oil + aqueous) Yield (% wt)		Gas Yield (% wt)
5°C min^{-1}				
300	69.0	18	(2.4 + 15.6)	13.0
420	50.3	31.2	(6.8 + 24.4)	18.5
600	35.6	46.0	(16.4 + 29.6)	18.4
720	33.4	49.6	(20.4 + 29.2)	18.4
20°C min^{-1}				
300	70.8	18.4	(2.4 + 16.0)	10.8
420	50.4	30.4	(7.2 + 23.2)	19.2
600	35.2	49.2	(16.8 + 32.4)	18.6
720	29.4	52.2	(19.6 + 32.6)	18.6
40°C min^{-1}				
300	71.2	16.0	(2.8 + 13.2)	12.8
420	50.4	28.8	(8.4 + 20.4)	20.8
600	32.8	46.0	(17.6 + 28.4)	21.2
720	27.6	49.0	(28.8 + 20.2)	20.2
80°C min^{-1}				
300	71.9	16.1	(2.0 + 14.1)	12.3
420	49.2	28.6	(9.2 + 19.4)	21.2
600	31.7	51.2	(19.2 + 32.0)	21.8
720	27.3	55.7	(31.6 + 24.1)	20.3

Rampling and Hickey (7) have shown that the char consists of carbon and partially pyrolysed material such as hydrocarbons of high molecular weight. Therefore, as the temperature was increased, the increased yield of liquid was most probably derived from the

volatilisation and thermaldegradation of the high molecular weight hydrocarbons within the char.

The maximum conversion of RDF to liquid occurred at 720°C, with the conversion of more than 50%. Rampling and Hickey (7) have shown similar product yield results for the slow static batch pyrolysis of RDF. They reported that as the pyrolysis temperature was increased from 350°C to 700°C, char yield decreased from 50% to 30%, liquid increased from 32% to 49% and gas increased from 18% to 22%.

The liquid yield consisted of an aqueous phase and viscous oil phase. Table 3.13 shows the percentage oil and water of the liquid phase. The water and oil phases of the liquid show an increase in percentage yield as the temperature of pyrolysis was increased. The yield of oil reached a maximum at the highest heating rate of 80°C min^{-1} and final pyrolysis temperature of 720°C. These results show the potential of pyrolysis of municipal solid waste to generate oils.

Roy et al (109) using a vacuum pyrolysis system, but at a lower pyrolysis temperature of 455°C, found similar yields of oil at 35% for RDF.

Slightly higher yields of oil were obtained by Pober and Bauer (110) as 40% for pyrolysis of shredded and screened municipal solid waste, however, their system utilised flash pyrolysis, known to increase the yield of oil.

The aqueous phase has been shown to be composed largely of water, organic acids and miscible hydrocarbons (6, 7, 109, 110). Mallya and Helt (6) using slow pyrolysis of RDF in a fixed-bed reactor, produced a liquid with 50% water content, whereas, Roy et al

(109) using vacuum pyrolysis of RDF, obtained a liquid with lower water content of 9%.

The effect of heating rate is seen in Table 3.13. The higher heating rates of 40°C min^{-1} and 80°C min^{-1}, produced an increased yield of gas and a corresponding decrease in char. The higher heating rates to the final temperature of 720°C, resulted in a significantly higher yield of the oil phase of the liquid. The heating rates of 40°C min^{-1} producing 28.8% oil and 80°C min^{-1} producing 31.6% oil. The properties of oil derived from RDF heated to 720°C are shown in Table 3.14, in relation to heating rate.

Table 3.14. Properties of RDF pyrolysis oils. Final temperature 720°.

	Heating Rate °C min^{-1}			
	5	20	40	80
C	59.5	61.3	60.9	61.65
H	9.04	9.1	9.57	9.6
N	0.87	0.85	0.82	0.95
O	29.77	27.95	27.96	27.1
S	0.82	0.80	0.75	0.70
CV MJ kg^{-1}	33.41	40.4	40.0	40.7

The increased heating rate does not affect the oils ultimate analysis significantly. The carbon content shows a small increase and oxygen content shows a decrease as the heating rate increases.

The determined calorific values of the oils derived from RDF can be compared with the literature. It is seen that the amounts in Table 3.14 are quite high. Mallya and Helt (16) reported much lower

calorific values of 22.2 MJ kg^{-1} for RDF tars. Similarly, Rampling and Hickey (7) reported a maximum calorific value for the aqueous/oil liquid of 18.9 MJ kg^{-1}. Also, Pober and Bauer (10) reported the calorific value of flash pyrolysis oil of the shredded and screened organic components of municipal solid waste as 24 MJ kg^{-1}.

The calculated calorific values of the oils from the elemental analysis data (Table 3.14), would be also about 25 MJ kg^{-1}.

In this research, oil was separated from aqueous phase and dried before testing its calorific value.

Therefore, the calorific value of 40 MJ kg^{-1}. must be the result of drying or deoxygenation of the samples.

Gas Composition.

Detailed analysis of the gas composition from the pyrolysis of the RDF showed the main gases were CO_2, CO, H_2, CH_4, C_2H_6 and C_3H_8, with lower concentrations of C_2H_4, C_3H_6, C_4H_8 and C_4H_6 and other hydrocarbon gases.

The maximum evolution of each gas was dependent on the temperature and heating rate with the main gas evolution occurring between 400°C and 600°C. Fig. 3.9 shows the total yield of each gas in relation to heating rate for the waste heated to the final pyrolysis temperature of 720°C.

The total yield of each gas increased as the heating rate increased. The total calorific values of the yield gases also increased with the increased heating rate (Table 3.15).

It has been shown that the main gases produced during the pyrolysis of shredded and screened municipal solid waste or RDF to be CO_2, CO, H_2 and CH_4 and also the minor hydrocarbons to consist of C_2H_4, C_2H_6, C_3H_6 and C_3H_8 (7, 109, 110).

Table 3.15. Total calorific values of yield gases from RDF pyrolysis.

Heating Rate C min^{-1}	Calorific Value MJ m^{-3}
5	13.9
20	14.9
40	17.7
80	18.0

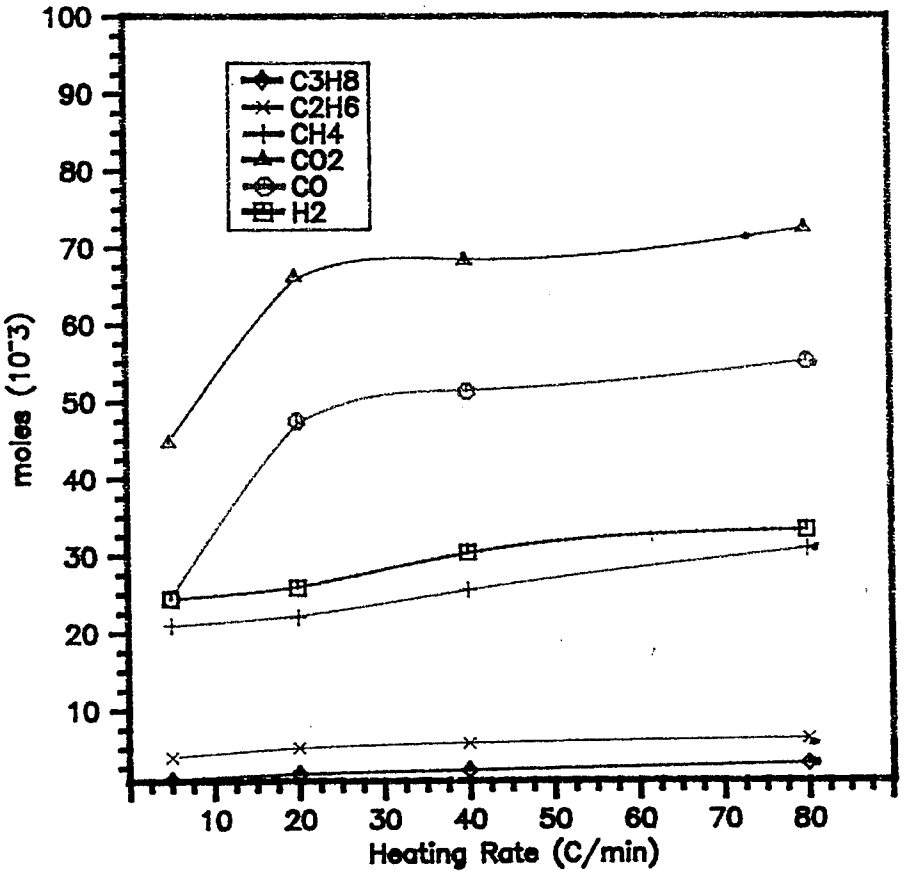

Fig. 3.9. Total gas yield versus heating rate for the pyrolysis of RDF.

Over 50% of municipal solid waste constituents are cellulosic, for example, paper, newsprint, packaging materials and wood wastes (141). It is expected that the pyrolytic behaviour of cellulose will influence the overall pyrolysis of the refuse derived fuel. Shafizadeh (48) showed that the major products from pyrolysis of cellulose were dependent on temperature, at lower temperatures below 300°C, CO_2 and CO dominate with water and char. Above 300°C, the cellulose is decomposed by an alternative pathway and the major evolved product is tar which contains levoglucosan as the major constituent with aldehydes, ketones and organic acids in addition to CO_2, CO, H_2 and char (69). Other components of the RDF, such as plastics and textiles, will contribute to the gas composition and concentration.

The elemental analysis of char produced at the heating rates of 5, 20,40 and 80°C min^{-1} heated to 420°C and 720°C are shown in Table 3.16.

The oxygen content of the chars was shown to be dependent on temperature, higher temperatures producing a reduction in oxygen. The oxygen and ash results for the RDF pyrolysed at 420°C may reflect incomplete pyrolysis of the RDF since the RDF waste material contained components with higher thermaldegradation temperatures than the 420°C.

Table 3.16. Elemental analysis of the char derived from pyrolysis of RDF in relation to temperature and heating rate.

		Heating Rate (C min^{-1})			
Temperature °C	Element	5	20	40	80
420	C	60.06	57.17	52.09	51.72
	H	4.94	3.0	3.54	3.56
	N	0.85	1.41	1.5	1.52
	S	0.59	0.60	0.57	0.55
	O	13.60	13.02	14.04	14.73
	Ash	19.96	24.80	28.06	27.92
720	C	57.30	56.04	55.97	55.09
	H	1.61	1.72	1.42	1.34
	N	0.85	0.81	0.67	0.59
	S	0.42	0.39	0.40	0.38
	O	5.22	5.94	5.93	5.09
	Ash	34.60	35.10	35.60	37.51

The nitrogen contents appeared to show an increase with heating rate when the chars were pyrolysed at 420°C, but a decrease when pyrolysed at 420°C. These trends are tentative and require more work. The nitrogen contents were generally lower for the higher pyrolysis temperature. Sulphur content of the chars appeared to be lower for the chars pyrolysed at the higher temperature and were independent of heating rate.

The calorific value of chars (shown in Table 3.17) pyrolysed to 720°C at 5, 20, 40 and 80°C min^{-1} were independent of heating rate.

Table 3.17 Calorific Values Of Chars Of RDF Pyrolysis.

Heating Rate C min^{-1}	Calorific Value (MJ kg^{-1})
5	19.1
20	20.1
40	18.7
80	19.4

The use of chars as solid fuels may be limited because of the high ash contents. Fig. 3.10 shows the surface areas of the chars formed from the pyrolysis of RDF at 420, 600 and 720°C at heating rates of 5, 20, 40 and 80°C min^{-1}. The surface areas of the char increased with both pyrolysis temperature and heating rate. The solid high molecular weight hydrocarbons shown (7) to be present on the char surface, could become volatilised at the higher temperatures and consequently, increase the surface area of the chars. The surface area of the chars is rather low, but, comparable to certain carbon blacks used in rubber products, for example AS7M designated carbon black numbers N-991 and N-907 nave surface areas of 7 and 11 m^2 g^{-1} respectively. However, the use of chars as carbon blacks does not depend entirely on surface area and other properties such as particle size, ash content and the presence of solid hydrocarbons would limit the use of RDF chars as carbon blacks.

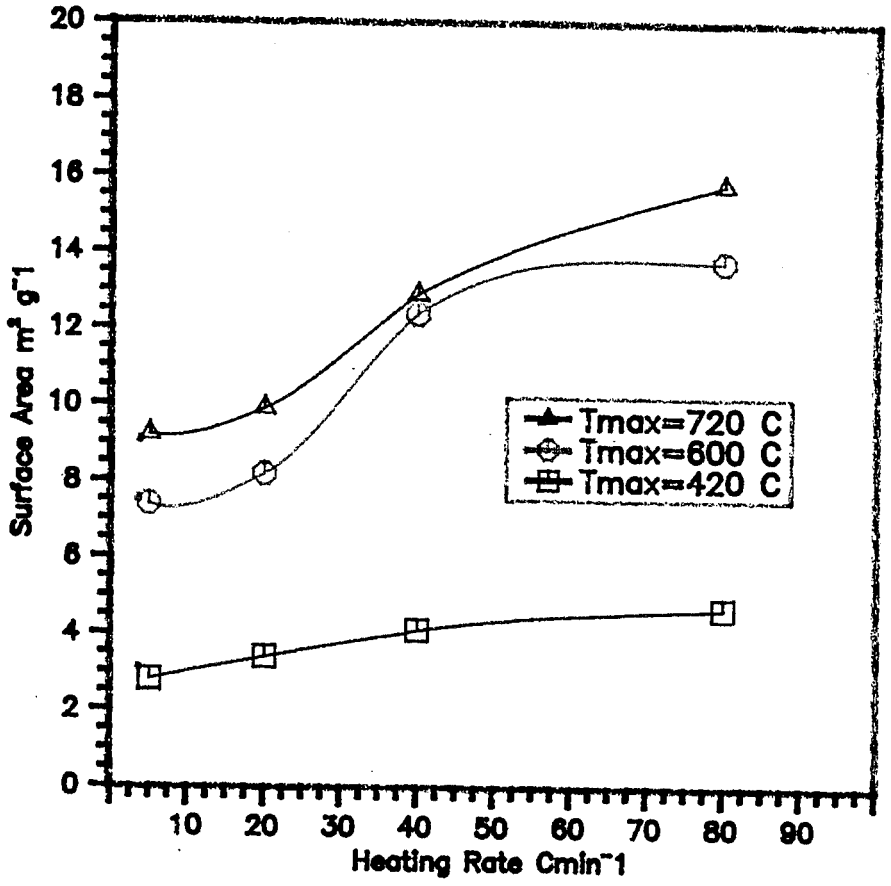

Fig. 3.10. Surface Areas Of Chars For RDF Pyrolysed At 420, 600 and 720°C Versus Heating Rate.

3.2.3 Conclusion

The fixed-bed reactor pyrolysis of RDF showed that as the temperature of pyrolysis was increased, there was a corresponding increase in gas yield from 300°C to 420°C. Above 420°C, the gas yield remained essentially constant. Higher heating rates and temperatures produced the highest conversion of the RDF to oil. The elemental analysis of the oils showed the oils were highly oxygenated. The oil derived from pyrolysis of municipal solid waste is most probably not an economic viability when compared to other

energy from waste schemes. However, the oil from pyrolysis of RDF has been shown by Roy et al (109) to contain chemicals of high economic value, such as maltol (3-hydroxy - 2-methyl - 4-pyrone) which is present in high concentration in the oil.

Gas yields showed dependence on temperature and heating rate. Their calorific value also increased with both the temperature and heating rate. Gas yields may be considered to have the potential to heat the pyrolysis system.

Chars were high in ash content and showed an increase with temperature and heating rate. Also, surface areas of the chars increased with both pyrolysis temperature and heating rate. Chars may be considered as fuel or carbon black, but still need more work.

3.3. Pyrolysis of Scrap Tyre

3.3.1 Introduction

Pyrolysis of rubber and tyre wastes seems a convenient way for recovering energy and reusable chemicals, in fact, rubber and tyres are energy rich wastes.

As defined before, pyrolysis consists of heating solid raw materials in an oxygen-free environment, causing the polymer structure to be ruptured and organic components to thermally degrade through complex reactions.

The most common pyrolysis way is gas-solid contact, which has been tested via various reactor technologies, such as vacuum, fluidised-bed, rotary kiln reactor, screw conveyor kiln reactor,

fixed counter flow bed reactor, retort reactor and for tyres, liquid-solid contact pyrolysis tested by Bouvier et al (117, 142).

The advantages of the pyrolytic treatment of scrap tyres may be significantly enhanced if the process conditions can be used to optimise the final product composition and yield for the required end use.

Pyrolysis of scrap tyres involves a series of complex mass and heat transfer phenomena. This fact must be recognised before any attempt is made to build a capable plant which will turn scrap rubbers into fuels and fine chemicals. Bench scale, process development unit and pilot plant phases are required prior to building a demonstration unit (124).

In this section of research, a fixed-bed reactor was employed to pyrolyse scrap tyre pieces in a nitrogen environment, in order to observe the effects of heating rate and final maximum temperature on the yield of products.

3.3.2 Results and Discussions

Shredded scrap tyre pieces (2-5 cm^2), were pyrolysed in a fixed-bed reactor with nitrogen as the carrier gas at a fixed metered flow rate. The properties of the scrap tyre are shown in Table 3.18.

Table 3.18. Composition of scrap tyre feedstock.

Elemental Composition (% wt)		Gross Calorific Value (MJ kg^{-1})
C	85.9	40.0
H	8.0	
N	0.4	
O	2.3	
S	1.0	
Ash	2.4	

Table 3.19 illustrates the total mass yield results for the tyre samples heated 5, 20, 40 and 80°C min^{-1} to 300, 420, 600 and 720°C. For each heating rate, as the temperature was increased, there was a decrease in the yield of char and an increase in the yield of gas and oil. Dodds et al (118) suggest that higher pyrolysis temperature volatilises some of the solid hydrocarbon content of char, since there is no obvious mechanism for carbon loss.

The maximum conversion of tyre to pyrolysis products occurs up to 600°C, after which there is only a small change in product yield. It was also shown by Dodds et al (118) that the maximum yield of oil occurred at 600°C.

There was only a small effect of heating rate at the rates used at 40 and 80°C min^{-1}, higher gas yields are reached at lower temperatures than at the slower heating rates and there was a corresponding decrease in oil and char yields.

Table 3.19. Yield of tyre pyrolysis products.

	Char (wt %)	Liquid (oil + aqueous) (% wt)		Gas (% wt)
5°C min^{-1}				
300	94.0	3.6	(1.2 + 2.4)	2.4
420	56.0	40.0	(36.8 + 3.2)	4.0
600	40.2	54.0	(49.2 + 4.8)	5.8
720	38.8	54.8	(50.4 + 4.4)	6.4
20°C min^{-1}				
300	92.2	4.2	(3.2 + 1)	3.6
420	54.5	40.8	(39.2 + 1.6)	4.7
600	39.2	54.0	(48.4 + 5.6)	6.8
720	34.0	57.2	(55.6 + 1.6)	8.8
40°C min^{-1}				
300	89.2	6.0	(4.8 + 1.2)	4.8
420	47.3	41.3	(39.6 + 1.6)	11.4
600	33.2	54.8	(52.8 + 2)	12.0
720	29.2	58.0	(56.4 + 1.6)	12.8
80°C min^{-1}				
300	87.6	8.0	(5.6 + 2.4)	4.4
420	41.6	52.4	(50.8 + 1.6)	6.0
600	32.8	54.8	(53.2 + 1.6)	12.4
720	26.4	58.8	(57.2 + 1.6)	14.8

The liquid yield consists of oil and aqueous phases. The amount of aqueous phase for the slow heating rate (5°C min^{-1}) was approximately 4-5%. The amount for rapid heating rates stayed between 1.6-2.4%. The oil content of the liquid phase also increased as the temperature and heating rate increased.

The yield of oil is high, representing the potential of scrap tyres as a substitute for fossil fuels and chemical feedstocks. Kawakami et al (125) obtained 53% oil using rotary kiln. Collin (145), who used a rotary kiln at 700°C, obtained a lower oil yield, of 23%. The oil yields obtained by Kaminsky and Sinn (112) using a

fluidised-bed reactor were 40% and 27% for the temperatures of 640°C and 840°C respectively.

In this research, pyrolysis products were removed from the pyrolysis zone quickly to prevent the occurrence of secondary reactions. Various research groups experimented were high heating rates with rapid quenching of the products and they agree that quick removal of the products favours the formation of liquid products (112, 125, 145). Also, Roy and Unsworth (113) used a fixed-bed vacuum pyrolyser in which the products were removed from the hot zone by vacuum pump. They reported high yields of oil (56.6%) at 415°C. Cypres and Bettens (123) increased the rate of removal of pyrolysis vapours derived from scrap tyres from a secondary hot zone by increasing the flow of nitrogen carrier gas. They found that this increased the yield of oil by reducing the secondary reactions. They also pyrolysed different makes and brands of tyre and found small but significant differences (of the order of 10%) in the yields of solid liquid and gaseous products. The composition of the gas phase hydrocarbons and liquid phase constituents was found to be dependent on tyre type.

The ultimate analyses and calorific values of pyrolysis product oils are shown in Table 3.20. As the heating rate increased, the carbon content of the yields showed a small increase, also, the hydrogen content showed an increase while oxygen and sulphur contents showed a decrease.

The calorific values of the product oils increased by a small amount. Similarly, Roy (124) reported the ultimate analyses of vacuum pyrolysis oil as follows:

C: 85.9%, H: 10.62%, N: 1.35%, O: 1.20%, S: 0.9% and gross heating value of 43 MJ kg^{-1}.

Also, similar calorific values for tyre derived pyrolysis oil have been reported by Kawakami et al (125) for light and heavy oil fractions as 43.9 and 42.5 MJ kg^{-1} and sulphur contents of 1.01 and 1.65% respectively.

Table 3.20. Chemical composition of pyrolysis oil derived from scrap tyres.

	Heating Rate C min^{-1}			
Elemental Composition	5	20	40	80
C	84.3	86.7	87.15	87.6
H	9.8	10.5	10.65	10.7
N	0.4	0.35	0.35	0.55
O	3.68	0.7	0.38	0.02
S	1.82	1.75	1.47	1.13
Gross CV (MJ kg^{-1})	41.99	41.97	42.04	42.25

The pyrolytic oil derived from scrap tyres can be used as a heating fuel and it is grossly classified as a No. 4 ASTM bunker fuel. It can also be refined as a crude oil or upgraded by catalysts and it is reported by Pakdel et al (126) that pyrolysis oils obtained from scrap tyres contain a significant portion of volatile, naphta-like fraction with an octane number similar to petroleum naphta. The benzene, toluene and xylene (BTX) content of the naphta fraction was reportedly high. It was also reported that the naphta fraction

contains approximately 15% limonene, which has a potentially high market value.

In this research, the tyre oil properties tests were also carried out with the oils obtained using AEA-Beven Commercial pyrolyser (this will be discussed in chapter 5).

Detailed analysis of the gas composition from the pyrolysis of the tyre waste revealed the main gases were hydrogen, carbon dioxide, carbon monoxide, methane, ethane and butadiene. There were also lower concentrations of propane, propene, butane and other hydrocarbon gases (Fig. 3.11). The onset of gas evolution occurred at higher temperatures as the heating rate was increased. The main gas evolution also shifted to higher temperature levels as the heating rate was increased.

For example, maximum carbon dioxide evolution occurred at 340°C at 5°C min^{-1} heating rate, 500°C at 20°C min^{-1}, 530°C at 40°C min^{-1} and 560°C at 80°C min^{-1}. Also, the volume of each gas increased with increasing heating rate. Roy and Unsworth (113), Douglas et al (145) and Kaminsky and Sinn (112) have also shown the gas phase to mainly consist of hydrogen, carbon dioxide, carbon monoxide and hydrocarbons including methane, ethane, ethene, propane, propene, butene, butadiene and butane.

Thermaldecomposition of the hydrocarbon polymers making up the tyre gives rise to the resultant gases. Butadiene for instance is derived from the breakdown of the polymer butadiene styrene-rubber used in the manufacture of the tyres.

The structure of a natural rubber molecule is shown in Fig. 3.12.

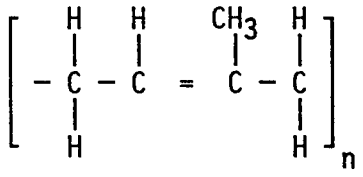

Fig. 3.12. Structure of natural rubber molecule.

The presence of double bonds in the molecular chains and preferred location for thermal rupture of the carbon-to-carbon bonds are the main characteristics of all vulcanisable elastomers.

The rubber used in tyre manufacture are characterised by carbon-carbon double bonds within the rubber molecule. The presence of the double bonds directs the thermal rupture to the B location, which is the second carbon-carbon bond from the double bond.

During the thermal degradation, highly reactive free radicals are formed by the propagation of the chain rupture. The free radicals tend to be sub-chains of the original rubber molecule. This is the explanation for the presence of styrene, butadiene and alkanes in the pyrolysis products.

The predominant monomers of styrene and polyaromatic hydrocarbons (PAH) such as benzene, toluene, naphthalene and phenanthrene would be expected through reactions of styrene. Also, the ethylene compounds disappear at higher temperatures. They are aromatised producing H_2 and CH_4 in accordance with the following general reactions (123).

$$C_4H_8 + C_2H_4 \longrightarrow C_6H_6 + 3H_2$$

$$C_4H_8 + C_3H_6 \longrightarrow C_6H_6 + CH_4 + 2H_2$$

Lee et al (192) list the relative carcinogenicities of certain PAH, they show that chrysene, benzofluoranthene and benzo(e)pyrene give positive results in carcinogenity tests. Longwell (193) has also shown that phenanthrene and methylphenanthrenes give positive results in human and bacterial cell tests.

The biologically active PAH, such as phenanthrene and naphthalene are found in the tyre pyrolysis oils in high concentrations. Consequently, the tyre pyrolysis oils may be a health hazard (this will be discussed in chapter 7).

Figure 3.13 shows the total yield of each gas when the tyres were heated to 720°C. It is seen that for most gases, as the temperature was raised, there was an increase in the volume release of gases with heating rate.

The gases generated have a significant calorific value. The total calorific values of the gases are shown in Table 3.21.

The increase in the total gas emission with heating rate, corresponds with the decrease in oil yield. Kaminsky and Sinn (112) reported an increase in methane, hydrogen and other hydrocarbon gases on increasing the reactor temperature from 640°C to 840°C.

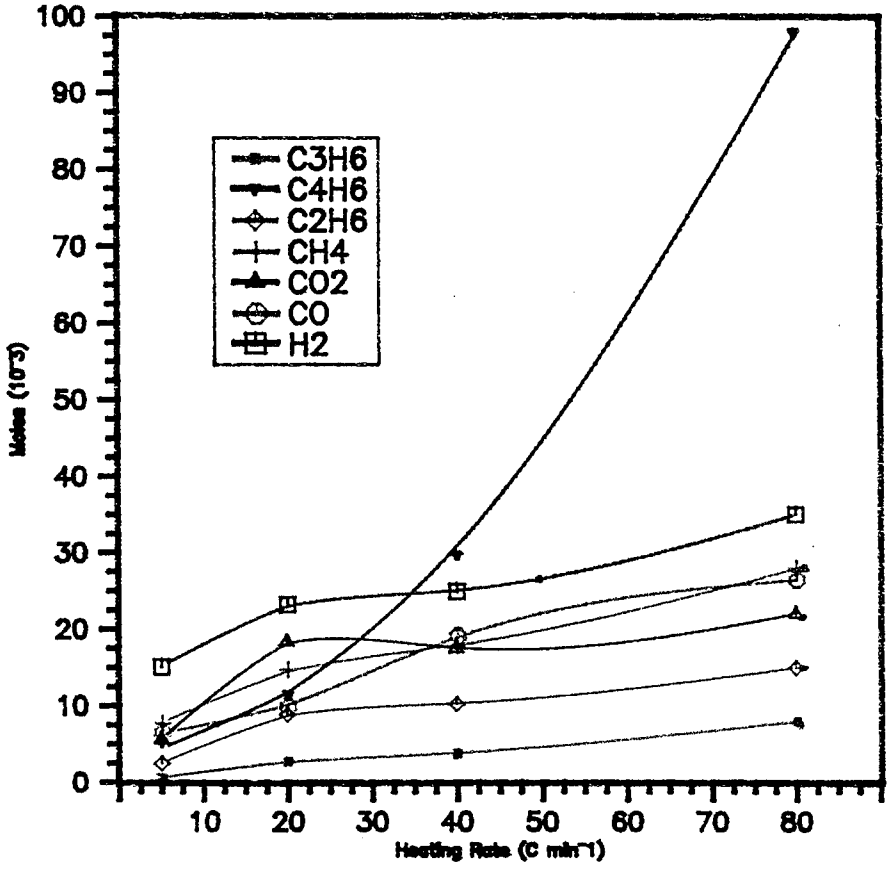

Fig. 3.13. Total gas yields evolved from pyrolysis of scrap tyres versus heating rate.

Table 3.21. The calorific values of total gas yield of tyre pyrolysis gases.

Heating Rate	Calorific Value ($MJ\ m^{-3}$)
5	36.37
20	38.56
40	51.95
80	64.68

Table 3.19 illustrates that char yields decreased as the final temperature and heating rate increased. Elemental compositions and calorific values of the chars are shown in Table 3.22.

Table 3.22. Elemental composition of pyrolysis chars derived from scrap tyres.

	Heating Rate C min^{-1}			
Elemental Composition	5	20	40	80
C	84.6	84.82	84.9	85.71
H	0.78	0.66	0.68	0.75
N	0.08	0.07	0.05	0.06
O	1.46	1.34	1.52	0.58
S	2.5	2.47	2.15	2.32
Ash	10.58	10.66	10.7	10.58
Gross Calorific Value (MJ kg^{-1})	28.7	29.14	29.02	29.2

The carbon contents increased in small amounts corresponding with the small increase in heating value as the heating rate increased. The other content of chars show independent characteristics from heating rate. Bilitewski et al (121) measured the heating value of tyre char as 31.4 MJ kg^{-1} and carbon content of approximately 87% weight.

Figure 3.14 shows the surface areas of the chars formed from the pyrolysis of tyres at 420, 600 and 720°C at heating rates of 5, 20, 40 and 80°C min^{-1}. It is seen that the surface areas of chars increase with both pyrolysis temperature and heating rate.

Wolfson et al (146) determined surface areas of between 19 and 40 $m^2\ g^{-1}$ for char from pyrolysis of heavy duty truck tyres.

Bilitewski et al (121) measured tyre char surface areas between 40 and 80 $m^2\ g^{-1}$ for a variety of reaction conditions. Dodds et al (118) showed that the solid fraction derived from tyre pyrolysis contains carbon black and a solid hydrocarbon residue which is reduced by increasing the pyrolysis and heating rate. Removal of the solid hydrocarbon residue would increase the surface area of the char and improve the carbon black properties of the char. The surface is high and comparable with the surface area of carbon blacks used in rubber products including tyres.

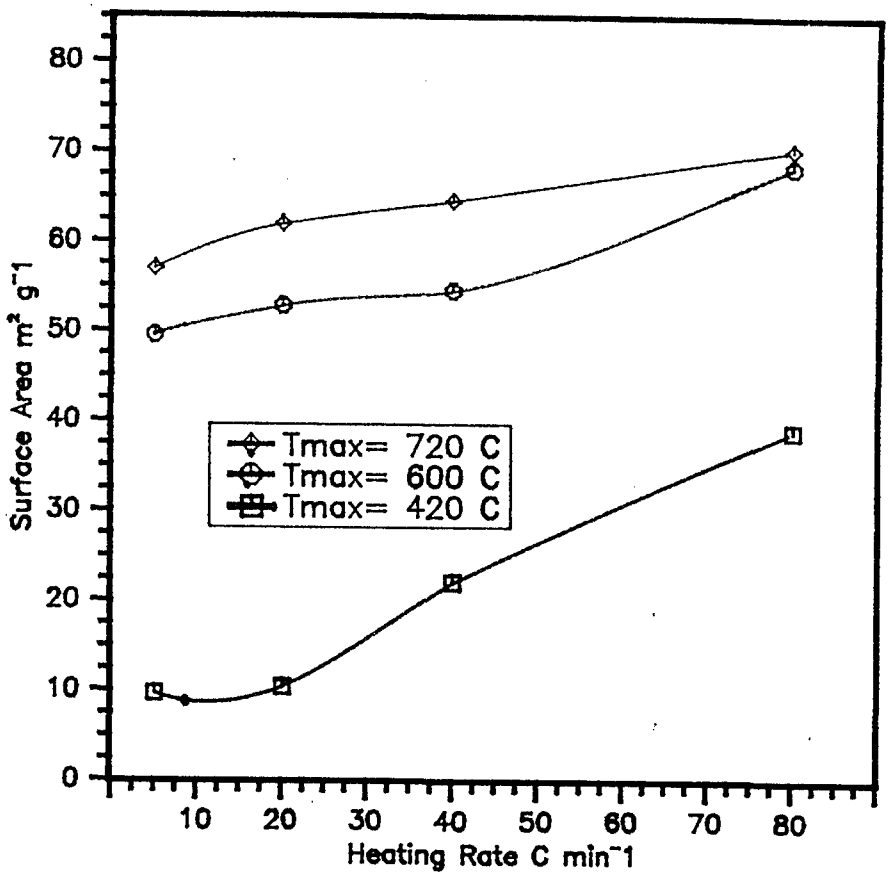

Fig. 3.14. Surface areas of chars obtained from tyre pyrolysis.

Roy (124) reported the surface area of char from vacuum pyrolysis of tyre as 60 m^2 g^{-1}. Carbon black samples produced at a pilot plant were shipped to two rubber product manufacturers. It was concluded that this carbon could partially replace commercial blacks for the preparation of low grade rubber parts. Manufacturers also concluded that chars could be used as a substitute up to 20-40% of N-990 and N-774 commercial grade. Roy (124) also concluded that carbon blacks produced from vacuum pyrolysis have numerous potential uses including reinforcement or semi-reinforcement for bicycle tyres, shoes, auto flaps, foot wear, conveyor belts and dock fenders.

The carbon black samples, namely N-351 and N-650, have nitrogen absorption surface areas of 73 m^2 g^{-1} and 38 m^2 g^{-1} respectively (147). The quality of carbon black is also important with a number of properties including particle size, shape and purity as well as surface area to be considered (118).

Kawakami et al (125) have shown that the physical properties of tyre derived carbon black, such as tensile strength, elongation and hardness are dependent on the type of tyres used and the pyrolysis conditions at particular temperatures.

Roy (124) reported the compared results of tyre char properties with various carbon black samples such as surface area, iodine index, volatile matter, tint strength, ash and pH.

From the results of this research, along with information from the literature, it can be concluded that char from scrap tyre pyrolysis cannot be satisfactorily reutilised without further treatment.

The char may be effectively activated and improved in quality.

3.3.3 Activation of Chars

The scrap tyre pyrolysis chars were activated by keeping the chars in a Gray-King furnace for 20 minutes and 1 hour in order to determine the pore size distributions of the activated chars and investigate the improvement in their surface areas. Fig. 3.15, a, b, c and d show the pore size distribution curves and Table 3.23 gives the surface areas of the activated chars.

The surface areas show an increase after activation of 20 minutes and 1 hour. The increase in surface area is more significant for the chars obtained from the maximum temperature of pyrolysis of 420°C. The total area of all pores to 16 Å radius was found as 39.0 $m^2\ g^{-1}$. This surface area is less than the one calculated with BET, because this calculation does not include the surface area contributed by micropores. Somehow, an area larger than the BET area would be exhibited by ink-bottle pores in which a larger volume of gas is condensed in pores having a relatively small area.

From the activation of chars, it can be concluded that the surface areas of the chars from the pyrolysis of scrap tyre, can be increased by activation.

Table 3.2.3 The Surface Areas of the Scrap Tyre Chars After Activation (m^2 g^{-1})

Heating Rate $Cmin^{-1}$	Before Activation	20 minute Activation	1 hour Activation
Max Temp = 420°C			
5	9.72	34.3	64.5
20	10.4	37.0	66.2
40	22.08	38.2	67.3
80	39.37	42.3	71.8
Max Temp = 720°C			
5	57.0	59.3	64.9
20	62.57	62.9	65.6
40	64.68	65.1	65.9
80	70.49	72.1	73.9

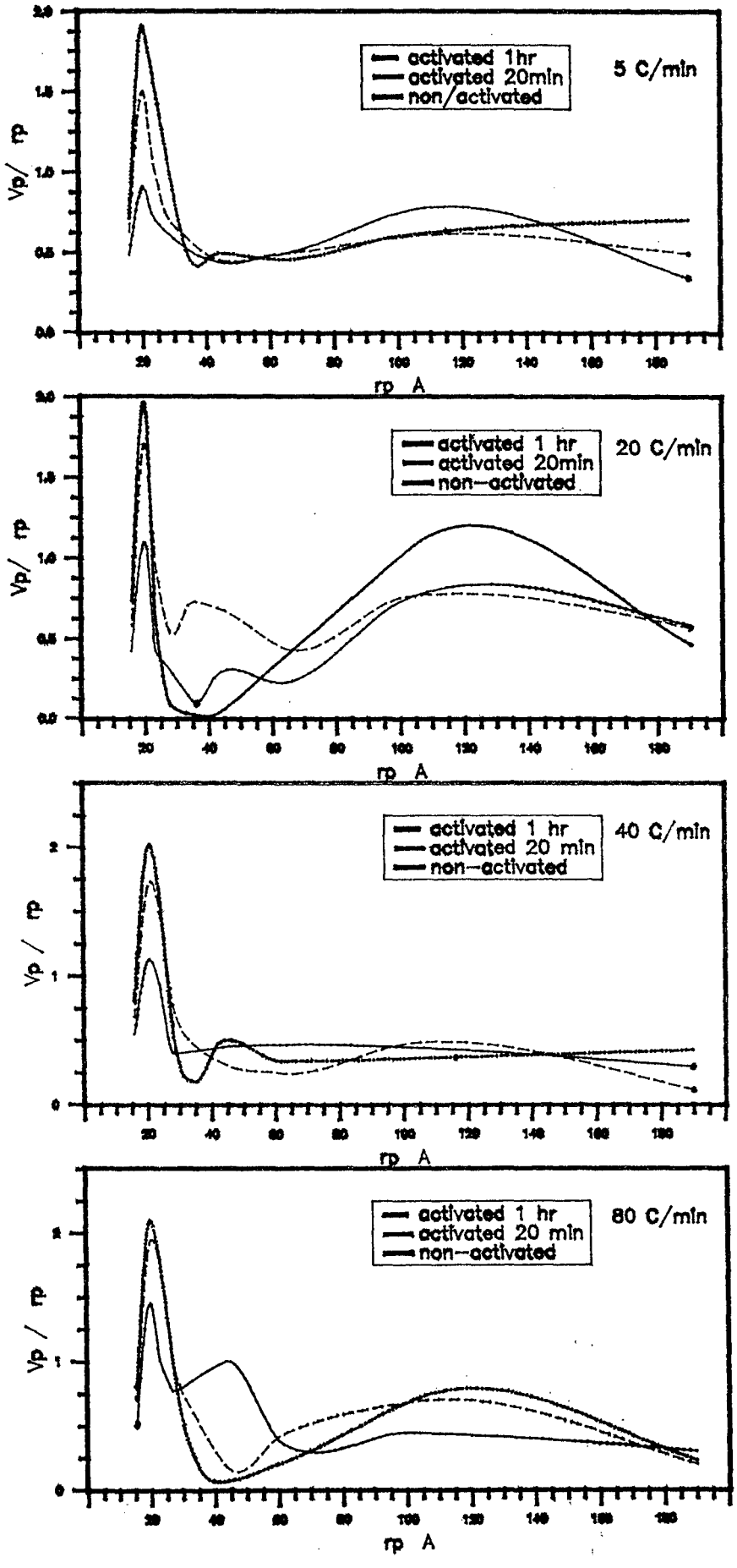

Fig.3.15 Pore Size Distribution of Tyre Chars

CHAPTER 4

FLUIDISED BED REACTOR PYROLYSIS

4.1 Introduction

The work presented in this chapter is concerned with the fast pyrolysis of biomass and waste material in a fluidised bed reactor.

As indicated earlier (Chapter 1), pyrolysis technologies can be classified into different groups depending on heating rate, residence time and maximum temperature employed.

Fast pyrolysis is defined by Beenackers and Bridgwater (15) as heating at fairly high heating rate up to a maximum temperature of 650°C, with a residence time of 0.5 - 5s. Liquid is the major product from fast pyrolysis processes.

Fast pyrolysis is usually carried out at or near atmospheric pressures. It requires small particles as well as a reactor configuration capable of very high heating rates. One of the most appropriate designs is the fluidised bed reactor, in which nearly all fast pyrolysis, moreover, flash pyrolysis studies are carried out.

The temperature is a very important parameter in a fluidised bed, where heat is transferred extremely quickly from fluidised-sand to waste particles. Also, if the residence time of the tar vapours produced in the bed is long enough, then further cracking will occur to low molecular weight hydrocarbon gases, CO, CO_2 and N_2.

Nimmo (195) reports that the formation of primary products at low temperatures (< 500°C) is difficult to monitor since they quickly react to form other final products, mainly tars through

polymerisation reactions. On the other hand, at higher temperatures (> 500°C), information regarding the primary reaction steps can be obtained from the final products since they often closely resemble the primary products or in fact are themselves the primary products.

In this part of the research, two biomass samples which were wood and rice husks and RDF and scrap tyre samples were pyrolysed in a fluidised-be reactor whose technical properties were described in Chapter 2.

The pyrolysis experiments were conducted at two different temperatures of 400°C and 550°C. For wood samples the effects of bed depth and particle size were also investigated for the reaction temperature of 550°C. The temperature profile is seen in Fig. 4.1. The theromocouples were located as follows, 1 was the pre-heater zone, 2 and 3 were the bed temperatures and 4 and 5 in the freeboard.

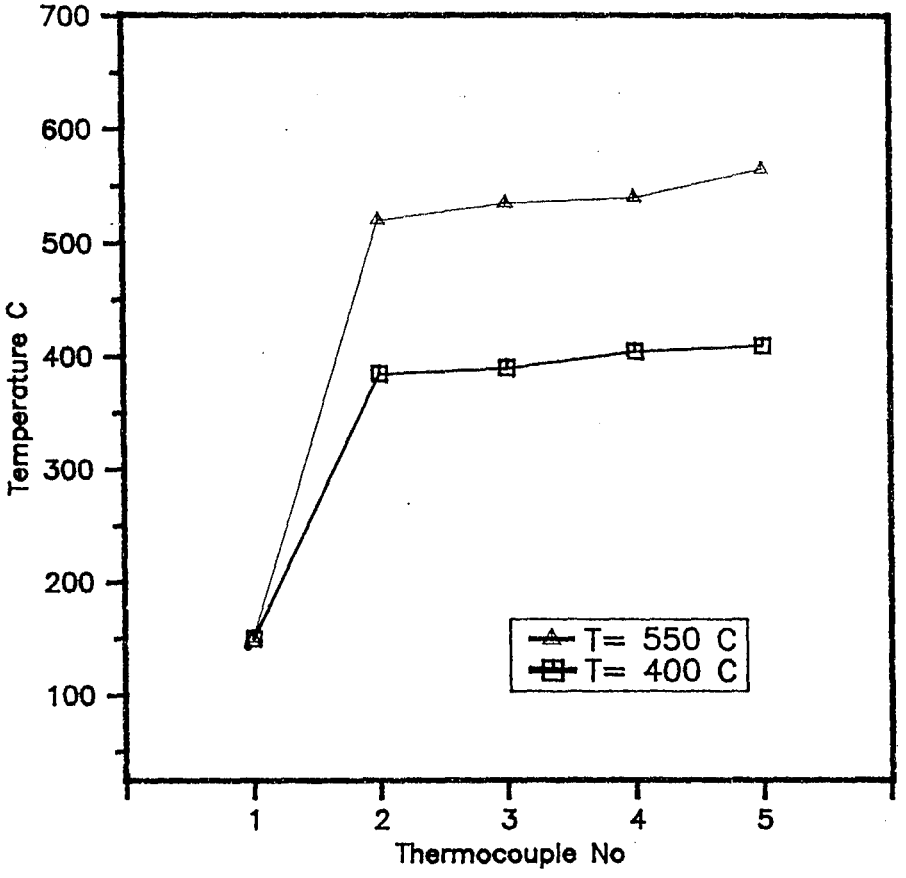

Fig. 4.1 Temperature Profile of the Fluidised-Bed

Pyrolyser Experiments

4.2. Fast Pyrolysis of Biomass

In recent years, a number of published works have appeared about pyrolysis of biomass in fluidised bed reactors. In these processes, the products are gases, chars, tars and light oils. The results of research carried out by different authors differ one from the other due to numerous factors. Therefore, the comparison of these result with one another or extract a certain conclusion is rather difficult.

The product distribution of biomass pyrolysis in a fluidised bed depends on;

(1) Pyrolysis environment (N_2, CO_2, Steam etc).

(2) Type of biomass.

(3) Size of biomass.

(4) Pyrolysis temperature.

(5) Pressure.

(6) Presence or absence of primary catalysts.

(7) Heating rate.

(8) Amount of char since the char has some catalytic effect on the yield production.

(9) Fluidised velocity.

(10) Bed depth.

(11) Type of solid bed.

It is also reported that the scale or size of the reactor has influence on the product distribution.

4.2.1 Fast Pyrolysis of Wood

As it is described by Scott and Piskorz (197), the pyrolysis of wood is an ancient art. Earlier wood pyrolysis was performed to produce many basic organic chemicals such as acetone, acetic acid and methanol. The wood pyrolysis was also practised as a method of producing charcoal. However, recently the importance of the rapid heating of wood particles has drawn more attention than slow heating.

Fast pyrolysis of wood is carried out at moderate temperatures, typically from 400°C to 550°C in which the yield of condensable products is maximised at the expense of gas and char yields. Short vapour and solid residence times are required bo maximise the desired products and to prevent the occurrence of secondary decomposition reactions (198).

In wood pyrolysis, since the cellulose is the most important content of wood, it can be said that cellulose pyrolysis would help to understand more about the pyrolysis of wood.

Cellulose is a polymer of d-glucose and the work of Piskorz et al (76) showed that the high yields of hydroxyacetaldehyde derive primarily from fragmentation of this polymer chain.

It was reported that (78) the native cellulose in wood gives significant yields of hydroxyacetaldehyde and other low molecular weight oxygenated compounds, but low yields anhydrosugars while highly altered micro-crystalline cellulose gives the reverse.

In fast pyrolysis, the decomposition of cellulose can follow one of two major pathways, each of which is capable of minor

rearrangement reactions in order to account for the variety of different products observed.

The morphology of cellulose, degree of polymerisation and temperature will determine the choice of major decomposition pathway (Fig. 1.19).

In this part of the work, wood particles (< 0.5 cm) were pyrolysed at two different temperatures of 400°C and 550°C. The wood samples had the same physical properties of those used in the fixed-bed pyrolysis experiments. The experimental information is summarised in Table 4.1.

After building up the fluidised bed reactor, during the test runs it was seen that the condenser part was inadequate to condense all the vapours derived, therefore, the condenser part was extended with another set of condensers.

At identical experimental conditions, the extended condenser system gave more liquid than the former design, but at the same time, char yields were the same from both types.

Suggesting that the condensing section was not efficient since the liquid yield was still lower than the yields of different groups who carried out similar experiments and a mass balance of the product streams did not approach 100%. Several further configurations of condenser were used to improve the condenser system and increase the yield of liquid product.

Table 4.1. Pyrolysis of Wood in The Fluidised-Bed Reactor

Temperature (°C)	400	550	550	550
Vapour Residence Time (s)	10	10	10	8
Particle Size (cm)	0.5	0.5	0.1	0.5
Max Fluidisation Velocity (cm s^{-1})	2.9	2.9	2.9	2.9
Bed Depth (cm)	10	10	10	5
Feed Rate (g min^{-1})	16	15	12	16
Yields				
Liquid	19	16	21	20
Char	27	24	20	22
Gas (real)	48.65	52	48.8	51.2
Gas (by difference)	54	50	59	58
Gas Analysis	%	%	%	%
H_2	6.7	7.5	7.1	5.9
CO	14.65	15.4	16.1	15.1
CO_2	14.3	12.5	12.6	11.4
CH_4	4.9	6.7	4.5	6.9
C_2H_6	3.7	4.3	4.5	7.1
C_3H_8	1.8	2.3	1.5	1.5
C_3H_6	1.9	1.5	2.1	2.4
C_4H_{10}	0.7	1.2	0.4	0.9
Total	48.65	52	48.8	51.2
CV MJ m^{-3}	16.7	17.7	17.8	17.1

Subsequent designs incorporating an off gas sample with seven condensers in series have shown an improvement in the condenser efficiency. Unfortunately, due to the lack of time, the liquid yield could not be increased more. The maximum liquid yield was about 22%. In the literature, the liquid yield was reported as 60% by Scott and Piskorz (197).

Corella et al (196) has reported the difficulty of comparison of the results from different research groups. They compared their results with those of two different research groups and the results were all different. Also, the char yields of this work were not as low as the char amounts reported in the literature (196, 78). However Bridgwater and Bridge (18) compared different pyrolysis technologies and they reported the char yield from fast pyrolysis experiments were about 7 - 20%.

When the temperature increased from 400°C to 550°C, it was seen that the gas yield increased while the char and liquid yields decreased. The gas yield increases at high temperatures at the expense of char and liquid yield in fast and flash pyrolysis systems. Also, in this work, secondary reactions probably affected the gas yield because the product vapours residence time in the hot zone was in the range of 10 - 12 seconds.

Residence time is one of the most important parameters which affect yield amount and nature. Because of the lack of time, the effect of flow rate and residence time could not be investigated. However, Stiles (21) suggests that decreased flow rates which creates longer residence times would affect the yields and it was reported by him that char and tar amounts decreased and gas amount increased with the decreased flow rate.

The yield and calorific value of the gases also increased with the increased temperature.

From the gas analysis, the calculated gas yield was lower than the amount calculated by difference. The difference for the

temperature of 400°C was 5% and for 550°C 10%. This was most likely caused by the inadequate condenser system.

Piskorz et al (77) have reported from fast pyrolysis of different woods, observed similar gas composition, but lower amounts than this research. This could be explained again by the inefficient condenser system.

Table 4.1 shows the influence of particle size for the 550°C reactor temperature. For the particle sizes 0.1 cm there was a lower production of char and increased production of liquid compared to the 0.5 cm particle size. Also, the bed depth at 550°C was compared at 5 cm and 10 cm, this comparison also coinciding with a reduced vapour residence time for the shallower bed. The results showed that liquid yield was increased and char yield decreased.

Table 4.2 shows the properties of the liquid from the fluidised bed reactor. The oils from the fluidised bed show an increase in calorific value over the static batch reactor oils.

Rapid pyrolysis such as that found in the fluidised bed reactor has been shown to produce lower viscosity oils indicating more volatile compounds compared to slow pyrolysis oils such as those produced in the static batch reactor (18). In addition, oils from slow pyrolysis tend to have higher water contents than rapid pyrolysis oils (18). Both these factors would produce higher calorific values in the fluidised bed pyrolysis oils.

Table 4.2. Properties of Wood Oil Derived From Fluidised bed Reactor.

	wt (%)
C	58.04
H	8.02
N	0.1
O	33.24
S	0.24
Calorific Value ($MJ\ kg^{-1}$)	28.9

4.2.2 Fast Pyrolysis of Rice Husks

The rice husks samples were pyrolysed in the fluidised bed reactor at the identical experimental conditions to those of wood. The reason for employing the rice husk was to compare the oil characteristics and liquid yields from fixed-bed and fluidised bed reactors in order to achieve the re-utilisation of agricultural wastes. Scott et al (197) suggest that it is possible to use any lignocellulosic material and to obtain similar results to those obtained with wood. Although there will be differences in overall yields of gas, liquid and char as well as in specific compounds because of the wide variations in holocellulose/lignin amounts as well as in the amounts of a number of impurities.

Another reason was to investigate the efficiency of the reactor in which pyrolysis of different biomass waste materials was carried out without doing any changes in reactor configuration for the different types of waste.

Peel (199) suggests that agricultural residues are mostly seasonal and would need to be used in conjunction with other fuel resources in order to provide year round operation. A reactor using these residues would therefore need to be suitable to pyrolyse all kinds of wastes.

Scott et al (197) emphasize that employing lignocellulosic materials would also be very useful in the research of fast pyrolysis with fluidised bed reactors.

The introduction of fluidised bed technology may bring advantages in convenience, efficiency and versatility in the re-utilisation of biomass and biomass waste.

The rice husks samples whose physical properties are reported in Chapter 3, were pyrolysed at 400°C and 550°C in a fluidised bed reactor. During the experiments, there were still condensing problems as in the experiments with wood.

The pyrolysis information is summarised in Table 4.3. Similarly to wood, in rice husks pyrolysis experiments, the liquid and char yield decreased with the increased temperature. Conversely, the gas amount increased with the increased temperature.

When the liquid yields are compared with the fast pyrolysis of wood, it is seen that the rice husks pyrolysis oils are lower than wood oils.

Scott et al (197) also obtained lower liquid yields from agricultural biomass and they generalise that the yields of products obtainable may be roughly estimated from a knowledge of the amounts of each of the three main lignocellulosic constituents.

The physical properties of oil derived from rice husks pyrolysis in fluidised bed reactors are seen in Table 4.4.

As in wood oils, the rice husk oils from fluidised bed pyrolysis reactors show an increase in calorific value over the static batch reactor oils.

The biomass derived pyrolytic oils have a significant calorific value and could be used directly as fuels although they are clearly highly oxygenated, which influences the viscosity and calorific value of the oils.

Table 4.3. Pyrolysis of Rice Husks

Temperature (°C)	400	550
Vapour Residence Time (s)	10	8
Particle Size (cm)	< 0.5	< 0.5
Min Fluidisation Velocity (cm^5)	2.3	2.3
Gas Flow Rate (cm^5)	8.7	8.7
Bed Depth	8	8
Feed Rate ($g\ min^{-1}$)	12	12
Yields		
Liquid	19	17.5
Char	38	34
Gas (real)	33	38.1
Gas (by difference)	43	48.5
Gas Analysis		
H_2	4.2	5.3
CO	11.8	12.3
CO_2	9.9	10.9
CH_4	4.3	4.9
C_2H_6	1.8	2.1
C_2H_4	0.8	1.4
C_3H_6	0.2	1.2
Total Gas CV ($MJ\ m^{-3}$)	33	38.1

Table 4.4 Properties of Rice Husks Oil Derived From Fluidised bed Reactor

C	56.00
H	6.35
N	1.45
O	35.89
S	0.31
Calorific Value (MJ kg^{-1})	26.2

The distillation range by gas chromatography simulated distillation for the derived oils compared to refined petroleum products are shown in Fig. 4.2.

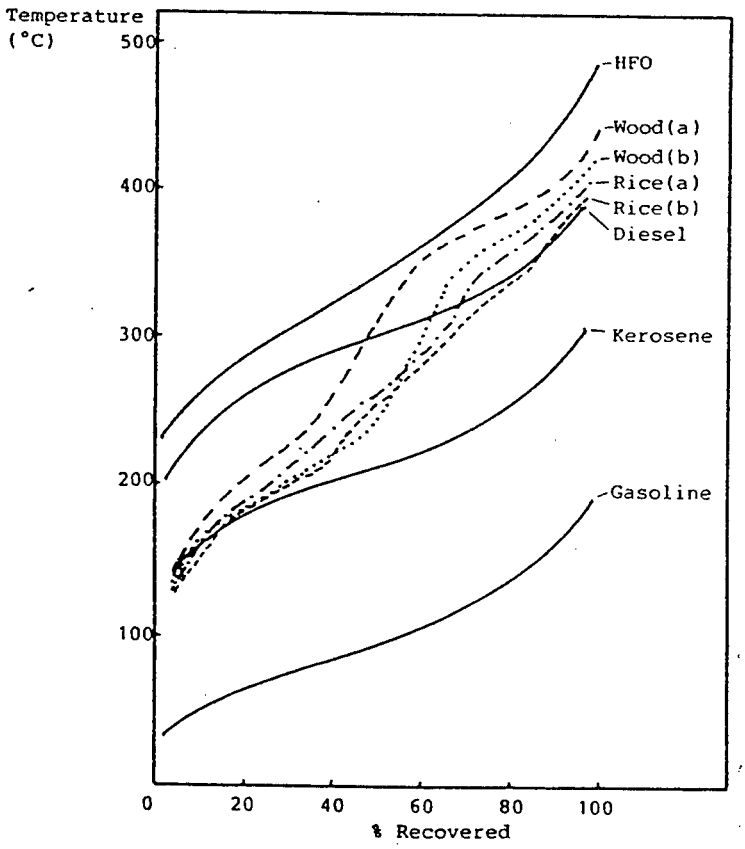

Fig. 4.2. Distillation Range of Biomass Derived Pyrolytic Oils (HFO: Heavy Fuel Oil, a: Fixed-bed, b: Fluidised bed)

The first distillation fraction for the fixed-bed and fluidised bed reactors for biomass oils were similar to kerosene. However, the middle distillation range showed the high molecular mass range of the oils with high boiling point compounds being present approaching heavy fuel oil. The slow pyrolysis static batch reactor produced higher distillation range oils compared to the more rapid pyrolysis in the fluidised bed pyrolyser.

The distillation range of oils shows that they could be added to petroleum refinery feedstocks to produce refined fuels, however, the oils are highly oxygenated. The production of liquid fuels from biomass has a number of advantages over other energy recovery from biomass systems in that since the fuel is liquid, it can be stored and transported and hence, does not have to be used at or near the recycling plant.

The pyrolysis process produces a char which can be used as a solid fuel or as a char/water or char/oil slurry liquid fuels. The fluidised bed reactor gives chars with a calorific value of 25.9 MJ kg^{-1} and 15.4 MJ kg^{-1} for wood and rice husks respectively.

The calculated overall calorific values of the gases based on composition and yield from the fluidised bed were 16.5 MJ m^{-3} and 15.4 MJ m^{-3} for wood and rice husks respectively. The total calorific value of the gases increased with the reaction temperature. Also, the calorific values of gases from the fluidised bed are higher than the calorific values of the gases from the fixed-bed reactor.

4.3. Fast Pyrolysis of RDF

The various contents of refuse derived fuel undergo distinctly separate physical processes. As Nimmo (195) reports, the effect of heat on the organic or combustible fractions can be represented simply

$$\text{Fuel} \longrightarrow \text{Char} + \text{Volatiles}$$

The residual char enters the solids circulation pattern in the bed while the volatiles enter the upward flowing stream of fluidising gas. The individual particles behave differently on heating. Where paper pyrolyse and char rapidly, the plastic contents melt before releasing volatiles thereby producing a char of porous nature. The char produced from paper is more prone to attrition or breaking down by abrasion to eventually be elutriated from the bed. Plastic materials because of their melting characteristics may cause agglomeration with sand. Nimmo (195) argues that those agglomerates are dense lumps which sink to the bottom of the bed and cause disruption to the fluidising pattern.

Also, the inert fractions if present can cause problems such as agglomeration, defluidisation etc.

In this work the RDF employed was in the form of municipal solid waste where the inert fraction had largely been removed.

In their work, Schoeters and Buekens (104) proposed a decomposition pattern for the thermaldecomposition of synthetic polymers as follows:

(1) Depolymerisation into monomer

(2) Random fragmentation of the polymer chain yielding a broad spectrum of products.

(3) Charring of the polymer chain accompanied by the evolution of cracking products.

Koo et al (107) also reported similar decomposition patterns to the above:

(1) Depolymerisation (thermaldecomposition) producing monomer or other small molecules.

(2) Chain fragmentation producing low molecular weight materials.

(3) Production of unsaturated and aromatic compounds by radicals.

(4) Char formation.

The final products include gas (saturated and unsaturated compounds), oil (saturated, unsaturated and aromatic compounds) and char.

It was also suggested that the recycling of polymer waste by thermal conversion into its monomer is restricted to only a few types of polymers. The others yield products that are especially suitable as fuel (202).

Cameron (202) reports the yield of monomer on pyrolysis of some most common polymers (Table 4.5). According to Cameron (202), polyethylene does not give monomer. The pyrolysis of polyethylene was revealed to be on the basis of a free radical mechanism by Tsuchiya and Sumi (100). Conversely, they suggest that initiation consisted of the preferential scission of weak bonds caused by the

irregularity in the polymer chain and by random scission of ordinary carbon-carbon bonds. The propagation reaction produced the ethylene monomer.

Table 4.5. Yield of Monomer on Pyrolysis of Some Polymers

Polymer	Monomer Yield %
Polytetrafluoroethylene	99
Polymethylmetacrylate	98
Polystyrene	45
Polypropropylene	2
Polyethylene	0

For the thermaldecomposition of polystyrene, Cameron and Maccallum (203) suggested that the initial decomposition occurs randomly through weak link scission. Various pyrolysis products are then formed by intra-molecular H-transfer at the chain end.

Koo et al (107) report that the formation of aromatic compounds from pyrolysis of plastics can be explained by the Diels-Alder theory. The yields of these products can be controlled by reaction time, pyrolysis temperature and the ratio of plastics in the feedstock.

In this work, the formation of aromatic compounds in pyrolysis oils will be discussed in Chapter 7.

The RDF pellets were firstly shredded, but the feeding of them into the reactor was unsuccessful. To solve this problem, the RDF pellets were kept in liquid N_2 for 15 minutes, then smashed by a hammer into particle size of 0.2 - 0.5 cm. The pyrolysis experiments

were carried out in the fluidised bed reactor which was employed in the biomass pyrolysis experiments.

The feeding problem was solved for the time being with liquid N_2, but the author believes that using a screw feeder would solve easily the feeding problems of such samples. The experimental conditions and results are summarised in Table 4.6.

The char yield decreased as the temperature increased. The liquid yield did not show significant change, but gas yield increased with the increased temperature.

The cellulose content of the RDF affects the thermaldecomposition pathway since the cellulosic materials constitute over 50% of RDF.

Nishizaki et al (106) pyrolysed polystyrene chips in a fluidised bed reactor and obtained more than 50% oil.

Increased temperature changed the properties of the oil which showed a lower viscosity compared to the oil from the fixed-bed. During the experiments the main problem was plugging in the condenser tubes. Apart from problems of efficient condensation, RDF pyrolysis in the fluidised bed did not cause any major problem. Also, there was no sign of carbon build up or deposition on the reactor walls.

The calorific value of the oil yield increased with the increased temperature from 23.6 to 24.7 MJ kg^{-1}. As reported in Chapter 3, RDF pyrolysis oils from fixed-bed reactors were dried then their calorific values were measured. In this part of the work, the calorific values of pyrolysis oils were determined as soon as they were removed from the reactor and without any pre-treatment.

Gas analysis shows that main gas yields are H_2, O, O_2 and Hydrocarbon gases to C_4. The amount and calorific values of the total gas yields did not change significantly with the increased temperature of pyrolysis.

Kaminsky et al (103) pyrolysed polyethylene (PE), polyvinylchloride, PVC and polystyrene (PS) separately and the mixture of polyethylene and polyvinylchloride in a fluidised bed reactor. They observed similar gas compositions.

Schoeters and Buekens (104) also observed similar gases from polyethylene pyrolysis in a fluidised bed reactor

Char calorific values are also significant from fast pyrolysis of RDF. For the reaction temperature of 400 and 550°C chars calorific values of the chars were 15.0 and 15.8 MJ kg^{-1} respectively.

The experimental results showed that the fluidised bed employed in the experiments to pyrolyse biomass materials can also be used to pyrolyse RDF without doing any major redesign work apart from the problems of efficient condensation of pyrolysis oils.

Table 4.6. RDF Pyrolysis in Fluidised bed Reactor

Temperature °C	400	500
Bed depth (cm)	10	8
Sand particle size (mm)	0.1-0.3	0.1-0.3
Minimum fluidising velocity (cm s^{-1})	2 - 9	2 - 9
Residence time (s)	10	10
Expanded bed height (cm)	40	40
Feed rate (g min^{-1})	20	20
Yields		
Liquid	23	23.5
Char	31	28
Gas (real) (by difference)	34.3 46	36.1 48.5
Gas Analysis		
H_2	6.9	8.3
CO	8.2	8.9
CO_2	9.8	9.8
CH_4	4.1	5.3
C_2H_6	2.4	2.4
C_3H_8	1.8	2.1
C_3H_6	0.7	0.9
C_4H_{10}	0.4	0.5
Total	34.3	36.1
Calorific Value (MJ m^{-3})	16.05	16.2

Fluidised bed pyrolysis of RDF seems one of the best ways to re-utilise the waste materials while producing energy, the system consumes waste which is one of the most important issues of today.

Table 4.7. Scrap Tyre Pyrolysis

Temperature °C	400	550
Bed depth (cm)	8	8
Sand size (mm)	0.1 - 0.3	0.1 - 0.3
Min fluidisation velocity (cm s^{-1})	2.9	2.9
Residence time (s)	12	12
Expanded bed height	40	40
Feed rate (g min^{-1})	20	20
Yields		
Liquid	22	20
Char	38	54
Gas (real)	33.9	37.9
(by difference)	42	43.6
Gas Yields		
H_2	4.5	4.9
CO	4.2	5.2
CO_2	3.6	3.9
CH_4	3.9	4.6
C_2H_6	4.3	4.9
C_4H_6	7.8	8.4
C_3H_6	3.2	3.5
C_3H_8	2.4	2.5
Total	33.9	37.9
CV (MJ m^{-3})	26.4	32.4
Liquid CV (MJ kg^{-1})	42.1	43.09

In rapid pyrolysis of scrap tyres, it was found that the char and liquid yields decreased with the increased temperature. Conversely, gas yields increased with the increased temperature.

Kaminsky and Sinn (112) reported similar char yields of scrap tyre pyrolysis in a fluidised bed reactor. The liquid yield was found to be 27% by them.

From pyrolysis of different brands of tyres, Cypres and Bettens (123) obtained a liquid yield in the range of 38% - 42%, char yield between 41% - 45% and gas yield between 16% - 19%. Some researchers also reported similar gas composition in this research, but, depending on the tyre employed gas yields percentages varied.

Kawakami et al (125) observed 40% char and 53% oil from scrap tyres in pilot plant at rapid heating conditions.

Pakdel et al (126) reported that 55% oil and 25% carbon from rapid pyrolysis of scrap tyres in a vacuum reactor.

In this research, the liquid yields vary in the range of 20% - 22% by weight. It is believed that the yield would be increased with necessary improvements on the condenser section and experimental conditions such as changing the bed height, residence time etc.

Fluidised bed pyrolysis of scrap tyres yields oil with quite a high calorific value, 43.1 MJ kg^{-1}. The calorific value of scrap tyre char is 31.3 MJ m^{-3}, but the percentage yield of gas is more than for the fixed-bed pyrolysis.

As is indicated earlier, the degradation of scrap tyre generally occurs in the temperature range of 260°C - 420°C. When the temperature is increased, the residence time of vapours in the hot reaction zone would affect the characteristics of the yields and composition.

The polycyclic aromatic hydrocarbons (PAH) are mainly the result of secondary cracking reactions.

The formation of PAH occurs via a Diels-Alder type reaction, involving the aromatisation of olefinic compounds. In this research, the PAH formation in pyrolysis oils from fixed-bed and fluidised bed reactors will be discussed in Chapter 7.

Scrap tyre pyrolysis also yields very useful chemicals such as Dipentene (di-limonene).

Fluidised bed pyrolysis of scrap tyre, as reported in the literature, seems a useful way to dispose of scrap tyre and obtain fine chemicals and char which can be used as active carbon after treatment to improve its quality.

CHAPTER 5

COMMERCIAL SCALE PYROLYSIS

5.1 Introduction

Each year, scrap tyre production is estimated as 1.5 million tonnes and 0.4 million tonnes in the European Community and the U.K. respectively.

Although incineration is considered as an alternative to dumping in an effort to utilise the calorific value of scrap tyres, this disposal route may not maximise the potential economic recovery of energy and chemicals from the waste.

As indicated earlier, pyrolysis of tyres is currently receiving renewed attention since the derived oils may be used directly as fuels or added to petroleum refinery feedstocks. They may also be an important source of refined chemicals. The derived gases are also useful as fuel and the solid char may be used either as smokeless fuel, carbon black or activated carbon.

There appears to be only a few scrap tyre commercial pyrolysis plants in the world, although there have been numerous attempts to pyrolyse tyres. For example, Kaminsky and Sinn (112) used a fluidised-bed and Kawakami et al (125) tested a rotary kiln pyrolyser.

On a commercial scale, most of the scrap tyre pyrolysis experiments have been carried out in Japan (148).

In this part of the research, commercial scale pyrolysis of scrap tyres was carried out.

The pyrolysis unit was manufactured by AEA-BEVEN, which is a joint venture company of the Atomic Energy Authority of the U.K. and a private company H. Beven Ltd. Although the unit has been designed to dispose of all kinds of waste, it is now employed to dispose of only scrap tyres.

The capacity of the pyrolyser is 2 tonnes per day in two 12 hour batches. The capacity of the recycler, compared with the other existing commercial scrap tyre pyrolysis plants (Table 5.1), shows that the unit tested is significantly smaller in capacity.

Table 5.1. Existing commercial scrap tyre pyrolysis plants (119).

Process/Company	Capacity	Location	Start-up Date
Hyber Recycler	Batch	Britain and Japan	1977
Kobe Steel	1 ton h^{-1}	Aioi, Japan	1978
Onahama Smelting and Refining	1 ton h^{-1}	Iwaki, Japan	1981
Kleenair	1 ton h^{-1}	Centralia, Washington USA	1986 (now closed)

In Canada (Laval University), vacuum pyrolysis process development units header capacity reported as 13 kg h^{-1}. Also, in the same place, a vacuum pyrolysis pilot plant was tested, with the capacity of 200 kg h^{-1} (124).

The pyrolyser examined in this part of the research was a commercial unit, manufactured and marketed by AEA-Beven.

5.2 Results and Discussions

Scrap tyre pyrolysis runs were carried out at different temperatures. The experimental conditions for each run carried out are presented in Table 5.2.

Table 5.3 illustrates the product yield of oil, char, residual steel core and gases (by difference) in relation to the process conditions. Also, Table 5.4 shows the data of Table 5.3 corrected to omit the mass of steel content of the tyre sample.

Table 5.2. Experimental conditions for the batch pyrolysis of tyres.

Experiment Number	1	2	3	4	5
Kiln Temperature (C)	700	800	850	900	950
Tyre Mass (kg)	310	305	771	770	1015

Table 5.3. Product yield from the pyrolysis of tyres in relation to process conditions.

Experiment Number	1	2	3	4	5
Oil (kg)	70.5	78.8	215.5	160.4	212.4
%	22.7	25.8	27.9	20.8	20.9
Char (kg)	153.5	113.3	328.9	303.8	413.8
%	49.5	37.1	42.6	39.4	40.7
Gas (kg)	34.5	N/A	119.4	187.4	242.8
%	11.1	N/A	15.5	24.3	23.9
Steel (kg)	51.5	N/A	107.2	98.3	131.1
%	16.6	N/A	13.9	12.7	12.9
N/A = Not Available					

Table 5.4. Product yield from the pyrolysis of tyres in relation to process conditions for the steel core.

Experiment Number	1	2	3	4	5
Tyre Mass (corrected)	258.5	N/A	663.8	672.0	884.2
Oil (%)	27.3	N/A	32.5	23.9	24.0
Char (%)	59.4	N/A	49.5	45.2	96.8
Gas (%)	13.3	N/A	18.0	27.9	27.4
N/A = Not Available					

It is seen that (Table 5.4), as the pyrolysis temperature was increased from 700°C to 950°C, the amount of char yield decreased from 59.4% to 46.8%, however, the char does not appear to decrease in percentage mass above 900°C.

The oil yield also appears to slightly decrease from a value of 27.3% at 950°C. These results are consistent with the literature which has shown that higher pyrolysis temperatures favour the increased formation of gas and reduced formation of char (113).

The oil yield is somewhat lower than that reported from other pyrolysis experiments. For example, Roy and Unsworth (113) reported a maximum oil yield of 56.6%, Kawakami et al (125) 53% and Kaminsky and Sinn (112) 40%.

The experimental apparatus favoured the formation of oil by either high heating rates, with rapid quenching of the derived pyrolysis vapours or rapid removal of the products from the hot zone which reduces the extent of secondary reactions which are known the yield of char at the expense of oil formation.

As a commercial scale pyrolyser, the Kobe plant yielded 31% oil, 29% carbon black, 15% gas, 10% steel, 5% sludge and 2% water. Also, it was reported that the Onahama plant yielded 25-30% oil, 35-40% carbon black and 10% steel (119). The process development unit (Canada) yielded at 513°C 54% oil, 37.8% carbon black and fibre, 4-2% gas and 4.0% water and at the same place, the pilot plant at the identical conditions has resulted in yields of 55% oil, 25% carbon black, 9% steel, 5% fibre and 6% gas (124).

When the yields of the AEA-Beven multi-purpose tyre recycler are compared with the other pilot plant, by the results above it is seen that the oil and gas results do not differ, from the other commercial scale applications except the vacuum pyrolysis techniques used in Canada.

In commercial scale pyrolysis equipment, the over loading of tyres may serve to decrease the transfer of heat to the tyres, since in the low mass loaded experiments, a higher proportion of the tyres will be in contact with the hot outer surface of the kiln.

The product yield results show some variability, this is most probably due to the mixture of different types loaded in the pyrolysis unit. Cypres and Bettens (123) have shown that pyrolysing different brands and makes of tyre results in significant differences of the order of 10% in the yields of solids, liquid and gaseous products.

Table 5.5 shows the fuel properties of the oils from the five pyrolysis experiments carried out. Table 5.6 illustrates the fuel properties of the petroleum derived fuel diesel, kerosene light fuel oil and heavy fuel oil for comparison.

Table 5.5. Fuel properties of oils derived from the pyrolysis of scrap tyres.

Sample No.	1	2	3	4	5
Carbon Residue (%)	0.5	1.16	1.16	2.1	2.1
Mid Boiling Point (C)	229	282	245	278	264
Viscosity 60°C (centistokes)	2.15	2.47	2.24	2.47	2.38
40°C (centistokes)	3.10	3.75	2.35	3.50	6.30
Density (kg m^{-3})	0.91	0.95	0.93	0.96	0.96
API Gravity	21.81	17.44	19.35	14.35	15.51
Cetane Index	14.45	19.78	14.42	13.10	11.35
Flash Point (C)	14	15	15	21	20
Hydrogen Content (%)	10.58	9.97	9.84	9.42	942
Initial Boiling Point (C)	80	87	90	98	100
10% Boiling Point (C)	140	145	135	145	139
50% Boiling Point (C)	229	282	245	278	264
90% Boiling Point (C)	340	352	349	352	355
Calorific Value (MJ kg^{-3})	42.9	42.6	42.9	42	42.1
Sulphur	0.5	1.1	1.1	1.1	1.1

The carbon residue results show an increase in percentage carbon residue with increasing pyrolysis temperature. The carbon residue test is a measure of the tendency of the oil to form carbon, particularly when the oil is combusted in the absence of a large excess of air, or when the fuel is subject to evaporation and

pyrolysis. For example, a high carbon residue result may lead to coking of the fuel injector nozzles in a diesel engine.

A typical diesel fuel would have a carbon residue of approximately 0.2%, whereas, Table 5.5 shows that the tyre oils have a range from 0.5% to 2.20%. However, fuel oil used in very large diesel engines may have carbon residues up to 12%.

The viscosity of the tyre oils showed no particular trend with increasing temperature of pyrolysis. The viscosity of a fuel is an important property since it affects for example the flow of the fuel through pipes and other plant items, the atomisation of the fuel and the performance and wear of diesel pumps. Comparison with the petroleum derived fuels shown in Table 5.6, shows that the viscosity of the tyre oils lie between those of a diesel fuel and a light fuel oil.

The relative density of the tyre oils show an increase with increasing pyrolysis temperature and a corresponding decrease in the API (American Petroleum Industry) gravity. The API gravity allows values of relative density, which have been made from hydrometers to be corrected. The values for the tyre oils have relative densities and API gravities between those of a light fuel oil and a heavy fuel oil.

The Cetane Index was calculated to evaluate the tyre oils in relation to their use in diesel and compression ignition engines. The Cetane Index was calculated rather than an experimental determination of Cetane number. The Cetane Index is derived from the API gravity and the mid-boiling point of the oil. The index has a number of limitations and cannot strictly be used for alternative

fuels to those derived from petroleum. However, the index gives a comparison figure for the tyre oils in relation to pyrolysis temperature. The results shown in Table 5.5 suggest a decrease in Cetane Index with increasing pyrolysis temperature. Typical values for diesel fuel lie in the range 48-52.

Table 5.6. The fuel properties of the petroleum derived fuels, diesel, kerosene, light fuel oil and heavy fuel oil (194)

Sample	Kerosene	Diesel	LFO	HFO
Carbon Residue (%)	< 0.15	< 0.35		
Mid Boiling Point (C)	200	300	347	
Viscosity				
60°C (centistokes)	0.65	1.3	4.3	24
40°C (centistokes)	1.2	3.3	21	30
Density (kg m^{-3})	0.84	0.78	0.89	0.95
API Gravity	47	31	26.6	17.5
Cetane Index		48.52		
Flash Point (C)	40	75	79	110
Hydrogen Content (%)	13.6	12.8	12.4	11.8
Initial B. Point (C)	140	180	200	252
10% Boiling Point (C)				
50% Boiling Point (C)	200	300	347	
90% Boiling Point (C)	315			
Calorific Value (MJ kg^{-3})	46.6	46.0	44.8	44.0
Sulphur (%)	0.1	0.9	1.4	2.1

LFO = Light Fuel Oil
HFO = Heavy Fuel Oil

The flash point of a liquid fuel is the temperature at which the oil begins to evolve vapours in sufficient quantity to form a flammable mixture with air. The temperature is an indirect measure of volatility and serves as an indication of the fire hazards associated with storage and application of the fuel (159).

The flash point of the tyre derived oils showed an increase with increasing pyrolysis temperature. The flash points are low when compared to petroleum refined fuels, for example kerosene has a required minimum flash point of 23°C (159). The low flash points of the tyre oils are not surprising since they represent an un-refined oil with a mixture of components having a distillation range from a minimum of 80°C to over 350°C. The low flash point temperatures of the tyre oils have implications for safe storage and handling and those fuels having flash points below 66°C are subject to special regulations (159).

The hydrogen content of the oils showed a decrease from 10.58% to 9.42% as the temperature of pyrolysis was raised from 700°C to 950°C. Hydrogen contents for petroleum derived fuels shown in Table 5.6, show that hydrogen contents range from about 13.6% for a kerosene to about 11.8% for heavy fuel oil.

The distillation range of the oils reflects the fact they are un-refined oils and consequently have a wide range of boiling points for the components of the oils. The results show that the oil produced at a pyrolysis temperature of 700°C has the lowest boiling point range of the tyre oils. The initial boiling points of the oils show an increase with increasing temperature of pyrolysis. However, the 50% and 90% boiling point temperatures of the tyre oils are

similar. The petroleum refined fuels shown in Table 5.6 have boiling point ranges consistent with their derivation, that is from the fractional distillation of crude petroleum oil. The distillation ranges of the refined fuels showing an increase in temperature for each fraction.

The calorific value of the tyre oils were similar for all the oils representing approximately 42 MJ kg^{-1}. The calorific value of the oils is high and comparable with that of a light fuel oil, indicating the potential for the use of tyre derived oils as fuel. Similar high calorific values for tyre derived pyrolysis oil have been reported.

For example, Kawakami et al (125) collected light and heavy oil fractions with calorific values of 43.9 and 42.5 MJ kg^{-1} respectively. Roy and Unsworth (113) found a calorific value of 43 MJ kg^{-1}.

The sulphur contents of the tyre oils showed that the oil produced at 700°C was 0.5%, whereas, that of the oils produced at the higher pyrolysis temperatures was more than twice this value at 1.1%.

The sulphur contents are similar to those of a diesel fuel or light fuel oil. Similar sulphur contents for tyre derived pyrolysis oils have been reported in the literature (113, 125).

5.3 Economic Appraisal

An economic appraisal for tyre pyrolysis depends entirely on the market for the products of the pyrolysis process. In addition, the economic viability is also improved if a tipping fee for the disposal of the tyres is included. Table 9 shows the process

economics for the AEA-Beven tyre pyrolysis unit. The appraisal is based on a three unit system with three different projected throughputs of tyres depending on the number of pyrolysis cycles per unit per year. The percentage mass of products, the projected fuel costs and annual running costs are also included. The capital costs of the three units, including interest payments are included as annual payments for ten years. The main product income is for the carbon char which is used for the clean up of polluted chemical plant effluent and water. Three cases are presented with income from the carbon at three different values per tonne. The economic appraisal is also dependent on the tipping fee for each tyre and three cases are also presented for three different tipping fees. Table 5.7 presents two profitability scenarios, a worst case and best case, depending on the tyre tipping fee, the income from the carbon and the number of pyrolysis cycles per year. The profitability is sensitive to all three input parameters, however, all show a projected annual profit. In the best case scenario with a high number of pyrolytic cycles per year, the projected profit is high.

In the process economics presented in Table 5.7 it can be seen that no value was placed on the oil derived from the pyrolysis of the tyres. However this work has shown that the tyre derived pyrolytic oil is suitable to be used as fuel as a substitute for light petroleum oil. The income from the sale of the tyre derived oil would further improve the process economics. In addition, the pyrolytic oils have been shown to contain chemicals of potentially high value. For example, this work has shown that benzene, xylene, toluene, styrene and limonene are present in significant concentrations and the oils have a significant aromatic content. The

potential use of the oils as chemical feedstocks would also improve the process economics.

Other research groups have assessed the process economics for the pyrolysis of scrap tyres. Dodds et al (8) have presented an economic appraisal for several tyre pyrolysis plants throughout the world. They suggested that generalities could not be made on a world-wide basis since some countries subsidised such technology, or were covered by Government grants for start-up. Similarly the assessment depended on the tipping fee for the tyres and a long term guarantee of tyre supply. For conservative estimates of the revenues from the char to be sold as carbon black and oil as heating fuel and using high interest rates they concluded that a tipping fee was required in all cases for the process to be profitable. However, the tipping fee was modest at less than one dollar per tyre. In addition, the economic viability was increased if the oil yield could be improved or a higher quality carbon black could be produced.

Cypres and Bettens (123) have shown that the char derived from tyre pyrolysis can be successfully upgraded to high quality activated carbon by steam heating at high temperature. The activated carbon can have adsorbent qualities very similar to commercially produced types. Their work also showed that the oil produced by tyre pyrolysis was high in benzene, xylene and toluene which could be used as a chemical feedstock. An economic appraisal of the process was shown to be profitable for smaller scale units of the order of 2000 tonnes per annum and in addition, would also solve a serious environmental problem.

More recently, Roy et al (119) and Pakdel et al (126) have presented an economic study for a 3 tonnes per hour (20,000 tonnes per year) continuous tyre pyrolysis plant and have suggested that if the pyrolysis conditions can be optimised to produce high value chemicals for the chemical industry, such as dl-limonene, benzene, xylene and toluene then the economic viability for tyre pyrolysis is markedly increased.

Table 5.7 Process Economics for the AEA Beven Batch Pyrolysis Unit

Assumptions	
Cost per plant (approx)	£295,000
Cost per 3 unit system (approx)	£790,000
Value of oil (p/litre)	0
Value of steel (£/tonne)	16
Cost of Diesel (p/litre)	45
Diesel reqd/tonne (litres)	50
Products/tonne (%)	
Oil	20.9
Carbon	40.8
Steel	12.9
Gas	0

Annual Running Costs	
Space - Ren/Rates	9000
Electricity	10500
Plant costs over 10 years	176984
Nitrogen	8000
Manpower	72000
Crane maintenance	1000
Other maintenance	5000
Insurance	2500
Contingency	5000
Total costs	289984

No. of cycles per year/unit		500	550	600
No. of units	3			
Weight per batch (kg)	1080			
Tyres per tonne	150			
Tyres/year		243,000	267,300	291,600
Weight/year (tonnes)		1620	1782	1944
Income Streams				
Tyres pence each	30	£72,900	£80,190	87,480
Tyres pence each	35	£85,050	£93,555	£102,060
Tyres pence each	50	£121,500	£133,650	£145,800
Steel		£3,384	£3,722	£4,060
Carbon (£/tonne) tyres	400	£264,307	£290,738	£317,169
Carbon (£/tonne) tyres	450	£297,346	£327,080	£356,815
Carbon (£/tonne) tyres	500	£330,384	£363,423	£396,461
Costs				
Annual		£289,984	£289,984	£289,984
Fuel		£36,450	£40,095	£43,740
Profitability: Worst Case				
Tyres (pence each)	30	Carbon	(£/tonne)	400
Income		£340,591	£374,650	£408,709
Costs		£326,434	£330,079	£333,724
Profit - per annum		£14,157	£44,571	£74,985
Profitability: Best Case				
Tyres (pence each)	50	Carbon	(£/tonne)	500
Income		£455,268	£500,795	£546,321
Costs		£326,434	£330,079	£333,724
Profit - per annum		£128,834	£170,716	£212,597

CHAPTER 6

THERMOGRAVIMETRIC ANALYSIS OF BIOMASS AND WASTE

6.1 Thermogravimetric Analysis Of Biomass And Components

6.1.1 Introduction

In this part of the work, wood and rice husks as biomass samples, cellulose, hemicellulose and lignin as the main components of biomass and model carbohydrate compounds represented by the monosaccharides (maltose), trisaccharides (melezitose), tetrasaccharides (stachyose) were separately pyrolysed in the thermogravimetric analyser.

The chemistry of biomass is complicated, but, the major components which can be isolated by analytical methods are cellulose, hemicellulose, lignin and extraneous compounds (47). Also, it has been shown that various monosaccharides, oligasaccharides and polysaccharides can be identified in biomass, cellulose, hemicellulose and lignin (46, 47). In addition, monosaccharides, oligasaccharides and polysaccharides have been identified as pyrolysis products or cited as intermediaries in the pyrolysis of biomass (162). Pavlath and Gregorski (169, 170) investigated the pyrolysis of various mono-, oligo and polysaccharides in a thermogravimetric analyser and showed that even small changes in chemical structure could influence the thermaldegradation and composition of the pyrolysis products.

6.1.2 Thermogravimetric Analysis of Wood, Rice Husks and Main Components

The thermogravimetric analysis (TGA) thermograms and differential calculation of the weight loss to give the rate of weight loss for the wood and the main components of cellulose, hemicellulose and lignin extracted from wood are shown in Figures 6.1 to 6.4 at heating rates of 5°C min^{-1}, 20°C min^{-1}, 40°C min^{-1}, and 80°C min^{-1} respectively. Also, Figures 6.5 to 6.8 show TGA and DTG curves of rice husks and lignin extracted from rice husk.

The TGA curves of wood show that completion of moisture evolution from samples occurs at 115°C, 150°C, 168°C and 247°C for the heating rates above respectively. This first weight loss range is between 3.8% - 8.5% by weight. Connor and Salazar (81) for the Eucalyptus Delegatensis wood showed that the first weight loss range is between 9% - 12% which occurs between the temperatures of 50 - 220°C.

The thermograms show that the moisture loss step of the rice husk starts at 105°C, 110°C, 130°C and 150°C and completes at approximately 230°C, 250°C, 260°C and 275°C for the heating rates of 5°C min^{-1}, 20°C min^{-1}, 40°C min^{-1} and 80°C min^{-1} respectively. The first step of moisture loss range is between 4.8% - 8% by weight.

Cellulose which is one of the main components of biomass, starts to lose moisture ~100°C and total weight loss for all heating rates above approximately 2% weight.

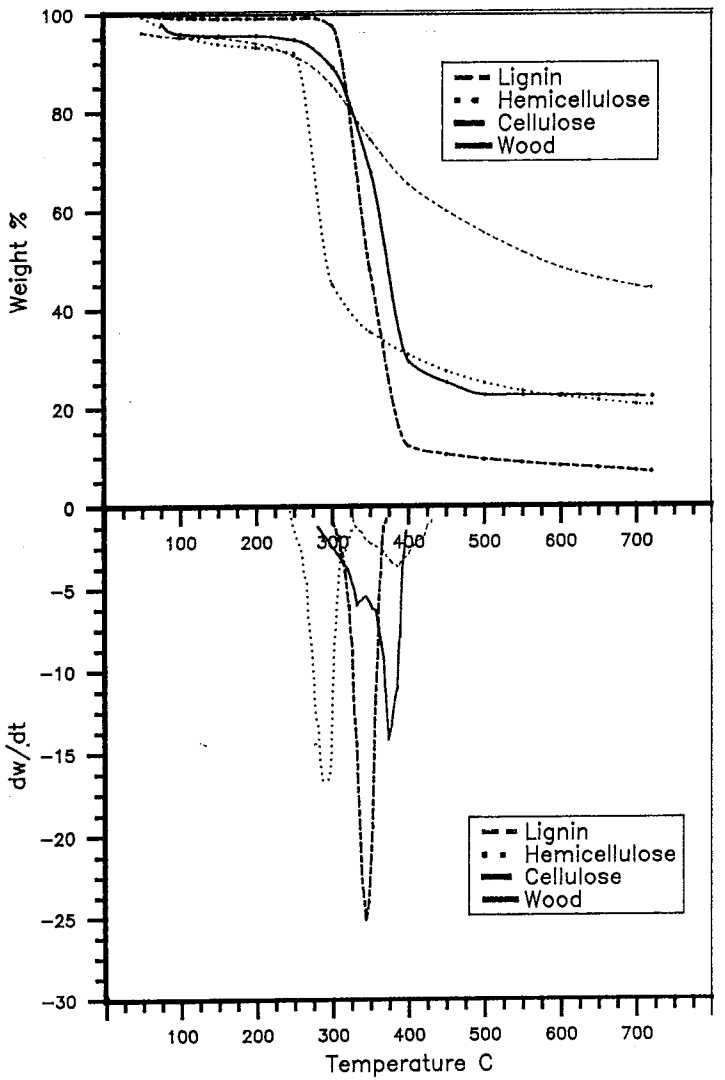

Fig.6.1 TGA and DTG curves for 5 C/min

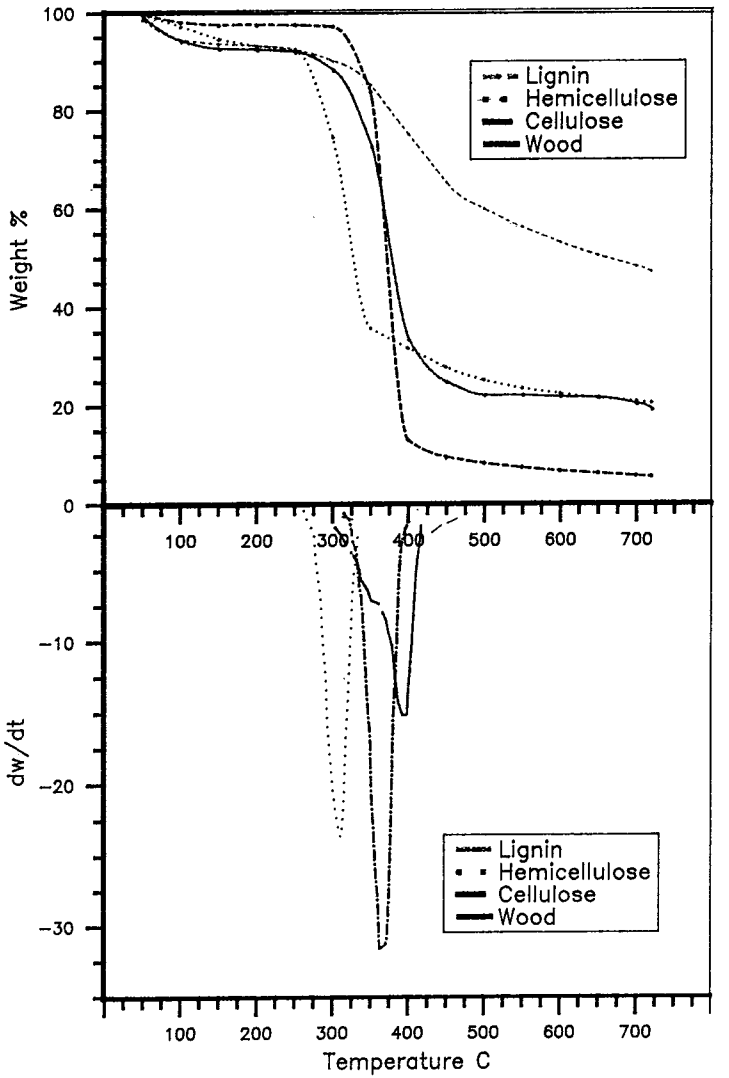

Fig.6.2 TGA and DTG curves for 20 C/min

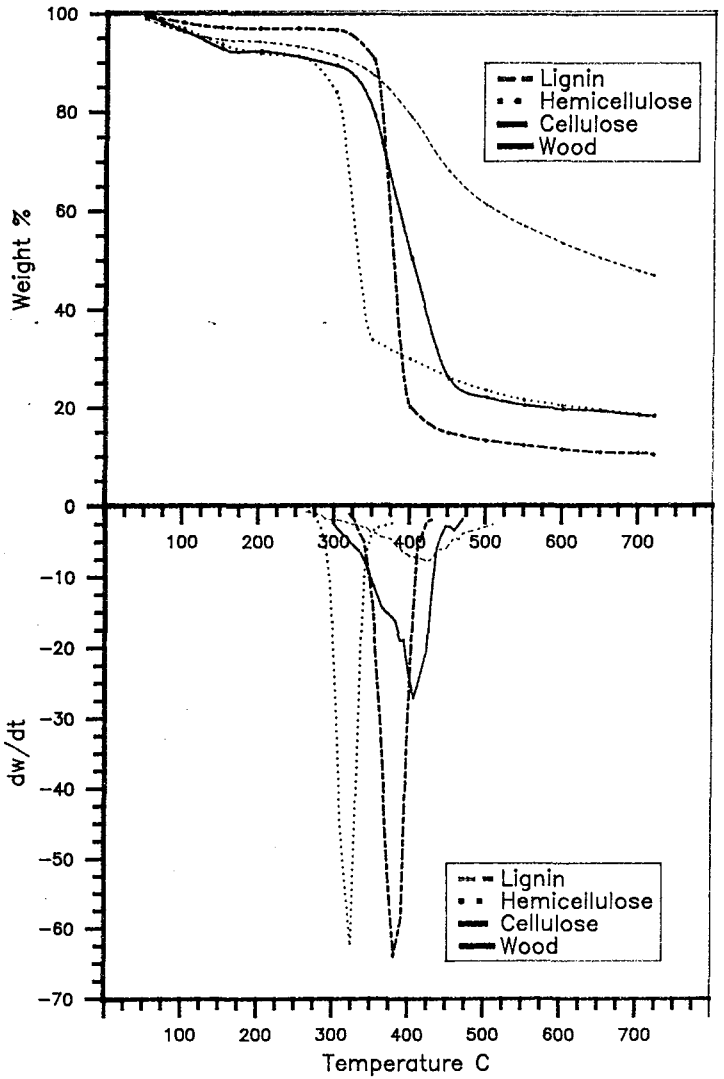

Fig.6.3 TGA and DTG curves for 40 C/min

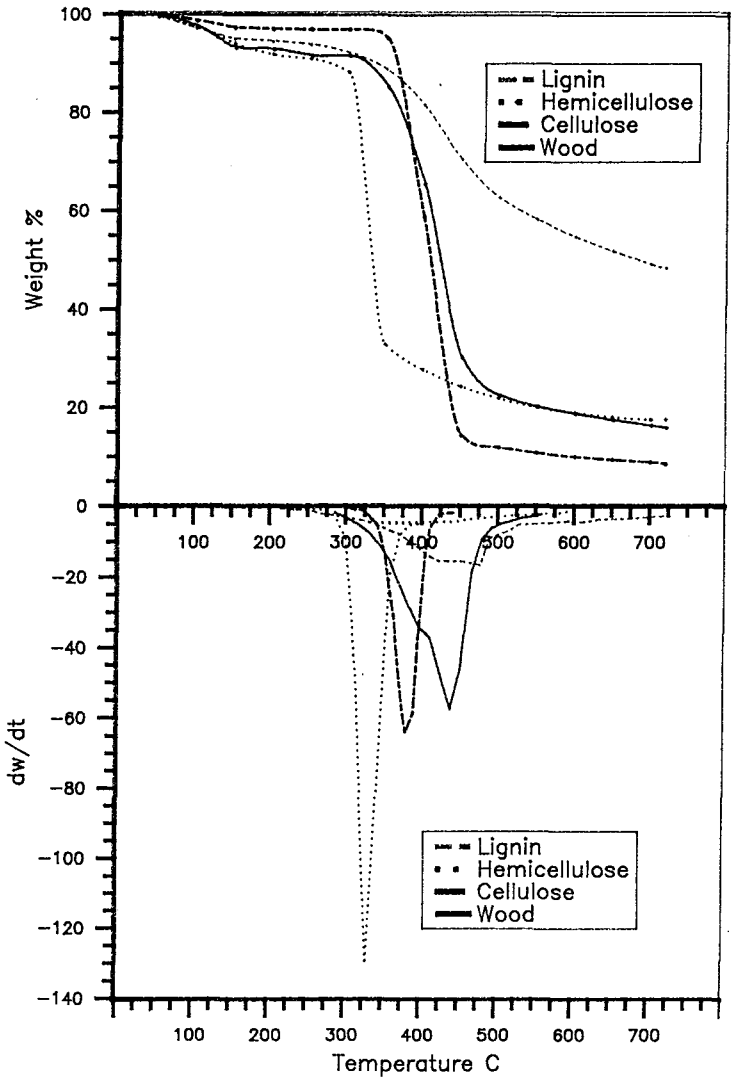

Fig.6.4 TGA and DTG curves for 80 C/min

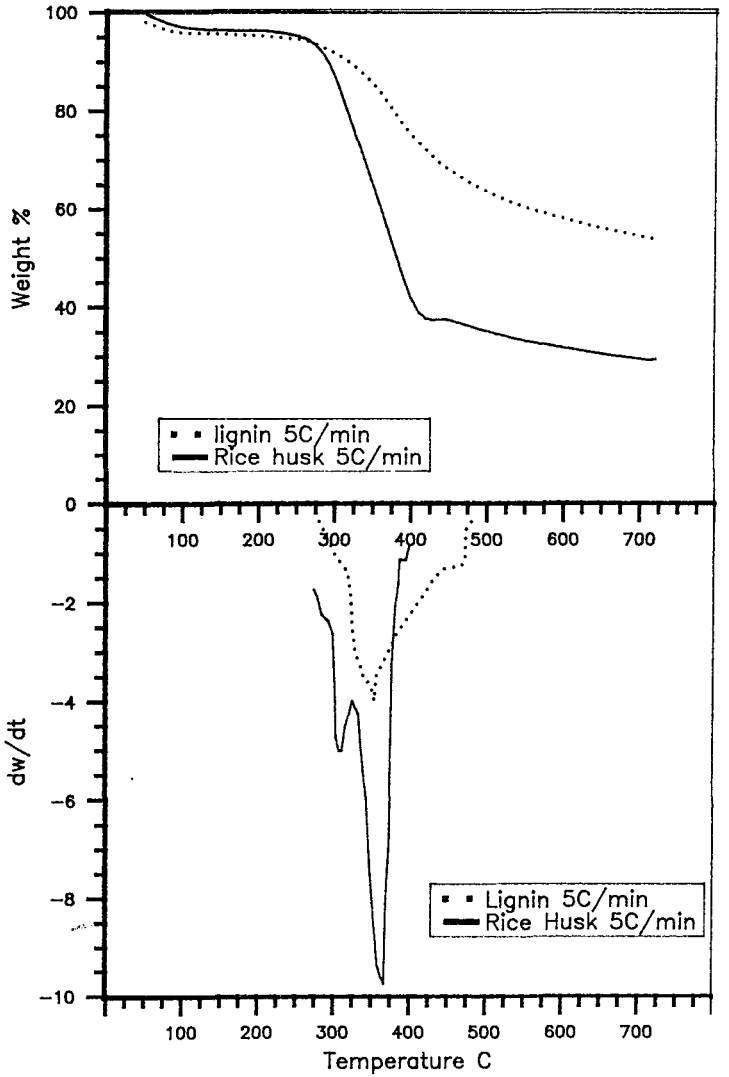

Fig.6.5 TGA and DTG curves for 5 C/min

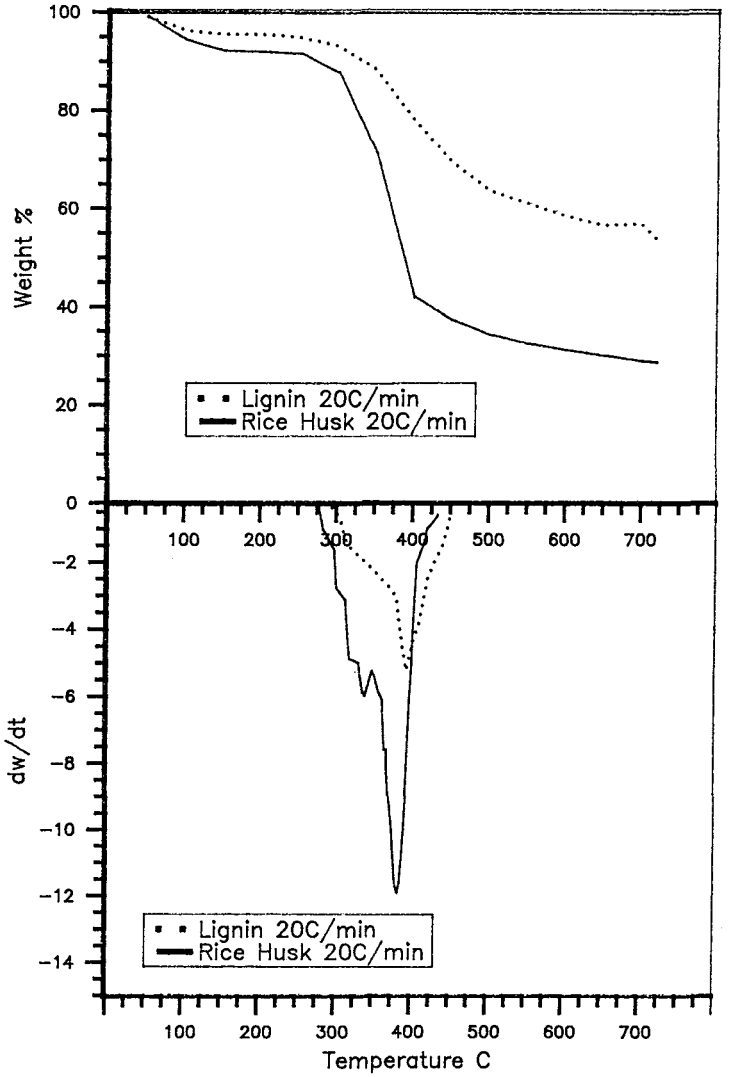

Fig. 6 TGA and DTG curves for 20 C/min

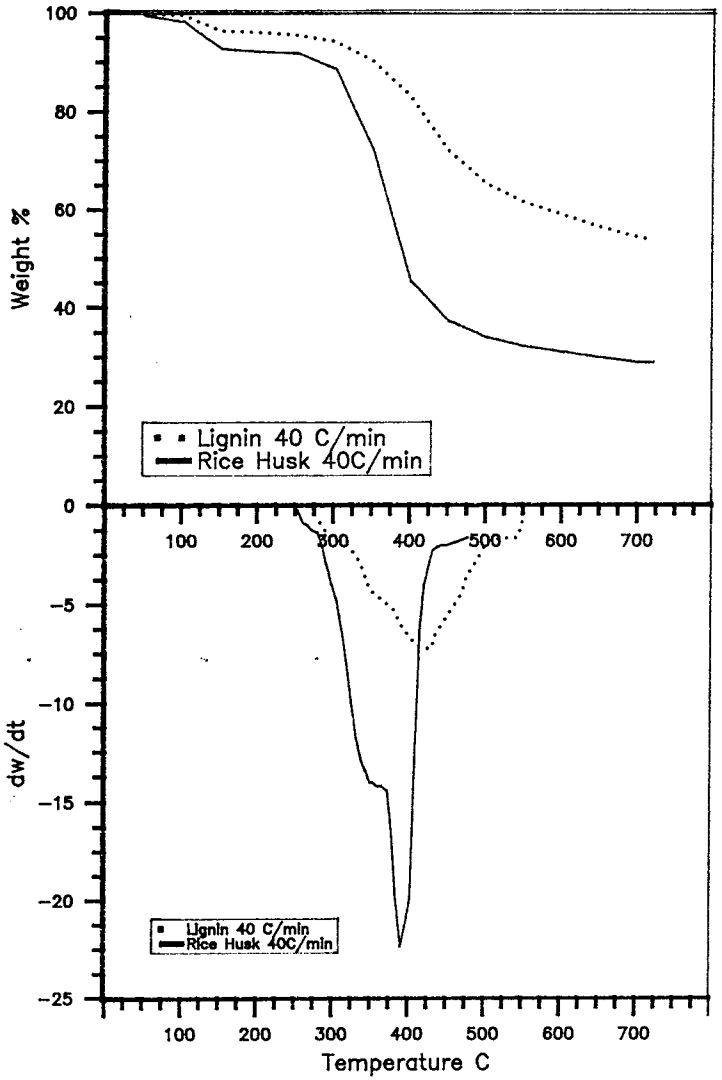

Fig.5.7 TGA and DTG curves for 40 C/min.

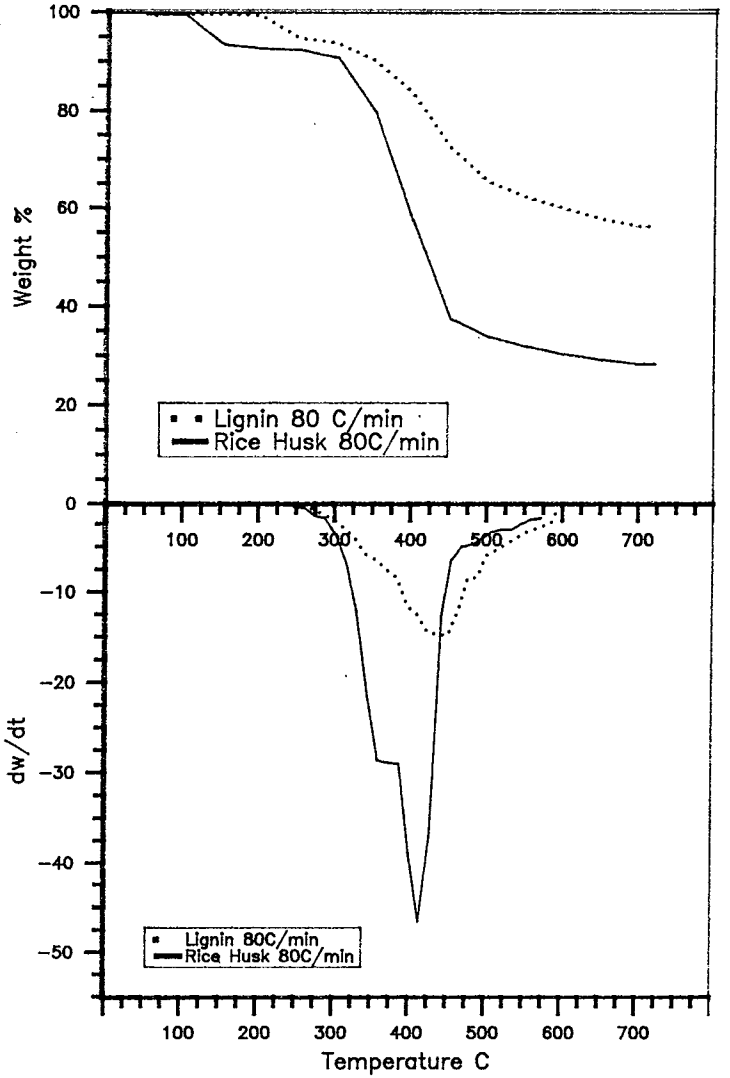

Fig.5.8 TGA and DTG curves for 80 C/min

The moisture loss step of hemicellulose for the heating rates of 5°C min^{-1}, 20°C min^{-1}, 40°C min^{-1} and 80°C min^{-1} at 100 - 150°C and total moisture weight loss is in the range of 5% - 8%.

The lignin extracted from wood starts to lose moisture almost at the same temperature of wood and moisture loss is 5% for all heating rates. The lignin extracted from rice husk starts to lose moisture in the temperature range of 125°C - 150°C and the weight loss is about 7% - 8.5% weight.

The second weight loss which is the main thermaldegradation step for the wood chips starts at between 245°C - 275°C. This second weight loss completes approximately between 423°C - 488°C. After this temperature, there is a slow weight loss until the maximum temperature of 720°C. After 720°C, there is no further loss of weight. The residual char amounts are approximately 23%, 19%, 18.2% and 16% by weight for the heating rates of 5°C min^{-1}, 20°C min^{-1}, 40°C min^{-1} and 80°C min^{-1} respectively. When these char amounts are compared with the char yields of the fixed-bed reactor (chapter 3), it can be seen that both fixed-bed and thermogravimetric analyser char yields in percentage weight are very similar. These results also show that using the thermalgravimetric analyser for investigation of pyrolysis reactions is a useful technique.

When the DTG curves of wood are examined, it is seen that for the lower heating rates there are two peaks on the curve. This makes it clear that there are two weight loss steps for the main thermaldegradation of wood. Connor and Salazar (81) also reported that there were two peaks on the DTG curve when the main thermaldecomposition proceeds.

For the higher heating rates, these two peaks become closer. The smaller one which is also the earlier one, becomes a shoulder on the second peak. It was shown by Connor and Salazar (81) that the first peak on the DTG curve for the thermaldecomposition of wood starts at 230° and ends between 280°C - 310°C and when this peak ends, weight loss is about 17% - 20%. This peak has also been identified as the thermaldecomposition of hemicellulose by Connor and Salazar (81). For xylan, the degradation range is given between 195°C - 325°C by Ramiah (63). In this work for hemicellulose which was represented by xylan, DTG curves start at 258°C, 270°C, 280°C and 282°C and end at 318°C, 331°C, 378°C and 422°C for the heating rates of 5°C min^{-1}, 20°C min^{-1}, 40°C min^{-1} and 80°C min^{-1} respectively.

Table 6.1. Temperature ranges and temperatures of maximum weight loss for the pyrolysis of wood, rice husks, hemicellulose, cellulose and lignins (extracted from both wood and rice husks). (Nomenclature defined in Fig. 6.9).

Substance	Heating Rate °C min^{-1}	T_1 °C	T_{max1} °C	T_2 °C	T_{max2} °C	T_3 °C
Wood	5	250	325	330	385	400
	20	260	350	360	400	410
	40	270	375	380	410	440
	80	272	400	410	450	470
Rice Husk	5	250	310	325	360	390
	20	275	330	345	380	410
	40	270	350	375	410	425
	80	270	350	375	410	425
Hemicellulose	5	258	285	318	-	-
	20	270	309	331	-	-
	40	280	320	378	-	-
	80	282	330	422	-	-
Cellulose (microcrystalline)	5	-	-	310	350	380
	20	-	-	325	370	405
	40	-	-	300	380	425
	80	-	-	310	410	500
Lignin (extracted from wood)	5	-	-	330	380	420
	20	-	-	300	400	460
	40	-	-	300	430	500
	80	-	-	300	460	530
Lignin (extracted from from rice husk)	5	-	-	295	354	492
	20	-	-	300	401	505
	40	-	-	288	430	601
	80	-	-	290	450	601
Paper	5	-	-	310	375	420
	20	-	-	300	390	430
	40	-	-	310	410	470
	80	-	-	305	415	495

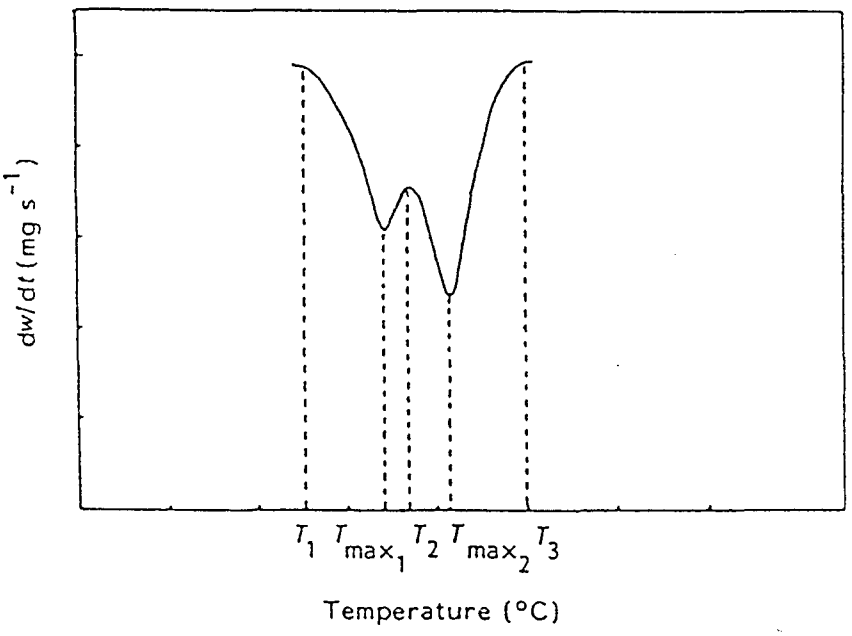

Fig. 6.9. DTG nomenclature for Tables 6.1, 6.5, 6.6, 6.7, 6.8, 6.10, 6.11

It is seen that wood decomposition starts approximately at the same temperature with the hemicellulose for each of the heating rates. The first peaks on the DTG curves of wood (Table 6.1) end at 330°C, 360°C, 380°C and 410°C for the heating rates as above. These temperatures are very close to the final temperatures of the hemicellulose DTG curves. After these observations it can be said that the thermaldecomposition of wood starts with the decomposition of hemicellulose content of wood and the first peak on the DTG curve of wood is represented by the thermaldecomposition of hemicellulose.

The thermograms show that thermaldecomposition of the rice husk starts at approximately 250°C, followed by major weight loss where the main devolatilisation occurs and is virtually complete by 450°C and there follows a slow further weight loss until 720°C after which

there is essentially no further weight loss. The residual char amount was approximately 29% and ash 11% by weight and was unaffected by heating rate. There was a lateral shift in the TGA curves to higher temperatures as the heating rate was increased.

From the DTG curves it is seen that after the thermaldecomposition of rice husk, there are clearly two areas of weight loss producing two peaks on the DTG curves and as the heating rate was increased, the two peaks become progressively merged.

As reported earlier, the components of biomass effect the thermaldecomposition route (47, 171). Also, Lipska-Quinn et al (38) report that rice husks are mainly composed of hemicellulose and cellulose.

In the DTG curves of rice husks for different heating rates, two different weight loss regions can be observed. As with wood, the first peak which coincides with the DTG curves of hemicellulose can be identified as the thermaldecomposition peak of the hemicellulose content of rice husks.

Connor and Salazar (81) identify the peak which appears on the DTG curve of wood between 280°C - 360°C as the thermaldecomposition of cellulose.

Ramiah (63) agrees that cellulose decomposes in the temperature range of 295°C - 380°C. Also, Bradbury et al (65) summarise that pyrolysis of cellulose occurs within the temperature range of 260°C - 340°C. Table 6.1 shows that in this work, cellulose decomposes more or less in the same temperature range. There was a lateral shift to higher temperatures as the heating rate was increased. On the DTG

curve of wood, it seems that the second peak is coinciding with the cellulose DTG curve. The pure cellulose and hemicellulose always decompose at lower temperatures than wood. This can have an inhibiting effect on the decomposition reactions.

It was also shown that purity and physical properties of cellulose have a significant effect on the decomposition of cellulose by Shafizadeh (47).

In the DTG curves of rice husks, the second peak observed coincides with the DTG curves of cellulose thermaldecomposition. Figures 6.1 - 6.4 show that lignin, which was extracted from wood, decomposes between approximately 250°C - 500°C. For the thermaldecomposition of aspen wood, the peak appears between 350°C - 420°C and has been identified as due to the pyrolysis of cellulose and lignin by Grandmaison et al (172). It is pointed out that the weight loss at 700°C was 89.4%. From the DTG and TGA curves (Figures 6.1 - 6.4), it can be said that lignin is the most thermally stable component of wood.

The same conclusion can be made for the lignin extracted from rice husk. When the DTG curves are compared, it is seen that lignin decomposition occurs throughout the temperature range used, but the main weight loss occurs at the higher temperatures.

Lignin was found by Ramiah (63) as the most thermally resistant. Cellulose is intermediate and the hemicelluloses are the least stable. Lignin has been shown to be the major source of char in biomass pyrolysis, whereas, the carbohydrates, cellulose and hemicelluloses are the precursors of the volatile products and hence

contribute more to the weight loss of the biomass samples in relation to the production of volatile products (171).

6.1.2.1 Estimation of Biomass Contents From TGA and DTG Curves

Figures 6.1 to 6.4 show that during decomposition of cellulose, essential amounts of lignin also decompose and from the DTG and TGA curves it is possible to make comments about their amount although overshadowing of those two decomposition reactions.

As described in the experimental techniques section lignin samples were extracted from wood chips and rice husks and 27.5% and 18.6% of lignin content were determined respectively.

The hemicellulose content of wood has been found to be 24.5% from the TGA curves and final temperatures of the first peaks of the wood DTG curves. These figures also give approximately 40.5% of cellulose content in wood examined in this work. Cellulose and hemicellulose contents of rice husk were also determined as approximately 40.4% and 35% respectively.

These figures above show that the use of TGA to estimate the major contents of cellulose is possible. The sum of the wood and rice husks major contents were 92.5% and 94% respectively. Probably the rest of the biomass samples were other extractables and moisture.

6.1.2.2 Biomass Thermaldegradation Models

In the pyrolysis of biomass, the major components cellulose, hemicellulose and lignin are likely to react independently (53). Many researchers studying the kinetics of wood pyrolysis prefer to

simplify the wood as a single reactant. Thurner and Mann (173), calculated kinetic parameters in the model

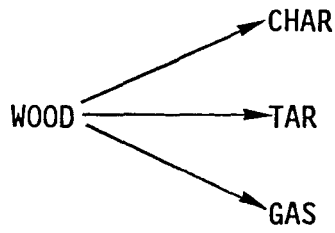

assuming the reactions were first order. Also, Cordero et al (174), after testing a number of reaction models, have found that the first order reaction model provides a fairly good description of the kinetics of holm oak pyrolysis.

Chan et al (175) also used the model:

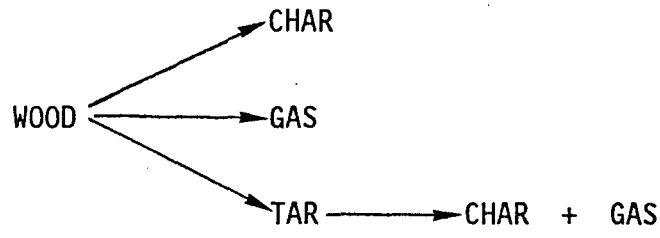

Considering secondary reactions of tars to char and gas.

In this work, evolved gases were removed straight away from the reaction zone to prevent secondary reactions.

It was shown that purity and physical properties of cellulose have a significant effect on the decomposition of cellulose by Shafizadeh (62). Packing density of cellulose and alteration of physical structure effect the nature of the pyrolysis reactions and the yield of levoglucosan. Also, the presence of even low concentrations of impurity either catalyse or inhibit the degradation of cellulose (62).

As reported earlier in this work, cellulose in the form of Whatman filter paper no. 1 was also employed in the TGA investigations. When the degradation temperatures were compared with the microcrystalline cellulose, the filter paper decomposed at higher temperatures than the microcrystalline cellulose (Table 6.1).

Shafizadeh (62) reported that the presence of trace metals results in a shift to lower thermaldecomposition of cellulose. In this work, most probably the crystalline structure of the cellulose dominates the catalytic effect of any trace metals present in the filter paper cellulose. It was also shown by Lipska-Quinn et al (38) that cellulose extracted from rice straw thermally degrades at a higher temperature than pure cellulose.

In their review, Antal et al (63) report the mechanisms for the pyrolysis of cellulose. In this mechanism, the first step is a decrease in the degree of polymerisation with no significant weight loss, followed by either a thermal autocrosslinking reaction leading to the formation of anhydrocellulose, which may continue to react further to join most of the char and some volatile species. Competing with the anhydrocellulose reaction is a series of sequential depolymerisation reactions which eventually produce a levoglucosan tar. This tar may either form char and some volatiles or mainly volatiles, depending on the experimental conditions.

Zaror et al (176) have suggested that for slow pyrolysis, primary char may form directly from the cellulose.

There are less data on the mechanism for the pyrolysis of hemicellulose. It was suggested by Soltes and Elder (83) that hemicellulose degradation occurs in two steps; decomposition of the

polymer into water soluble fragments followed by conversion to very short or monomeric units that in turn decompose into volatiles. The degradation reactions occurring in a narrow temperature range between 220°C and 320°C.

Thermal degradation of lignin reactions involve the breaking of relatively weak aliphatic bonds releasing large hydrocarbon fragments, which undergo secondary reactions such as cracking and repolymerisation.

The approach adopted by many researchers in kinetic analysis of TGA data is to assume a first order rate of reactions for the pyrolysis of biomass devolatilisation. Cordero et al (179) studied different models for the wood pyrolysis and they concluded that first order reaction is the best fit to describe the wood pyrolysis.

In this work, the adopted approach is to assume a first order reaction with respect to the amount of undecomposed material. The pyrolysis of complex materials like wood and lignocellulosic biomass can be studied by focusing the attention on gaseous and condensable products or by following the solid weight loss. This second method has been widely used.

The sample size used is small to eliminate heat transfer effects (80). It was shown that the pyrolysis of cellulosic material is chemical reaction controlled for sizes less than 0.2 cm, between 0.2 cm and 6 cm it is controlled by both heat transfer and chemical reaction, whilst above 6 cm, the pyrolysis is controlled by heat transfer. In this work the size of the samples employed were less than 0.2 cm.

In the literature, there is not an agreement on the measured rates of cellulose pyrolysis. After reviewing the data in the literature about large samples, Antal et al (69) suggest that the analysis of the results from large samples is complicated by heat and mass transfer phenomenon and secondary reactions, all of which tend to obscure the interpretation of the experiment.

Heat transfer from the furnace to the sample has been shown to be a problem in determining kinetic parameters (69) and close coupling of the measuring temperature thermocouple to the sample is desirable. In this work, the thermocouple measured the temperature of the sample boat.

6.1.2.3 Kinetics

The Arrhenius equation has been popularly used in the pyrolysis studies of cellulosic materials to present the rate as a function of temperature.

The rate of decomposition is given by;

$$\frac{dw}{dt} = -k\,(w - w_f) \qquad (6.1)$$

Where w is the weight of undecomposed material, w_f is the weight of residue at the end of the reaction and k is the rate constant. The reaction rate constant k is also defined by the Arrhenius equation;

$$k = A\, e^{-E/RT} \qquad (6.2)$$

Where A is the pre-exponential or frequency factor, E is the activation energy of the decomposition reaction and R and T the universal gas constant and the absolute temperature respectively.

From equations 6.1 and 6.2

$$\ln k = \ln A - E/RT \qquad (6.3)$$

A plot of ln k versus 1/T gives straight line of -E/R slope. The continuous recordings of the TGA of weight loss with time and temperature enable dw/dt and k to be determined.

Agrawal (190) suggests that the Arrhenius law applies only to a simple homogeneous gas-phase reacting system. In many cases, complex reactions appear to follow a simple kinetic order over a range of limited experimental conditions. In other systems, a relation between lnk and 1/T is non-linear. This non-linearity may suggest a change in the reaction mechanism or that the heating system may have become physically limited due to heat and mass transfer effects. Some reasons for non-linearity between lnk and 1/T in some biomass pyrolysis studies are; complexity of the reaction, possible errors in sample temperature measurement and temperature gradient within the sample.

In this work, the kinetic data will be presented in this chapter. It has been checked and non-linearity was not found (Fig. 6.10).

Chornet and Roy (184) defined the relationship between log A and E as a compensation effect. They report a compensation effect during the pyrolytic decomposition of a number of highly oxygenated solid fuels, namely wood, peat, lignin, cellulose, hemicellulose and α-cellulose.

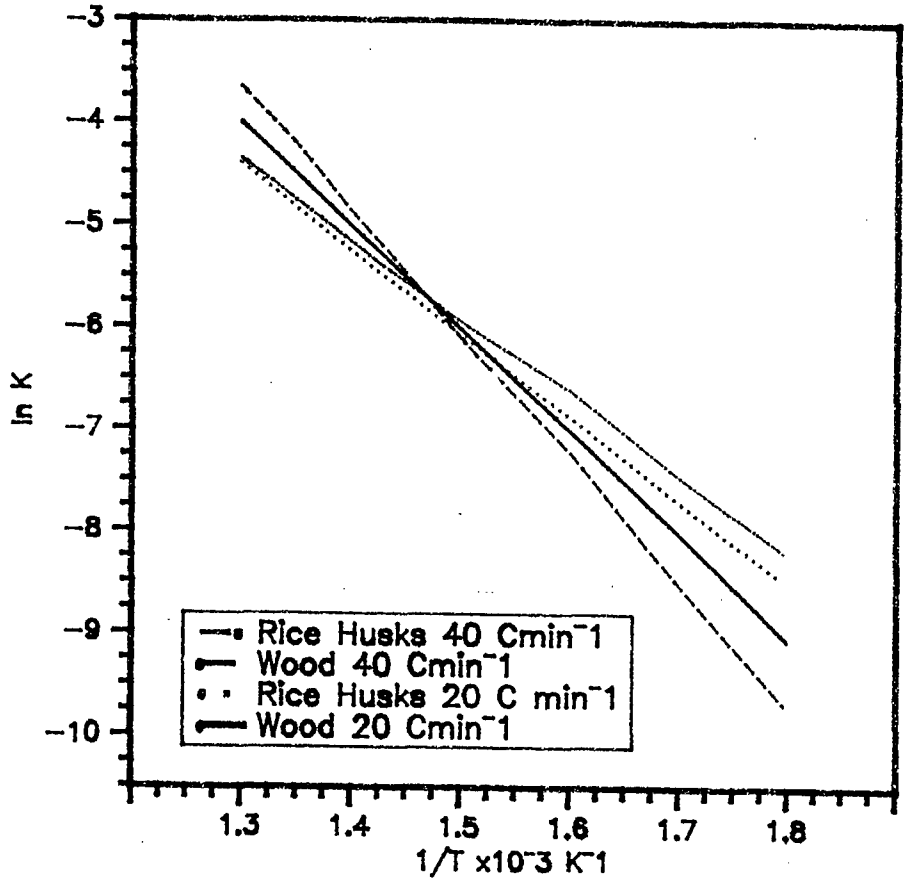

Fig. 6.10. Arrhenius plots for some wood and rice husks.

Agrawal (191) conversely suggests that the compensation behaviour for the pyrolysis of cellulosic materials reported by Chornet and Roy (184) is primarily due to inaccurate temperature measurement and large temperature gradients within the sample. The linear relation between ln A and E has no physical significance.

The activation energies and pre-exponential factors for the pyrolysis of wood and rice husk at different heating rates are seen in Table 6.2 and 6.3. The information also includes overall reaction kinetic parameters in order to compare with literature figures. Kinetic parameters for wood, rice husk, hemicellulose, cellulose and two lignin samples extracted from wood and rice husk have been calculated using thermogravimetric analysis.

As can be seen in Table 6.2, the activation energies of wood decreased as the heating rate increased. Similar trends were also reported by Antal et al (69). They tested various heating rates between 2.16 - 55°C min °C to pyrolyse cellulose in nitrogen environment and they found that activation energies decreased when the heating rate increased.

For the heating rates of 5°C min^{-1} and 20°C min^{-1} first and second step reaction activation energies differ significantly. This difference disappears when the heating rate of 40°C min^{-1} and 80°C min^{-1} are considered.

Arsenau (68) regarded that the initial low value of the activation energy as being caused by the char forming and latter activation energy as being caused by tar forming reactions.

Shafizadeh (177) confirmed that at higher temperatures, the tar forming reactions accelerate rapidly and overshadow the production of char and gases.

Barooh and Long (178) reported activation energies for wood as 18 kJ mol^{-1} below 330°C and 84 kJ mol^{-1} above 330°C. Font et al (179) report an activation energy 108 kJ mol^{-1} for the overall decomposition of almond shells.

Another activation energy for wood as 150 kJ mol^{-1} was reported by Browne and Tang (180). Also, Figuerido et al (181) reported for "pinus pinaster" wood activation energies were in the range of 77 - 146 kJ mol^{-1} and for chestnut tree wood 85 - 188 kJ mol^{-1}.

As can be seen in Table 6.3, rice husk decomposition activation energy show similarities to wood and decreased as the heating rates

were increased. Conversely, Boateng et al (182) calculated activation energies of rice husk at the heating rates of 40, 80 and 160°C min^{-1} and reported a mean activation energy as 183 kJ mol^{-1}. They also suggested there was no influence of heating rate on the activation energy. Similar conclusions were also found by Raman et al (183) reporting the activation energy as 175 kJ mol^{-1}.

Consequently, from a survey of the number of published data it can be seen that the reported kinetic parameters are variable because of the use of wide variety of experimental techniques and different calculation methods by various researchers. Important factors which influence the nature of the kinetics of the pyrolysis reactions include heating rate of the biomass, the temperature range of the operation and the residence time of the volatiles in the reactor (69).

Table 6.2. Kinetic Parameters For The Decomposition of Wood by TGA. Analysis For The Low and High Temperature Reaction Regimes and For The Overall Decomposition.

Heating Rate °C min^{-1}	Pre-exponential Factor A s^{-1}	Activation Energy kJ mol^{-1}
5 Low	3.52×10^4	84.5
High	1.5×10^{12}	176.0
Overall	4.79×10^5	97.0
20 Low	9.2×10^4	88.9
High	4.2×10^9	147.1
Overall	6.4×10^4	87.2
40 Low	2.8×10^4	81.7
High	1.47×10^5	89.8
Overall	7.57×10^4	86.2
80 Low	1.3×10^4	77.1
High	6.2×10^4	84.1
Overall	5.9×10^4	83.9

Table 6.3. Kinetic Parameters For The Decomposition of Rice Husks by TGA. Analysis For The Low and High Temperature Reaction Regimes and For The Overall Decomposition.

Heating Rate °C min^{-1}	Pre-exponential Factor A s^{-1}	Activation Energy E kJ mol^{-1}
5 Low	1.96×10^6	100.1
High	5.56×10^9	143.2
Overall	8.84×10^6	108.8
20 Low	4.46×10^9	134.6
High	2.24×10^8	131.5
Overall	8.47×10^5	105.3
40 Low	1.35×10^7	110.3
High	7.25	37.2
Overall	4.7×10^4	85.9
80 Low	5.37×10^7	98.2
High	5.25×10^2	28.6
Overall	1.12×10^5	84.9

Another important parameter was pointed out by Agrawal et al (69) that of the location of the thermocouple measurements. The heat transfer from the furnace to the sample is important factor to be considered in determining kinetic parameters. Close coupling of the measuring temperature thermocouple to the sample is desirable.

In this work, the thermocouple measured the temperature of the sample boat. As a result, the shift in thermograms with increasing heating rate is to be due to changes in the kinetics of the thermal decomposition. Also, the data in the literature for the activation energy of biomass decomposition is clearly dependent on the type of biomass. It is obvious since they include different compositions of cellulose, hemicellulose and lignin and different trace metal compositions. This is also seen in Table 6.4. Activation energies for cellulose in microcrystalline form differ from activation energies for cellulose in the form of Whatman filter paper no. 1 which is fibrous and contains trace metals. In the literature there

is a disagreement about the precise activation energy value for the decomposition of cellulose (Table 6.5). Also, Arsenau (68) reports an activation energy of 190 kJ mol^{-1}, Lewellen et al (185) 140 kJ mol^{-1}, Shafizadeh and Bradbury (186) 155 kJ mol^{-1} and Agrawal (5) 205 kJ mol^{-1} for the pyrolysis of cellulose.

Table 6.4. Kinetic Parameters For The Decomposition of Hemicellulose, Cellulose in Microcrystalline Form and as Whatman Filter Paper No. 1 and Lignins (from wood and rice husks) by TGA

Substance	Pre-Exp Factor s^{-1}	Activation Energy kJ mol^{-1}
Hemicellulose		
5°C/min	1.86×10^{22}	258.8
20°C/min	2.67×10^{21}	257.2
40°C/min	2.94×10^{15}	194.0
80°C/min	1.61×10^{9}	125.1
Cellulose (microcrystalline)		
5°C/min	6.49×10^{19}	260.4
20°C/min	2.52×10^{17}	233.2
40°C/min	3.70×10^{16}	225.0
80°C/min	1.45×10^{13}	187.6
Cellulose (Filter Paper)		
5°C/min	1.23×10^{14}	197.8
20°C/min	9.95×10^{12}	188.5
40°C/min	2.84×10^{10}	157.7
80°C/min	1.48×10^{8}	128.3
Lignin (From Wood)		
5°C/min	2.77×10^{7}	124.3
20°C/min	3.57×10^{2}	64.5
40°C/min	0.57	52.6
80°C/min	0.29	45.8
Lignin (From Rice Husks)		
5°C/min	1.93×10^{5}	97.8
20°C/min	1.91×10^{3}	72.4
40°C/min	1.76×10^{2}	58.4
80°C/min	2.25×10^{2}	55.9

It was suggested by Antal (47) that the variation in literature values of cellulose pyrolysis kinetic data reflect the complex pyrolysis mechanism which cannot be adequately simulated by simple rate law. Antal (47) also suggests the form of the cellulose and the presence of trace metals influence the activation energy as already referred to.

As it can be seen in Table 6.4 for both forms of cellulose, hemicellulose and lignin, there is a significant decrease in activation energy and pre-exponential factor with increasing heating rate. As mentioned earlier, Antal et al (69) reported that there was a decrease in the activation energy from 222 kJ mol^{-1} to 153 kJ mol^{-1} as the heating rate was increased from 2°C min^{-1} to 55°C min^{-1}.

The activation energy for the thermaldegradation of the components of the biomass was in the order of cellulose > hemicellulose > lignin as also shown by Ramiah (63) and Lipska-Quinn et al (38).

In this work, hemicellulose, cellulose (microcrystalline form) and lignin decomposition activation energies show same order for the heating rates of 5°C min^{-1}, 40°C min^{-1} and 80°C min^{-1}. Only at the 20°C min^{-1} heating rate is the activation energy of cellulose decomposition lower than that of hemicellulose.

Table 6.5. Some Arrhenius Parameters Reported In Literature. (Data used by Chornet and Roy (184) establishing the compensation effect for pyrolysers of cellulosic materials)

Material	T Range	E	A
Wood	280 - 325	96.3	9.9×10^{7}
Wood	325 - 350	226.1	3.9×10^{18}
Lignin	260 - 344	87.9	9.9×10^{18}
Lignin	344 - 435	37.6	5.6×10
Lignin	280 - 300	145.7	4.3×10^{12}
Lignin	360 - 500	141.5	7.6×10^{9}
Cellulose	300 - 420	227.3	1.8×10^{18}
Cellulose	280 - 360	166.6	2.4×10^{13}
Cellulose	250 - 1000	139.8	4.0×10^{11}
Cellulose	230 - 400	125.6	4.2×10^{9}
Cellulose	275 - 360	234.5	2.4×10^{19}
Hemicellulose	240 - 350	124.0	8.7×10^{10}
Hemicellulose	220 - 280	119.3	2.9×10^{10}
α-Cellulose	240 - 308	146.5	3.9×10^{11}
α-Cellulose	308 - 360	234.5	2.4×10^{19}
α-Cellulose	230 - 560	55.6	1.1×10^{4}
α-Cellulose	240 - 580	48.1	1.1×10^{4}
α-Cellulose	280 - 700	79.5	1.0×10^{6}
Filter Paper	160 - 380	163.7	1.3×10^{13}
Filter Paper	280 - 400	45.2	1.1×10^{4}
Peat	100 - 800	108.8	1.1×10^{10}

6.1.3 Thermogravimetric Analysis of Mono and Oligosaccharides

In this part of the work, the model carbohydrate compounds represented by the monosaccharides hexose (glucose) and pentose (xylose), disaccharide (maltose), trisaccharide (melezitose) and tetrasaccharide (stachyose) and also levoglucosan were pyrolysed in the thermogravimetric pyrolyser at the identical experimental conditions with the biomass and compounds (Fig. 6.11).

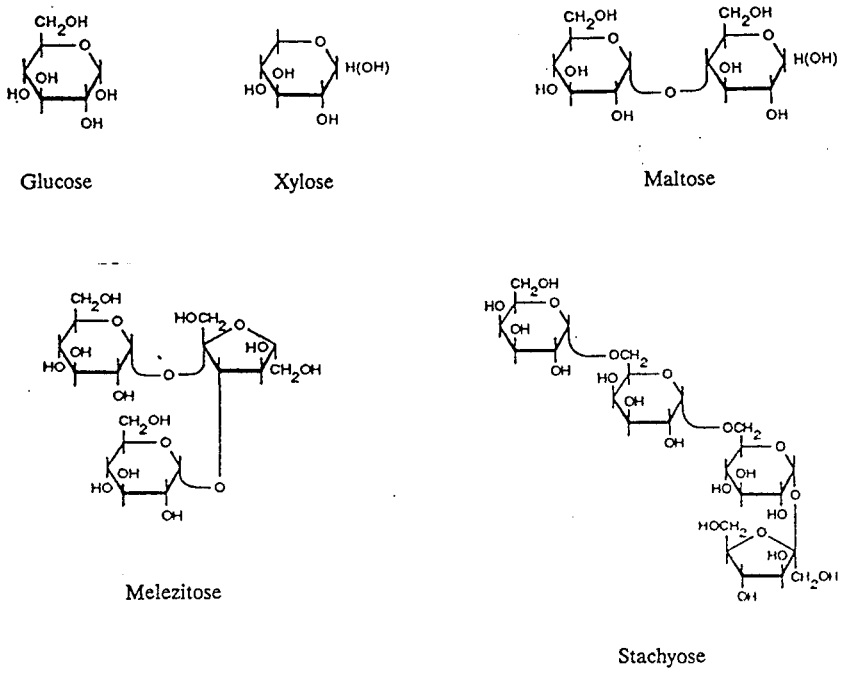

Fig. 6.11 Formulas of the monomeric sugars (47)

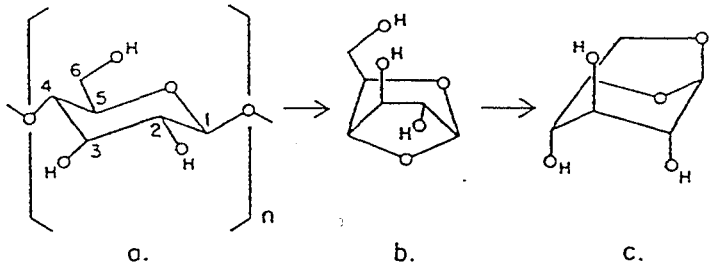

Fig. 6.12 Proposed mechanism for the formation of levoglucosan.

(a) The Glucopyrasonic Monomer
(b) 1,4-Anhydro-α-D-Glucopyranose
(c) 1,6-Anhydro-β-D-Glucopyranose (Levoglucosan)

Carbohydrate based biomasses have the best potential to supplement energy and chemical feedstuff needs which are presently derived from fossil fuel (170).

The reason those particular mono and oligasaccharides were chosen was because they were identified in the biomass structure. Over the years, research has shown cellulose to be a linear polysaccharide composed of anhydroglucose units.

The non-cellulosic polysaccharide and related substances comprise the hemicelluloses. These hemicelluloses are further characterised as polyuranides, mannan, galactan, xylan or araban. The hemicelluloses are sometimes characterised as pentosans and hexosans. Glucose is the prevalent monomer in the structure of cellulose. Mannose in the hemicellulose component of coniferous (soft) woods and xylose in deciduous (hard) woods (47). Levoglucosan, the major constituent of pyrolytic tars is an isomer of the cellulose monomer. For each molecule of levoglucosan produced from cellulose two bonds must be broken and one formed. The mechanism of levoglucosan formation is shown in Fig. 6.12 (66).

Figures 6.13 to 6.16 show TGA and DTG curves of xylose, alpha-D-glucose and maltose respectively. Similarly, TGA and DTG curves of melezitose, stachyose and levoglucosan are shown in Figures 6.17 to 6.20.

As is seen from the TGA curves, stachyose has a quite significant initial weight loss, while the others have lesser initial weight loss. The monosaccharides which are comprised of glucose and xylose start the main weight loss earlier than the other oligosaccharides at about 175°C and 179°C respectively (Table 6.6).

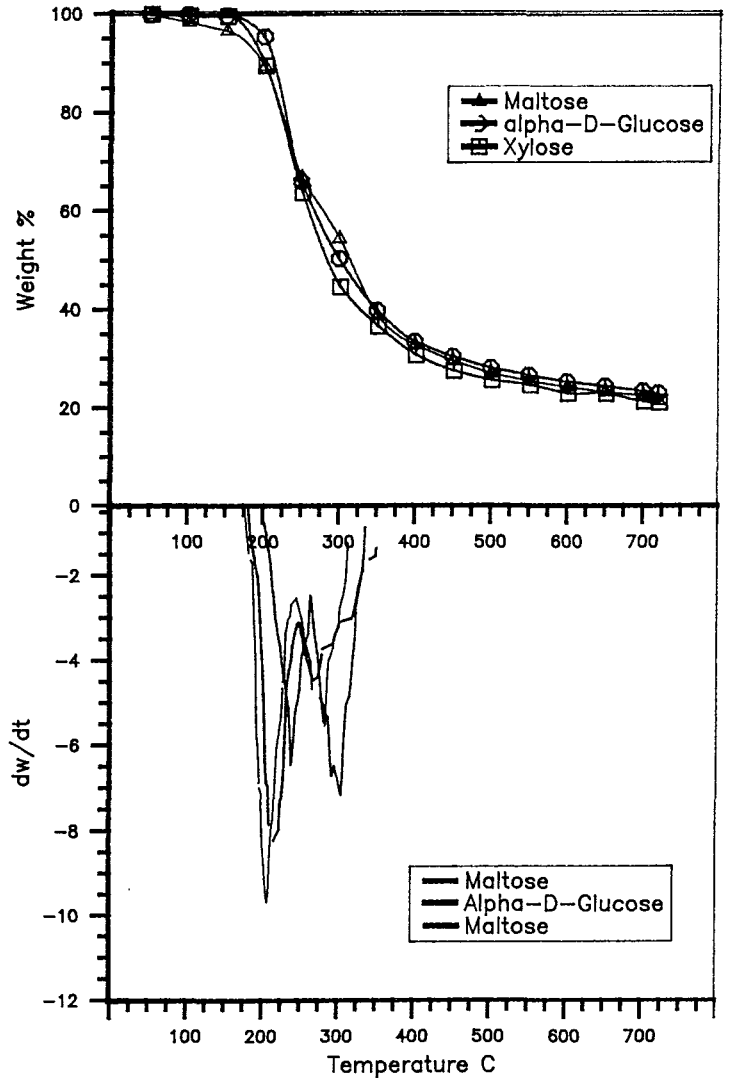

Fig.6.13 TGA and DTG curves for 5 C/min

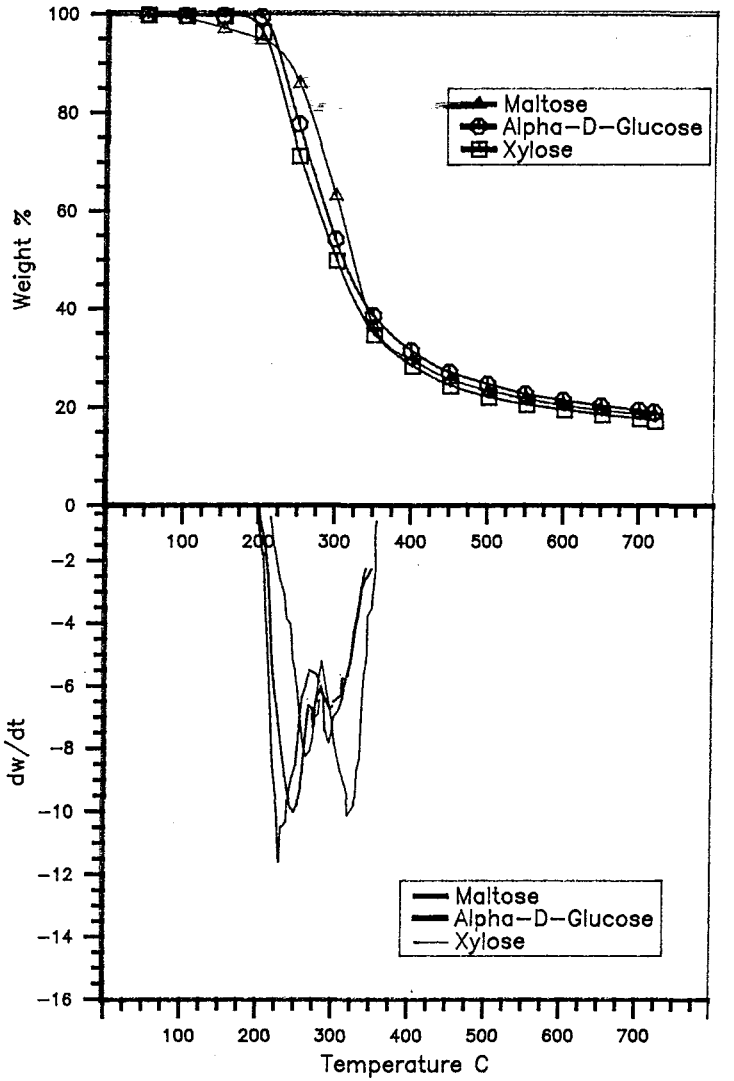

Fig.6.14 TGA and DTG curves for 20 C/min

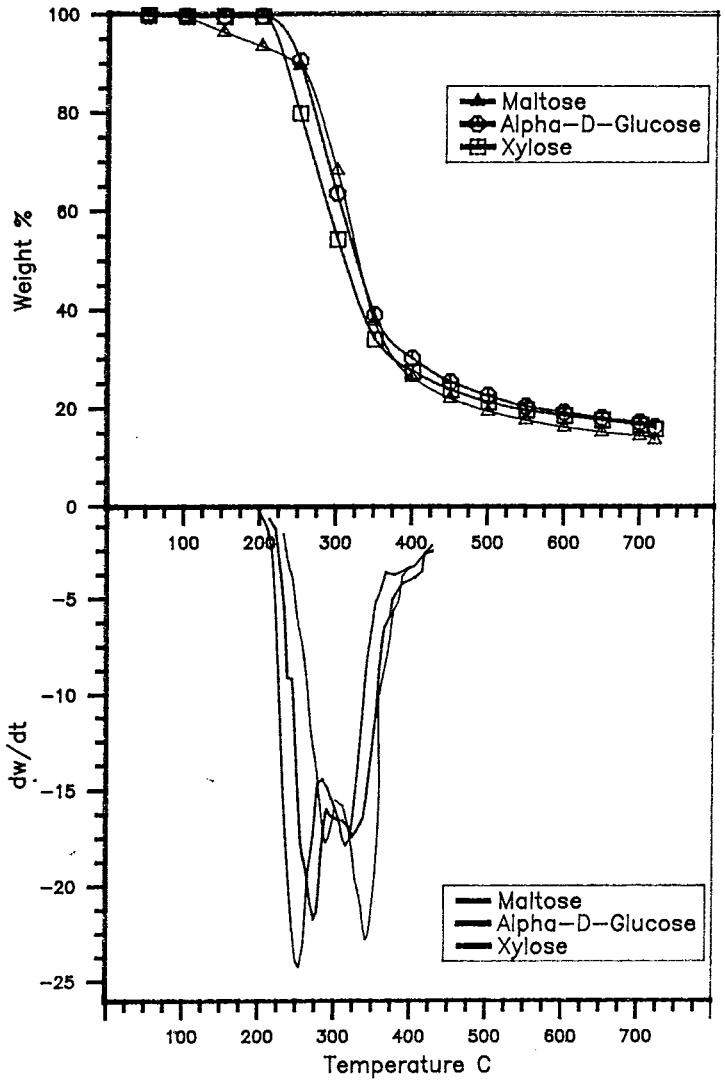

Fig.6.15 TGA and DTG curves for 40 C/min

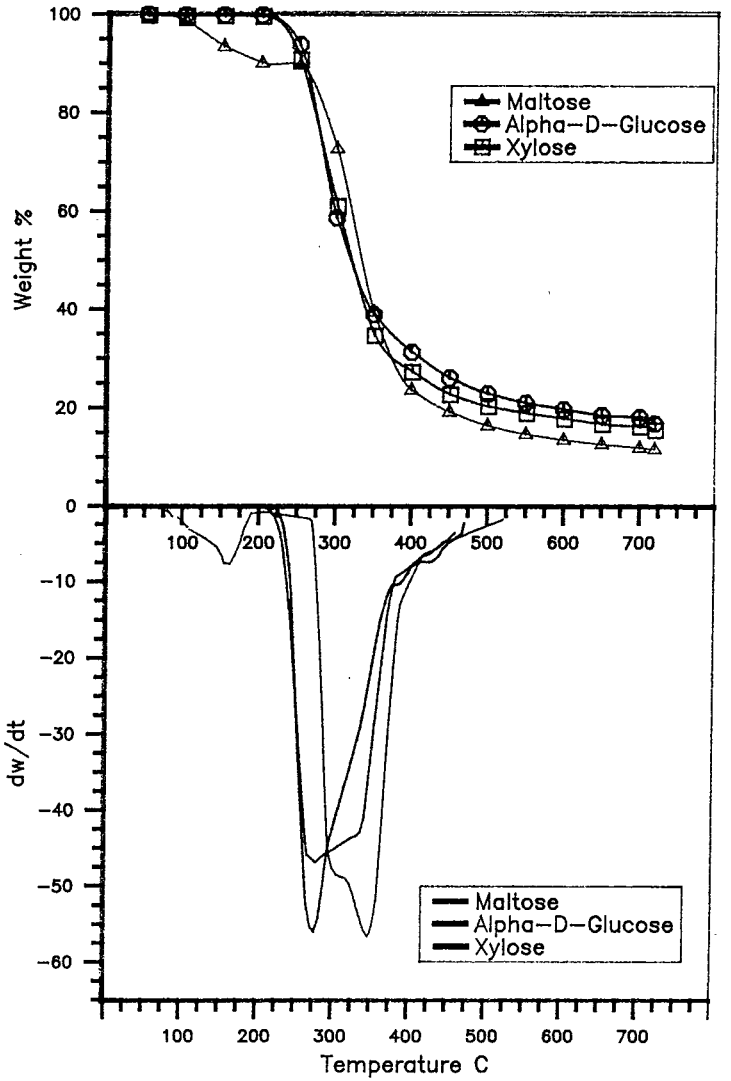

Fig.6.16 TGA and DTG curves for 80 C/min

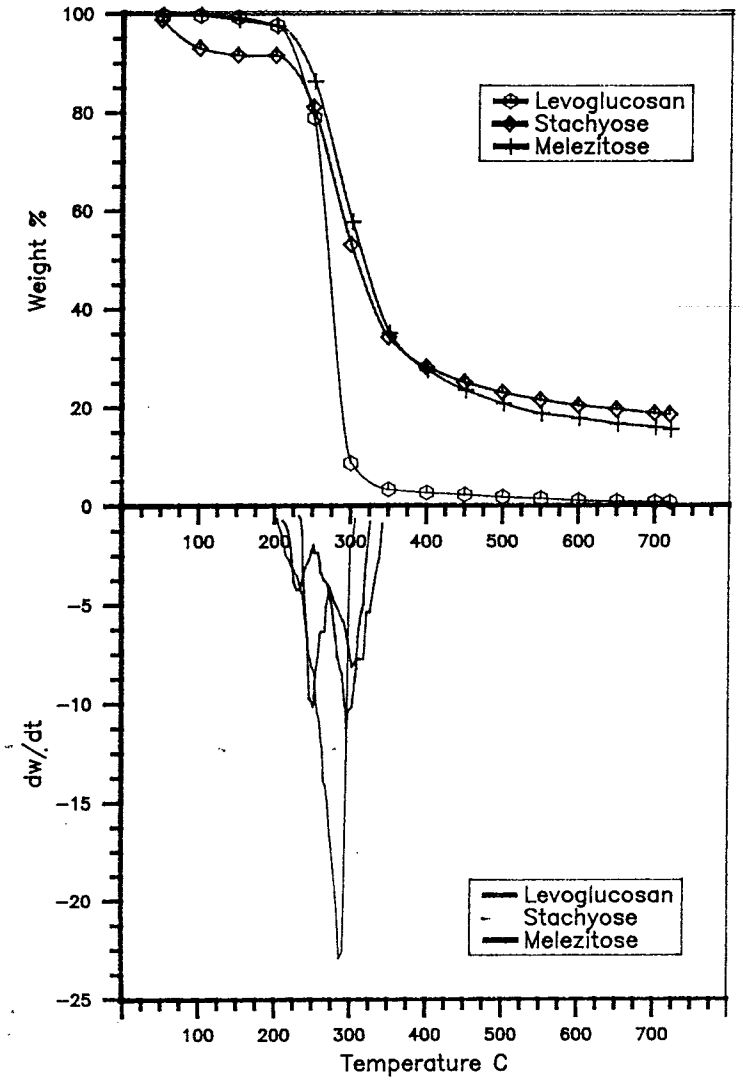

Fig.6.17 TGA and DTG curves for 5 C/min

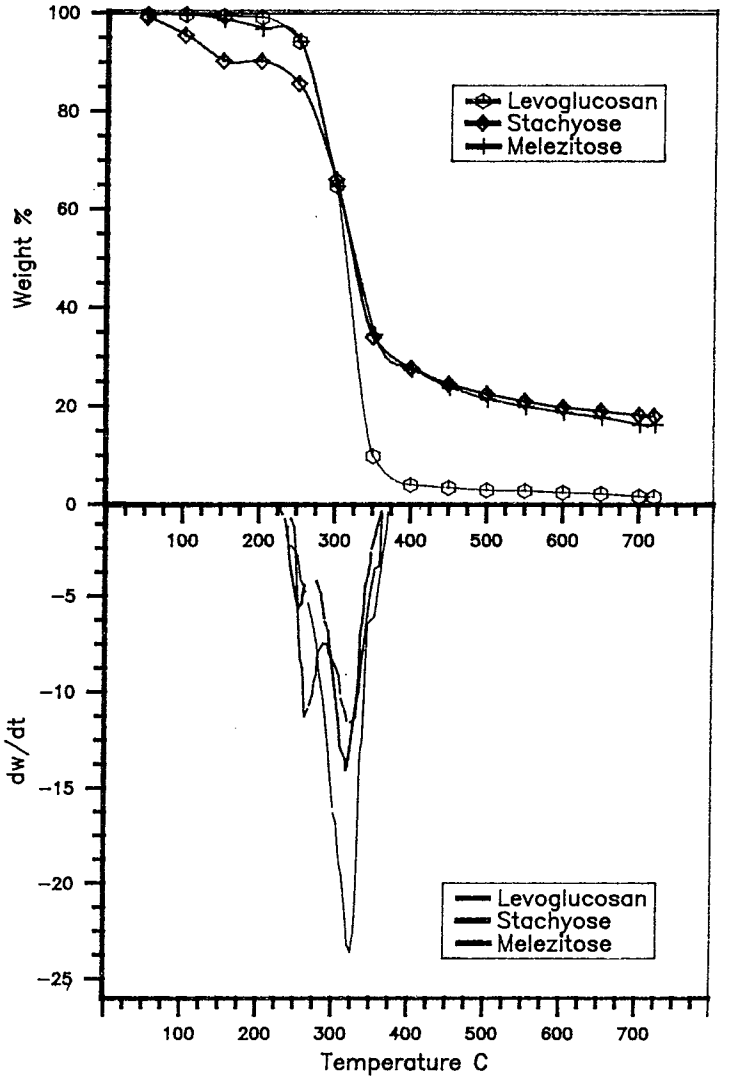

Fig.6.18 TGA and DTG curves for 20 C/min

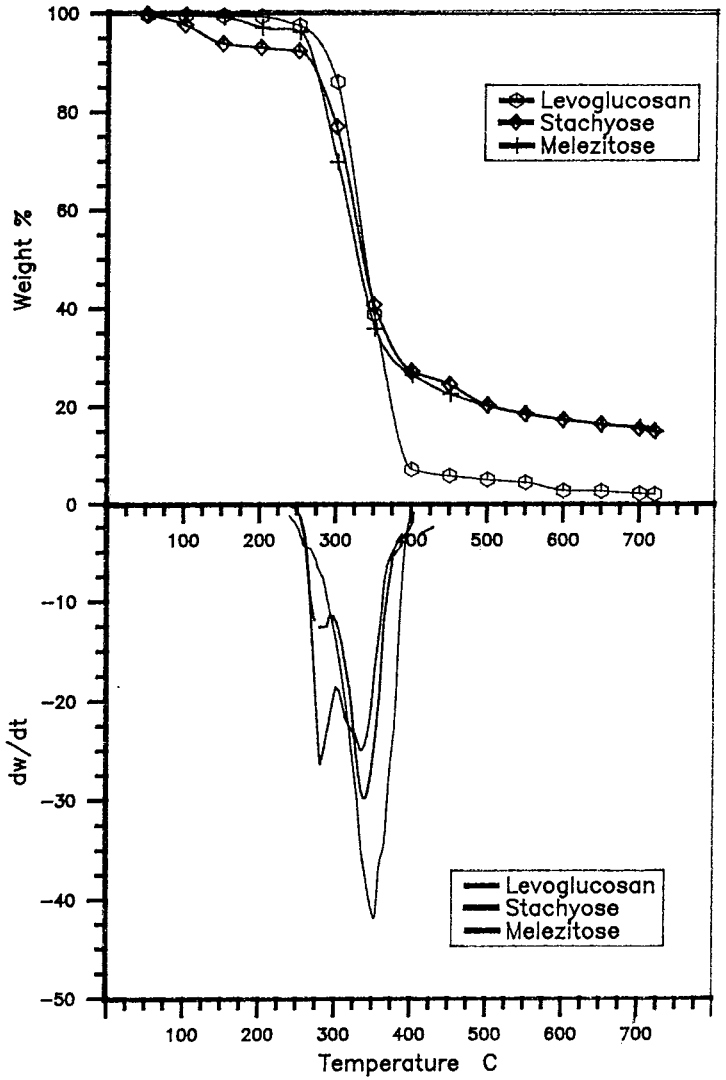

Fig.6.19 TGA and DTG curves for 40 C/min

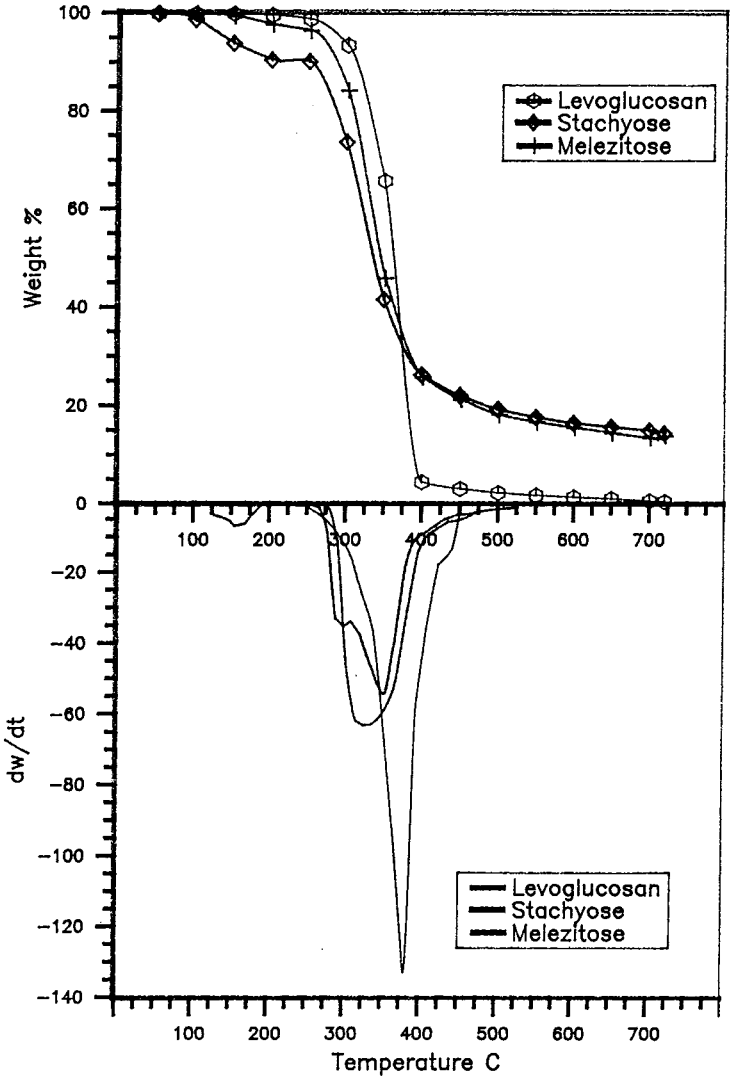

Fig.6.20 TGA and DTG curves for 80 C/min

Table 6.6. Temperature Ranges and Temperatures of Maximum Weight Loss For The Pyrolysis of Saccharides

	T_1 °C	T_{1max} °C	T_2 °C	% wt	T_{2max} °C	T_3 °C	% wt	T_{end} °C	% char
lose									
	175	207	240	31	275	312	58	720	23
	200	225	270	32	300	340	62	720	20
	203	248	275	32	315	365	68	720	15
pha-D-glucose									
	179	225	250	32	275	350	46	720	26
	203	250	275	32	300	350	58	720	20
	210	275	290	32	325	400	72	720	17
	226	278	400	68	-	-	-	720	17
ltose									
	200	240	275	34	309	330	95	720	17
	215	265	280	34	325	360	64	720	20
	225	290	315	34	348	380	72	720	15
	290	350	415	77	-	-	-	720	13
lezitose									
	210	230	245	27	298	340	37	720	16
	230	265	285	30	325	360	45	720	15
	252	280	300	34	327	400	74	720	15
	276	325	425	75	-	-	-	720	13
achyose									
	203	230	250	20	300	330	39	720	20
	225	252	265	20	325	365	46	720	18
	250	285	300	27	340	450	53	720	16
	275	361	450	78	-	-	-	720	14
voglucosan									
	200	280	305	92	-	-	-	720	3
	225	325	370	95	-	-	-	720	2
	230	350	400	93	-	-	-	720	2
	255	380	450	97	-	-	-	720	1

The disaccharide maltose is the next saccharide to decompose. The tetrasaccharide stachyose decomposes earlier than the trisaccharide melezitose. Also, levoglucosan starts to lose weight at the same

time as stachyose. The weight loss percentages for the end of each step and final char yields are listed in Table 6.6.

The final char yields for the heating rate of 5°C min^{-1} are in the range of 17% - 26%. These amounts decreased as the heating rate increased. The char yields for the decomposition of carbohydrates employed at the heating rate of 80°C min^{-1} were in the range of 13 - 17%. In contrast to saccharides, thermaldecomposition of levoglucosan yielded a char percentage mass in the range of 1 - 2% weight.

Pavlath and Gregorski (170) obtained similar weight loss percentages for glucose and maltose decomposition. They also suggest that the pyrolysis of such complex molecules as carbohydrates must involve various competing simultaneous and consecutive reactions.

The DTG curves (figures 6.13 to 6.20) show that the thermaldecomposition of carbohydrates occur in two steps except for the heating rate of 80°C min^{-1}. The two peaks on the DTG curves become closer as the heating rates increased.

Consequently, for the heating rate of 80°C min^{-1} depending on the dominance of reactions one overshadows the other. For xylose, glucose and melezitose the first decomposition step becomes dominant and for the fast heating rates the second decomposition step appears as a shoulder on the first decomposition peak while the second decomposition peaks become dominant on the first ones of maltose and stachyose.

It is shown by Pavlath and Gregorski (170) that minor changes in chemical structure can influence the thermal degradation of

saccharides. They showed that the monosaccharides mannose and glucose which differ only in a steric configuration of the hydroxyl group on the second carbon produced a difference in the pattern of thermaldegradation.

Various carbohydrates including cellulose, xylose, glucose and maltose were pyrolysed at 300°C to 500°C by Heyns and Klier (187). It was found that they gave the same degradation products. They suggested that thermaldecomposition of cellulose, monosaccharides and disaccharides involves similar polymeric intermediates which then undergo secondary degradation. The similarity in the TGA and DTG traces for the different saccharides shown here would suggest a similar thermaldegradation process. A low temperature, below 300°C and a high temperature, above 300°C group of degradation reactions. The data however suggests that the intermediate polymer formed is not the same for each saccharide since the DTG trace gives a different maximum rate of weight loss temperature regime for each saccharide.

When the TGA and DTG traces for the saccharides are compared to those of wood, rice husks, cellulose, hemicellulose and lignin, it is seen that the thermaldecomposition of saccharides starts earlier than both wood and components and also rice husk and components. As seen in Figures 6.1 to 6.4 the thermaldecomposition of wood and main components occur in the temperature range of 240°C to 450°C, also, Figures 6.5 to 6.8 show similar decomposition ranges for rice husk and the main components of rice husk. Only the lignin derived from rice husks completes its decomposition at about 500°C.

However, the DTG traces for the saccharides wood and rice husks show two areas of weight loss whilst cellulose and hemicellulose show

a single DTG peak. The saccharides have been shown to be the products of the thermaldecomposition reactions of biomass materials. Essig and Richards (188) determined the yields of 1,5-anhydro-L-arabinofuranose from pyrolysis of agricultural wastes. Bradbury and Sakai (65), Shafizadeh (62), Shafizadeh et al (72) confirm that the thermaldecomposition of cellulose and hemicellulose are complex reactions involving a number of stages. Also, the mono and oligosaccharides are known to be the thermaldegradation products of cellulose and hemicellulose. Thermaldegradation of cellulose and transformation of the products are shown in Fig. 6.21 (189).

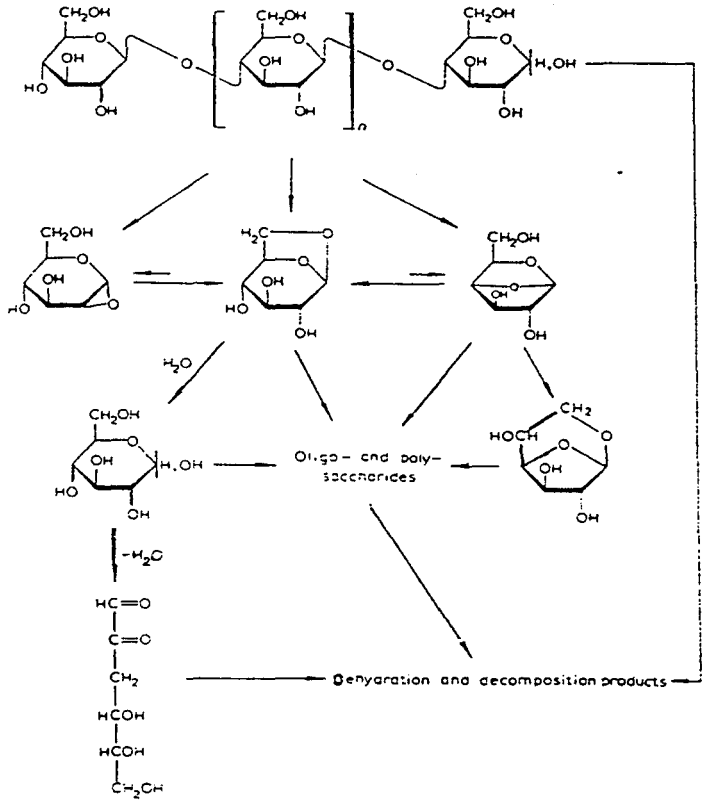

Fig. 6.21. Thermaldegradation of cellulose and transformation of products.

Table 6.7. Arrhenius Parameters for Thermaldecompositions of Saccharides.

Heating Rate C min^{-1}	A sec^{-1}	E kJ/mol^{-1}
Glucose		
5	2.56×10^{14}	156.4
20	4×10^{13}	156.1
	0.1	14.9
40	3.68×10^{10}	129.6
	67.3	42.3
80	5.52×10^{12}	150.42
Xylose		
5	2.21×10^{19}	197.5
	2.89×10^{2}	51.7
20	9.57×10^{16}	184.4
	8.26×10^{3}	67.1
40	7.07×10^{17}	194.5
	3.9×10^{3}	61
80	6.7×10^{13}	159.5
Maltose		
5	8.47×10^{9}	121.4
	7.52×10^{4}	78.9
20	2.18×10^{8}	110.1
	1.15×10^{5}	81.7
40	3.73×10^{7}	103.1
	3.44×10^{5}	85.5
80	2.63×10^{12}	156.7
Melezitose		
5	1.35×10^{44}	461
	9.51×10^{3}	69.8
20	1.14×10^{26}	269.4
	2.24×10^{5}	81.9
40	1.09×10^{23}	260
	1.24×10^{5}	81.6
80	2.01×10^{15}	189.4
Stachyose		
5	2.3×10^{21}	240.9
	2.88×10^{8}	118.2
20	5.14×10^{20}	225.4
	1.37×10^{9}	123.4
40	2.01×10^{17}	206.3
	1.3×10^{8}	114.6
80	1.8×10^{11}	144.7
Levoglucosan		
5	4.26×10^{8}	111.6
20	9.72×10^{6}	100.7
40	2.1×10^{6}	95.14
80	9.79×10^{5}	91.6

6.1.3.1 Relations Between Biomass Components and Saccharides

The activation energies and pre-exponential factors of the thermaldecomposition reactions of the saccharides are shown in the Table 6.7. It is seen that the activation energies decreased as the heating rate increased. Only with the heating rate of 80°C min^{-1} maltose decomposition which shows a higher activation energy than the other heating rates. This is probably the result of the more complicated decomposition pathway of maltose at higher temperatures.

Pavlath and Gregorski (170) suggest that during the decomposition of saccharides, additional occurrence of secondary reactions are inevitable. In this work, it was not possible to remove any products from the reaction zone for further analysis in the thermogravimetric analyser.

As indicated earlier, the reason for investigation of carbohydrates pyrolysis was to determine the thermaldecomposition of biomass waste in this work for wood and rice husk.

Since cellulose is one of the main components of biomass, determination of cellulose thermaldecomposition helps to understand the thermaldecomposition of biomass. Theoretically, pyrolytic degradation of the cellulose molecule may take place through cleavage of the glycosidic group of dehydration, elimination and breakdown of the sugar molecule takes place, resulting in gradual charring and depolymerisation of the molecule. According to Shafizadeh and Fu (189), these reactions take place very slowly until ~300°C, when sufficient energy becomes available for a rapid cleavage of the glycosidic bond and evaporation of the products. In the time,

levoglucosan may be formed directly from cellulose or indirectly through the intermediate formation of 1,2 or 1,4-anhydro-l-D-glucopyranose which could generate the two 1,6-anhydro sugars. Since the pyrolytic reactions can proceed through alternative pathways, the fate of the anhydro sugars, which are formed from the cleavage of the glycosidic linkage in cellulose, depends on the relative stability of the compound and the prevailing conditions.

6.2 Thermogravimetric Analysis of RDF and Components

Thermogravimetric analysis of the RDF and the components known to occur in municipal solid waste were performed using thermogravimetric analysis at the identical experimental conditions to the fixed-bed rig.

Figure 6.22 shows the TGA thermograms and DTG curves at the heating rates of 5, 20, 40 and 80°C min^{-1}. From the thermograms it can be seen that the heating rate shows little influence on the thermaldecomposition of RDF.

When the DTG curves are examined it is seen that RDF starts to decompose at about 270°C for all heating rates afterwards of initial loss of moisture.

Although heating rate seems not to affect the starting temperature for the oil heating rates, it rather influences quite significantly the final temperature of pyrolysis. Also, another decomposition step appears as the heating rate is increased. The two distinct areas of weight loss indicate two separate reactions are taking place.

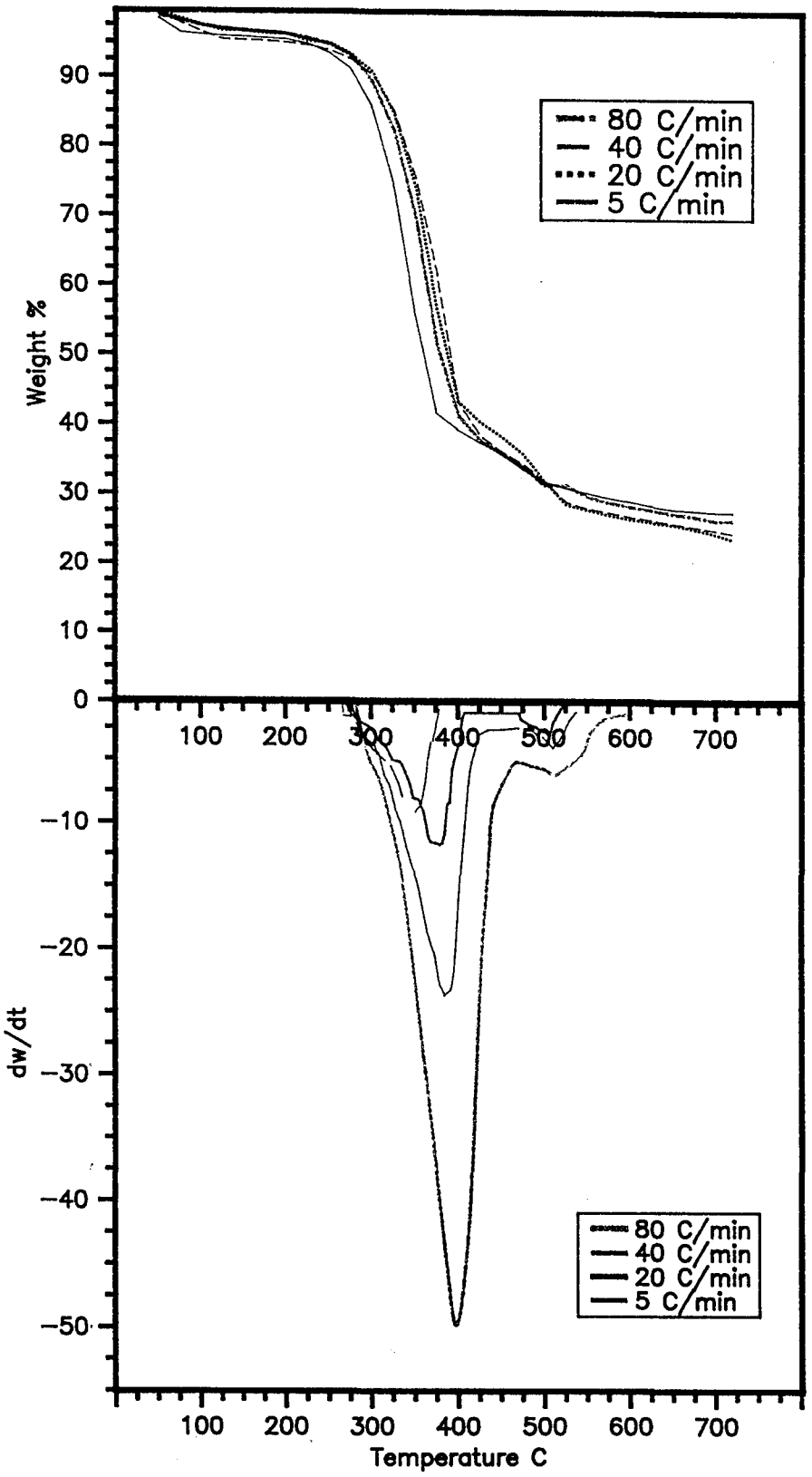

Fig.6.22 TGA and DTG curves for RDF

In contrast to the other samples employed in this work, RDF has a heterogeneous nature and consists of mostly biomass in the form of mainly cellulose, also in significant amounts of plastics, rubber and the others which vary through location and season.

Table 6.8 summarises the temperatures of the start of the maximum weight loss, also the final temperature of weight loss at the different heating rates. The weight loss reaches a maximum at temperatures of 350, 375, 385 and 400°C for the heating rates of 5, 20, 40 and 80°C min^{-1} respectively.

The second weight loss step does not appear for the heating rate of 5°C min^{-1}. The maximum weight loss for the second step occurs at about 502, 510 and 520°C for the heating rates of 20, 40 and 80°C min^{-1} respectively.

Table 6.8. Temperature Ranges and Temperatures of Maximum Weight Loss for the Pyrolysis of RDF and Possible Components.

°C min^{-1}	T_1	T_{1max}	T_2	T_{2max}	T_3
RDF					
5	280	350	380	480	510
20	280	375	402	502	520
40	280	385	420	510	530
80	280	400	460	520	565
PVC					
5	273	288	363	442	492
20	276	330	400	481	545
40	279	344	414	502	590
80	281	353	442	517	605
Waxed Cardboard					
5	299	359	377	470	493
20	300	381	404	496	514
40	313	407	438	518	552
80	317	429	460	520	516
Polyethylene					
5	300	502	522	-	-
20	310	510	536	-	-
40	353	524	617	-	-
80	425	530	630	-	-

6.2.1. Comparison of the Thermaldecomposition of RDF and Components

It is important, especially for the wastes like RDF which are immediately to be characterised and re-utilised, to understand their decomposition pathways for optimum and efficient disposal.

In order to compare the thermaldecomposition pathway of RDF with the known components occurring in municipal solid waste, the following components were chosen: PVC plastic, rubber tyre, pinewood, cardboard packaging, waxed cardboard packaging, cotton textile material, polyethylene plastic, newsprint, expanded polystyrene food packaging and synthetic carpeting were pyrolysed in the thermal analyser.

It is shown in Fig. 6.23 and 6.24 for the cellulosic wastes, newsprint, cardboard and wood that there was an initial loss of moisture. The main weight loss occurs depending on the type of waste component.

The cellulosic materials wood cardboard, waxed cardboard and newsprint start to lose weight earlier than the other samples at about 150°C - 180°C. During this step, moisture loss proceeds. The moisture loss of these samples are about 7.5% - 8%. Cotton also starts to lose weight in the same temperature range, but the moisture loss is only 2.5% - 5% wt.

The cellulosic materials above complete their moisture loss and start their main thermaldegradation step as follows; wood; 280°C, cardboard; 285°C, newsprint; 290°C, waxed cardboard; 300°C and cotton; 330°C. Also, the main thermaldecomposition step of wood, cardboard, newsprint, waxed cardboard and cotton complete at 480°C, 510°C, 490°C, 540°C and 520°C respectively.

For the PVC waxed cardboard and carpet there are two distinct areas of weight loss. The first step of main thermaldegradation of PVC, waxed cardboard and carpet starts at 280°C, 300°C and 260°C and completes at the temperatures of 450°C, 465°C and 460°C respectively.

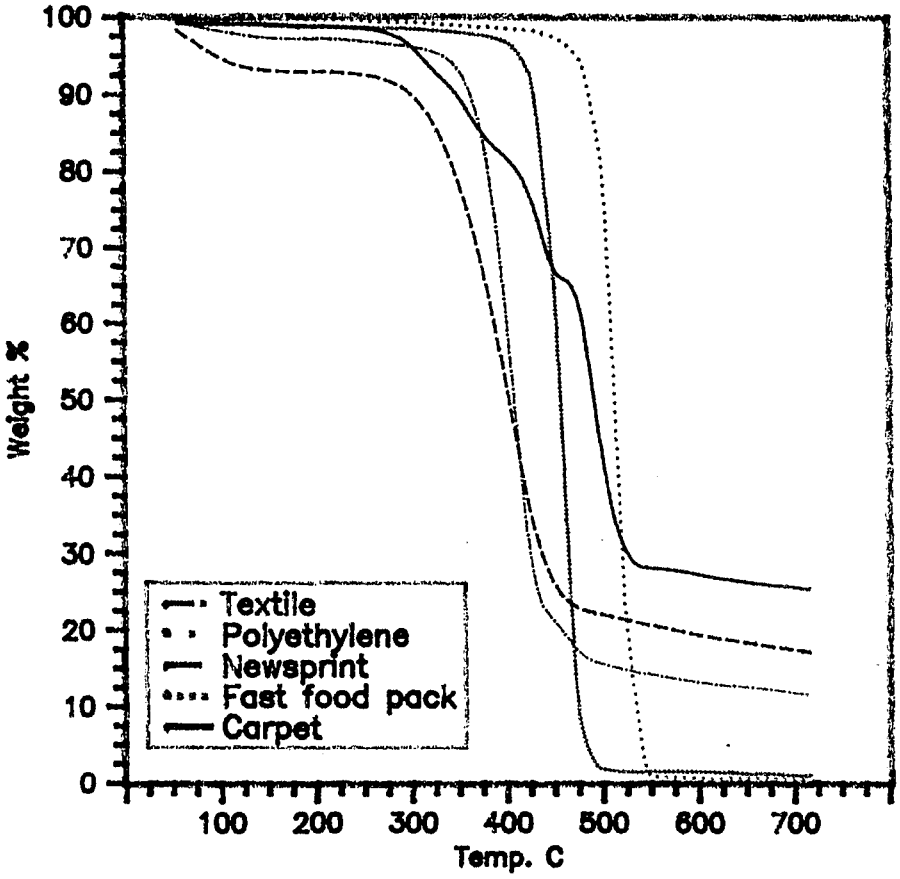

Fig 6.23 TGA Thermograms of Some RDF Components

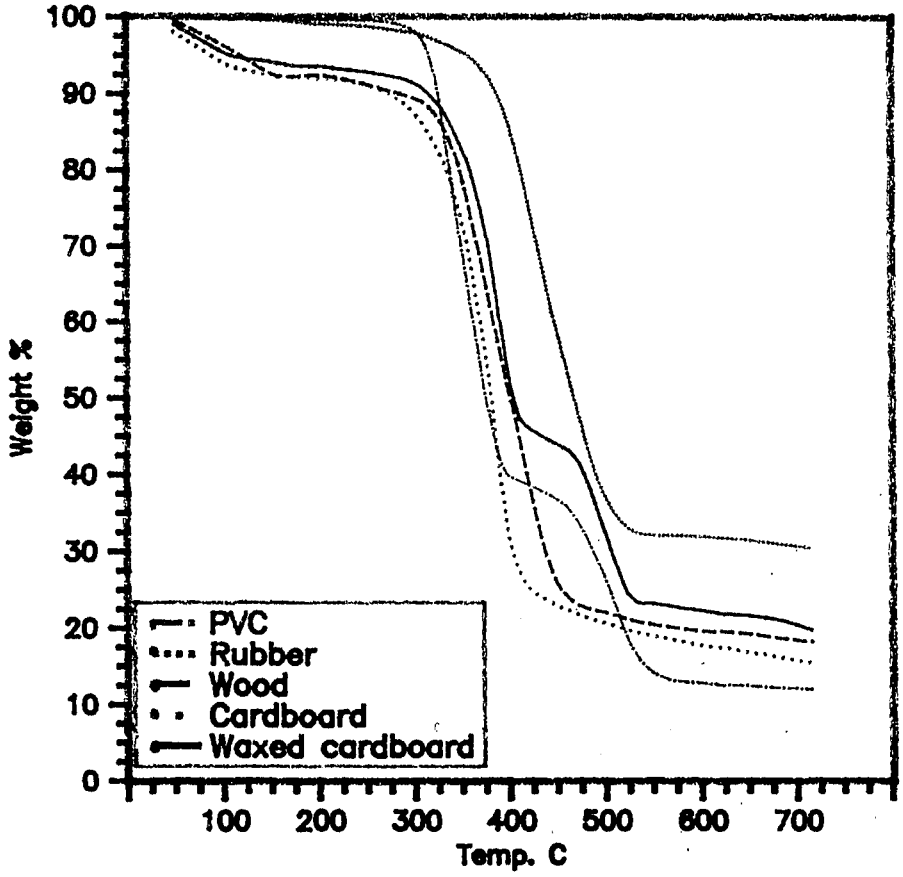

Fig 6.24 TGA Thermograms of Some RDF Components

The thermaldegradation of RDF also proceeds in two main steps after the moisture loss step (Fig. 6.22). The lower temperature degradation of RDF may be attributed to cellulosic wastes which are newsprint, the cotton textile, cardboard and wood and the higher temperature degradation may be attributed to plastics and includes rubber, polyethylene and polystyrene. This is also suggested by Agrawal (5), that cellulosic materials decompose earlier than plastics. In the thermaldecomposition of PVC, it is seen that there are two thermaldegradation regimes. The PVC plastic sample loses 60% of weight before the high temperature weight loss occurs.

Wilkins and Wilkins (99) have also shown that PVC has a two stage decomposition occurring in the temperature ranges of 180°C - 300°C and 350°C - 420°C for the low and high temperature stages respectively.

Figures 6.25 to 6.28 show the thermaldecomposition (TGA) curves and differential weight loss (DTG) curves of RDF, PVC, polyethylene and waxed cardboard for the heating rates of 5, 20, 40 and 80°C min^{-1}. PVC and plastic and polyethylene and waxed cardboard were chosen in order to compare their Arrhenius parameters with RDF. For the cellulosic content of the RDF, the data reported for wood and other lignocellulosics in section 6.1, also for the rubber content of RDF the results reported in section 6.3 can be compared with the data obtained from RDF.

The main decomposition peak of RDF coincides with the first degradation peak of waxed cardboard. For decomposition of waxed cardboard, the first decomposition step is most probably for the decomposition of the cellulosic part and the second step is for the

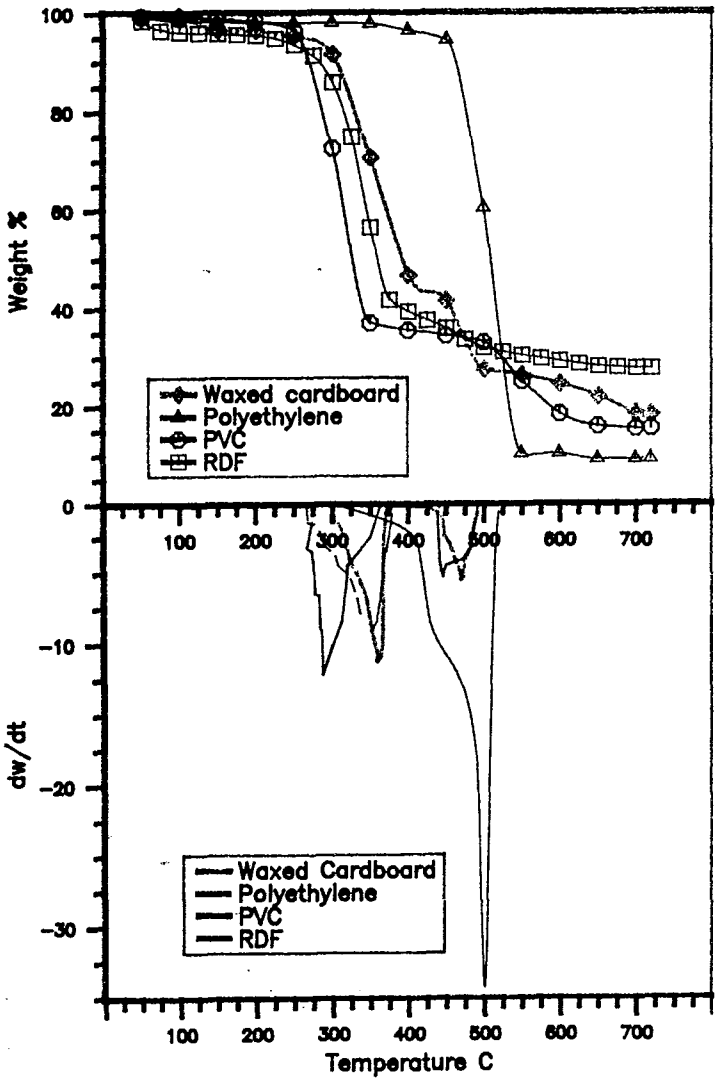

Fig.6.25 TGA and DTG curves for 5 C/min

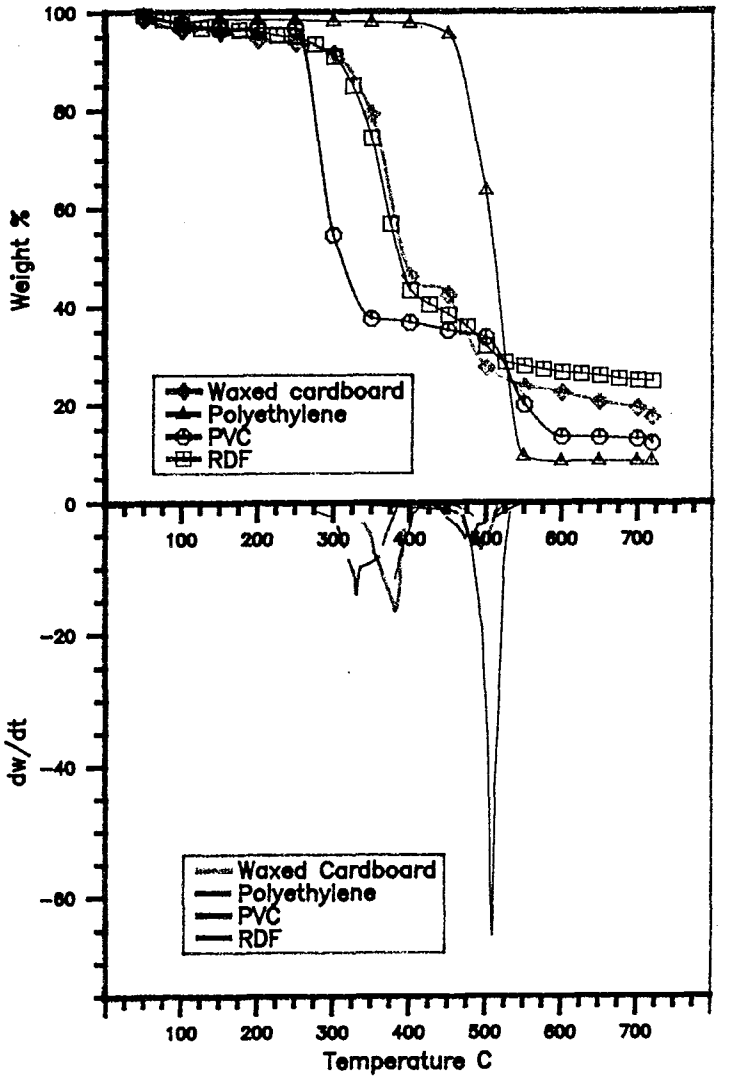

Fig.6.26 TGA and DTG curves for 20 C/min

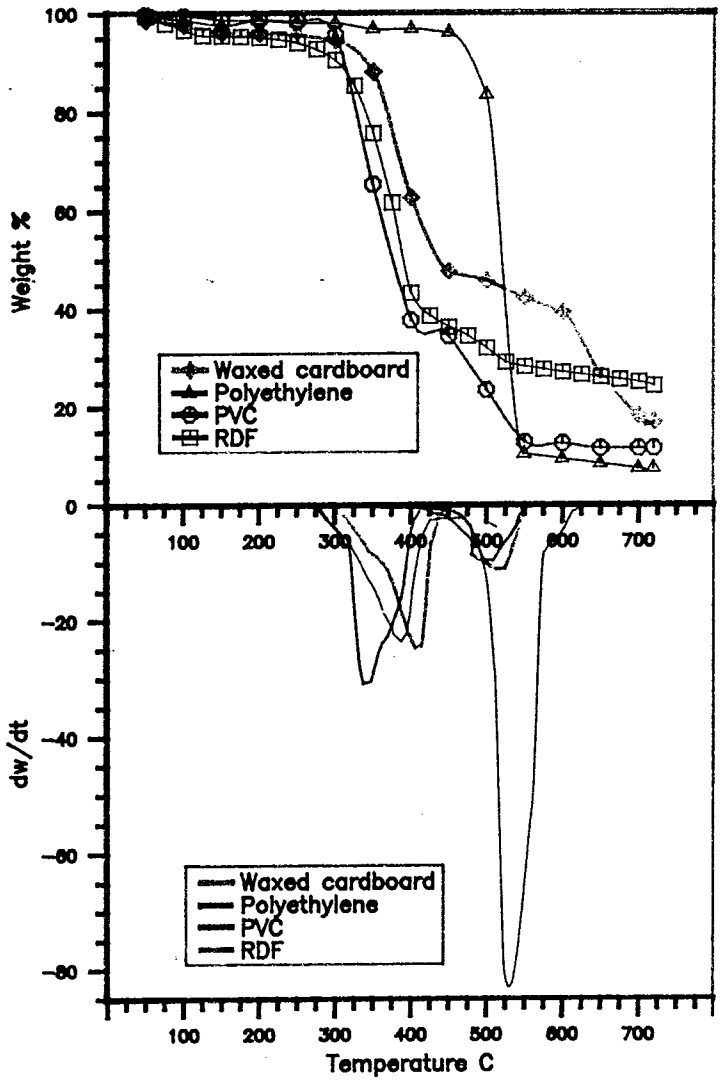

Fig.6.27 TGA and DTG curves for 40 C/min

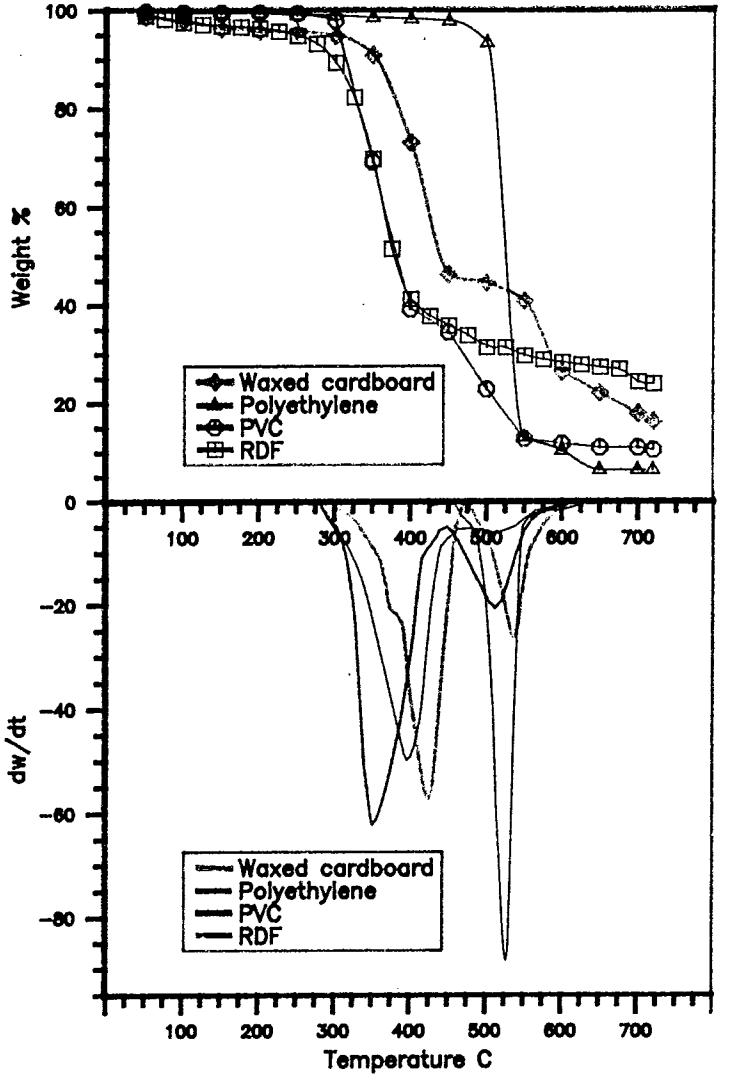

Fig.6.28 TGA and DTG curves for 80 C/min

plastic degradation. Also, the data reported in Table 6.1 for thermaldecomposition of wood, represents a similar temperature range for the first peak of the RDF. This confirms the conclusion made earlier that the earlier decomposition peak of RDF represents mainly decomposition of cellulosic materials.

Polyethylene decomposes in one step (Table 6.9) and the temperature range of decomposition was delayed with the increasing rate of heating. The thermaldecomposition range of low-density polyethylene for the heating rate of 20°C min^{-1} was reported by Kiron and Gillham (101) as 310°C - 510°C which is narrower than the data in Table 6.9. This was probably due to the difference in the density of the sample. Also, Agrawal (5) reported the activation energy of thermaldecomposition of polyethylene as 174.5 kJ mol^{-1} and pre-exponential factor as 4×10^{11} sec^{-1}, which coincide in this work the results of degradation of polyethylene at 40°C min^{-1} of E: 172.1 kJ mol^{-1} and $A = 1.17 \times 10^{11}$ sec^{-1}.

It is seen that the individual components activation energies are higher than the RDF activation energies, this is probably due to the heterogeneous nature of the samples. Also, the firm distinction between low temperature cellulosic and high temperature plastic thermaldegradation regimes for the components of RDF may not be applied to all the components which could be found in RDF.

The investigation of the RDF components separately would help to understand not only the nature of the thermaldecomposition reactions, but also complex interactions which might occur between primary products and other components of RDF.

Although it was reported by Rampling and Hickey (7) that the degree of bond scission is dependent on the quantity of energy supplied. Small energy additions tend to produce relatively large molecular fragments, whereas, larger energy additions yield much smaller fragments. In this part of the work, it has been found that RDF pyrolysis in the thermogravimetric pyrolyser is not affected greatly by the increased rate of heating. The pyrolysis investigations with the fixed-bed pyrolyser showed that (chapter 3) the yield amount differed significantly with the changing of heating rate.

From these data, it can be concluded that for the small particle size (2 mm) reaction is not heat transfer controlled. Conversely, for the bigger size particles, the reaction is ruled by heat transfer.

During the course of pyrolysis of RDF carbon, hydrogen and oxygen bonds are broken. Sometimes pyrolysers give monomers or further wide spectrum of smaller products which could be ultimate pyrolysis products. The thermaldecomposition of oxygenated compounds yields simpler and more stable compounds such as formaldehyde acetone and acetic acid (7).

Table 6.9 Arrhenius Parameters of Thermaldecomposition of RDF and Possible Components.

°Cmin^{-1}	A sec^{-1}	E kJ mol^{-1}
RDF		
5	1.9×10^{6}	100.3
20	2.6×10^{5}	93.8
	6.56×10^{7}	110.9
40	2.9×10^{4}	51.8
	9.8×10^{5}	76.1
80	2.9×10^{3}	65.6
	1.1×10^{2}	57.3
PVC		
5	1.28×10^{18}	231.7
	5.72×10^{16}	203
20	3.93×10^{12}	171.9
	4.82×10^{9}	197.3
40	1.19×10^{10}	141.4
	1.6×10^{10}	176.8
80	9.74×10^{9}	138.7
	1.31×10^{9}	158
Polyethylene		
5	7.1×10^{27}	414.2
20	3.21×10^{27}	391.7
40	1.17×10^{11}	172.1
80	2.4×10^{5}	118
Waxed Cardboard		
5	8.4×10^{12}	171.3
	6.2×10^{30}	180.4
20	2.39×10^{10}	154.8
	1.99×10^{31}	227.6
40	7.29×10^{5}	100.6
	2.62×10^{15}	229.6
80	9.13×10^{3}	76.2
	1.43×10^{13}	253.9

The weakest bond is C-C to be broken. C-H and O-H bonding are stronger than C-C, also, C=O, C=C and C≡C are quite strong bonds. Heteroatoms are very weak links.

The general description of the RDF pyrolysis can be summarised as follows:

(a) Just above 200°C, tight aromatic and aliphatic oils are evolved.

(b) Between 250°C - 300°C, gases containing mainly carbon oxides and tight hydrocarbons are evolved rapidly. The gas production starts to fall at ~450°C.

(c) Between 500°C - 600°C, a second step of thermaldecomposition occurs. This includes the evolution of viscous wax-like hydrocarbons and gas, mainly methane and hydrogen.

6.3 Thermogravimetric Analysis of Scrap Tyre and Main Components

Thermogravimetric analysis was employed to determine the thermal decomposition pathways of scrap tyre samples at the heating rates of 5°C min^{-1}, 20°C min^{-1}, 40°C min^{-1} and 80°C min^{-1}.

Various heating rates were chosen in order to investigate the effects of slow and medium heating rates on the thermaldecomposition of scrap tyre and tyre components within the heating rate limits of the TGA apparatus. In fact, those heating rates were employed during the fixed-bed reactor pyrolysis experiments.

Thermogravimetric analysis also helps to determine the percentage of highly volatile organics, elastomers, carbon black and inorganic residue for each sample.

The thermaldecomposition (TGA) and derivative thermal-decomposition (DTG) curves of scrap tyre are seen in Fig. 6.29 for the heating rates of 5, 20, 40 and 80°C min^{-1}.

It is seen that (Fig. 6.29) at lower heating rates, the scrap tyre starts to decompose earlier. When the heating rates were increased, thermaldecomposition started and finisheed later. The residual char amount was decreased as the heating rates increased. Also the DTG curves show that rubber tyre pyrolysis occurs in two steps which become merged for the higher heating rates. For the heating rates of 40°C min^{-1} and 80°C min^{-1} the second decomposition step appears as a shoulder on the first one.

To understand more about the decomposition of scrap tyres, DTG and TGA curves were compared with the DTG and TGA curves of rubber tyre components, which vary in percentage depending on the manufacturer.

The tyre components chosen were natural rubber (NR), Styrene-butadiene-rubber (SBR) and Polybutadiene rubber (BR).

The rubber polymers above are widely used in various percentages in the tyre manufacturing industry, depending on the desired end product.

Those polymers were pyrolysed in the thermogravimetric analyser at the identical heating ratesto those of the scrap tyre pyrolysis in the fixed-bed reactor to the final temperature of 720°C. The char yield results are shown in Table 6.10.

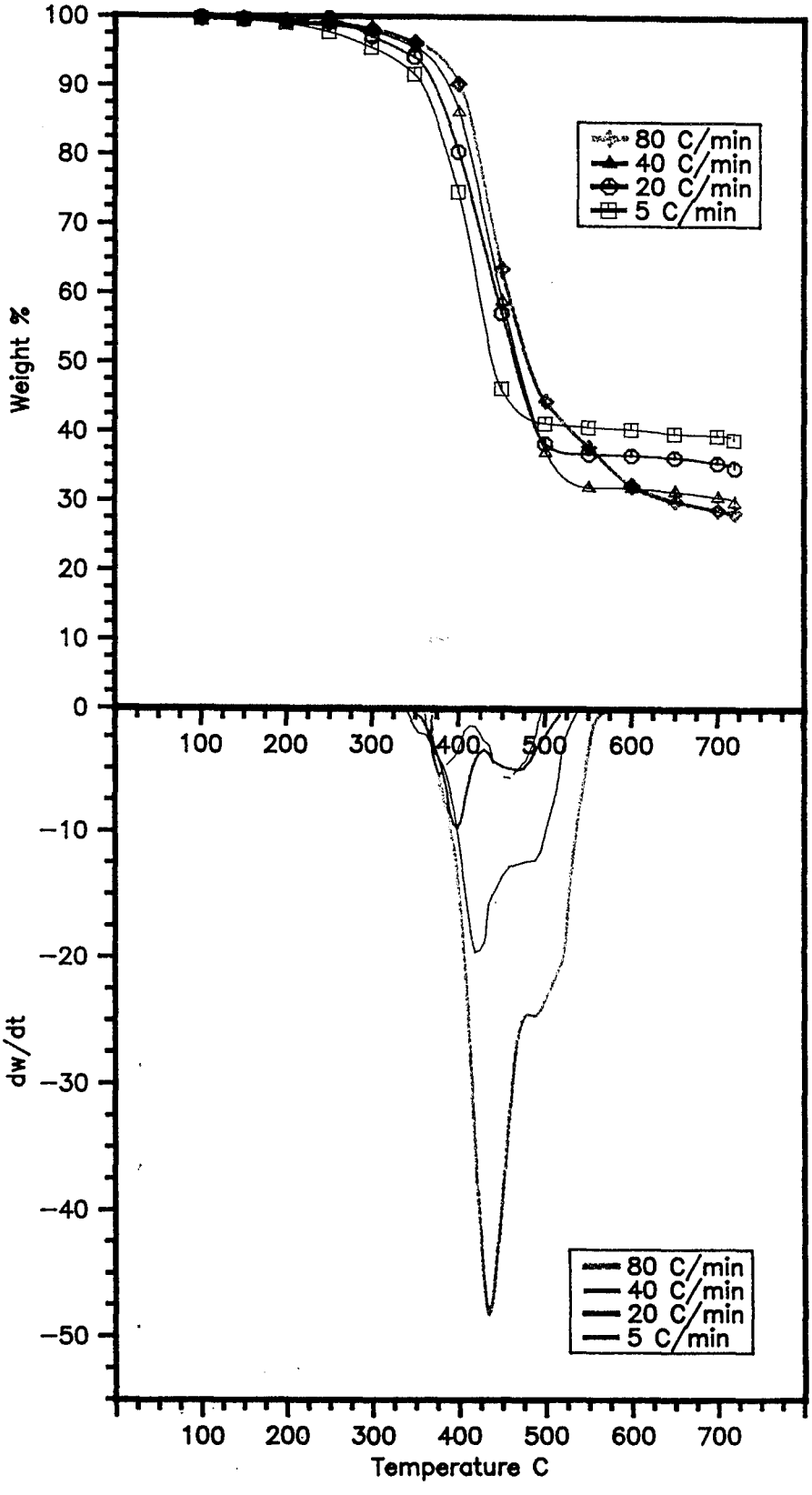

Fig.6.29 TGA and DTG curves for scrap tyre

Table 6.10 The Char Yields of Scrap Tyre and Components Pyrolysed in Thermogravimetric Analyser.

	Char Yield (% wt)			
Heating Rate (C min^{-1})	Tyre	NR	SBR	BR
5	39	3.0	2.0	4.0
20	35	2.0	2.0	3.0
40	29	1.5	1.0	2.1
80	27	1.0	1.0	1.0

When the scrap tyre TGA curves are compared with the other substances, it is seen that at the end of the reactions, scrap tyre samples gave residual char results of 39%, 35%, 29% and 27% for the heating rates of 5°C min^{-1}, 20°C min^{-1}, 40°C min^{-1} and 80°C min^{-1} respectively. The other substances complete their decompositions with much lower char amounts. The main reason for the observation of more char yield from tyre than their separate components is the carbon black which is added during the manufacturing of tyre. Brazier (167) reports that SBR and BR are non-carbonising elastomers and they leave less than 0.5% residue. It has also been suggested that the extender oil in the tyre has no effect on the carbon residue.

Figures 6.30 to 6.33 show thermaldecomposition curves and differential thermaldecomposition curves of natural rubber (NR) butadiene rubber (BR), styrene-butadiene rubber (SBR) and scrap tyre at the heating rates of 5°C min^{-1}, 20°C min^{-1}, 40°C min^{-1} and 80°C min^{-1} respectively.

NR starts to decompose earlier than the others at about 310°C for the heating rate of 5°C min^{-1}. SBR and BR follow NR to decompose

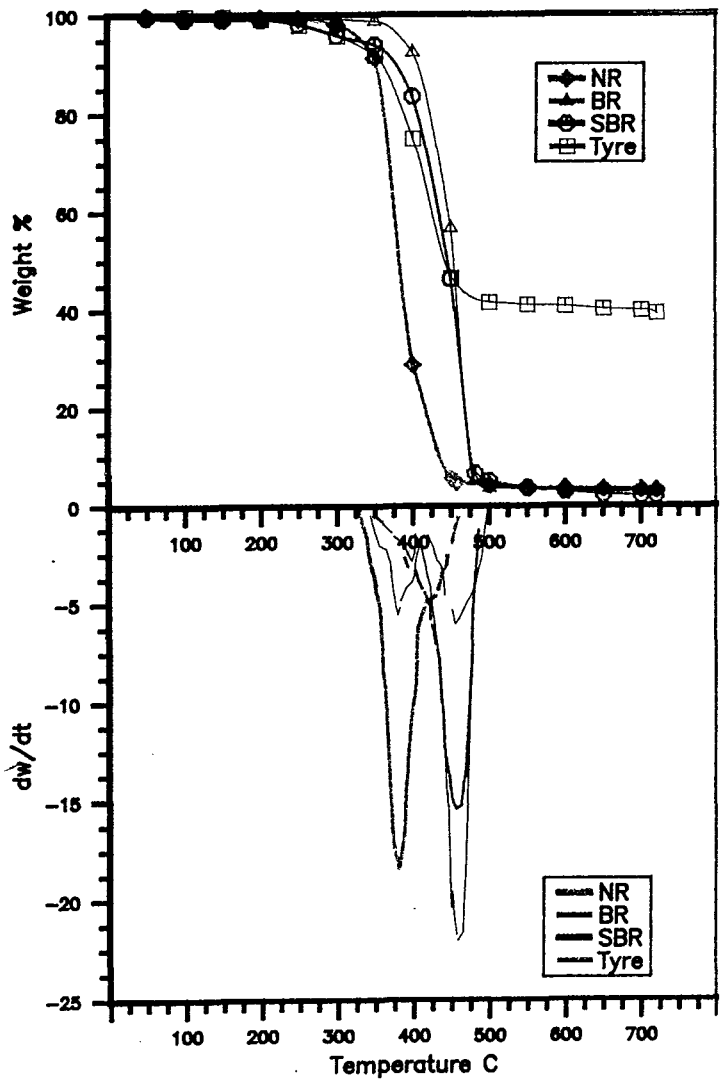

Fig.5.30 TGA and DTG curves for 5 C/min

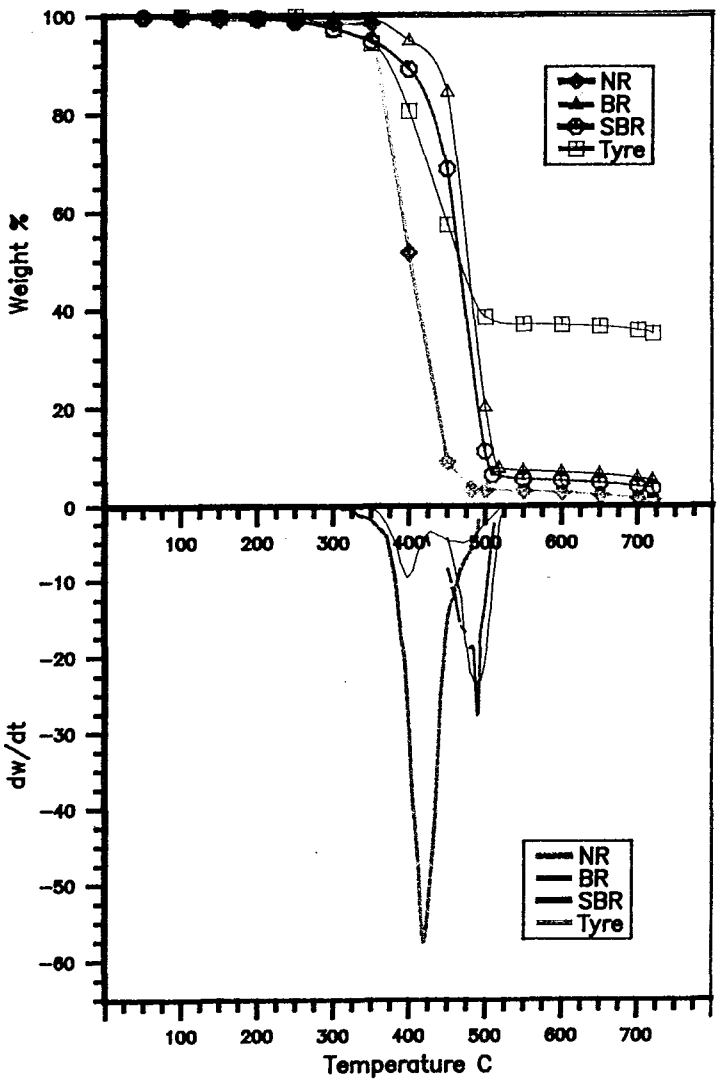

Fig.5.31 TGA and DTG curves for 20 C/min

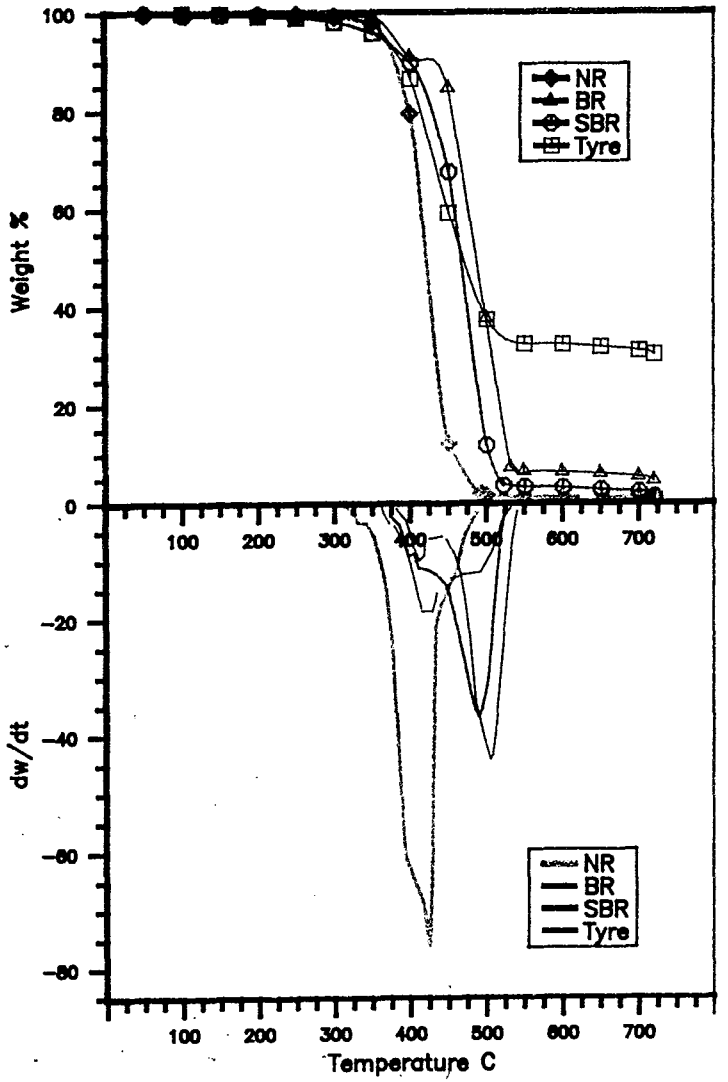

Fig.6.32 TGA and DTG curves for 40 C/min

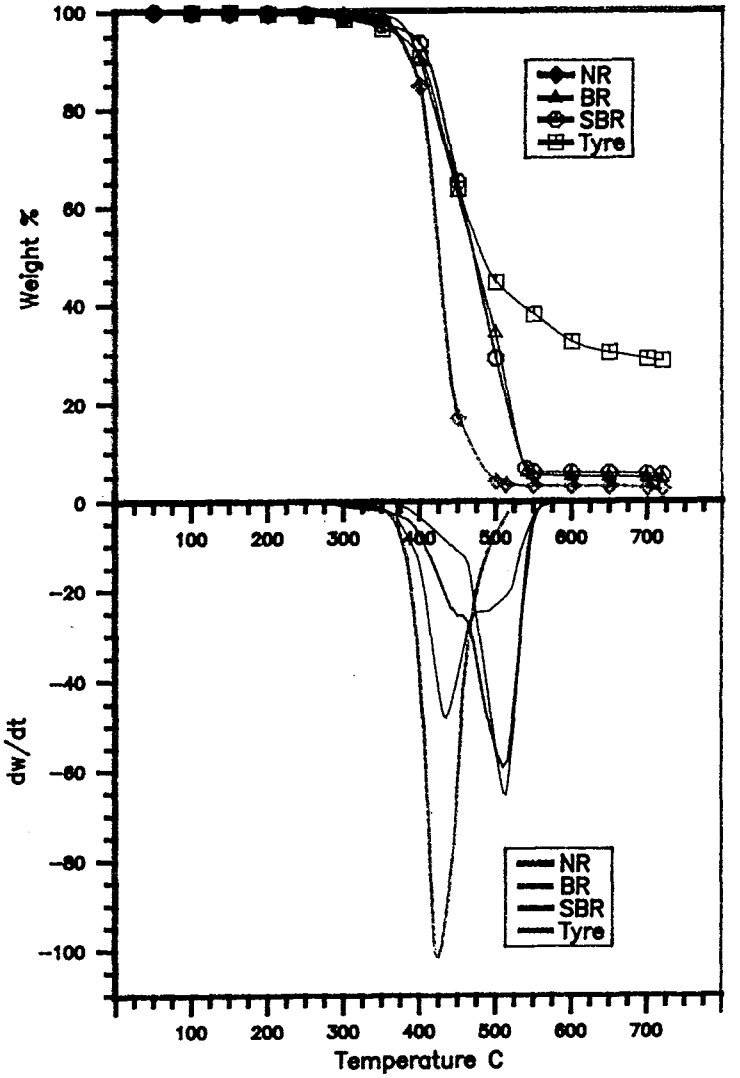

Fig.6.33 TGA and DTG curves for 30 C/min

respectively. Table 6.11 summarises the starting and ending temperatures of the decompositions of tyre and the components which are most probably ones to be in the scrap tyre samples.

Degradation of natural rubber starts between 310°C - 350°C and finishes between 465°C - 525°C (Table 6.11), depending on the heating rate. Bhowmick et al (164) also report the first degradation temperature of rubber in a nitrogen environment at 10°C min^{-1} heating rate as 330°C. It is also seen that (Fig. 6.34) in their work natural rubber completes its thermaldegradation at about 480°C.

Figure 6.30 shows that for the heating rate of 5°C min^{-1}, the first decomposition peak of scrap tyre coincides with the NR decomposition peak, but the first decomposition peak of scrap tyre completes earlier than NR. Also, for the other heating rates, scrap tyre decomposition coincides with the NR decomposition peaks. It is possible that NR could be one of the components of rubber tyre used in this work.

The decompositions of SBR and BR take place almost in the same temperature range. This is probably the butadiene component of SBR and BR. The second thermaldecomposition step of scrap tyre also occurs in the same temperature range of the SBR and BR. It is still difficult to decide precisely what the other main component(s) of scrap tyre could be, either SBR and BR or one of them.

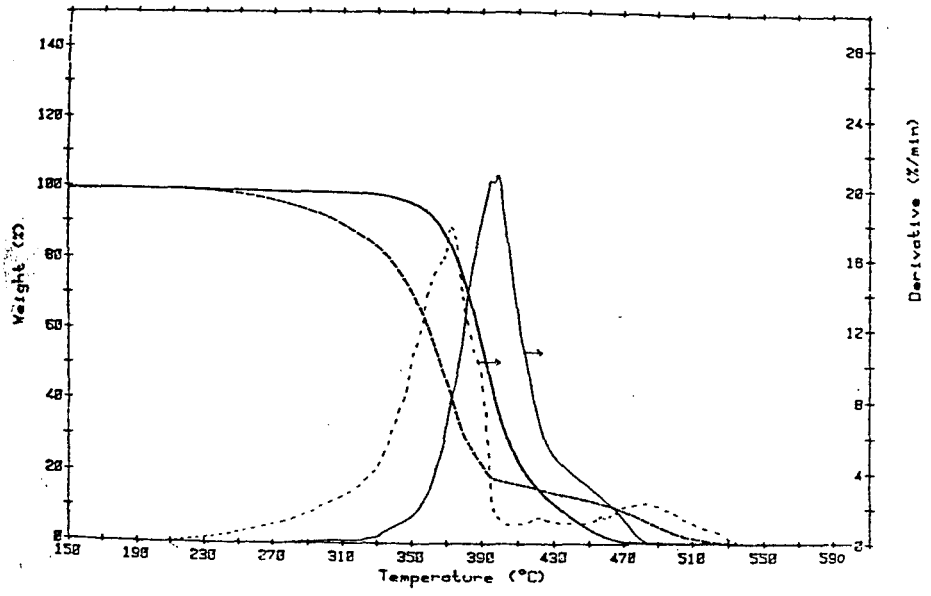

Fig. 6.34 Thermal degradation of rubber (164)
(—— in nitrogen, ---- in air)

Thermaldegradation of NR, SBR or BR (Fig. 6.35) in the scrap tyre, mainly contribute to the volatile parts of the pyrolysis products. Tamura et al (166) have postulated a mechanism for the thermaldegradation of rubber (Fig. 6.36).

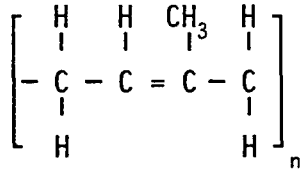

NR

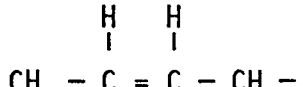

BR

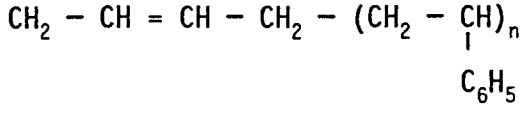

SBR

Fig. 6.35. Formulas of different compounds of scrap tyre.

Table 6.11 Temperature Ranges and Temperatures of Maximum Weight Loss for Scrap Tyre and Main Components.

°Cmin^{-1}	T_1	T_{1max}	T_2	T_{2max}	T_3
Tyre					
5	340	375	415	460	500
20	350	395	420	470	515
40	360	425	450	480	525
80	360	430	465	485	560
NR					
5	310	380	465	-	-
20	315	420	500	-	-
40	325	425	500	-	-
80	350	430	525	-	-
SBR					
5	350	460	490	-	-
20	360	480	415	-	-
40	370	495	530	-	-
80	380	510	550	-	-
BR					
5	360	460	500	-	-
20	335	460	500	-	-
40	380	505	540	-	-
80	390	515	550	-	-

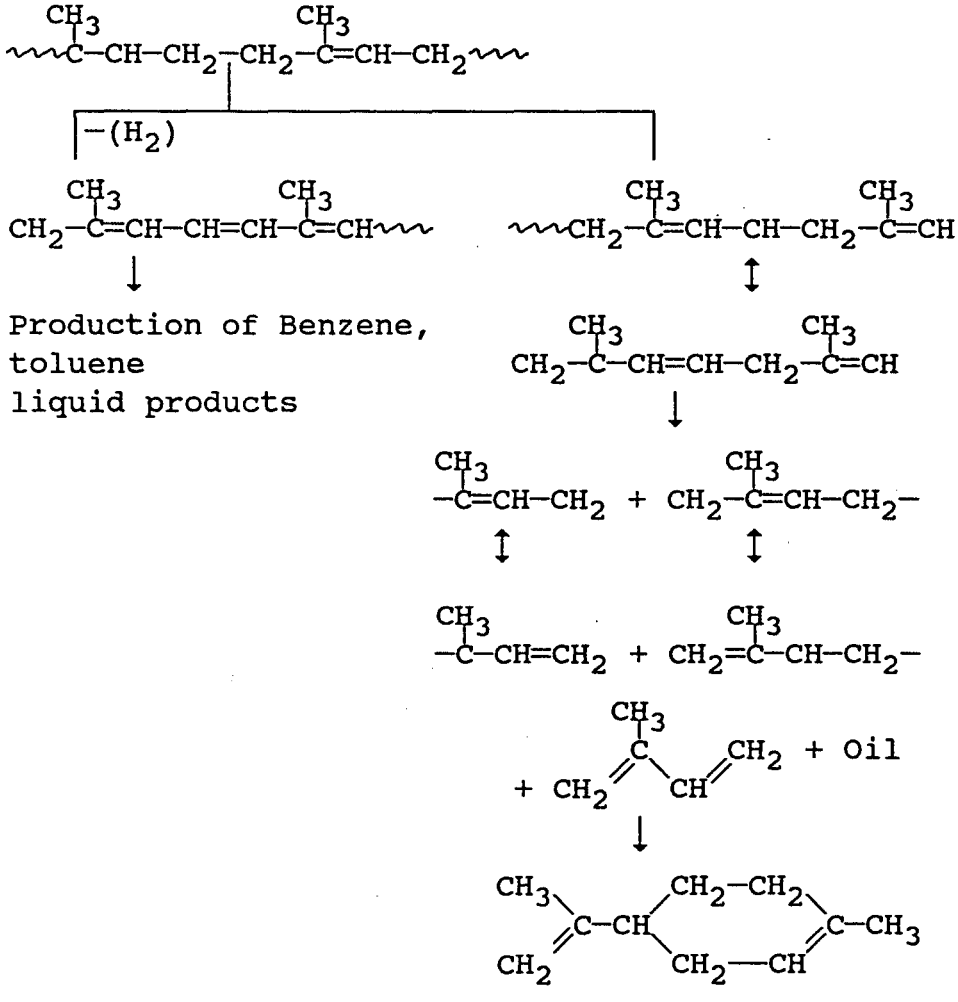

Fig. 6.36 Postulated mechanisms of thermaldegradation of rubber.

As it is seen in Figure 6.36, with the proceeding of the reaction thermal rupture occurs at β-location relative to the double bond in the polymer chain (the β-location is the second carbon-carbon bond from the double bond).

When chain rupture propagates along the chain, highly reactive free radicals are formed. From natural rubber thermaldegradation, two isoprene or butadiene molecules are formed and in the initial stages they are converted to secondary products of dipentene and 4-vinyl-1-cyclohexane by means of a Diels-Alder reaction.

In scrap tyre pyrolysis, oil dipentene (di-limonene) was found in large amounts by Pakdel et al (126). In addition, the presence of styrene and butadiene monomers is the liquid products of tyre pyrolysis has been reported by Dodds et al (118).

Scrap tyre thermograms and derivative thermaldecomposition curves were also compared with the rubber tyre samples obtained directly from manufacturers where the three components of the tyre were known. The components of the rubber tyre are shown in Table 6.12. Figures 6.37 to 6.40 show TGA and DTG curves of scrap tyre and three different rubber tyre samples.

The results suggest that the first decomposition step is for depolymerisation of NR. The second step is much more complicated because the decompositions of SBR and BR occur in the same temperature range and during the second decomposition step it is difficult to suggest that the components decompose whether together or one is become on the other.

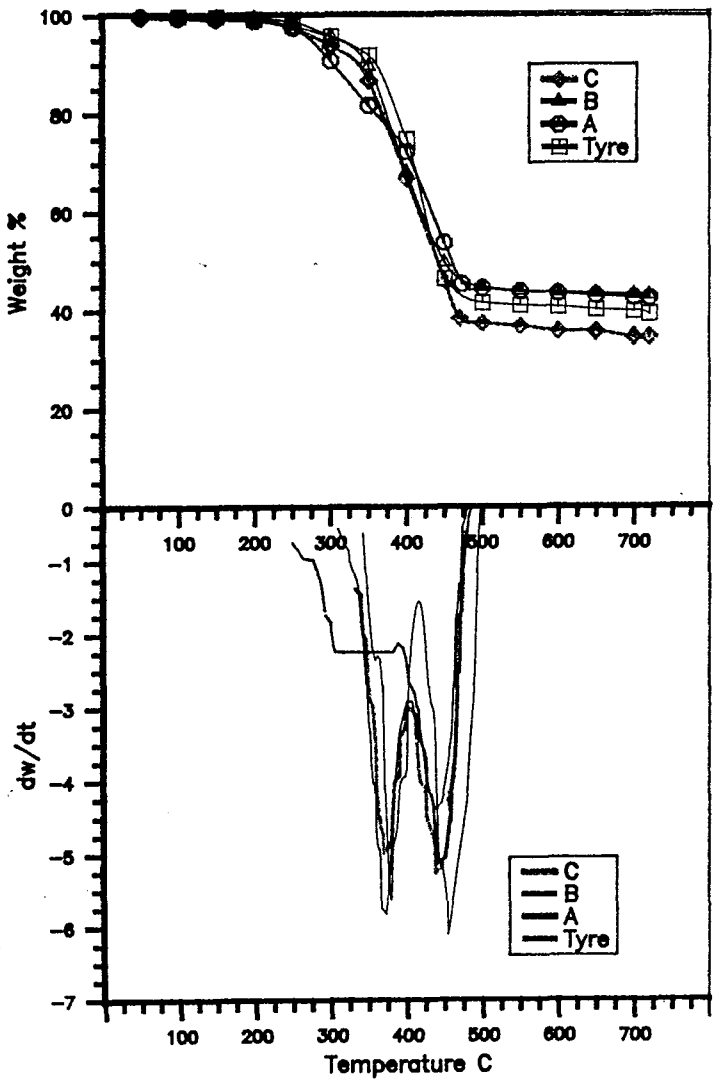

Fig. 6.37 TGA and DTG curves for 5 C/min

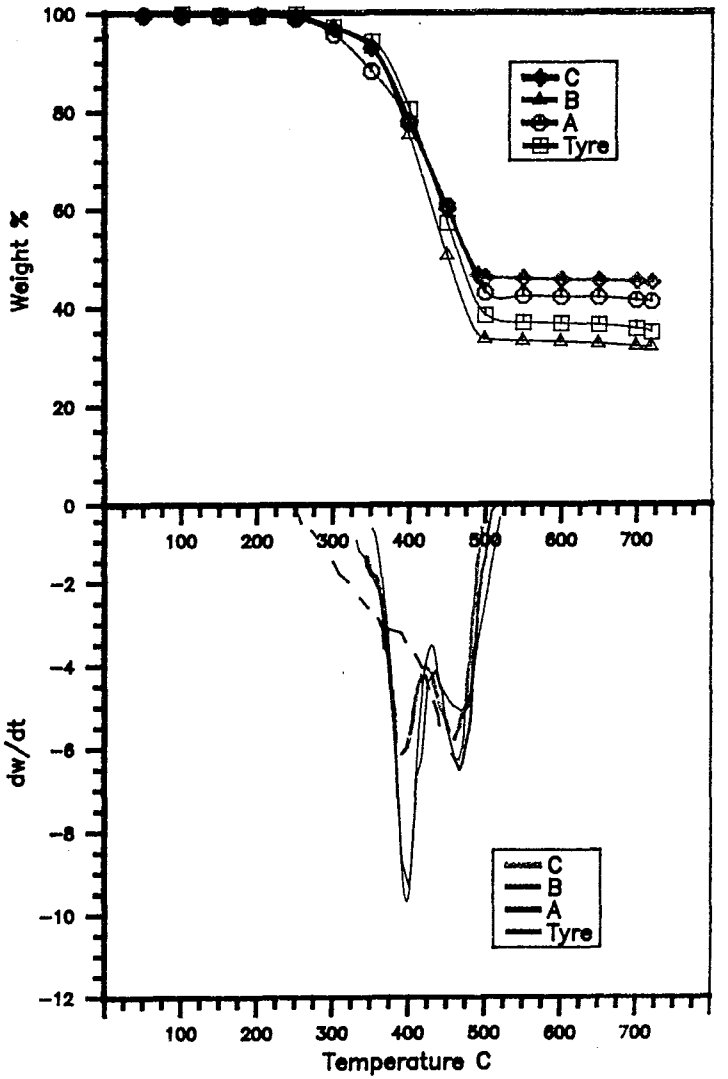

Fig. 6.38 TGA and DTG curves for 20 C/min

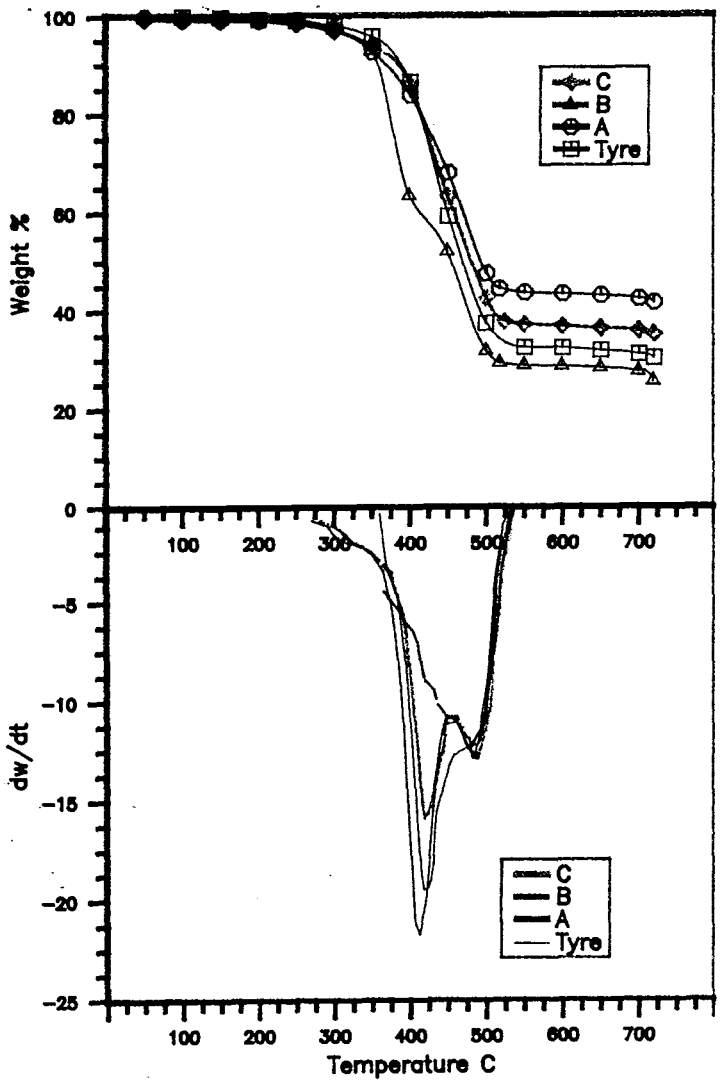

Fig.6.39 TGA and DTG curves for 40 C/min.

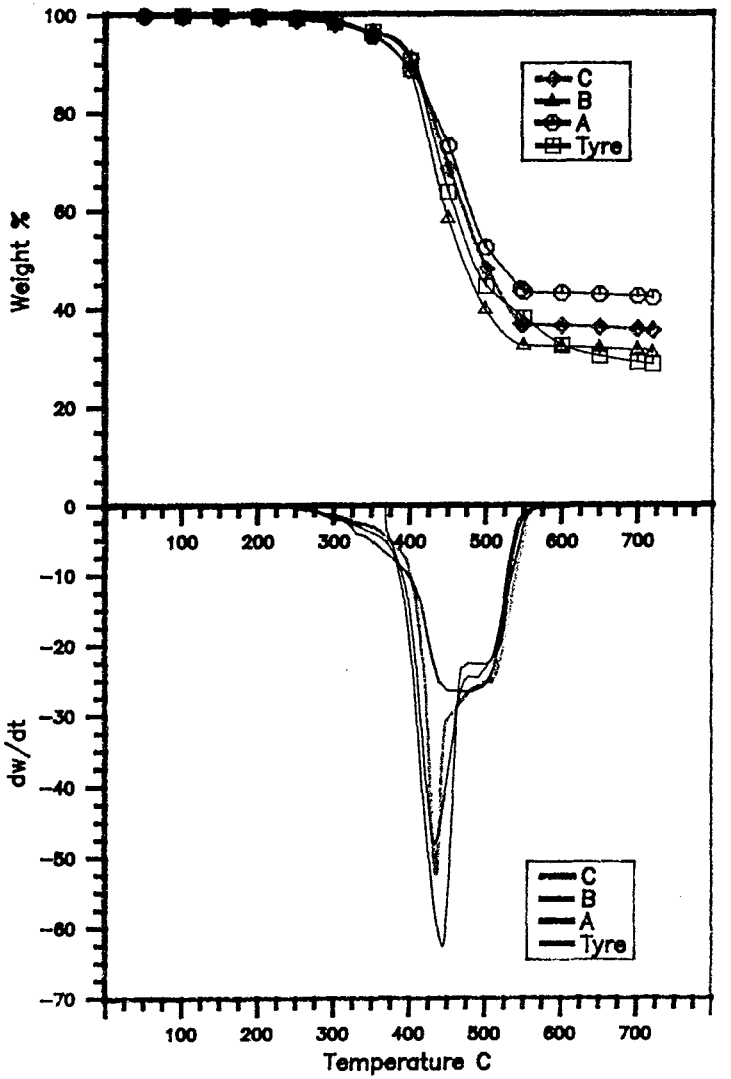

Fig.6.40 TGA and DTG curves for 80 C/min.

These observations are confirmed by Macoione et al (120). In their work, SBR-NR diblend decomposes in the temperature range of 400°C - 500°C. Also, for the decomposition of SBR-NR-BR, two separate peaks were obtained. The first one refers to NR depolymerisation while the second one refers to depolymerisation of SBR-BR.

Table 6.12 Compositions of the Tyre Samples Obtained From Manufacturers.

	A	B	C
SBR	39.04	-	20
NR	-	41.34	45
BR	-	22.26	25
C. Black	36.9	23.21	-
Oil	19.52	4.13	-
Other	4.54	9.06	9

Brazier (167) has also reported the DTG maximum peak temperatures as 573°C, 461°C and 449°C for the thermaldecompositions of natural rubber, butadiene and styrene, butadiene copolymer respectively.

The DTG curves of different elastomers (NR, BR and SBR) are seen in Figure 6.41. Their thermaldecomposition peak temperatures are reported as 365°C, 447°C and 465°C for NR, SBR and BR. Also, the TG and DTG thermograms of NR-BR diblend are seen in Figure 6.42.

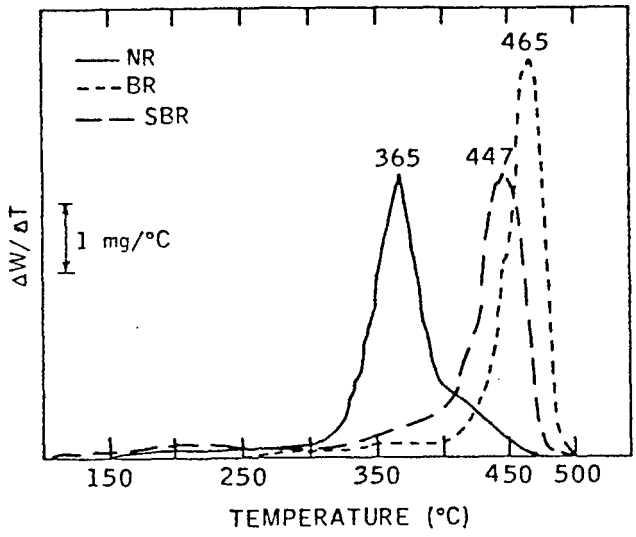

Fig. 6.41. DTG curves of different elastomers in nitrogen (167).

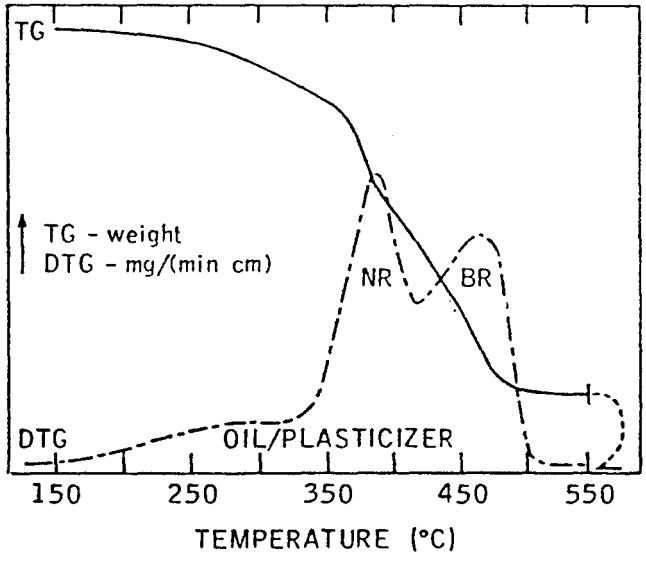

Fig. 6.42. TG and DTG thermograms of NR-BR diblend.

When scrap tyre DTG curves are compared with the other samples, it can be seen that for all heating rates, sample B and scrap tyre DTG peaks seem similar. Compounded elastomers like rubber tyre are complex mixtures of polymers, carbon black or mineral filters, curatives, plasticisers and other ingredients. This makes scrap tyre extremely difficult to characterise. Using TGA however, is a potentially effective analytical technique for the compositional analysis of compounded elastomers, even though such analyses are not completely accurate.

The activation energies and pre-exponential factors of the thermaldecomposition of scrap tyre, SBR, BR, NR and different tyre samples which are A, B and C are listed in Table 6.12 and Table 6.5.

Activation energies generally decreased as the heating rate increased. Brazier (167) has reported the activation energies as 151 kJ mol^{-1}, 163 kJ mol^{-1} and 170 kJ mol^{-1} for the thermaldecompositions of NR, BR and SBR respectively.

The reported activation energy of SBR is in close agreement with the results in Table 6.13, but the activation energies for NR and BR are reported lower than the data in Table 6.13. This is probably due to different thermal analysis equipments employed, also different calculation methods. It is seen that thermaldegradation activation energies and pre-exponential factors of scrap tyre samples and sample B for each heating rate have quite similar figures (Table 6.14).

Activation energies generally decreased as the heating rate increased for scrap tyre and also for the components.

When pure substances activation energies are compared with the scrap tyre and the other samples called A, D and C, it is seen that activation energies of individual components are much higher than rubber tyre samples as expected.

Table 6.13. Kinetic Parameters for the Decomposition of Scrap Tyre and its Main Possible Components.

°Cmin^{-1}		A sec^{-1}	E kJ mol^{-1}
Tyre			
5	Low	4.2×10^{7}	132.4
	High	7.3×10^{10}	144.8
20	Low	4.7×10^{6}	135.2
	High	8.4×10^{9}	141.5
40	Low	6.9×10^{3}	54.9
	High	7.1×10^{7}	140.5
80		1.28×10^{4}	79.8
SBR			
5	Low	4.68×10^{5}	110.9
	High	9.6×10^{12}	208.5
20	Low	1.24×10^{16}	168.0
	High	4.5×10^{11}	195.2
40	Low	1.21×10^{8}	138.8
	High	1.1×10^{10}	168.6
80		2.2×10^{3}	36.2
BR			
5	Low	2.6×10^{3}	86.0
	High	1.06×10^{18}	278.1
20	Low	2.67×10^{14}	223.8
	High	8.61×10^{14}	244.4
40	Low	5.6×10^{18}	277.7
	High	3.45×10^{13}	223.8
80		2.1×10^{3}	78.62
NR			
5		2.4×10^{16}	212.1
20		1.18×10^{14}	199.9
40		4.41×10^{11}	176.5
80		4.99×10^{4}	89.4

Table 6.14. Kinetic Parameters for the Decomposition of Some Tyre Samples.

°Cmin^{-1}		A sec^{-1}	E kJ mol^{-1}
Sample A			
5		2.1×10^{8}	142.76
20		2.62×10^{4}	90.8
40		1.26×10^{3}	70.4
80		1.11×10^{3}	66.4
Sample B			
5	Low	9.31×10^{7}	102.8
	High	1.12×10^{8}	145
20	Low	3.31×10^{5}	128.3
	High	2.07×10^{8}	137.7
40	Low	5.9×10^{2}	66.1
	High	6.3×10^{7}	136.2
80		1.3×10^{2}	55.6
Sample C			
5	Low	1.18×10^{8}	130.8
	High	2.05×10^{8}	142.4
20	Low	1.22×10^{8}	132.7
	High	4.91×10^{7}	134.8
40	Low	6.45×10^{2}	67.58
	High	9.81×10^{6}	125.95
80		1.42×10^{3}	68.7

CHAPTER 7

CHARACTERISATION OF PYROLYTIC OILS

7.1 Introduction

The identification of the chemical compounds present in waste and biomass derived oils is important since the oils may contain valuable chemicals in significant, economically recoverable concentrations or on the other hand hazardous chemicals of environmental importance.

For wood, scrap tyre and RDF derived oils, extensive characterisation of the functional groups present in pyrolytic oils by Fourier - Transform infra-red spectroscopy and identification of polycyclic aromatic hydrocarbons in pyrolysis oils by gas chromatography and gas chromatography and mass spectroscopy was carried out.

7.2 Functional Group Analysis by Fourier-Transform Infra-Red Spectroscopy

7.2.1 Samples From the Fixed-Bed Reactor

7.2.1.1 Characterisation of Biomass Derived Oils

7.2.1.1.1 Introduction

The breakdown of the complex polymer structure of biomass leads to a large number of products. The proportions of these products are very sensitive to the rate of heating. The use of biomass pyrolysis to produce char, tars etc has been known since antiquity. As reported by Desbene et al (206), pyrolignous acid is well known but only a few data are available on the composition of tars. Until 1980, no attempts were made to characterise pyrolysis oils as a

function of temperature. But now it is well understood that the production of tars depends on temperature. In fact, the structural complexity of oils is influenced by various factors i.e. methods of derivation, parent raw material used etc.

The oils are constituted of a number of individual compounds which can be grouped in many different functional groups. Fourier-Transform infra-red spectroscopy is one of the useful tools to give information about the whole oil.

In this part of the research, characterisation of the pyrolytic oils obtained from biomass, namely wood (pine), rice husks and refuse derived fuel (RDF) pyrolysis will be reported. In addition, the influence of the maximum temperature and heating rate on the functional groups, particularly hydrocarbons (linear and aromatic) of the oils will be summarised.

Functional group compositional analyses were performed on the pyrolysis oils separated from the condensed liquid product. As indicated earlier (Chapter 2), KBr discs were employed during the experiments.

7.2.1.1.2 Results and Discussion

Figure 7.1 shows typical FT-ir traces for pyrolysis oil derived from wood, rice husks and refuse derived fuel (RDF). The infra-red spectra of the wood and rice husks pyrolysis oils present signals distributed in two zones between 3600 cm^{-1}, 2900 cm^{-1} and 1800 - 1000 cm^{-1}.

A very strong absorption band appears in the 3200 cm^{-1} - 3600 cm^{-1} region which corresponds to OH stretching. The appearance of OH

groups indicates the presence of the alcohols in the sample investigated. Also, in conjunction with the presence of C=O functional groups the presence of organic acids might also be indicated.

Desbene et al (206) reported the presence of furfuryl alcohol and methoxytetrahydrofuryl alcohol in the hornbeam pyrolysis oil derived by slow pyrolysis.

Fraga et al (225) also identified furfuryl alcohol and sinapyl alcohol in the sugar-cane bagasse pyrolysis tars derived at 600°C in the wire mesh reactor. The presence of methanol in the cellulose pyrolysis oil derived at 550°C was reported by Shafizadeh (48).

The FT-ir spectra of RDF oils indicate the presence of O-H vibrations between 3050 and 3600 cm^{-1}. The presence of C=O stretching vibrations at 1650 cm^{-1} and 1850 cm^{-1} indicates the presence of carboxylic acids and their derivatives. This is most probably the result of pyrolysis of the cellulosic contents of RDF.

Pakdel and Roy (204) report that low molecular weight carboxylic acids, formic acid and acetic acids in particular are one of the major groups in wood vacuum pyrolysis oil at 460°C. Shafizadeh (48) reported the existence of acetic acid in the cellulose pyrolysis oil. Formic, acetic, glycolic, malic and, acrylic acids (110) and derivatives of carboxylic acids (7) have been identified in pyrolytic oil derived from the pyrolysis of shredded and screened municipal solid waste and RDF.

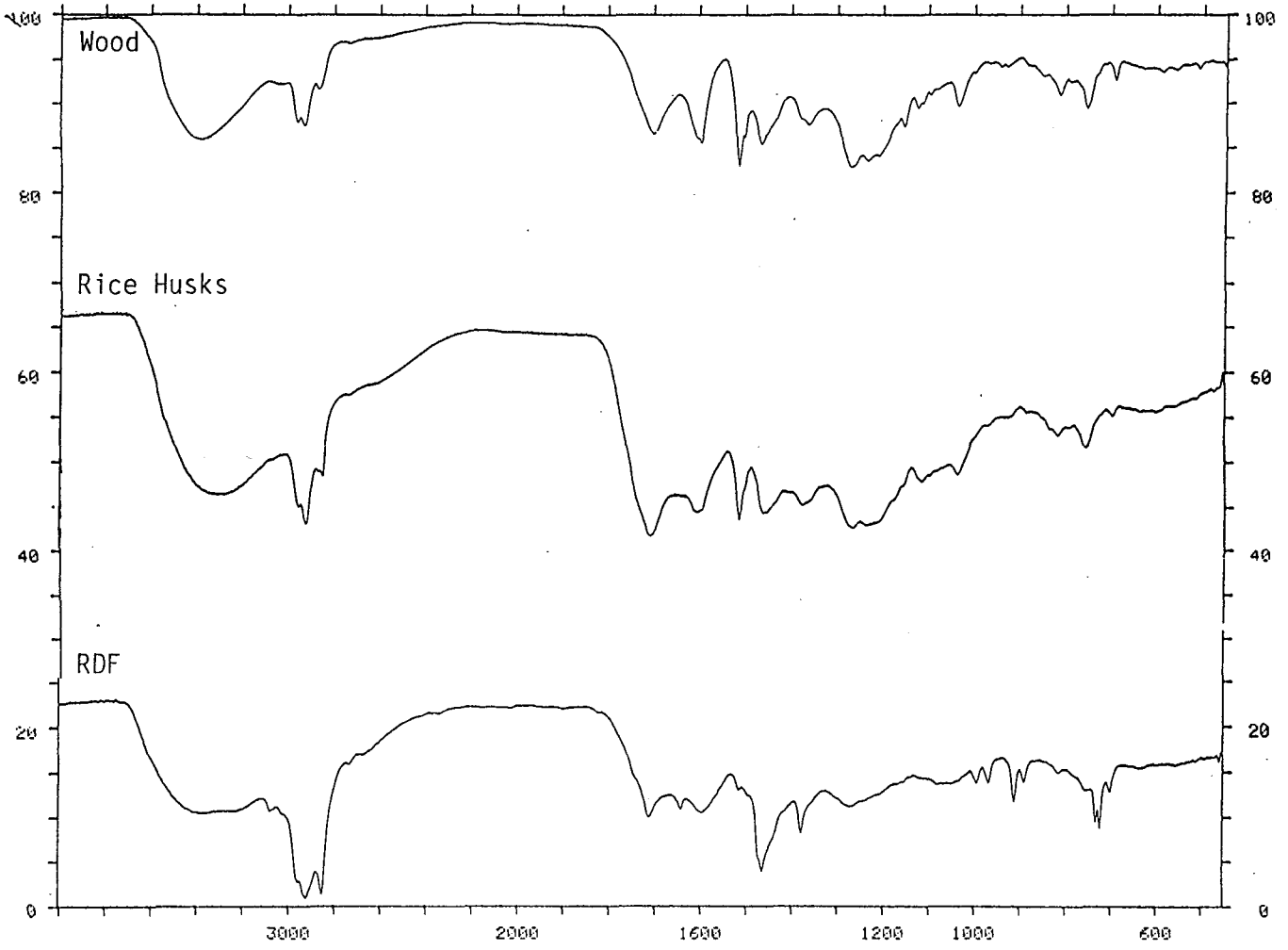

Fig.7.1 Typical FT-ir Traces of Wood, Rice Husks and RDF

Mallya and Helt (6) have suggested that the strong O-H vibrations between 3050 and 3600 cm^{-1} represent inter and intramolecularly hydrogen bonded hydroxyl groups which are mainly responsible for the high viscosity of the RDF derived pyrolysis oils.

The presence of CH_3 and CH_2 groups in the FT-ir spectra of wood and rice husks are shown by the peaks at 2957 cm^{-1} and 2926 cm^{-1} also signals at 2860 cm^{-1} and 2850 cm^{-1} are indicating the presence of CH_3 and CH_2 groups respectively. This is also confirmed by Churin et al (160).

The appearance of CH_3 and CH_2 groups indicates the presence of alkanes. Pakdel and Roy (204) identified alkanes in the wood vacuum pyrolysis oils. Desbene et al (206) have reported that the hornbeam slow pyrolysis oils constitutes some aliphatic hydrocarbon compounds i.e ethylcyclopentene, tridecane, hexadecane, pentadecane etc.

In the FT-ir spectra of wood, rice husks and RDF, the bands which appear at 1710 cm^{-1} - 1600 cm^{-1} correspond to C=O and C-O stretching absorptions in aldehydes and ketones. Lipska - Quinn et al (38) have identified aldehydes and ketones in the rice husk extracted cellulose derived pyrolysis oil at 500°C at the heating rate of 20°C min^{-1}. The presence of ketones and aldehydes have also been identified in the pyrolysis oil from wood and RDF (7). Helt and Agrawal (141) characterised the tars derived from municipal solid waste in a fixed-bed reactor and they reported that in general, the classes of compounds include furfurals, phenols, methoxy phenols, cyclic compounds such as methyl cyclo pentanones and methoxybenzenes.

The bands which appear at 1350 - 1500 cm^{-1} are due to C-H deformation (161). Pakdel et al (162) are agreed with this

conclusion and those bands appear in the wood derived pyrolysis oil FT-ir spectra are named by them as C-H deformation of CH_3COO-, CH_3CO-, -$COOCH_3$ and -CH_2-CO-. These groups indicate the presence of acids, esters and alcohols. In the pyrolytic oil of holocellulose extracted from rice straw, the presence of acids esters and alcohols have been reported (38, 164).

The presence of C-H stretching vibrations between 2800 and 3000 cm^{-1} and C-H deformation vibrations between 1350 - 1475 cm^{-1} indicate the presence of alkanes. This functional group has also been detected by other workers with RDF pyrolysis oils (6). For the FT-ir spectra of wood derived oils the bands of 1025 - 1250 cm^{-1} are due to C-O stretching which indicates

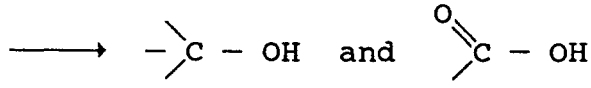

groups (161, 163)

The presence of those groups indicates the existence of carboxylic acids which have already been reported (161, 163).

Mono and polycyclic and substituted aromatic groups are indicated by the absorption peaks between 675 cm^{-1} and 900 cm^{-1} and 1575 cm^{-1} and 1625 cm^{-1}. The presence of mono and polycyclic aromatic compounds in the oil product from the pyrolysis of cellulose, a major component of the RDF, has been reported by Rampling and Hickey (7).

The presence of aromatic groups in wood has been identified (204, 205). Lipska-Quinn (38) reported the presence of some aromatics in the rice straw pyrolysate such as 1,4-dimethoxynaphthalene, 1-heptodecanyl-3-methoxy benzene, 4-hydroxy-3-methonyacetaphenone.

The formation of polyaromatic hydrocarbons can be explained by means of Diels-Alder reactions involving cyclisation of alkenes formed from the thermaldegradation of alkanes (this will be discussed later in this chapter).

In the FT-ir spectra of RDF derived oils, the absorbance peak between 1625 cm^{-1} and 1675 cm^{-1} represents C=C stretching vibrations indicative of alkenes. Mallya and Helt (6), Pober and Bouer (110) and Rampling and Hickey (7) have reported the presence of alkenes in the pyrolytic oils from municipal solid waste.

The peaks between 850 cm^{-1} and 950 cm^{-1} indicate the presence of ethers. A group of ethers were identified in the pyrolysis oil from municipal solid waste and RDF (6, 7).

The group of overlapping peaks between 950 cm^{-1} and 1325 cm^{-1} most probably represent the presence of primary, secondary and tertiary alcohols and also phenols due to the C-O stretching and O-H in plane deformations of these functional groups. Alcohols and phenols have been identified in RDF derived oils (11, 110).

7.2.1.1.3 Effect of Pyrolysis Temperature and Heating Rate

Pyrolytic oils derived from the fixed-bed pyrolysis of wood, rice husks and RDF were collected at temperatures of 300°C, 420°C, 600°C and 720°C as the pyrolysis was carried out at heating rates of 5, 20, 40 and 80°C min^{-1}.

Typical spectra to illustrate the influence of pyrolysis temperature on functional group compositional analysis of the pyrolytic oils are shown in Figures 7.2, 7.3 and 7.4 for wood, rice husks and RDF respectively. The heating rate was 5°C min^{-1} for wood

and rice husks and 20°C min^{-1} for RDF. Similar results for other heating rates were recorded.

It is seen that there are changes in peak intensities and therefore composition of the oils as the temperature of pyrolysis was increased for all the biomass waste.

As indicated earlier, the investigation of the temperature effect on the chemical composition of pyrolytic tars did not draw much attention until 1980. Elliott (27) has performed probably the first fundamental study. Elliott reported that low temperature pyrolysis of wood constituted acids, aldehydes, ketones, furans alcohols, complex oxygenates, phenols, guaiacols, syringols and complex phenolics. Conversely, at high temperature pyrolysis yields are reported as, benzenes, naphthalenes, biphenyls, phenanthrenes and benzofurans.

Pouwell et al (53) analysed the pyrolysis products of beech wood by wire point pyrolysis - gas chromatography - mass spectrometry. Aldehydes (formaldehydes, acetaldehyde, furaldehyde etc.) phenols, benzene, styrene, acids (acetic, furaic, carboxylic) were identified. Although no aromatic or polyaromatic compounds were reported. However, the pyrolysis temperature was 610°C. They also suggested that a number of pyrolysis products can be correlated with known chemical structures in hardwood.

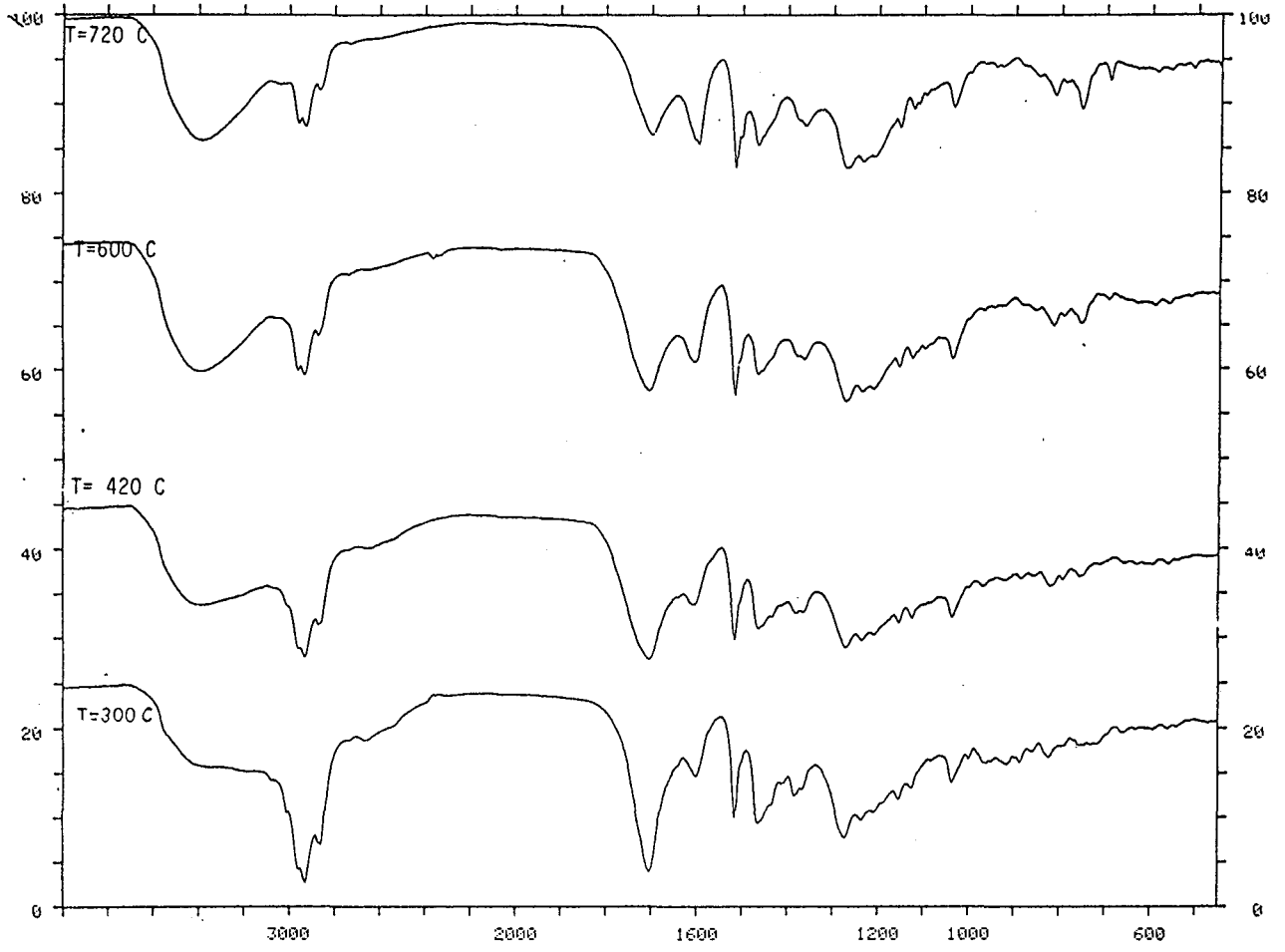

Fig.7.2 Temperature Effect on the FT-ir Traces of Oil Derived From Wood (Heating Rate of 5 C/min)

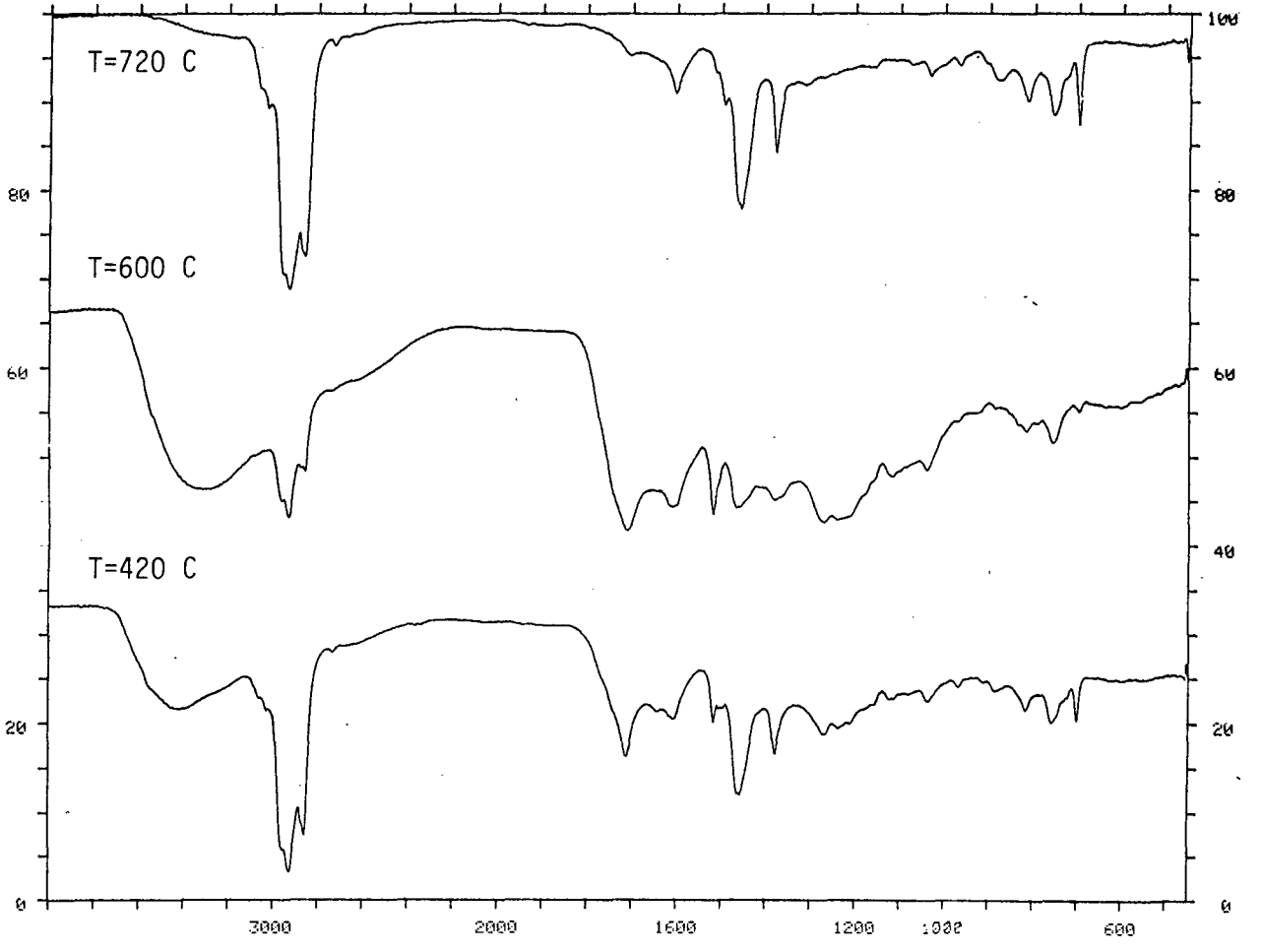

Fig.7.3 The Temperature Effect on the FT-ir Traces of Oil Derived From Rice Husks (Heating Rate of 5 C/min)

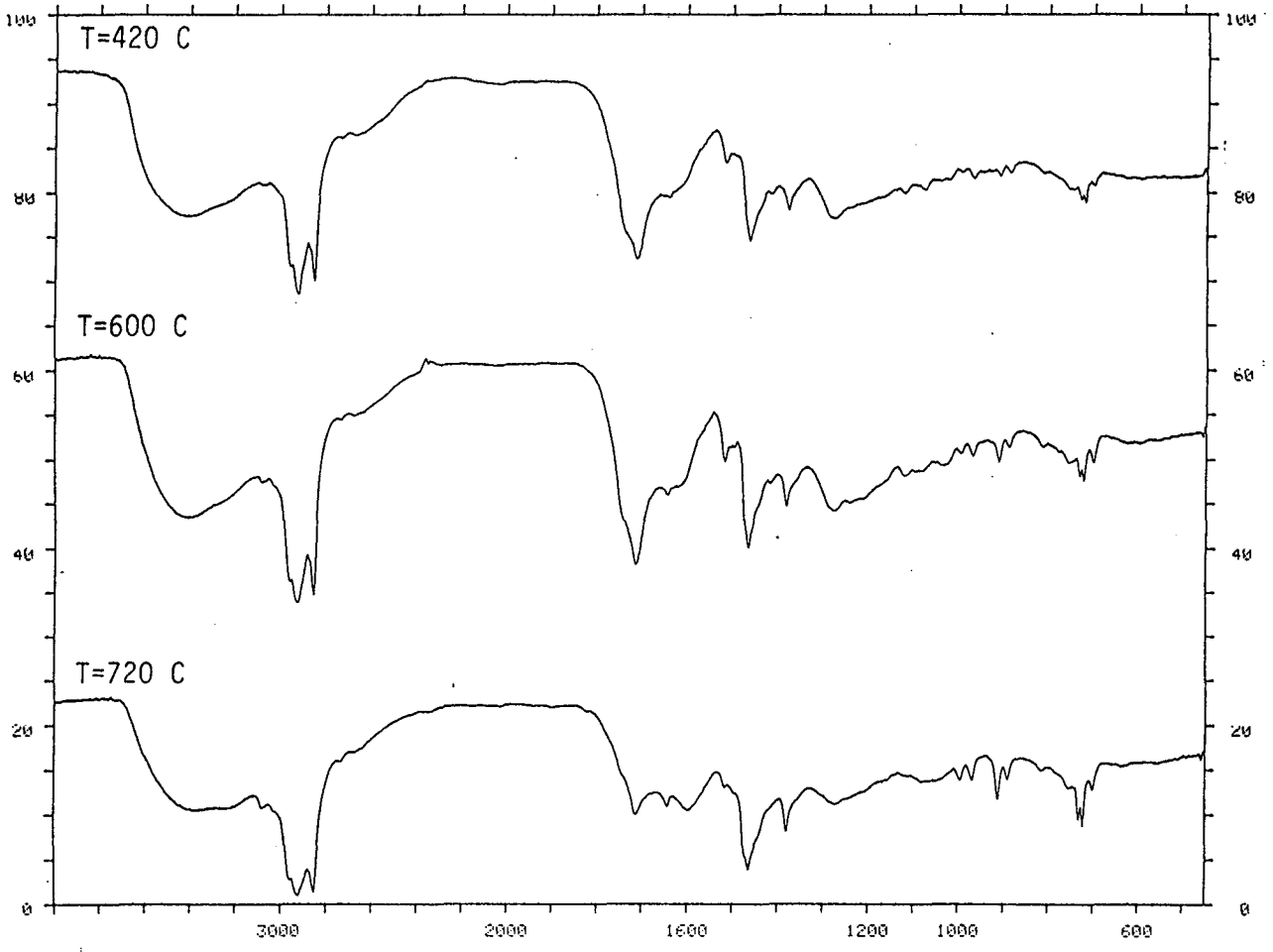

Fig.7.4 The Temperature Effect on the FT-ir Traces of Oil Derived From RDF (Heating Rate of 20 C/min)

In Figures 7.2, 7.3 and 7.4, the group of peaks between 675 cm^{-1} and 900 cm^{-1} and 1575 cm^{-1} and 1625 cm^{-1} representing mono and polyaromatic and substituted aromatic compounds show an increase in intensity as the temperature of pyrolysis was increased from 420°C to 720°C.

In contrast, the alkenes and alkanes represented by peak at 1625 cm^{-1} to 1675 cm^{-1} and 2850 cm^{-1} and 2900 cm^{-1} represent a decrease in intensity as the pyrolysis temperature was increased.

The results are presented in terms of relative peak heights in Figures 7.5, 7.6 and 7.7 for wood, rice husks and RDF oils respectively. The alkene peak measured was at 1675 cm^{-1}, the alkane peak measured was 2900 cm^{-1} and the three aromatic peaks were at 675 cm^{-1}, 1575 cm^{-1} and 1625 cm^{-1} The heating rate was 5 cm^{-1} for wood and rice husks and 20 cm^{-1} for RDF. In addition, Tables 7.1, 7.2 and 7.3 illustrate the temperature effect on the functional groups for the other heating rates of wood, rice husks and RDF respectively. Generally, for all heating rates the aromatic compounds show an increase while the alkanes and alkenes show a decrease. This is further evidence for Diels-Alder type reactions to form aromatic and polyaromatic compounds (discussed later).

FT-ir traces in Figures 7.8 for wood, 7.9 for rice husks and 7.10 for RDF show the effect of heating rates on the oils for different intervals of temperatures. The figures presented are for the final temperature of 720°C. The spectra for 420°C and 600°C temperatures showed similar results.

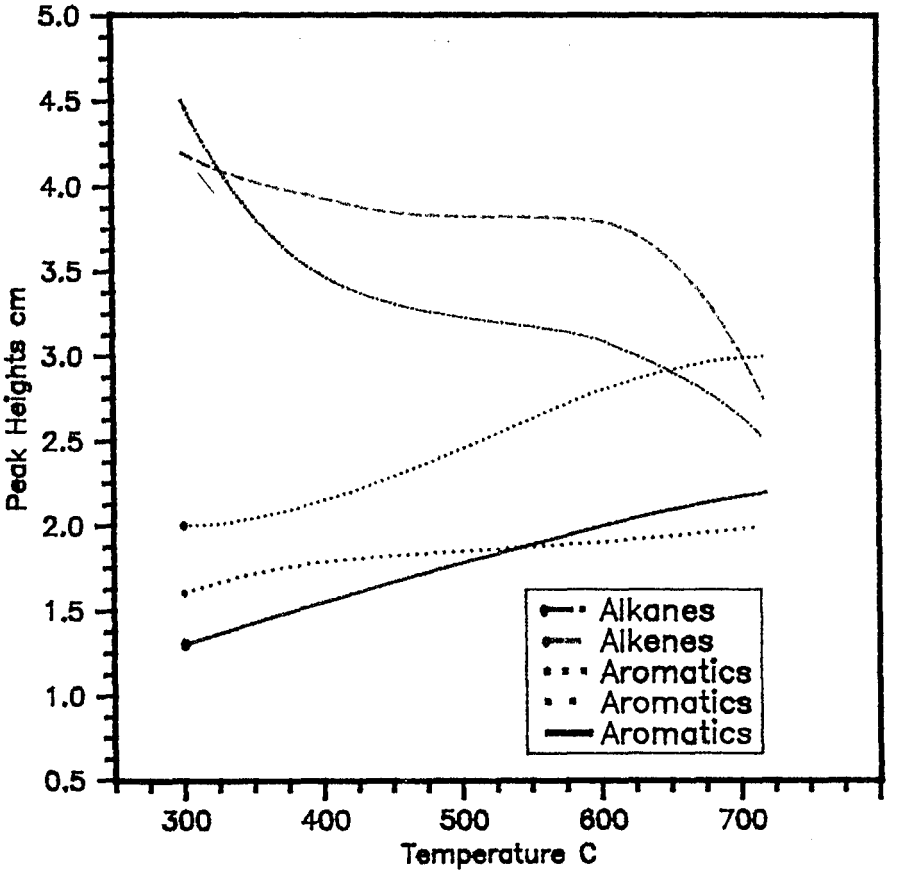

Fig. 7.5 The Temperature Effect on the Functional Groups in the Oil Derived From Wood.

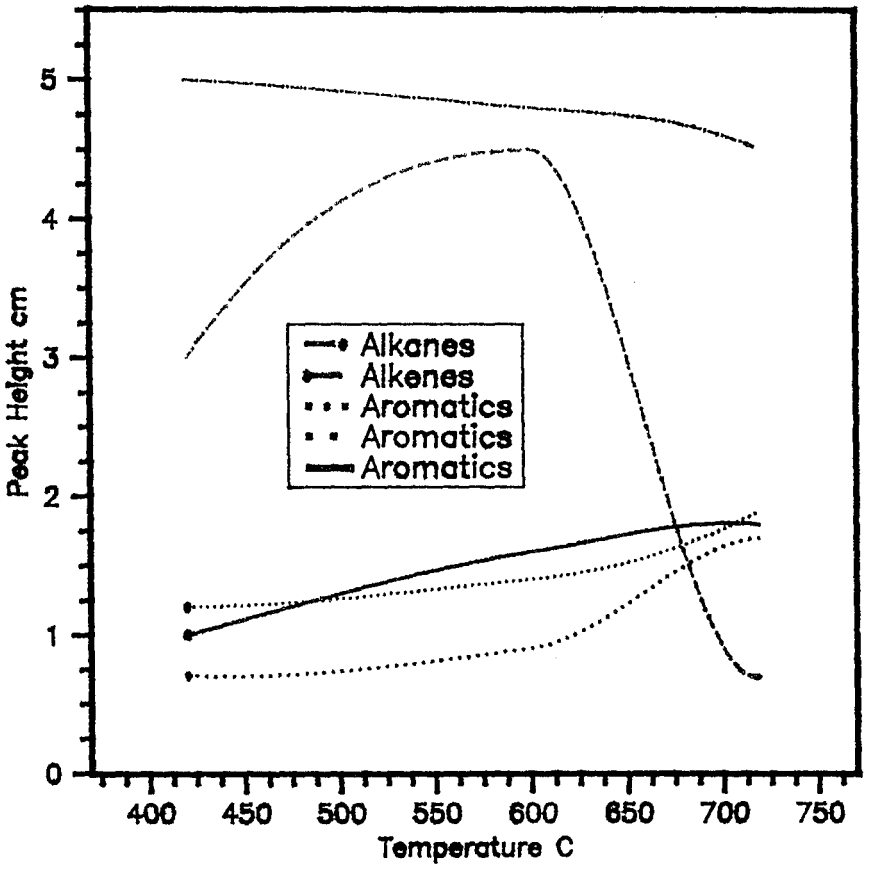

Fig. 7.6 The Temperature Effect on the Functional Groups in the Oil Derived From Rice Husks

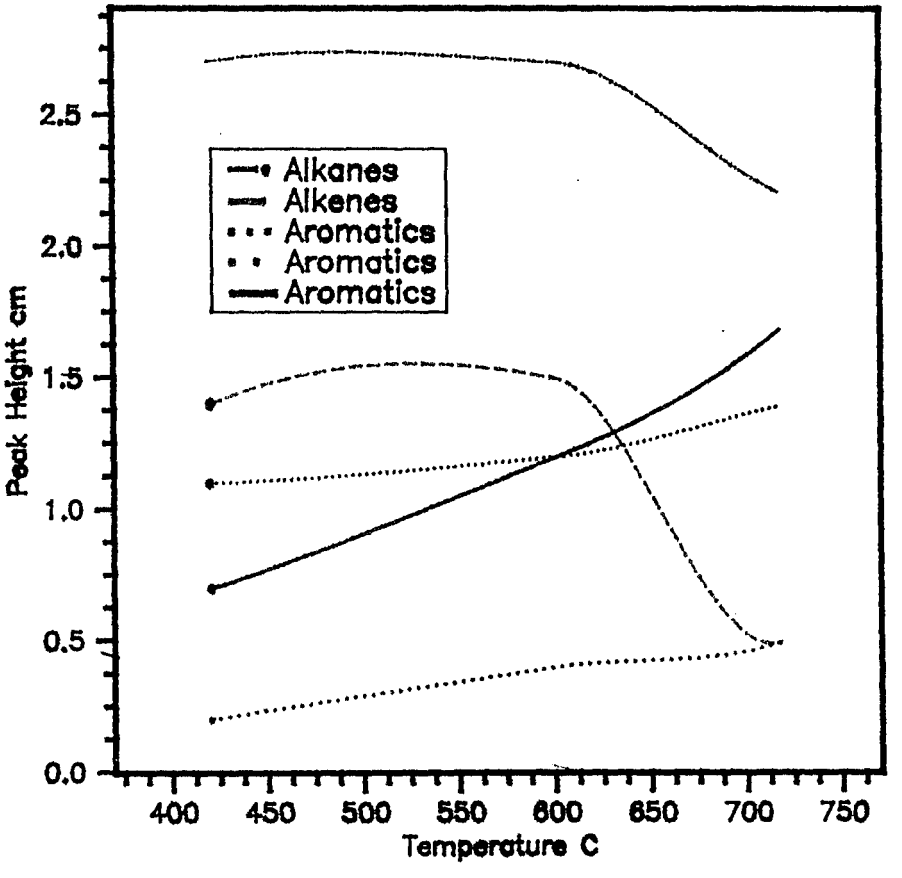

Fig. 7.7 The Temperature Effect on the Functional Groups in the Oil Derived From RDF

Table 7.1 Temperature Effect on the Functional Groups of Oils Derived From Wood

	(675-710) Aromatics 1	(710-900) Aromatics 2	(1575-1625) Aromatics 3	(1625-1675) Alkenes 4	(2850-2900) Alkanes 5
20°C min^{-1}					
420	0.7	0.9	0.6	2.9	3.3
600	1.0	1.1	0.7	1.6	1.9
720	1.3	1.2	0.8	1.5	1.5
40°C min^{-1}					
420	0.3	0.7	0.5	2.4	2.3
600	0.6	0.9	0.5	1.5	2.0
720	0.8	0.9	0.8	1.5	1.6
80°C min^{-1}					
420	0.4	0.7	0.7	2.6	2.4
600	0.5	0.8	0.7	1.3	1.3
720	0.8	0.9	0.9	1.3	1.5

Table 7.2 Temperature Effect on the Functional Groups of Oils Derived From Rice Husks

	(675-710) Aromatics 1	(710-900) Aromatics 2	(1575-1625) Aromatics 3	(2850-2900) Alkanes 4	(1625-1675) Alkenes 5
20°C min^{-1}					
420	0.8	0.6	0.4	2.1	1.8
600	0.8	0.6	0.4	1.4	1.2
720	1.2	0.8	0.4	2.0	1
40°C min^{-1}					
420	0.7	0.8	0.6	2	1
600	1.1	0.8	0.5	1.1	1.2
720	0.9	0.8	1.0	0.7	0.5
80°C min^{-1}					
420	0.9	0.6	0.5	0.9	0.2
600	0.4	0.3	0.2	0.7	0.4
720	0.7	0.5	0.4	0.7	0.4

Table 7.3 Temperature Effect on the Functional Groups of Oils Derived From RDF

	(675-710) Aromatics 1	(710-900) Aromatics 2	(1575-1625) Aromatics 3	(1625-1675) Alkenes 4	(2850-2900) Alkanes 5
20°C min^{-1}					
420	0.8	0.7	0.2	2.4	4
600	0.9	0.9	0.2	1.6	3.2
720	0.8	0.5	0.5	1	1.7
40°C min^{-1}					
420	0.4	0.3	0.6	0.8	3.4
600	0.8	0.3	1.2	1.4	2.0
720	1.5	0.5	1.3	1.1	2.0
80°C min^{-1}					
420	N/T	N/T	N/T	N/T	N/T
600	1	0.4	0.2	1.6	2.6
720	2.3	0.6	0.5	1.7	4.6

N/T = not tested

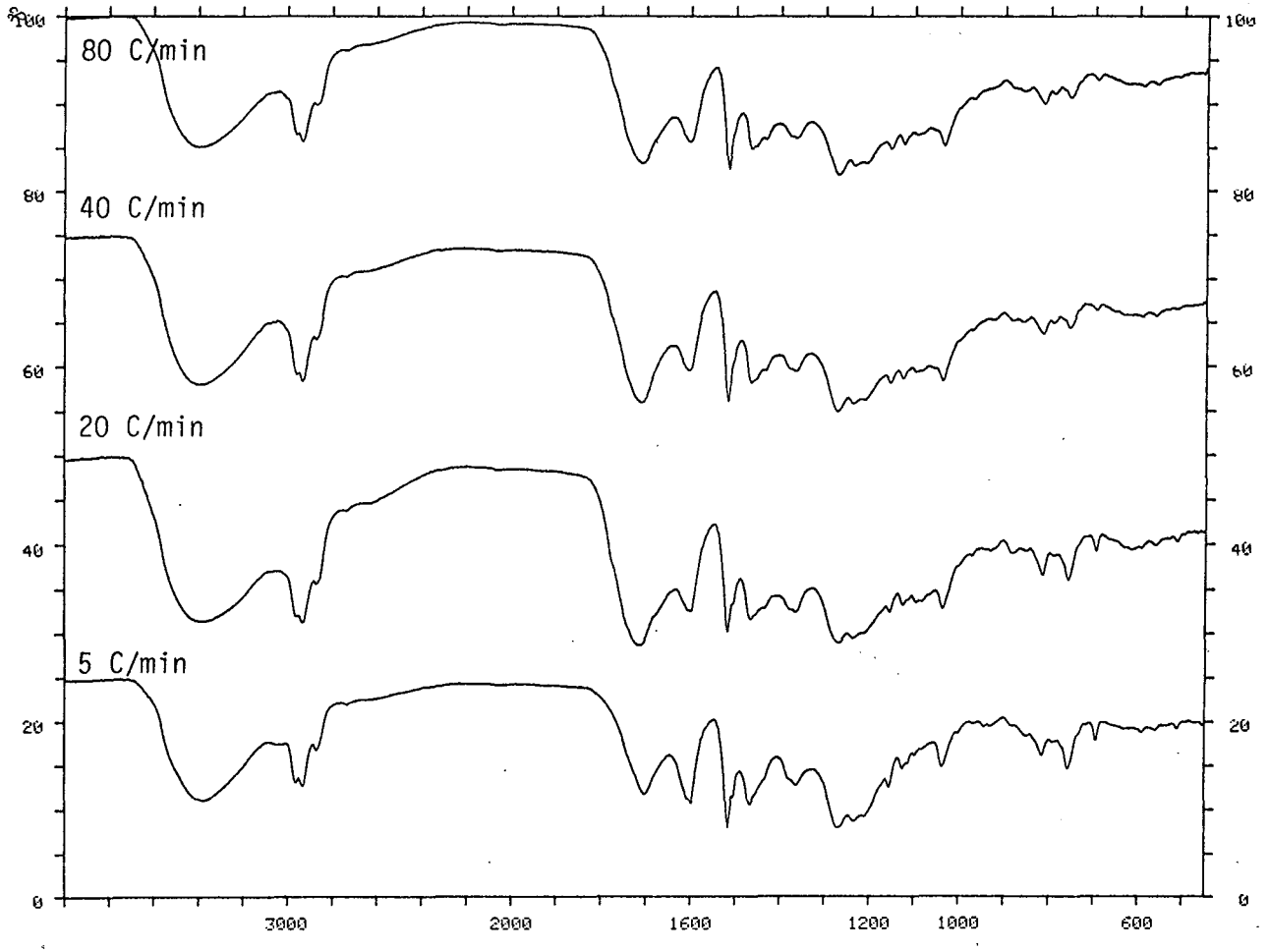

Fig.7.8 The Heating Rate Effect on the FT-ir Traces of the Oils Derived From Wood

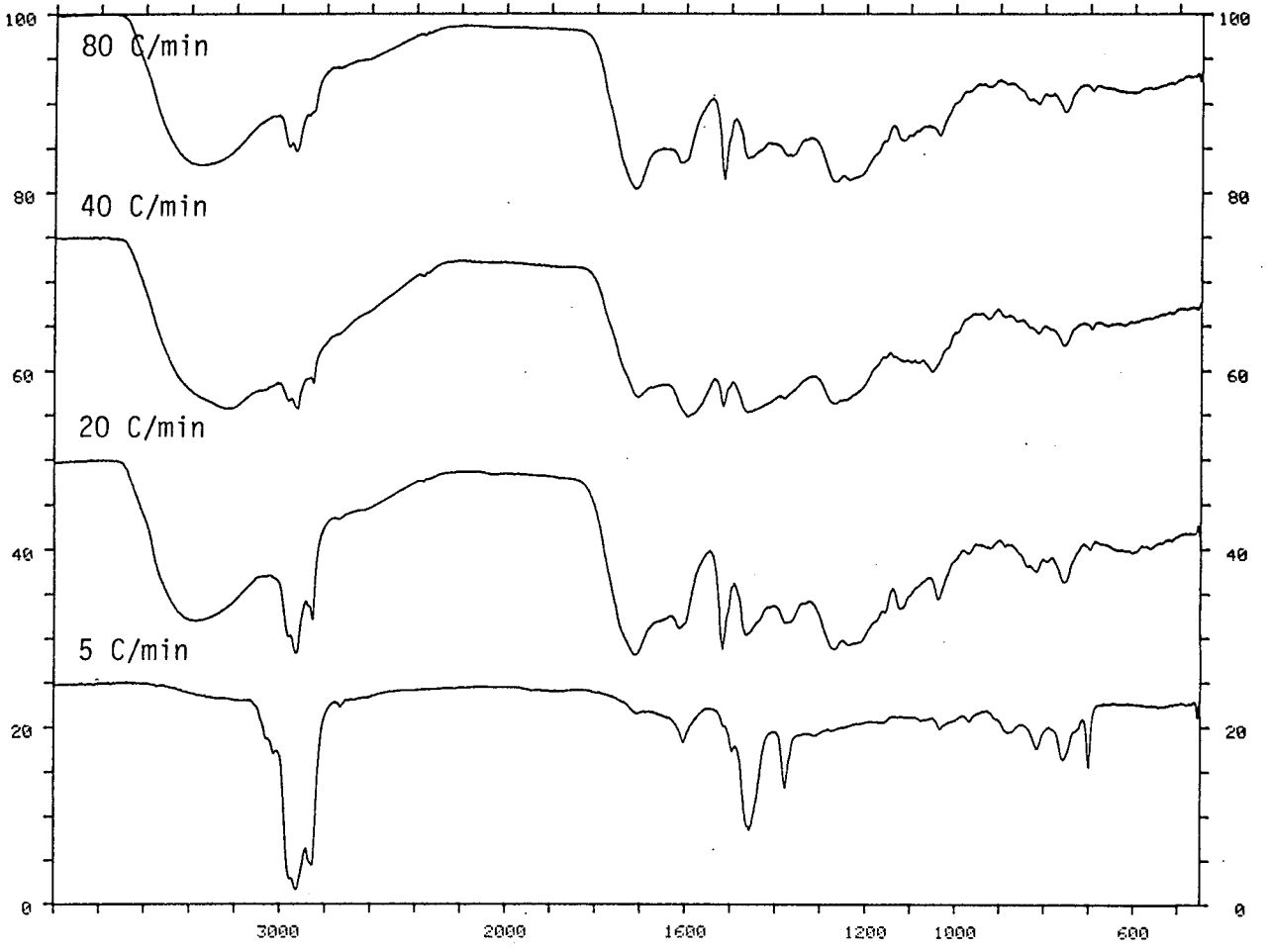

Fig.7.9 The Heating Rate Effect on the FT-ir Traces of the Oils Derived From Rice Husks

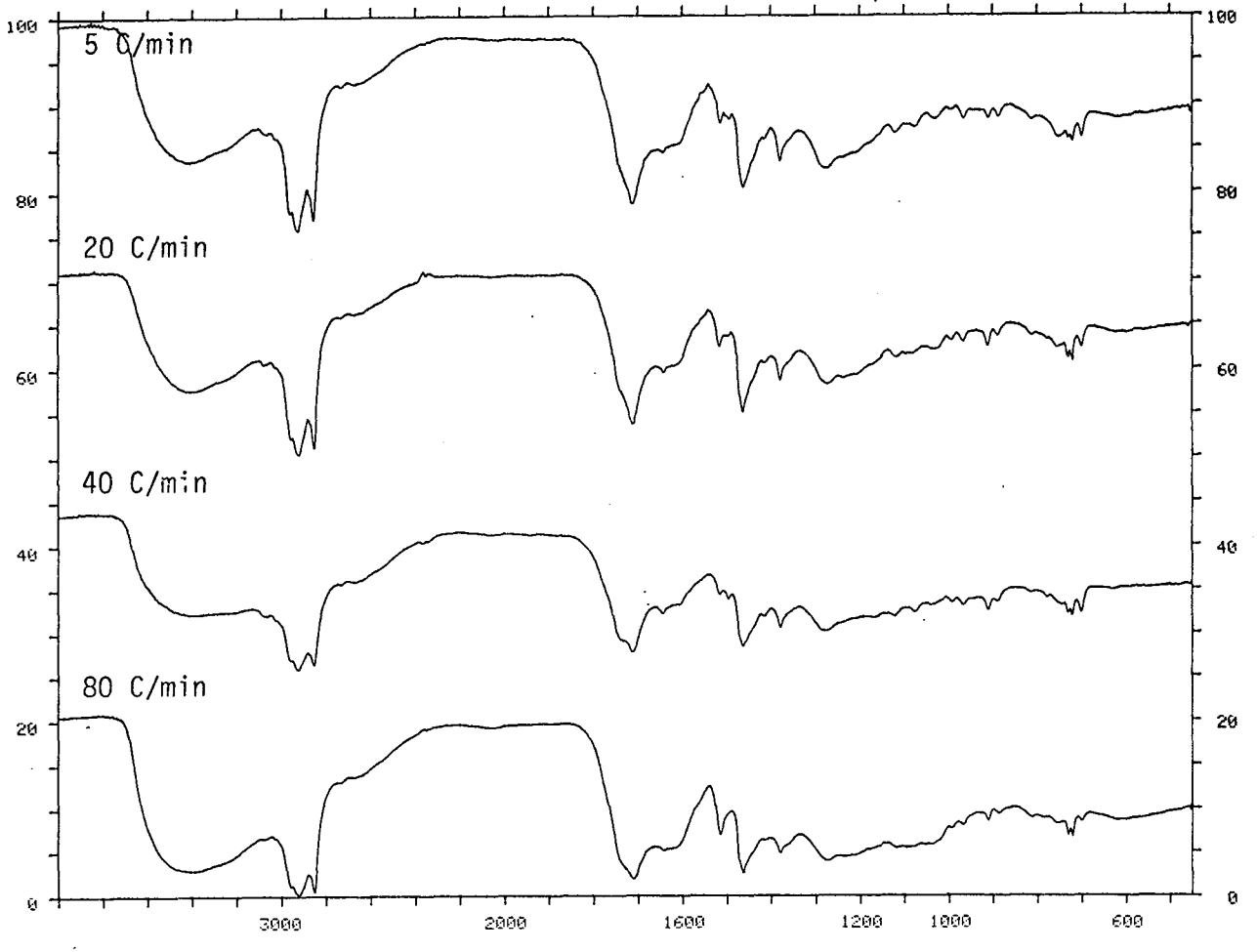

Fig.7.10 The Heating Rate Effect on the FT-ir Traces of the Oils Derived From RDF

The results presented in Table 7.4 shows the derived change in peak intensity in relation to heating rate for wood, rice husks and RDF. The data were derived from Figures 7.8, 7.9 and 7.10. When the changes in peak heights are investigated, it is seen that the aromatic groups decrease for wood and rice husks with the increased heating rate. For RDF it is seen that monoaromatics show an increase while the polyaromatics show a decrease as the heating rate was increased. It is known that long residence times at high temperatures accelerate the formation of aromatics. In this research, for all experiments at different heating rates, the sweeping gas flow rate was kept constant and the residence time did not change.

Therefore, it can be concluded that slower heating rates produce increased aromatics for the heating range used in this work of 5°C min^{-1} to 80°C min^{-1}. However, as will be shown later, for the fast heating rates in the fluidised-bed reactor, higher aromatic FT-ir intensities were found to those of the fixed-bed reactor heating rates reported here. However, for the fluidised-bed reactor, the residence time was much longer and consequently this factor may dominate the heating rate effect.

The RDF oils for the sampling temperature of 420°C for slow heating rates showed that carboxylic acids, aldehydes and ketone production showed a decrease with increased heating rate. For the sampling interval at 600°C and 720°C there was no significant difference between peak intensities of acids, aldehydes and ketones, but the peaks indicating the aromatics showed an increase in intensity with the increased heating rate.

Table 7.4 Heating Rate Effect on the Functional Groups of Oils Derived From Wood, Rice Husks and RDF

Heating Rate	Aromatics (675-710) cm^{-1}	Aromatics (710-900) cm^{-1}	Aromatics (1575-1625) cm^{-1}	Alkanes (2850-2900) cm^{-1}	Alkenes (1625-1675) cm^{-1}
Wood					
5	2.2	2	2.0	2.5	2.7
20	1.3	1.2	0.8	1.5	1.5
40	0.8	0.9	0.8	1.6	1.5
80	0.8	0.9	0.9	1.5	1.3
Rice Husks					
5	1.8	1.7	1.9	5.3	0.2
20	1.2	0.8	1.4	2.0	0.5
40	0.9	0.6	1.0	0.7	0.3
80	0.7	0.5	0.4	0.2	0.6
RDF					
5	1.5	0.5	1.4	2.2	1
20	0.8	0.5	0.5	1.7	1
40	1.5	0.5	1.5	2.8	1.1
80	2.5	0.6	0.5	4.6	1.7

7.2.1.2 Characterisation of the Tyre Derived Oils

The FT-ir spectra of scrap tyre pyrolysis oils collected for the temperature intervals of 300°C, 420°C, 600°C and 720°C for the heating rates of 20°C min^{-1} are shown in Fig. 7.11. The results for oils collected at 5°C min^{-1}, 40°C min^{-1} and 80°C min^{-1} showed similar FT-ir spectra.

The infra-red spectra of pyrolysis oils present signals distributed in three main zones between 2750-3100 cm^{-1}, 1300-1800 cm^{-1} and 675-925 cm^{-1}.

The C-H stretching vibrations between 2800 and 3000 cm^{-1} and C-H deformation vibrations between 1350 and 1475 cm^{-1} indicate the presence of alkanes (161). The presence of aldehydes and ketones is indicated by the C=O stretching vibrations with absorbance between 1650 and 1750 cm^{-1}. The bands between 1575 and 1675 cm^{-1} and 875 and 950 cm^{-1} represent C=C stretching vibrations which indicate the presence of alkenes.

Mono, polycyclic and substituted aromatic groups are indicated (161) by the absorption peaks at 675-900 cm^{-1} and 1575-1625 cm^{-1}. The presence of alkanes, alkenes and aromatic compounds such as benzene, toluene, xylene, styrene and 2-6 ring PAH together with alkyl derivatives have been identified in the oil derived from pyrolysis of tyres (112, 113, 118, 123 and 144).

Mirmiran et al (114) have characterised the tyre oil derived with a vacuum pyrolysis process in the temperature profile of 200°C to 500°C. The hydrocarbons, mainly aromatics, oxygenated compounds

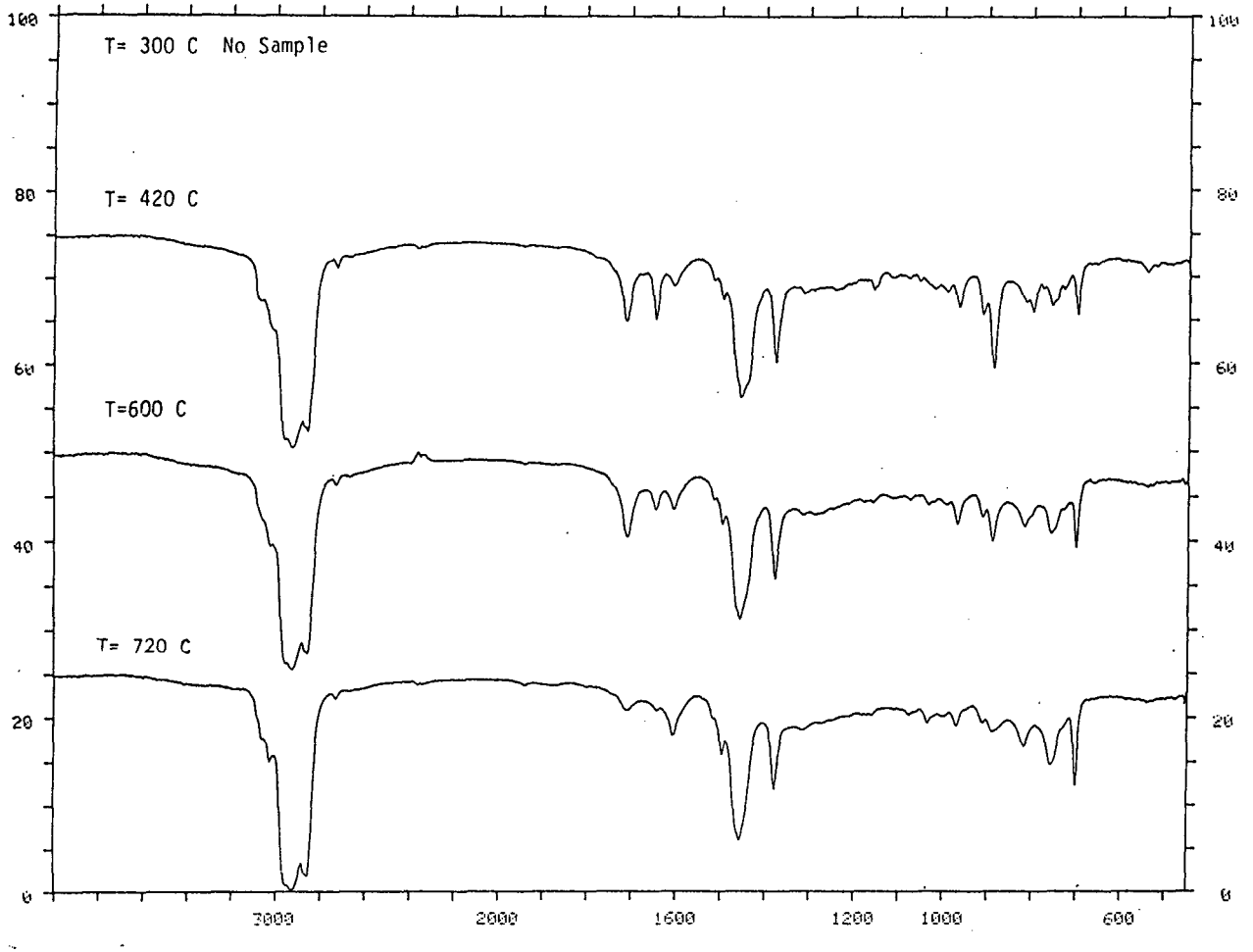

Fig.7.11 The FT-ir Spectra of Tyre Pyrolysis Oil
(Heating Rate of 20 C/min)

and nitrogenous compounds were identified. The presence of oxygen in the raw tyre compositional analysis indicates that oxygenated hydrocarbons such as aldehydes and ketones and indeed carboxylic acids might be expected in the reaction products. As hydrocarbons and oxygen, which are in the formulae of the natural rubber, SBR or BR, also nitrogen based accelerators which are added during the compounding and fabricating, can be expected to be the main sources of nitrogenous groups in the tyre oil.

The band which appears at 1690 cm^{-1} indicating C=O stretching vibrations and N-H bending vibrations at 1600 cm^{-1} and between 3100-3070 cm^{-1}, N-H stretching vibrations represent amids and secondary amins. The presence of amids, amins and alkyl derivatives in the tyre oil is confirmed by Mirmiran et al (114).

They report that aromatic hydrocarbons were distributed in a wide range of fractions in order of molecular dimension, for example mono to tetramethylbenzene and methyl to propylbenzene.

The naphtha-like fraction of vacuum pyrolysis tyre oil with an octane number similar to petroleum naphtha was separated and the benzene, toluene and xylene content of this naphtha fraction was found remarkably high by Pakdel et al (126). In addition, it was reported that the naphtha fraction contains 15% limonene (dipentene).

Another piece of work with tyre vacuum pyrolysis showed that the naphtha fraction (boiling point < 204°C) consists of 24.9% paraffins, 43.3% olefins, 6.6% naphthenes and 25.4% aromatics (124).

Cypres and Bettens (123) investigated scrap tyre pyrolysis in a two stage pyrolysis unit including low and high temperature stages.

Low temperature pyrolysis was performed at 400°C - 450°C and high temperatures were performed at 600°C to 800°C temperature range. They identified the presence of aromatic compounds which were benzene, toluene, naphthalene, methylnaphthalenes and acenaphthene etc.

7.2.1.2.A Effect of Temperature and Heating Rate

Figure 7.11 shows the effect of temperature on the absorbance spectra of the tyre derived pyrolytic oils for the heating rate of 20°C min^{-1}. It is seen that there are some changes in peak intensities which related to the compositions of the oils as the temperature was increased. The peak between 1650 cm^{-1} and 1750 cm^{-1} indicates the presence of aldehydes and ketones becomes reduced in intensity as the temperature was increased from 420°C to 720°C. The 1575 cm^{-1} to 1625 cm^{-1}, 1490 cm^{-1} to 1520 cm^{-1} and 700 cm^{-1} to 875 cm^{-1} peaks indicative of aromatic groups increased in intensity as the temperature was increased. The 1625 cm^{-1} to 1675 cm^{-1} and 875 cm^{-1} to 950 cm^{-1} absorbences indicative of alkenes showed a decrease in intensity as the pyrolysis temperature was raised to 720°C.

The results are presented in terms of relative peak height in Fig. 7.12 for the heating rate of 20°C min^{-1}. The FT-ir peaks used to compare temperature and heating rate effects were at 675 cm^{-1} and 1575 cm^{-1} the aromatic peaks, 2900 cm^{-1} the alkane and 1655 cm^{-1} the alkene peaks. Table 7.5 also illustrates the temperature effect on the functional groups for the heating rates of 5, 40 and 80°C min^{-1}. The trend observed is also confirmed by the fractional composition in section 7.2.

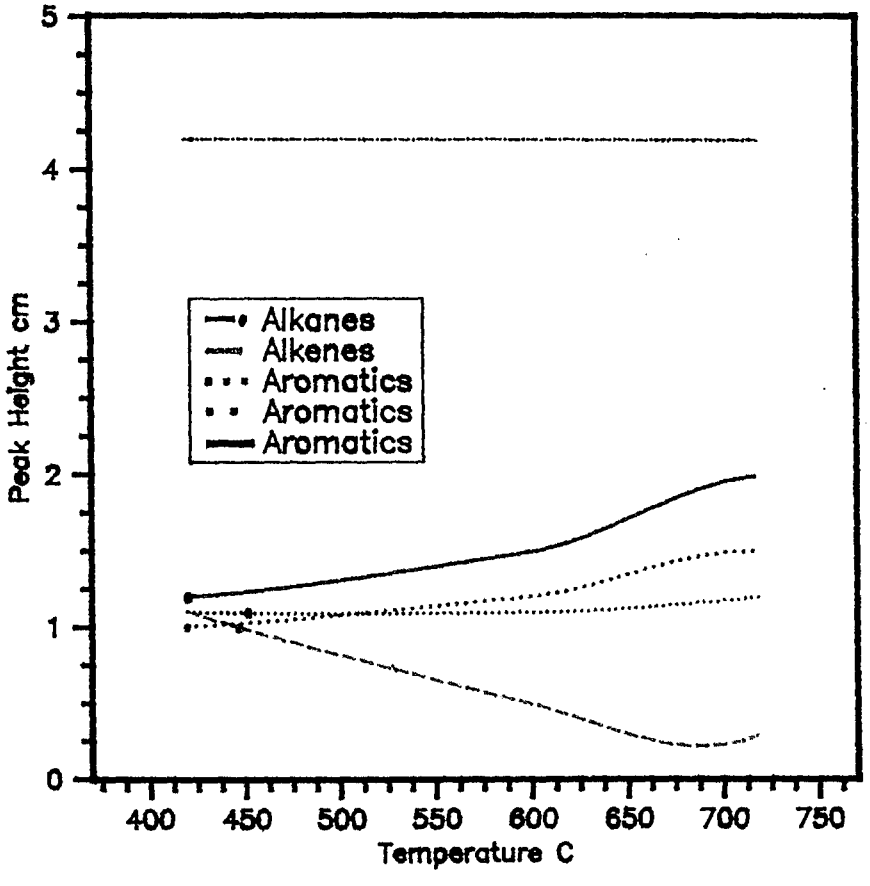

Fig. 7.12 The Temperature Effect on the Functional Groups in the Oil Derived From Scrap Tyre

Table 7.5 Temperature Effect on the Functional Groups of Oils Derived From Scrap Tyre

Temperature	Aromatics 1	Aromatics 2	Aromatics 3	Aromatics 4	Alkenes 5	Alkenes 6	Alkanes 7
5°C min^{-1}							
420	1.4	1.1	1.1	0.6	1.8	0.9	4.5
600	1.9	1.5	1.2	0.8	0.9	0.4	4.4
720	N/T	N/T	N/T	N/T	N/T	N/T	N/T
40°C min^{-1}							
420	N/T	N/T	N/T	N/T	N/T	N/T	N/T
600	1.5	1.2	0.9	0.8	1.5	0.9	4.4
720	1.9	1.5	1.1	0.9	1.0	0.3	4.3
80°C min^{-1}							
420	N/T	N/T	N/T	N/T	N/T	N/T	N/T
600	1.7	1.2	0.9	0.7	2.1	1.1	4.3
720	2	1.6	1.3	0.8	1.6	0.6	4.3

N/T = not tested

As indicated earlier, Cypres and Bettens (123) have tested two different temperature steps during scrap tyre pyrolysis. They report that at higher temperatures the ethylene compounds disappear. They are aromatised producing H_2 and CH_4 in accordance with the following general reactions:

$$C_4H_8 + C_2H_4 \longrightarrow C_6H_6 + 3H_2$$

$$C_4H_8 + C_3H_6 \longrightarrow C_6H_6 + CH_4 + 2H_2$$

Isoprene quickly disappears above 600°C. At high temperatures, naphthalene and phenanthrene seem to be most common aromatic compounds and 1,3 butadiene was also found. These induce aromatisation as a result of Diels-Alder reactions.

In this research, the increase of aromatic groups and decrease of alkenes can also be explained by means of Diels-Alder reactions (discussed later).

Fig. 7.13 shows the effect of heating rate on the functional groups present in the derived pyrolysis oil. As can be seen, the aromatic compounds increase in intensity for slow heating rates compared to faster heating rates. The alkenes and alkanes give lower results for slow heating rates compared to faster ones. Cypres and Bettens (123) have reported that with less contact time, the aromatic yield obtained was less than the longer contact time.

As with the experiments with biomass and RDF, the residence time was kept constant with all scrap tyre pyrolysis experiments.

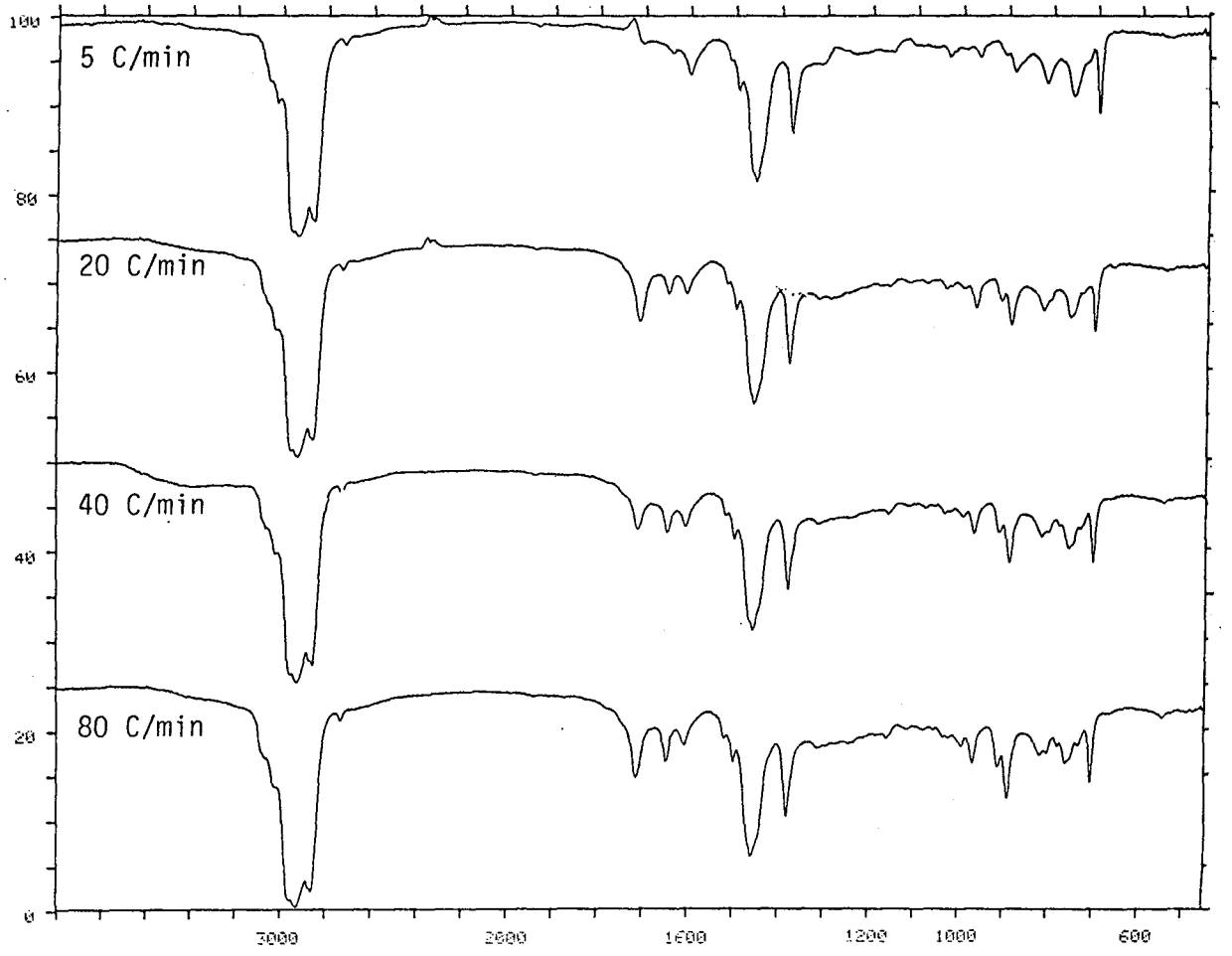

Fig.7.13 The Heating Rate Effect on the FT-ir Spectra of Scrap Tyre Derived Oils

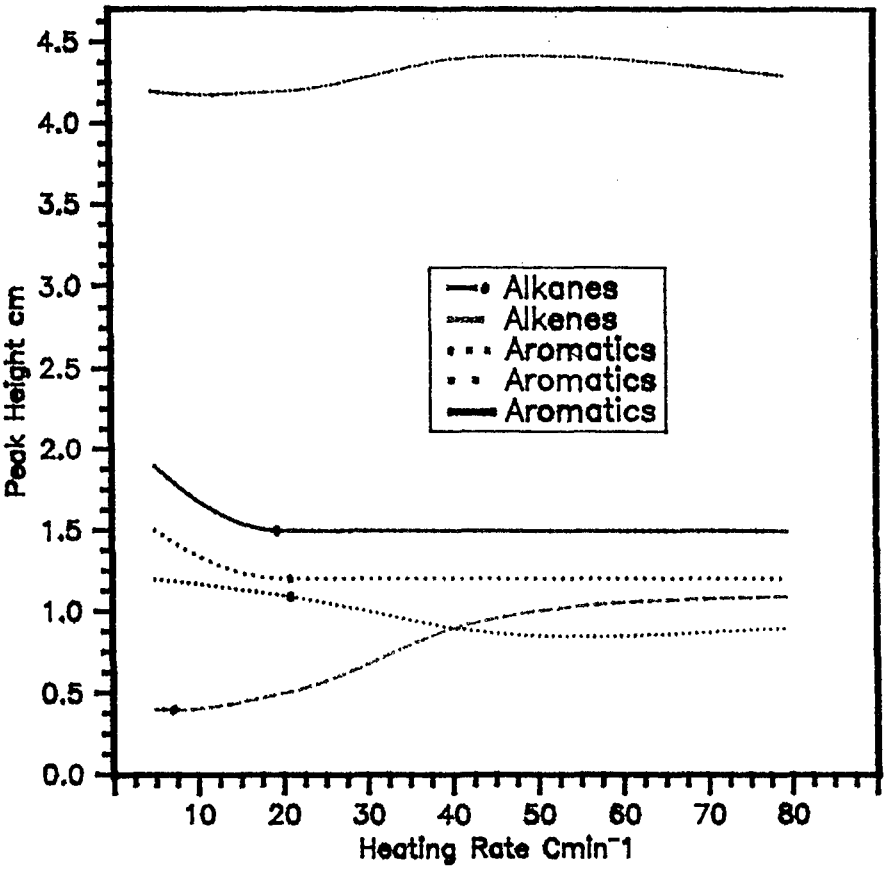

Fig. 7.14 The Heating Rate Effect on the Functional Groups in the Oil Derived From Scrap Tyre

7.2.2 Samples From Fluidised-Bed Reactors

7.2.2.1 Characterisation of Biomass and RDF Derived Oils

7.2.2.1.1 Introduction

The objective of the fluidised-bed pyrolysis employed in this research was to determine the effect of fast heating rate on the products of waste and biomass pyrolysis.

The work presented in this part is concerned with the chemical characterisation of the oils derived from biomass in a fluidised-bed reactor via the fast pyrolysis technique. Wood, rice husks and RDF were pyrolysed in the fluidised-bed reactor at the bed/freeboard temperatures of 400°C and 550°C. The oil was collected in the condensers and analysed by FT-ir.

7.2.2.1.2 Results and Discussions

The FT-ir spectra of the oils derived from wood, rice husks and RDF are shown in Figures 7.15, 7.16 and 7.17 respectively. The signals for the FT-ir spectra of oils derived from the fluidised-bed reactor display three different zones between 3600-2900 cm^{-1}, 1800-1000 cm^{-1} and 925-625 cm^{-1} similar to the FT-ir spectra of oils derived from the fixed-bed reactor.

The oils were similar in functional group composition to those obtained from the fixed-bed reactor. However, fast pyrolysis produces different concentrations of functional group species. The band between 3200-3600 cm^{-1} represents O-H stretching which indicates the presence of alcohols. The presence of alcohols in the wood pyrolysis oil derived at fast pyrolysis conditions is confirmed by a

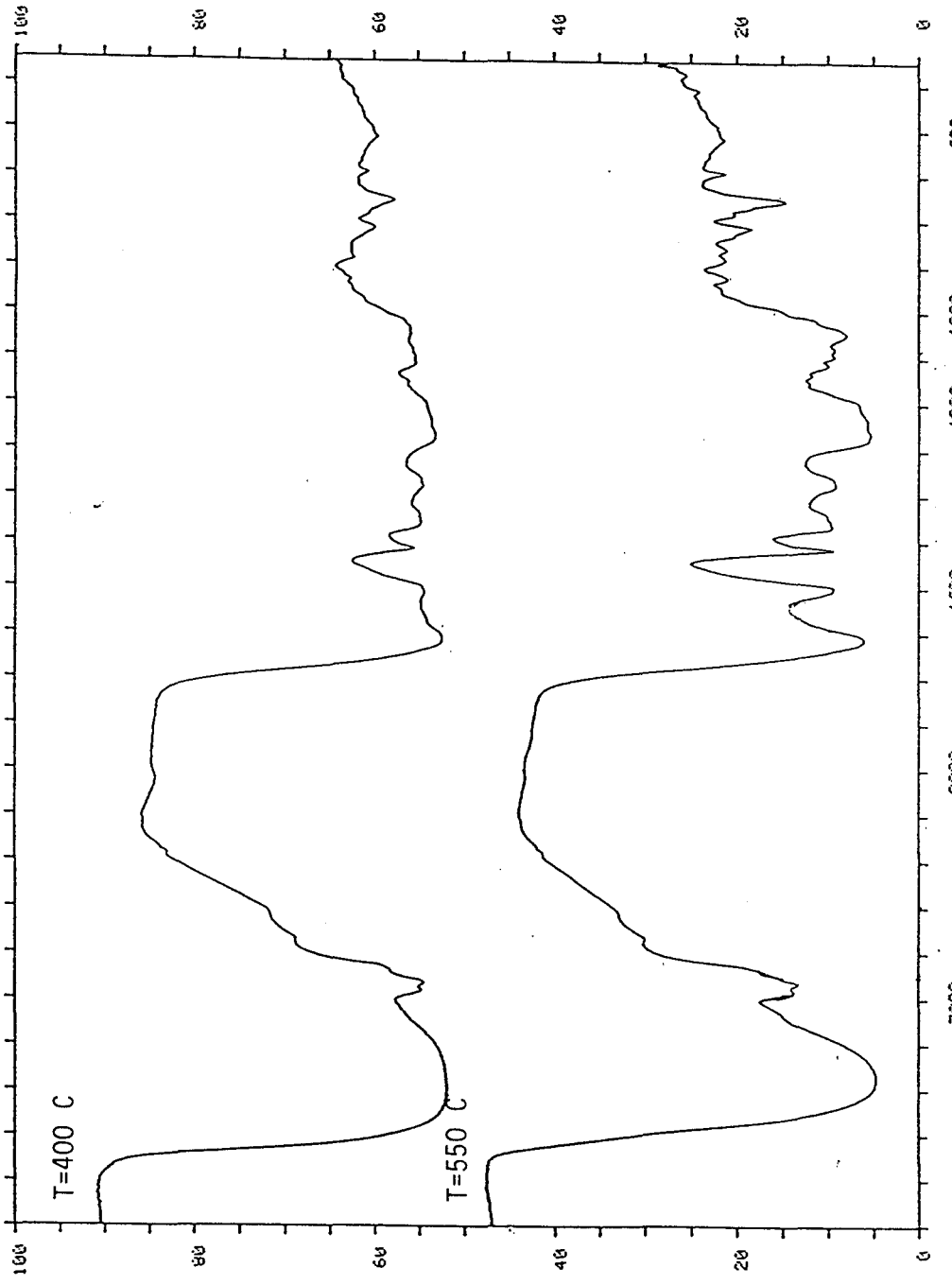

Fig.7.15 The FT-ir Spectra of Oils Derived From Fluidised-Bed Pyrolysis of Wood

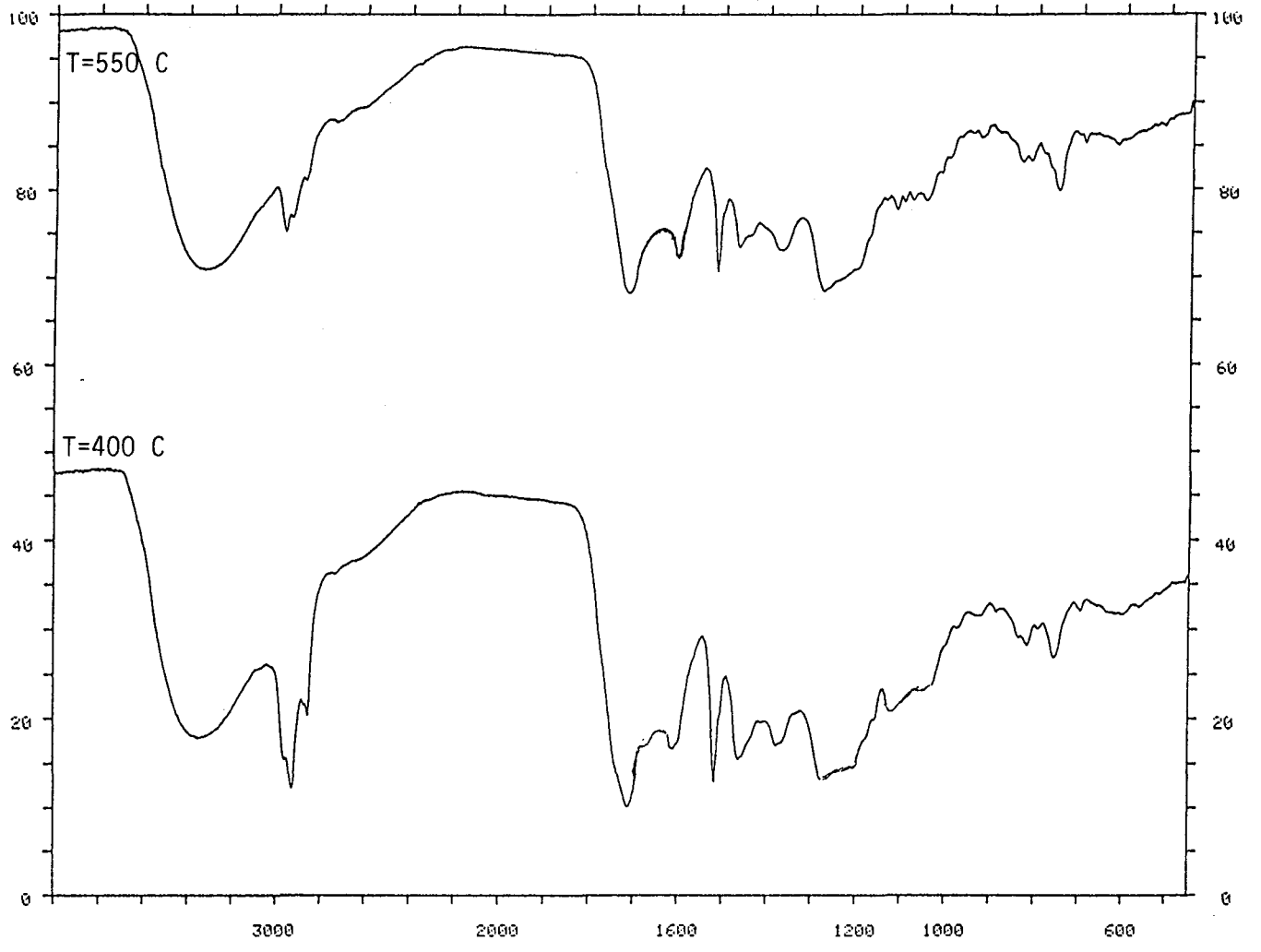

Fig.7.16 The FT-ir Spectra of Oils Derived From Fluidised-Bed Pyrolysis of Rice Husks

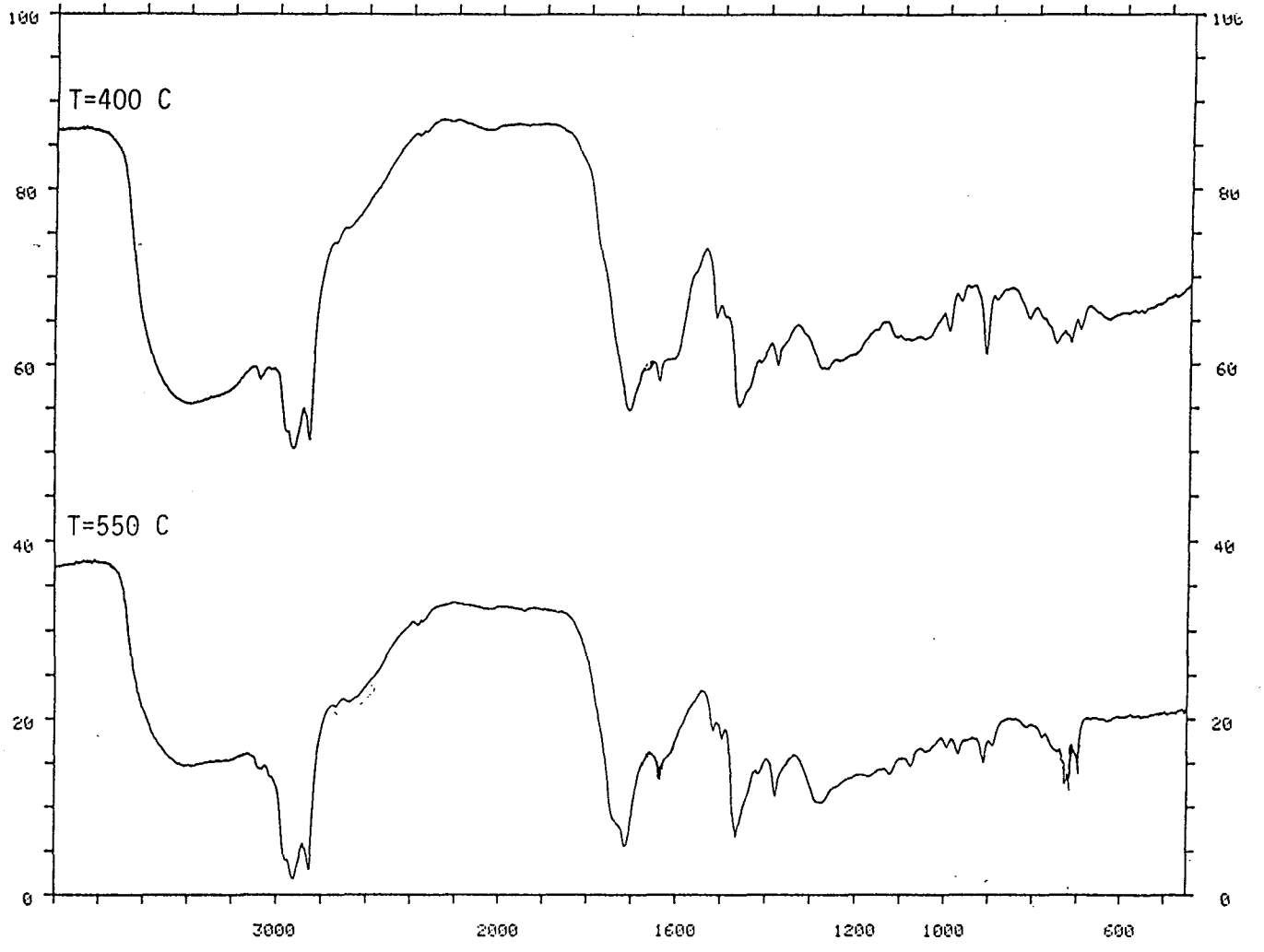

Fig.7.17 The FT-ir Spectra of Oils Derived From Fluidised-Bed Pyrolysis of RDF

number of researchers such as Nunn et al (226), Beaumont and Schwob (139) and Scott and Piskorz (197).

The yield of alcohols in the cellulosic materials pyrolysis oils is expected. This is also seen in FT-ir spectra of wood, rice husks and RDF fast pyrolysis oils.

The presence of CH_3 and CH_2 groups are displayed at 2960 cm^{-1} and 2930 cm^{-1}. Also, the signal at 2850 cm^{-1} indicates the presence of CH_3 and CH_2 groups. As indicated earlier, the presence of CH_3 and CH_2 groups indicates the presence of alkanes.

In the FT-ir spectra of RDF oils, the absorbance peak between 1625 and 1675 cm^{-1} represents C=C stretching vibrations, indicating the presence of alkenes. When the temperature was raised from 400°C to 550°C it is seen that the peaks show a decrease in intensity. Similarly, in the spectra of wood and rice husks oils, the alkene groups also decrease with the increased temperature.

The bands at 1100-1260 cm^{-1} are due to C-O stretching absorptions of C-O-H and at 1040-1140 cm^{-1} are due to C-O stretching in aliphatic ethers and alcohols.

Mono, polycyclic and substituted aromatic groups are indicated by the absorption peaks between 675 and 900 cm^{-1} and 1575 and 1625 cm^{-1}. The aromatic compounds of the oils as seen in the FT-ir spectra of the oils increase as the temperature is increased. Also, ethers, alcohols and aldehydes showed a decrease with the increased fluidised-bed temperature. Figure 7.18 illustrates the changes in the peak heights of aromatics, alkenes and alkanes for the oils derived from wood, rice husks and RDF.

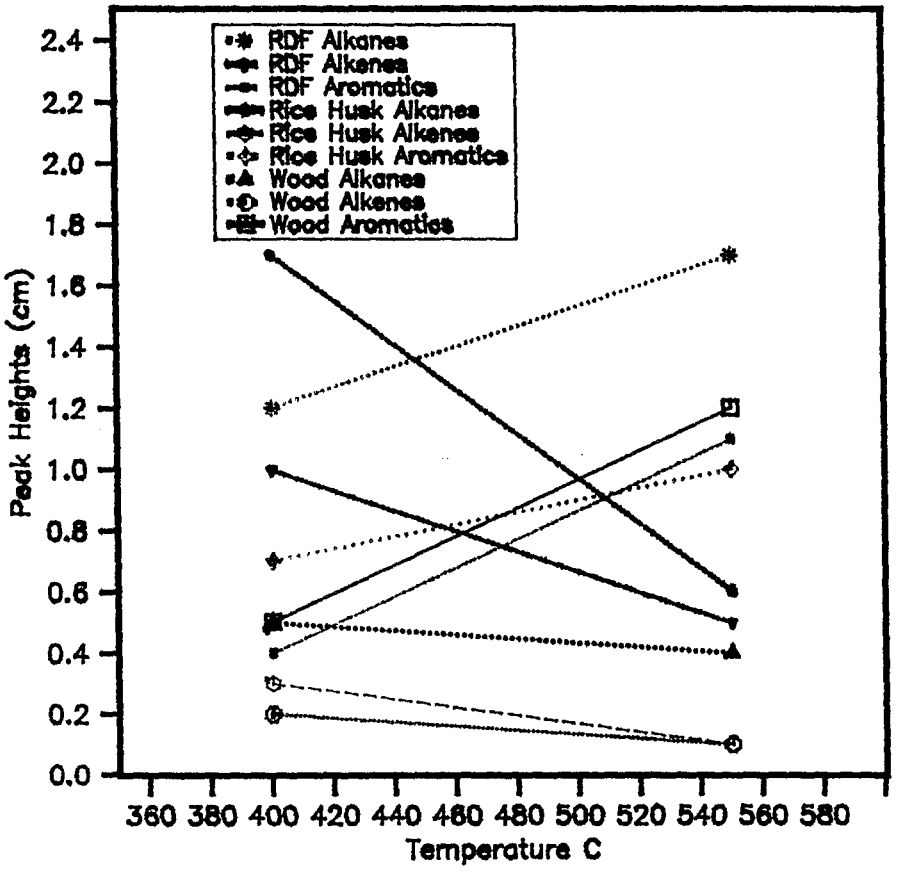

Fig. 7.18 Temperature Effect on the Liquid Yields of Wood, Rice Husks and RDF Fast Pyrolysis Oils

When the alkenes and alkanes decrease, the increase in aromatic compounds may well be explained by means of Diels-Alder reactions. These trends are also confirmed for the chemical class characterisation which will be illustrated in Section 7.3. The formations of polycyclic aromatic compounds by means of Diels-Alder reactions will also be discussed in the same section.

When the aromatic, alkane and alkene yields are compared with the yields from the fixed-bed reactor, it is seen that the oils from

the fluidised-bed reactor at 550°C give similar amounts of aromatics to the oils from the fixed-bed reactors at the temperature of 720°C.

7.2.2.2 Characterisation of Tyre Derived Oils

The FT-ir spectra of the oils obtained from the fluidised-bed reactor at the bed/freeboard temperatures of 400°C and 550°C are shown in Figure 7.19.

The signals presented are distributed in three main zones between 675-925 cm^{-1}, 1300-1800 cm^{-1} and 2800-3100 cm^{-1}. The FT-ir spectras from Figure 7.19 were analysed in terms of peak intensity for the alkane groups at frequency 2900 cm^{-1}, alkene groups at frequency 1675 cm^{-1} and aromatic groups at 675 cm^{-1} and 750 cm^{-1} which are illustrated in Figure 7.20.

It is seen that the aromatic groups dramatically increase as the temperature was increased, while alkenes showed a decrease (Fig. 7.20). Also, when the formation of aromatics are compared with the fixed-bed derived oils, it is seen that the oils derived from the fluidised-bed reactor consist of very high concentrations of aromatic compounds.

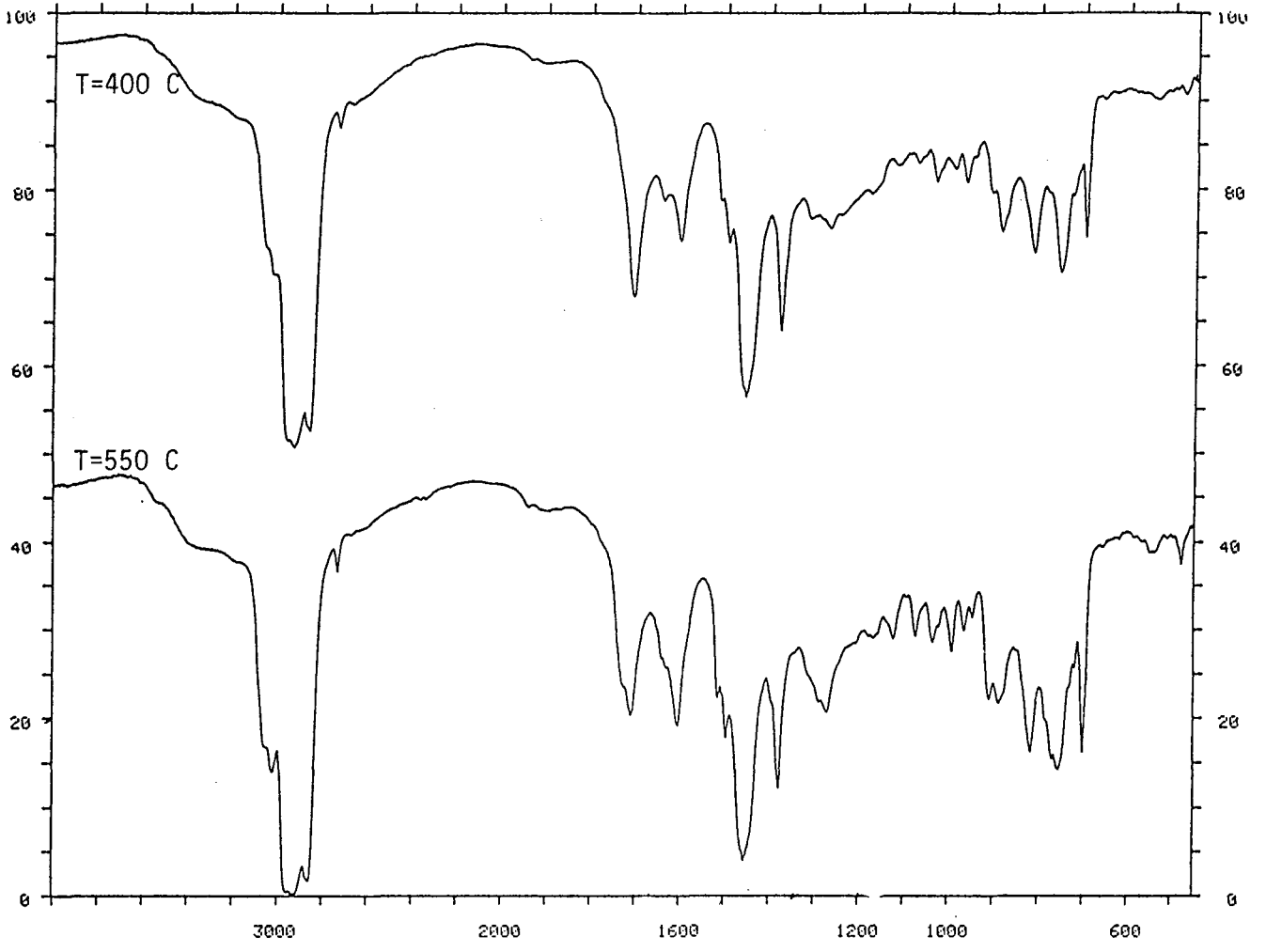

Fig.7.19 The FT-ir Spectra of Fluidised-Bed Pyrolysis of Scrap Tyre Oils

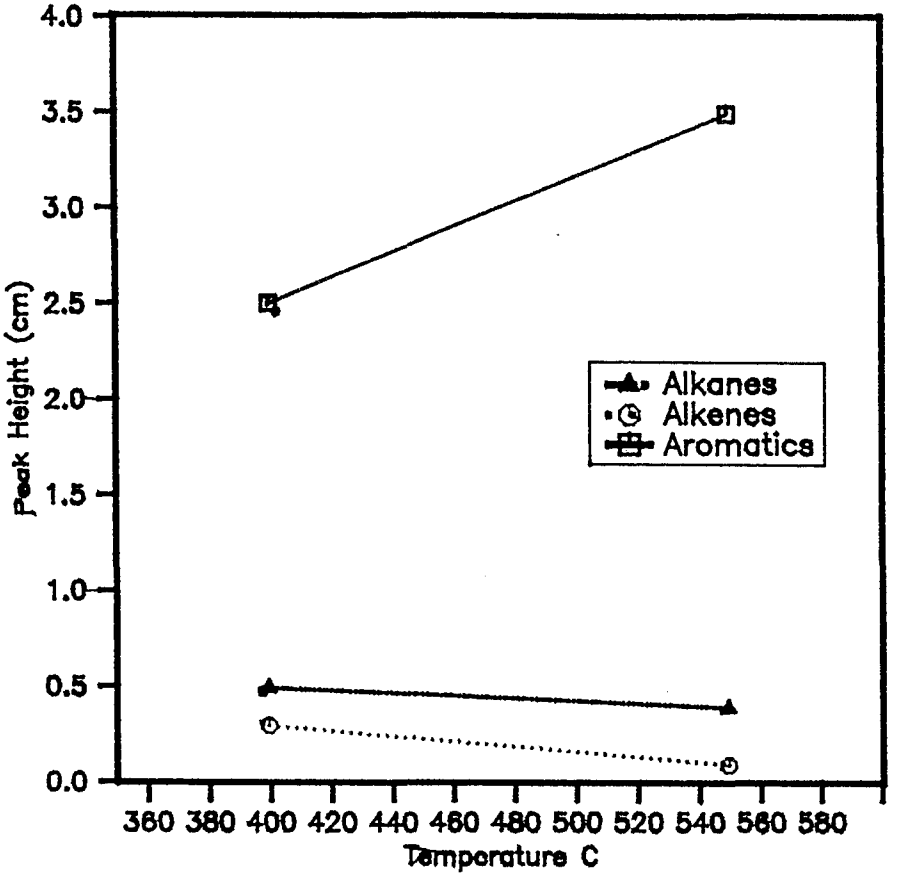

Fig. 7.20 The Temperature Effects on the Tyre Oil Derived From Fluidised-Bed Reactor

Comparison With Literature Work:

The common objective of the fast pyrolysis process developed was to obtain a maximum conversion of biomass to a liquid product which could serve as an alternative fuel oil and profitable source of chemicals. In addition, the derived chemical compounds in the oil should also not be hazardous.

Scott et al (205) have developed an atmospheric pressure fluidised-bed reactor. They pyrolysed poplar wood at 750°C and observed a wide range of chemicals such as hydroxyacetaldehyde, formic acid, acetic acid, acetol, methylglyoxalformaldehyde and aromatic compounds.

From the same research group, Radlein et al (79) have suggested that for fast pyrolysis at moderately high temperatures, cellulose appears to decompose, predominantly along one of two alternative pathways: depolymerisation to the monomer levoglucosan or fragmentation to lower molecular weight species among which hydroxyacetaldehyde is the most abundant. However, it was reported by Piskorz et al (77) that pyrolysis of wood, whether slow or rapid, normally gives very low yields of levoglucosan and it was also pointed out that if fast pyrolysis is employed prohydroxyacetaldehyde will be one of principal products (Fig. 7.21).

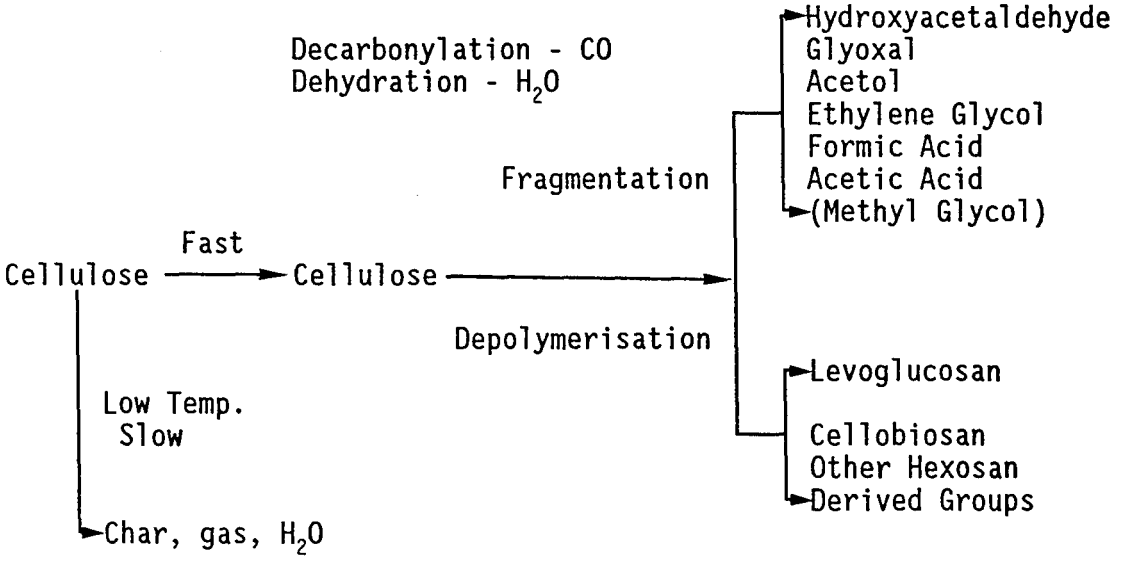

Fig. 7.21 Proposed Decomposition Mechanism in Fast Pyrolysis of Cellulose (205)

Fast pyrolysis of wood in a fluidised-bed reactor has also been tested by Beaumont and Schwob (139). They tested different fast pyrolysis temperatures and observed that furaldehyde and furfurylic alcohol yields decreased as the temperature was increased. Similar results are shown for the present work in Fig. 7.18. Also, they compared fast and slow pyrolysis cases and they observed higher

yields from fast pyrolysis experiments. They reported that the oil consists of water, methanol, ethanol, acetone, formic, acetic and propionic acids, furaldehyde and furfurylic alcohol. Their paper does not report any aromatic compounds in the yields. From the same research group, Beaumont (227) has revealed more detailed chemical characterisation of wood oils obtained from a fluidised-bed reactor, 57 compounds were identified in the wood fast pyrolysis oil. According to Beaumont (227), phenolics derive from lignin by cracking of phenyl-propane units of the macromolecule lattice. The phenolics are not found in the cellulose and xylone pyroligneous substances. Therefore, Beaumont (227) has reached the conclusion that the lignins are the main sources of phenolics. Degradation of xylan yields eight main products, water, methanol, formic, acetic and propionic acids, hydroxy-1-propanone, hydroxy-1-butanone and 2-furfuraldehyde. Water is formed by dehydration. Acetic acid comes from the elimination of acetyl groups originally linked to the xylose unit (227). Furfurol is formed by dehydration of the xylose unit. Formic acid proceeds from carboxylic groups of uranic acid. Methanol arises from methoxyl groups of uranic acid (227).

Scott et al (228) have pyrolysed different biomass samples in a fluidised-bed reactor at fast pyrolysis conditions at four different temperatures in the range of 450°C to 650°C. They observed in the liquid yield acetaldehyde, furan, acrolein and acetone. It was also reported that the yields of the compounds above increased as the temperature was increased.

Font et al (229) pyrolysed almond shells in a fluidised-bed reactor in the temperature range from 365°C to 710°C. They obtained acetic acid, 2-furaldehyde, formaldehyde, acetone, 2-propanol,

hydroxyacetone, 1-hydroxy-2-butanone, 3-methyl-1-butanol, propionic acid and acetaldehyde. No aromatics presence was reported. The amounts of those compounds above increased as the temperature was increased from 365°C to 500°C and then decreased with further temperature increases up to 710°C.

Pakdel et al (230) have characterised the vacuum pyrolysis oil of bark residues and primary sludges. They reported the pyrolysis temperature as 486°C and reactor pressure as between 3.3 and 5.3 kPa. The oil yields were first fractioned and then characterised. Aliphatic hydrocarbons, alicyclic hydrocarbons and benzene derivatives were identified. Polyaromatic hydrocarbons and derivatives were found in different fractions of primary sludge pyrolysis oil. A homologous series of n-alkanes and n-alkenes and numerous alicyclic hydrocarbons, benzene derivatives and polycyclic aromatic hydrocarbons e.g. 1.2 dimethyl benzene, 1, propenyl benzene, D-limonene, 4-methylene-1-cyclohexene, 2-ethenylnaphthalene, 9-H fluorene, 2-7 dimethyl phenanthrene and 2,3,5, trimethylphenanthrene were identified. A wide range of phenolic compounds and acids were also identified.

In the bark residues pyrolysis oils a homologous series of n-alkanes and n-alkenes (C_{11} to C_{29}), 1-methylnaphthalene, dimethylnaphthalenes, phenanthrene, anthracene, fluorene and methylanthracene and also a wide range of carboxylic acids, phenolic compounds and alcohols were identified.

Kaminsky et al (103) pyrolysed plastic materials such as polyethylene, polystyrene and polyvinylchloride at the reaction temperature of 740°C. The oils derived from polystyrene and

polyvinylchloride were found to be composed of phenanthrene, fluorene, diphenyl, methylnaphthalene, naphthalene, indene and styrene.

Kaminsky and Sinn (112) also performed the fast pyrolysis of scrap tyres in a fluidised-bed reactor at 750°C. The pyrolysis oil were characterised, besides aliphatic compounds the oil was found to consist of phenanthrene, fluorene, diphenyl, methylnaphthalene, indan, indene, styrene, xylene, toluene and benzene. They also showed, as was found in this work, that increasing the fluidised-bed temperature resulted in an increase in aromatic and polyaromatic compounds.

It is seen that besides so many attempts to characterise biomass oils, there are few investigations on the presence of polycyclic aromatic compounds in pyrolysis oils derived from biomass. Also, research on the polycyclic aromatic compounds in oils derived from the pyrolysis of plastic materials and scrap tyre, shows that there are few data in the literature.

The chemical characterisation of the oils derived from waste and biomass, were threrefore analysed for polycyclic aromatic hydrocarbons which are known environmentally hazardous compounds.

7.3 Characterisation of Polycyclic Aromatic Hydrocarbons by Gas Chromatography and Gas Chromatography-Mass Spectrometry

7.3.1 Introduction

The production of a liquid hydrocarbon product from biomass and waste via pyrolysis provides a number of advantages since the oil has a high energy density which reduces the costs of transport and storage and consequently the potential for premium fuel substitution.

The derived oils have a high calorific value similar to a medium heating oil and maybe used directly as fuel or added to petroleum refinery feedstocks. However, the use of plastics, tyre and biomass derived oils as fuels may be restricted since they have been reported to contain high concentrations of certain polycyclic aromatic hydrocarbons (PAH) (112, 206, 212).

The work presented in this section is concerned with the investigation of the identification and formation of polycyclic aromatic hydrocarbons in the pyrolysis oils derived from biomass and waste.

The oil was analysed for PAH by liquid chromatography, separating the oil into chemical class fractions, followed by gas chromatography-mass spectrometry for identification. Quantification was carried out using gas chromatography with flame ionisation detection using Lee retention indices and standard concentrations of standard PAH.

The column was eluted under vacuum with pentane, benzene, ethylacetate and methanol to produce aliphatic, aromatic, ester and

polar fractions respectively. The pentane fraction was further sub-divided into two fractions, namely pentane-1 and -pentane-2.

Williams and Taylor (210) have defined the pentane-1 fraction as aliphatics, pentane-2 fraction as light aromatics and the benzene fraction as heavy aromatics.

The pentane-2 and benzene fractions will consequently contain the PAH which are investigated in this study. The separation of each chemical fraction was confirmed by GC/MS and FT-ir analysis of each fraction.

7.3.2 Chemical Class Fractionation

7.3.2.1 Chemical Class Fractionation of the Oils Derived From Biomass And RDF

The chemical class fractionation in terms of the percentage mass ocurring in each fraction, which are pentane-1, pentane-2, benzene, ethylacetate and methanol of the biomass and waste derived oils, are presented in this section.

7.3.2.1.1 Oils Derived From the Fixed-Bed Reactor

Chemical class fractionation of the wood, rice husks and RDF pyrolysis oils collected during a single experiment at the temperature intervals up to 720°C at heating rates of 5, 20, 40 and 80°C min^{-1} are shown in Tables 7.6, 7.7 and 7.8 respectively.

Wood and Rice Husks Oils

For wood oils at each heating rate, as the temperature increased, the pentane-1 fraction decreased while the pentane-2,

benzene and methanol fractions increased. The ethylacetate fraction showed a very small increase. This data can be correlated with the change in composition of each fraction. It is seen that aliphatics showed a decrease, the benzene fraction and pentane-2 fractions indicating the heavy and light aromatic compounds showed an increase. The ethylacetate and methanol fractions which indicate the alcohols, aldehydes, esters, ethers and acids also increased as the temperature of pyrolysis increased.

Table 7.6 Wood Percentage Weight Composition of Each Fraction

T °C)	Pentane-1 (wt %)	Pentane-2 (wt %)	Benzene (wt %)	Ethyl Acetate (wt %)	Methanol (wt %)
5°C min^{-1}					
420	10	2	21	28	29
600	8	4	19	23	36
720	6	6	23	21	26
20°C min^{-1}					
420	9	1	24	28	29
600	6	5	21	21	35
720	5	6	23	22	34
40°C min^{-1}					
420	7	4	21	22	31
600	6	6	22	28	34
720	4	7	27	24	36
80°C min^{-1}					
420	-	-	-	-	-
600	4	7	24	28	35
720	3	6	26	20	32

Table 7.7 Rice Husks Percentage Weight Composition of Each Fraction

T °C)	Pentane-1 (wt %)	Pentane-2 (wt %)	Benzene (wt %)	Ethyl Acetate (wt %)	Methanol (wt %)
5°C min^{-1}					
420	6	9	24	22	28
600	6	11	24	23	26
720	5	11	25	23	21
20°C min^{-1}					
420	7	10	24	21	28
600	5	10	25	23	27
720	5	12	26	24	24
40°C min^{-1}					
420	7	12	24	24	20
600	6	11	22	30	25
720	4	13	27	29	24
80°C min^{-1}					
420	-	-	-	-	-
600	4	11	23	32	25
720	3	12	27	32	24

Table 7.8 RDF Percentage Weight Composition of Each Fraction

T °C)	Pentane-1 (wt %)	Pentane-2 (wt %)	Benzene (wt %)	Ethyl Acetate (wt %)	Methanol (wt %)
5°C min^{-1}					
420	18	7	28	24	15
600	17	8	30	20	15
720	14	8	35	21	12
20°C min^{-1}					
420	20	9	29	22	14
600	18	10	30	20	15
720	16	10	33	20	12
40°C min^{-1}					
420	14	10	20	21	13
600	16	12	28	22	10
720	20	11	28	20	12
80°C min^{-1}					
420	-	-	-	-	-
600	18	12	29	18	10
720	19	14	34	16	10

The chemical fractionation of rice husks also showed that the pentane-1 fraction, which indicates the aliphatic compounds, decreased as the temperature was increased.

The pentane-2 and benzene fractions, which indicate the light and heavy aromatics respectively, showed an increase with the increased temperature and heating rate. For example, for the heating rate of 20°C min^{-1}, the pentane-1 fraction decreased from 7% to 5% while the pentane-2 and benzene fractions increased from 10% to 12% and 24% to 26% respectively.

Sharma and Bakshi (211) reported that the yield of each fraction is dependent on temperature of pyrolysis. According to their results, as the temperature was increased, aliphatic hydrocarbons showed a small increase while aromatics showed a significant increase in the wood oils derived from their fixed-bed reactor at 370°C - 410°C. The phenolic content also decreased, whereas, the amount of aromatic hydrocarbons increased to a maximum as the temperature increased.

Scott et al (205) reported 24.6% aromatics in the liquid yield of poplar wood pyrolysis, similar to that found here. They suggest that the lignin fraction is the source for aromatics and that it can be readily separated from the pyrolysis liquid.

Elliott et al (207), after reviewing the elemental analysis of some biomass oils, suggested that the low hydrogen to carbon ratios dictate that the oil products must contain a large fraction of aromatic or at least highly unsaturated compounds.

In their detailed PAH work on poplar wood vacuum pyrolysis tars, Pakdel and Roy (212) report that the production of oils from biomass by thermal treatment depends on the pyrolysis temperature and residence time. The primary oxygenated oils produced during wood pyrolysis below 500°C can be changed to highly aromatic, de-oxygenated tar by additional thermal treatment at 700°C or above.

In their work, aliphatic hydrocarbons derived by vacuum pyrolysis from wood represented between 0.08% and 0.46% of the oil phase and 0.01% and 0.02% of the ageous phase. The aliphatic hydrocarbon fraction of the oil was dominated by n-alkanes in the range of n-C_{19} to n-C_{26}. Aromatic hydrocarbons were found between 0.06% and 0.24% of the oil phase and were detected only in trace amounts in the aqueous phase. Unlike the vacuum pyrolysis oil, wood gasification yielded tar with a high percentage of PAH's, about 55%.

The effects of increased temperature on the composition of the oils derived from wood pyrolysis were also investigated by Vassilatos et al (222). The wood oils were derived in the temperature range of 700°C - 900°C in a fixed-bed reactor. With increasing pyrolysis temperature, the amounts of aromatic compounds increased while the phenolics decreased. Naphthalene was reported to be the major single component for the pyrolysis temperature of 900°C.

The increased temperature effects on the reaction pathway is illustrated below by Elliott (27).

Mixed Oxygenates	Phenolic ethers	Alkyl phenolics	Heterocyclic ethers	PAH	Larger PAH
⟶	⟶	⟶	⟶	⟶	⟶
400°C	500°C	600°C	700°C	800°C	900°C

RDF Oils

The chemical class fractionation of the RDF oils showed that at each heating rate, as the temperature was increased, the ethylacetate and methanol fractions decreased and pentane-1 fraction showed a decrease for the heating rate of 5°C min^{-1} and 20°C min^{-1} and increased for the heating rates of 40°C min^{-1} and 80°C min^{-1}.

The light aromatic fraction first showed an increase, but for the heating rate of 40°C min^{-1} it decreased. The benzene fraction showed an increase with the increased temperature and heating rate.

Since the RDF contains more than 50% of cellulosic materials, it was expected that the RDF would show similarities to the cellulosics oil chemical fractionation as illustrated by the wood and rice husks results. However, the differences observed are probably due to the inhomogeneous nature of RDF and the decomposition of the plastics etc in the RDF.

Koo et al (107) observed similar results from the pyrolysis of polyethylene and polystyrene mixtures. As in this research, the decrease in the aliphatic compounds (pentane-1 fraction) with high temperature and the increase of light and heavy aromatic compounds (pentane-2 and benzene fractions) have been explained by means of Diels-Alder condensation reactions which are discussed in Section 7.3.3.

7.3.2.1.2 Oils Derived From the Fluidised-Bed Reactor

Chemical class fractionation of the wood, rice husks and RDF pyrolysis oils derived from the fluidised-bed reactor at fluidbed/freeboard temperatures of 400°C and 550°C are shown in Table 7.9.

Table 7.9 Wood, Rice Husks and RDF Oils Derived From Fluidised-Bed Reactor Weight Composition of Each Fraction

T (°C)	Pentane-1 (wt %)	Pentane-2 (wt %)	Benzene (wt %)	Ethyl Acetate (wt %)	Methanol (wt %)
Wood					
400	8	11	23	26	27
550	6	10	27	26	26
Rice Husks					
400	8	10	22	25	32
550	5	12	26	24	28
RDF					
400	13	10	24	17	17
550	16	12	39	17	12

For the bio-oils derived from wood and rice husks, the pentane-1 fraction which contained the aliphatic compounds decreased from 8% to 6% and 8% to 5% respectively as the temperature was increased.

The pentane-2 fraction which contained light aromatics showed a small decrease for the wood oils with increased temperature while the light aromatics of the rice husks oil increased. Also, the benzene fraction indicating the presence of heavy aromatics increased with the increased temperature. The ethylacetate and methanol fractions did not show any significant change for the wood oils while

the ethylacetate and methanol fractions of rice husks oil showed a decrease.

When the chemical fractions of the oils derived from the fixed-bed and fluidised-bed reactors are compared, it is seen that the benzene fraction percentage is higher in the oil derived from the fluidised-bed reactor. The aromatics yield at 550°C in the fluidised-bed reactor were higher than in the fixed-bed reactor at 600°C. This shows that aromatic compounds are produced in the fast heating system of the fluidised-bed reactor. This was also confirmed by Elliott (27). According to him, high temperature flash pyrolysis produces PAH's in significant amounts.

The liquids from the fast pyrolysis process were found to contain large amounts of relatively few chemicals with a number of minor components by Scott et al (205). They also suggested that the reaction mechanisms of fast pyrolysis were not clearly understood.

From the limited temperature data for the fast pyrolysis of wood and rice husks, it can be seen that the aliphatic compounds (pentane-1 fraction) show a decrease, while the light aromatics (pentane-2) and heavy aromatics (benzene fraction) increase with the increased temperature.

The fast pyrolysis of RDF also shows that the light and heavy aromatics increase with the increased temperature. Diels-Alder reactions have been cited as the mechanism of the formation of polycyclic aromatic hydrocarbons (Section 7.3.3).

7.3.2.2 Chemical Class Fractionation of the Oils Derived From Scrap Tyre

The chemical class fractionation of the tyre derived oils collected from the fixed-bed reactor at temperature intervals during a single experiment up to 720°C at heating rates of 5°C min^{-1}, 20°C min^{-1}, 40°C min^{-1} and 80°C min^{-1} and from the fluidised-bed reactor at temperatures of 400°C and 550°C are shown in Table 7.10.

Table 7.10 Tyre Oil Percentage Weight Composition of Each Fraction

Oils From Fixed-Bed Reactor	Pentane-1 (wt %)	Pentane-2 (wt %)	Benzene (wt %)	Ethyl Acetate (wt %)	Methanol (wt %)
5°C min^{-1}					
420	38	22	24	8	4
600	35	21	26	8	3
720	26	22	33	7	4
20°C min^{-1}					
420	34	23	25	8	4
600	30	24	25	6	3
720	26	25	33	9	6
40°C min^{-1}					
420	32	23	22	10	3
600	31	23	27	9	3
720	25	26	34	9	1
80°C min^{-1}					
420	-	-	-	-	-
600	30	23	27	10	2
720	25	21	37	6	1
Oils From Fluidised-Bed Reactor					
400	33	21	24	8	6
550	20	29	44	4	1

At each heating rate, as the temperature was increased, benzene and pentane-2 fractions increased and the pentane-1, ethyl acetate and methanol fractions decreased. The same trend can also be observed with the increased heating rate.

The increase of pentane-2 and benzene fractions reflect the increase of light and heavier aromatic compounds. The temperature effect was the same on the tyre oils derived from fluidised-bed reactor. As with the fixed-bed reactor, the aromatic fractions increased with the increased temperature.

Kaminsky and Sinn (112) have shown that the concentrations of aromatic compounds such as naphthalene, fluorene, phenanthrene, pyrene and some other aromatic compounds in the oil derived from scrap tyre via fluidised-bed pyrolysis increase as the temperature of pyrolysis increases. For example, as the temperature increased from 700°C to 750°C, the naphthalene, methyl naphthalene and diphenyl concentrations increased from 0.42, 0.67 and 0.39 to 0.85, 0.83 and 0.49% respectively.

Wolfson et al (146) for a batch pyrolysis unit also showed that as the temperature of pyrolysis was raised from 500°C to 900°C there was an increase in the volume percent of aromatic compounds and a corresponding decrease in the aliphatic fraction.

Collin (144) suggested that highly aromatic pyrolysis oils derived from pyrolysis of scrap tyres in a rotary kiln reactor can be obtained at reaction temperatures of about 700°C. Such pyrolysis oils could form the basis for the production of aromatics such as benzene, naphthalene and their homologues.

7.3.3 Characterisation of PAH Contents of Pyrolysis Oils

7.3.3.1 Bio Oils (From Wood, Rice Husks and RDF)

As indicated in the experimental section, the identifications of PAH's were carried out using GC-MS with ITD (ion-trap detector) and identities were confirmed and PAH were quantified with GC with FID (flame-ionisation detector) respectively.

The methodologies are illustrated in the following examples: Fig. 7.22 Shows an ITD chromatogram of the benzene fraction of RDF oil.

Fig. 7.23 illustrates a portion of the chromatogram (TOT) with single ion monitoring for phenanthrene mass number 178 and methyl phenanthrene mass number 192.

Figures 7.24 and 7.25 show the mass spectra of the phenanthrene and methylphenanthrene in the sample compared and identified with the NBS library spectra of the mass spectrometer.

The PAH yields of wood, rice husks and RDF oils are shown in Tables 7.11, 7.12 and 7.13 respectively.

The data shows for the oils derived from the fixed-bed reactor that PAH increase with increasing pyrolysis temperature. As was reflected in the chemical class fractionation for the PAH containing fractions i.e pentane-2 and benzene.

Elliott (27) has shown that aromatisation and condensation occur at high temperatures after investigating 450°C-500°C and 600°C-650°C as the pyrolysis temperature.

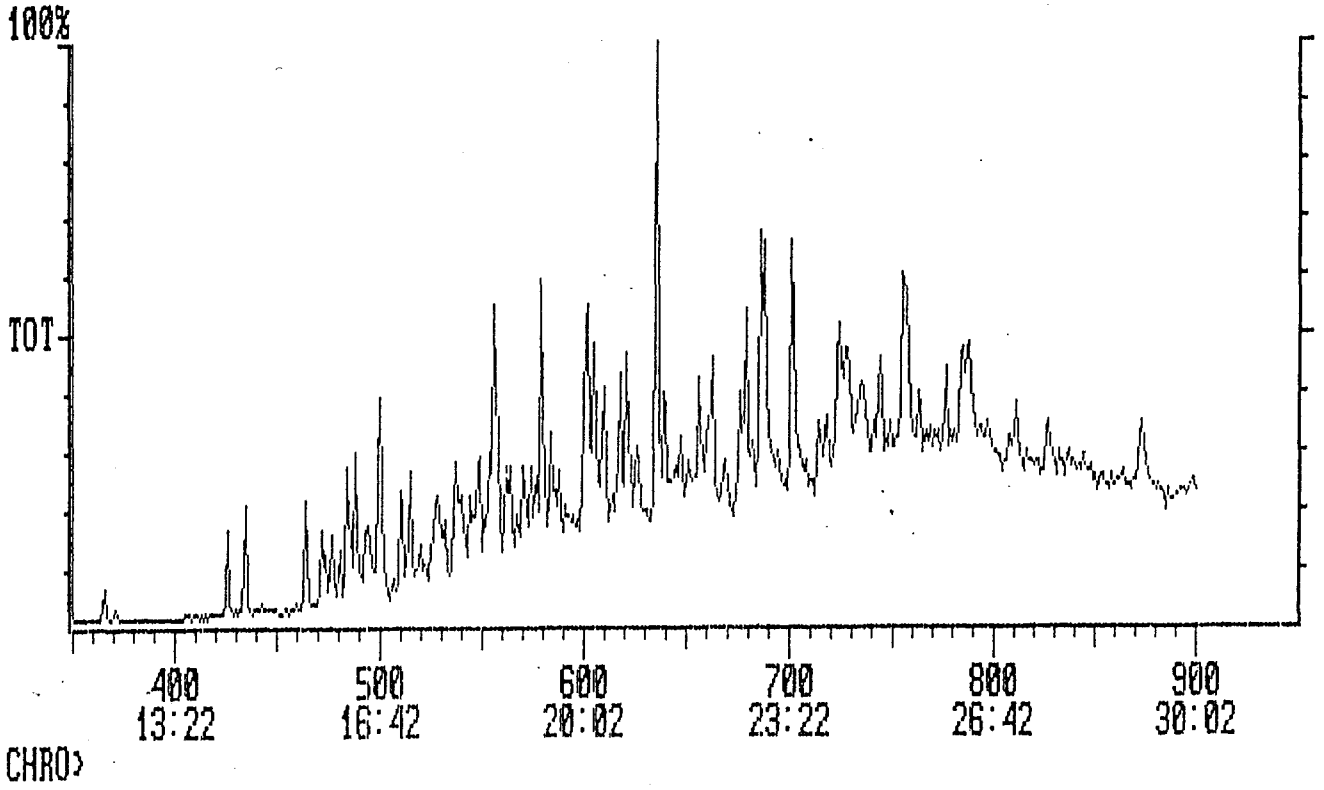

Fig.7.22 ITD Chromatogram of Benzene Fraction of RDF Oil

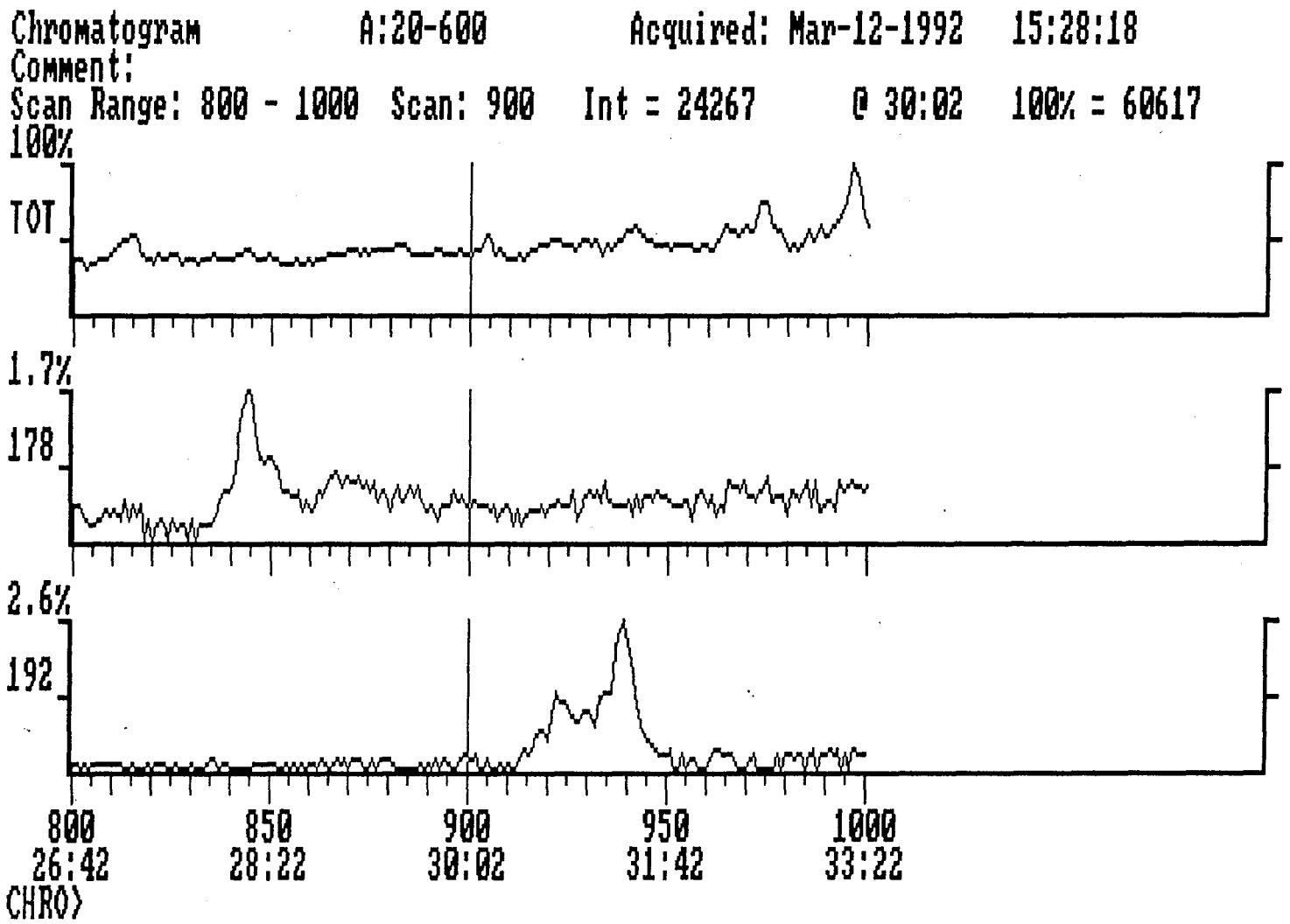

Fig.7.23 The Chromatogram (TOT) With Single Ion Monitoring

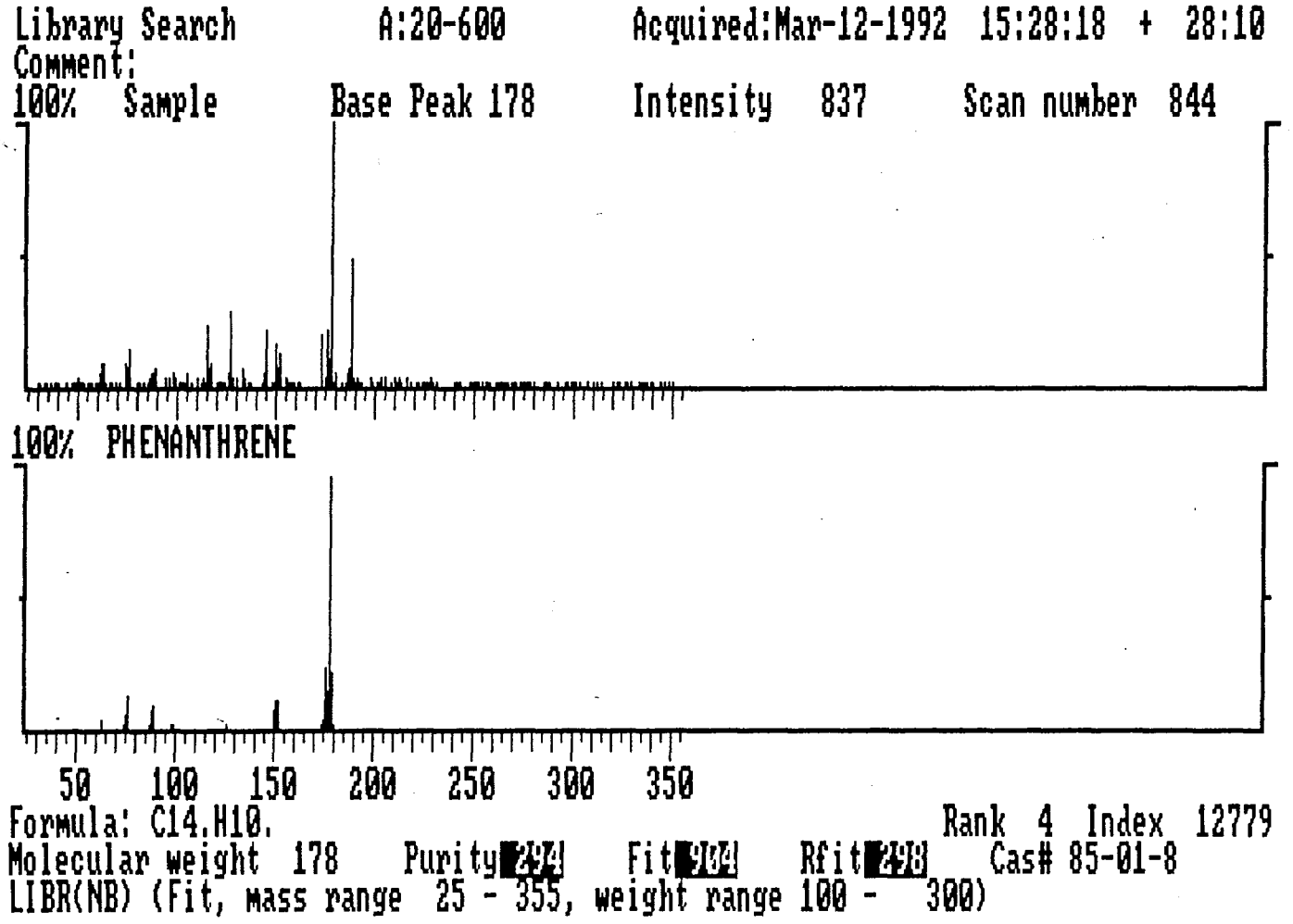

Fig.7.24 Mass Spectra of Phenanthrene

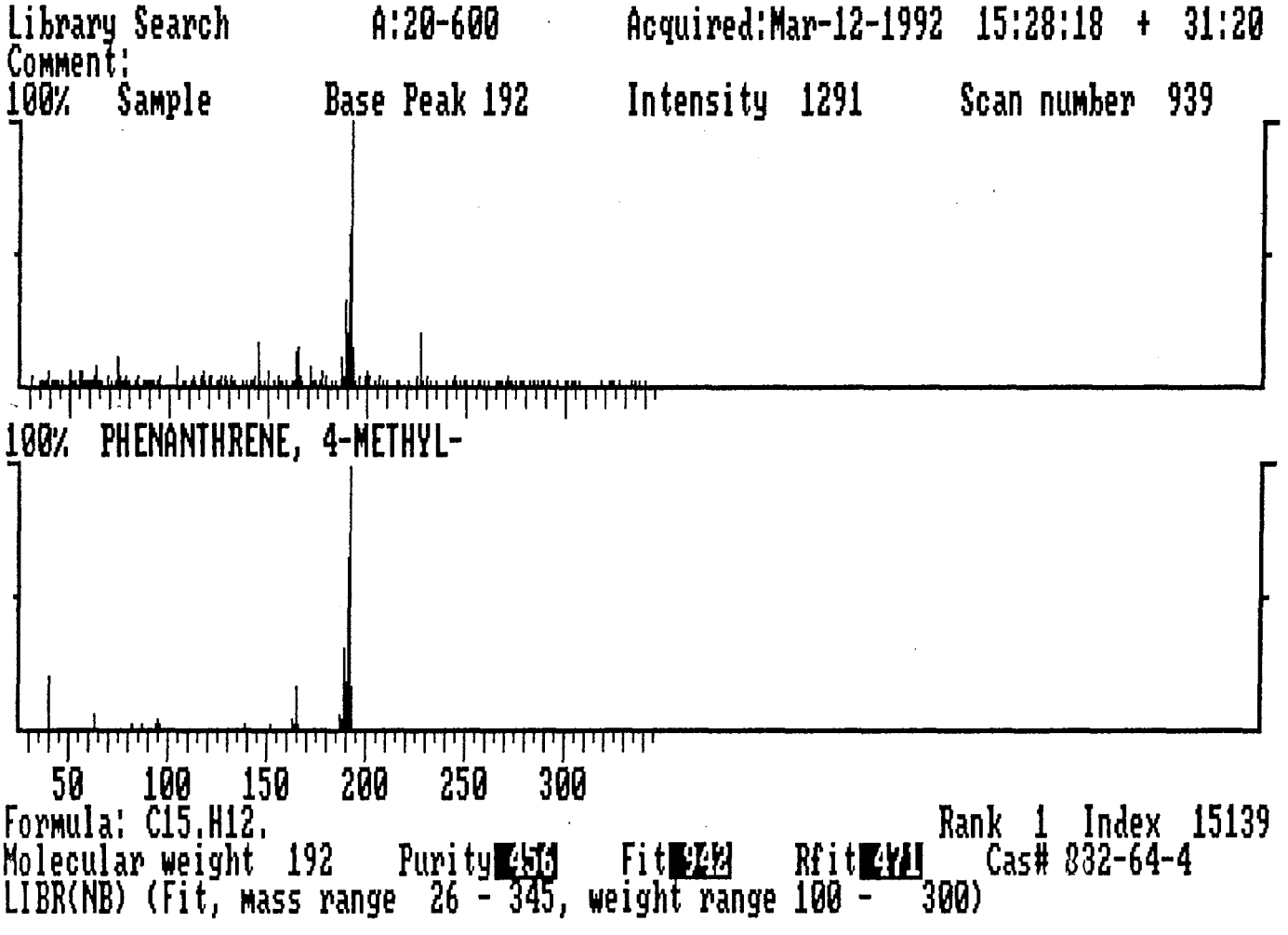

Fig.7.25 Mass Spectra of Methylphenanthrene

Table 7.11 PAH Contents of Wood Oils Derived From Fixed-Bed and Fluidised-Bed Reactors (ppm)

	Oils From Fixed Bed Reactor			Oil From Fluidised-Bed Reactor	Carcinogenicity
PAH 420°C	600°C	720°C	550°C		
1-Naphthalene	160	200	320	380	0
2-2-6 Dimethylnaphthalene	80	150	170	220	0
3-Methylbiphenyl	80	130	230	-	0
4-1-3 Naphthane	190	280	380	400	0
5-2-Methylfluorene	210	240	270	300	0
6-Phenanthrene	250	390	440	500	*
7-2 Phenylnaphthalene	310	450	510	580	0
8-Acenaphthylene	480	720	950	1100	0
9-Methylphenanthrene	220	230	310	400	*
10-Methylfluoranthene	190	220	290	300	+
11-Benzofluorene	360	210	320	400	0
12-Benzo(d)naphtho-(2-1)thiophene	190	160	230	400	0
13-Chrysene	180	280	300	310	+
14-Benzofluoranthene	160	180	210	250	++
15-Benzopyrene	140	160	310	350	++

* - Mutagenic
+ - Carcinogenicity

Table 7.12 PAH Contents of Rice Husks Oils Derived From Fixed-Bed and Fluidised-Bed Reactor (ppm)

	Oils From Fixed Bed Reactor			Oil From Fluidised-Bed Reactor	Carcinogenicity
PAH	420°C	600°C	720°C	550°C	
1- Naphthalene	380	410	520	890	0
2- 2 Methylnaphthalene	-	-	-	1120	0
3- 1 Methylnaphthalene	870	980	1110	1080	0
4-1,7 Dimethylnaphthalene	220	250	380	650	0
5-1,6 Dimethylnaphthalene	280	300	410	700	0
6- 1-3 Naphthalene	330	-	-	-	0
7- Fluorene	-	-	110	130	0
8- 9 Methylfluorene	380	-	-	170	0
9- Phenanthrene	420	500	520	320	*
10- 1 Methylphenanthrene	-	-	-	250	*
11- 3 Methylphenanthrene	180	220	340	-	0
12- Acenaphthylene	160	170	250	-	0
13- Chrysene	-	-	-	250	+
14- Methylchrysene	-	-	-	150	0
15- Pyrene	-	-	-	180	0

Table 7.13 PAH Contents of RDF Oils Derived From Fixed-Bed and Fluidised-Bed Pyrolyser (ppm)

	Oils From Fixed Bed Reactor			Oil From Fluidised-Bed Reactor	Carcinogenicity
PAH	420°C	600°C	720°C	550°C	
1- Naphthalene	100	140	170	300	0
2- Methylnaphthalene	300	400	440	700	0
3- Ethylnaphthalene	240	280	300	450	0
4- Dimethylnaphthalene	230	240	210	400	0
5- Acenaphthene	180	220	230	750	0
6- Methylbiphenyl	140	160	150	600	0
7- Fluorene	250	290	420	825	0
8- Dibenzothiophene	-	-	100	1100	0
9- Phenanthrene	250	300	600	1300	*
10- 2 Phenylnaphthalenes	500	550	650	1000	0
11- Pyrene	400	600	700	850	0
12-Methylphenylnaphthalene	300	400	500	900	0
13- Benzofluorene	400	500	700	900	0
14- Chrysene	-	-	400	650	+
15- Methylchrysene	-	-	-	300	+
16- Pyrene	-	-	-	300	0
17- Picene	-	-	100	300	0

It has been shown that benzopyrene and benzoperylene were the highest molecular weight PAH's detected in wood pyrolysis oils (212). In this research, dibenzoperylene has been identified as the highest molecular weight compound. Acenaphthylene has been detected as the most abundant compound in the wood oil. In addition, 2-methylnaphthalene in the rice husks oil and phenanthrene in RDF oils were identified as the most abundant PAH's.

The presence of 2-methylnaphthalene and some other PAH's in the rice husks oil were reported by Lipska-Quinn et al (38).

Koo et al (107) report the presence of naphthalene, trimethylbenzene and dimethylbenzene in the oil derived from

polyethylene and polystyrene pyrolysed at 500°C, 600°C and 700°C in a quartz retort. Desbene et al (206) also reported wide range aromatics content of bio-oils in their detailed work.

Elliott (27) suggests that just as physical properties of tars can be related to their chemical composition so can the biological activities of the tars.

As well as the short term acute toxicity of these tars is a valid concern, the carcinogenicity of the tars is also a very important issue before recommending the pyrolysis oils as a renewable good fuel or chemicals.

Elliott (27) employed the Ames Assay test in order to measure the tars mutagenicity and mammalian cell initiating activity. During the tests tars derived at low temperatures and high temperatures and also pure benzopyrene were compared and it was found that lower temperature tars did not have important long term toxicity.

The Ames Assay test was performed to estimate the mutagenic activity of vacuum pyrolysis of wood by Menard et al (216). The authors reported naphthalene and anthracene as the predominant aromatic hydrocarbons which showed a low mutagenic activity unless a large quantity of oil is considered.

Under the expression 'cancer', the medical profession now recognises a variety of neoplastic diseases with different symptoms and most likely of different origins. Their common characteristic is uncontrolled cell growth. As indicated earlier, polycyclic aromatic compounds are widespread in the environment (192). Ames et al (231) have shown that polycyclic aromatic compounds metabolites are very

powerful mutagens. A mutagenity test described by Ames et al (232) in a different publication is based on the conversion of polycyclic aromatic compounds by human autopsy or rat-liver homogenates to oxygenated metabolites which are subsequently assayed for mutagenic activity.

In this research, some mutagenic/carcinogenic PAH's such as phenanthrene, methylphenanthrene, chrysene, benzofluoranthene and benzopyrene have been identified. The amounts of PAH's in the bio oils are also significant. The oils derived from the fluidised-bed reactor contain more PAH compounds than the ones derived from the fixed-bed reactor. Pakdel and Roy (212) reported the PAH contents of the bio oils in the range of 0.2 - 11.8 ppm. When the PAH contents of bio oils of this research are investigated it is seen that PAH contents of the wood and rice husks oils are very high.

Petroleum derived fuels also contain PAH. Williams et al (220) have shown that total PAH in diesel fuels from a variety of sources shows a total PAH concentration of between 1.5% and 2.4%. Individual PAH of known biological activity are also present such as methylphenanthrenes, fluoranthene, chrysene, benzo(a)pyrene and benzo(e)pyrene. Longwell (193) has shown that phenanthrene, the methylphenanthrenes and fluoranthene are mutagenic in both bacterial and human cell tests, while methylfluorenes are active in mutagenicity bioassays.

Clearly, the secondary reactions of pyrolysis vapours with a long residence time of higher temperatures cause aromatising in the oils. The formation of aromatic and polyaromatic hydrocarbons via secondary reactions during pyrolysis has been attributed to Diels-

Alder reactions involving cyclisation of alkenes formed from the thermaldegradation of alkanes.

7.3.3.2 Characterisation of PAH Contents of Tyre Derived Oils

The PAH yields of tyre oils derived from the fixed-bed and fluidised-bed pyrolyser are shown in Table 7.14.

Table 7.14 PAH Contents of Tyre Oils Derived From Fixed-Bed and Fluidised-Bed Pyrolyser (ppm)

	Oils From Fixed Bed Reactor			Oil From Fluidised-Bed Reactor	Carcinogenicity
PAH	420°C	600°C	720°C	550°C	
1- Naphthalene	290	380	750	920	0
2- Dimethylnaphthalenes	150	250	420	2200	0
3- Acenaphthane	80	150	160	200	0
4- C-3 naphthalene	360	400	600	1800	0
5- Fluorene	200	250	310	350	0
6- Methylfluorene	380	560	530	-	0
7- Phenanthrene	400	600	1050	1780	0
8- Methylphenanthrenes	300	400	950	1800	*
9- Fluoranthrene	550	600	650	900	*
10- Benzofluorene	200	260	210	300	0
11- Chrysene	Tr	Tr	Tr	80	+
12- Benzofluoranthene	Tr	Tr	Tr	Tr	++
13- Benzopyrene	Tr	Tr	50	100	+

Tr = trace

Figures 7.26 and 7.27 show the pentane-2 and benzene fraction for tyre oil respectively.

As the reactor temperature for both the fixed-bed and fluidised-bed pyrolyser was increased, the total concentration of PAH increased. The formation of PAH in the tyre pyrolysis occurs via Diels-Alder reactions.

As indicated in Chapter 3, the presence of butadiene in the gas yields of scrap tyre pyrolysis shows the production of olefins. According to Cypres and Bettens (123), butadiene would combine with ethylene and form cyclohexane and further aromatics. The concentration of butadiene was however seen to increase as the pyrolysis temperature was increased. This is due to the high composition of butadiene, the removal to form PAH would not affect the overall concentration.

The PAH identified in the tyre pyrolysis oil consists largely of alkylated naphthalenes, fluorenes and phenanthrenes. Some of the PAH found in the oil have been shown to be carcinogenic and/or mutagenic. According to Lee et al (192), chrysene, benzofluoranthene, benzo(e)pyrene and benzo(a)pyrene give positive results in carcinogenicity tests.

Elliott (27) also reported that benzopyrene was tested with the Ames Assay test and found to be carcinogenic. This is also reported by Longwell (193) as mentioned before. These biologically active PAH are found in the tyre pyrolysis oils. From these it can be concluded that the pyrolysis oils may be a health hazard.

In this research, oils derived from the fluidised-bed pyrolyser contain more PAH than the oils from the fixed-bed pyrolyser. The residence time of vapours in the fluidised-bed reactor which included the hot freeboard and cyclone was between 10-15 seconds whilst the residence time in the fixed-bed reactor was 2-3 seconds. Therefore, high PAH concentrations have been observed in the fluidised-bed pyrolyser caused by long residence time. But, in the fixed-bed pyrolyser it is seen that increased temperature gives high PAH.

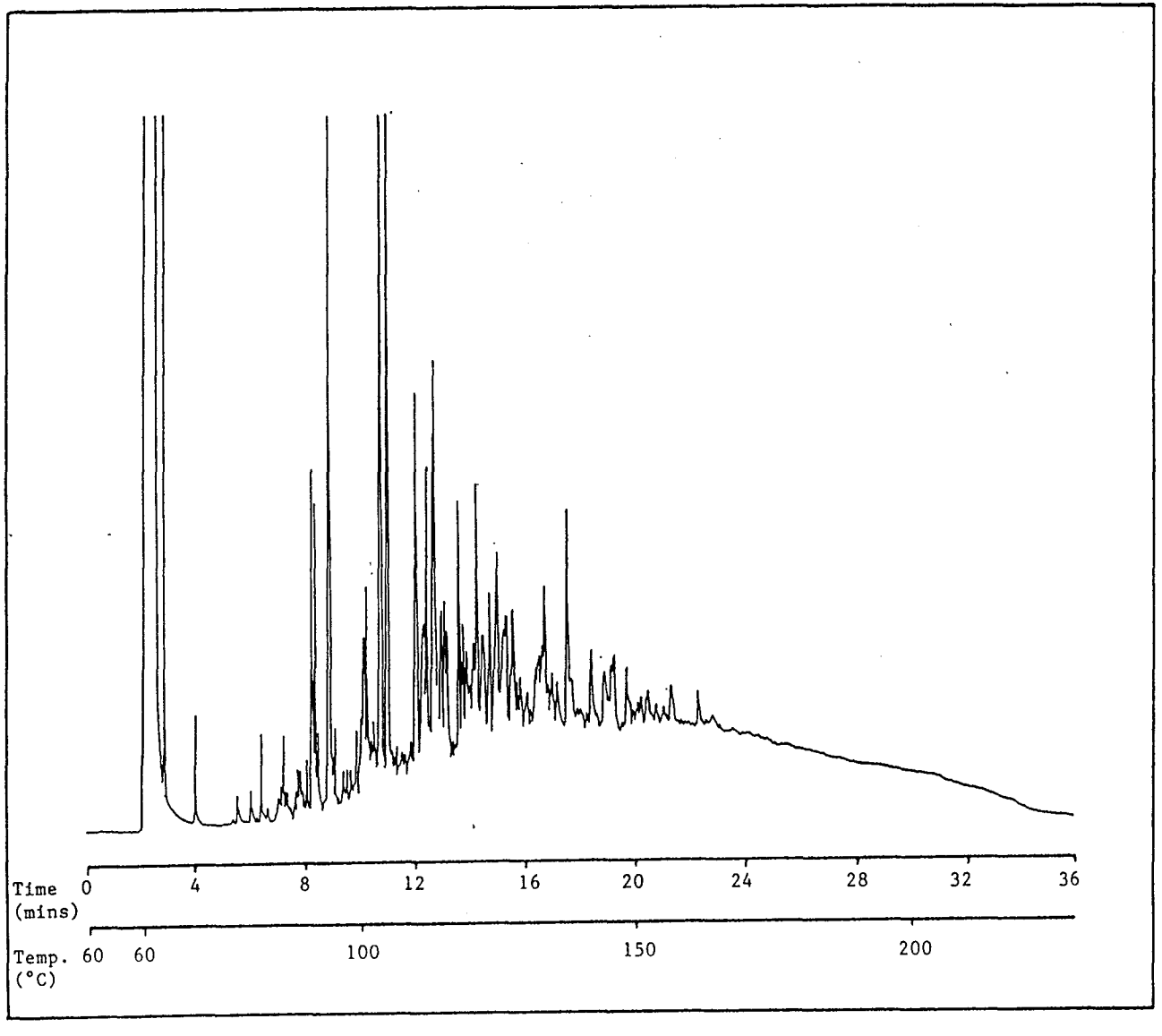

Fig.7.26 The GC of Pentane-2 Fraction of Tyre Oil

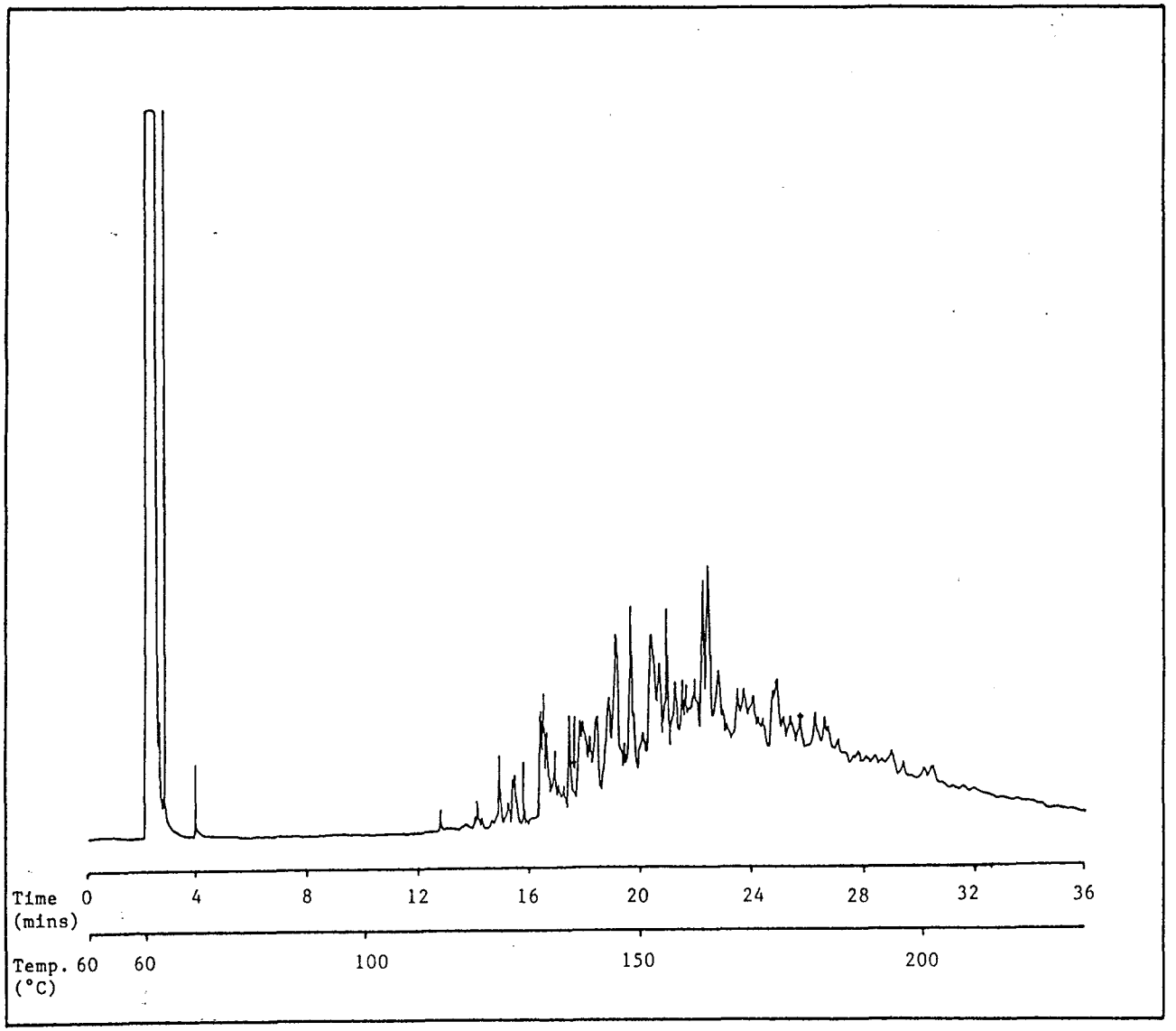

Fig.7.27 The GC of the Benzene Fraction of Tyre Oil

Therefore, the formation of PAH by Diels-Alder mechanism is influenced both by increased temperature and long residence time.

The process conditions affect the PAH composition of the tyre derived oils very significantly. Williams and Taylor (210) tested process temperatures and different residence times and they concluded that the pyrolysis process conditions for the thermaldegradation of scrap automotive tyres can be optimised to either limit or enhance the production of PAH.

The presence of PAH in the tyre oil as a potential fuel also has further significance in that the increased concentrations of PAH in the fuel may lead to increases in the emissions when the fuel is combusted.

Guerin (218) and Herlan (219) have found that the PAH in petroleum fuels contain significant amounts of PAH compounds. The PAH in diesel particulate emissions found in the organic fraction adsorbed to the soot have been shown to be derived from diesel fuel as an unburnt fuel fraction (220, 221).

Herlan (219) after combusting fuel has identified a wide range of PAH emissions in the soot and he concluded that the PAH emissions found on the soot were derived largely from the PAH of the fuel.

As a result, the presence of PAH in the tyre pyrolysis oils may lead to PAH in the combustion emissions depending on the PAH concentration of fuel.

This conclusion may limit the use of tyre pyrolysis oil as a directly combusted fuel without further treatments in order to improve the fuel properties of the oil derived from scrap tyre.

7.3.4 Polycyclic Aromatic Hydrocarbons

7.3.4.1 Formation of Polycyclic Aromatic Compounds Via the Diels-Alder Mechanism

The chemical fractionation of the pyrolytic oils derived from biomass in the form of wood, rice husks and RDF and scrap tyres, all show a similar trend of increasing temperatures of pyrolysis producing a decrease in aliphatic concentrations and corresponding increase in light and heavy aromatics. This trend has also been confirmed by analysis of the oils using FT-ir. In addition, the analysis of the biomass and tyre oils for PAH also show that increasing pyrolysis temperature and also longer residence times increase the concentration of PAH.

The pyrolysis of alkanes to produce olefins which are subsequently aromatised by Diels-Alder type reactions to form mono and polyaromatic species is well known (214, 217).

Breadel (213) reported that aromatic hydrocarbons are formed from light olefins by the successive thermal cracking of paraffins at 700°C for a 2 second contact time or possibly formed at lower temperatures with a longer contact time.

Fairburn et al (223) pyrolysed n-hexadecane and they suggested that paraffin pyrolysis proceeds via a free radical chain mechanism. According to Fairburn et al (223), at conversions less than 10%, n-hexadecane selectively cracks to form the primary products.

$$n\text{-}C_{16}\text{-}H_{34} \longrightarrow C_2\text{-}C_{15}\ 1\text{-olefins} + C_1\text{-}C_2\ \text{paraffins}$$

As the conversion of n-hexadecane was increased by an increase in temperature and/or reaction time, secondary reactions began to occur. Firstly, the unstable heavier 1-olefins decompose into the lighter 1-olefins, although not significantly until roughly 40% conversion of the n-hexadecane.

$$C_5\text{-}C_{15} \text{ olefins} \longrightarrow C_2\text{-}C_4 \text{ olefins} + C_1\text{-}C_3 \text{ paraffins}$$

At conversion levels greater than approximately 40%, C_4, C_6 and 1-olefins start to dehydrogenate to form diolefins such as 1.3 butadiene.

$$C_4\text{-}C_6 \text{ 1-olefins} \longrightarrow C_4\text{-}C_6 \text{ diolefins} + H_2$$

The butadiene then immediately combines with available ethylene/propylene to form simple aromatics such as benzene, toluene, ethylbenzene and styrene. This reaction proceeds according to the Diels-Alder mechanism with accompanying dehydrogenation; meanwhile, cyclic olefins are formed as intermediates.

$$C_2, C_3 \text{ olefins} + C_4H_6 \longrightarrow \text{Simple aromatics} + H_2$$

Once the conversion of n-hexadecane exceeds approximately 85% propane and propylene typically decompose to form ethylene, methylene and hydrogen.

Concurrently, available butadiene combines with the prevalent simple aromatics to form polyaromatics through a Diels-Alder mechanism. For example, naphthalene is formed through addition of butadiene to benzene.

$$C_4 + H_6 + \text{Simple aromatics} \longrightarrow \text{polyaromatics} + H_2$$

If the pyrolysis severity increases further, acetylene is produced via dehydrogenation of ethylene. Naphthalene combines with available butadiene to form three ring polyaromatics such as phenanthrene and anthracene.

Cypres and Bettens (123) suggest that the production of ethene, propene and 1,3 butadiene from scrap tyre pyrolysis will result in the formation of cyclic olefins. These reactions may be illustrated as

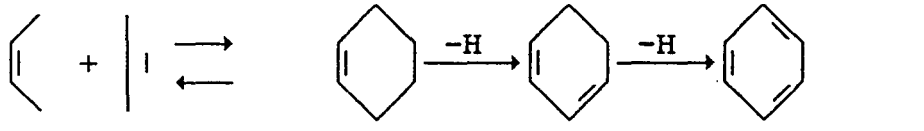

ethylene benzene

1.3 butadiene cyclohexene

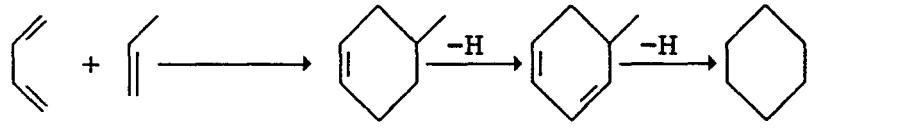

toluene

4 methyl-1-cyclohexene

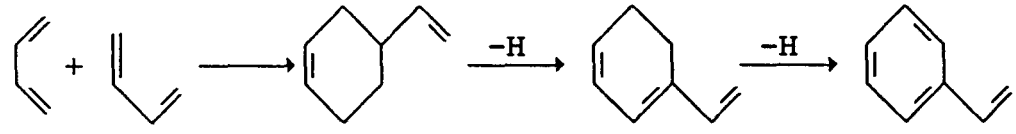

alkyl aromatics

4 vinyl-1-cyclohexene

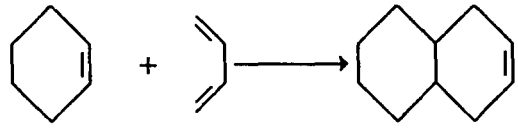

cyclohexane butadiene naphthalene

Dehydrogenation of the cyclic olefinic compounds with six carbon atoms occurs to produce single ring aromatic compounds and as a result of subsequent associated reactions may lead to the formation of PAH such as naphthalene and phenanthrene.

It was also suggested by Ren et al (224) that small aromatic ring compounds tend to condense to form larger ring compounds but, larger ring compounds have the tendency to decompose to smaller ring compounds. For example, benzene with short alkyl chains can be effectively de-alkylated to benzene or toluene, but benzenes with long chain alkyl chains tend to cyclise to diphenylnaphthalene or phenanthrene at high temperatures.

A number of researchers (107, 123, 214, 215) suggest that the Diels-Alder reaction is a reaction scheme for the formation of PAH from the pyrolysis of municipal solid waste and scrap tyres.

According to Cypres and Bettens (123), the pyrolysis of rubber leads to the production of ethylene, propene and 1,3 butadiene. These induce aromatisation as a result of Diels-Alder reactions.

Diebold (215) has shown that for the pyrolysis of solid wastes above 700°C, the primary pyrolysis products begin to immediately polymerise to form secondary products such as benzene and toluene as well as multiple ring aromatic tars.

Koo et al (107) reported that for pyrolysis of plastics, aromatic hydrocarbons are formed from light olefins by the successive thermal cracking of paraffins at 700°C for a 2 second contact time or possibly formed at lower temperatures with a longer contact time by Diels-Alder reaction.

CHAPTER 8

SUMMARY AND CONCLUSIONS

It is the aim of this chapter to summarise the findings of the studies of wood, rice husks, RDF and scrap tyre pyrolysis in the fixed-bed, fluidised-bed and thermogravimetric pyrolysers and scrap tyre pyrolysis in a commercial scale pyrolyser.

Full discussion of results is included in the relevant chapters, therefore, only brief conclusions will be presented here along with suggestions for further work.

8.1 Fixed-Bed Reactor Pyrolysis

8.1.1 Wood and Rice Husks

- Pyrolysis of wood and rice husks have shown a significant increase in liquid and gas yield and a decrease in char yield as either the heating rate and temperature was increased. It was also observed that after 720°C in wood pyrolysis the liquid yield decreased as it was accompanied by an increased gas yield.

- In wood pyrolysis, smaller particles yielded, more liquid and less char

- Detailed analysis of the gas compositions from the pyrolysis of wood and rice husks revealed the main gases were hydrogen, carbon dioxide, carbon monoxide, methane, ethane, propane and propene. The maximum evolution of each gas was dependent on temperature and heating rate.

- The calorific values of oils and gases increased as the heating rate was increased.

- The surface areas of chars increased with increased temperature and heating rate. The calorific values of chars decreased as the heating rate was increased.

After pyrolysis of two biomass samples, it can be concluded that pyrolysis of biomass waste is a promising technique in the reutilisation of waste biomass. The production of liquid fuels from biomass has a number of advantages over other energy recovery systems from biomass. The oils have a high energy density. They can be used directly or upgraded catalytically and/or added to other liquid fuels. They can easily be transported and stored. In addition, the char produced by pyrolysis from biomass can be used as a solid fuel or as char/water or char/oil slurry liquid fuels. The gas can also be used to provide the energy requirements of the pyrolysis plant.

8.1.2 Refuse Derived Fuel

- The fixed-bed reactor pyrolysis of RDF showed that higher heating rates and temperatures produced the highest conversion of the RDF to oil.

- Also, the elemental analysis of the oils revealed that the oils derived from refuse derived fuel were highly oxygenated and they are not an economic viability when compared to other energy from waste schemes due to the very inhomogeneous nature of the raw material.

- The gas yields may be considered to have the potential to heat the pyrolysis system.

- Chars may be considered as fuel or carbon black, but still need more work since in RDF and also municipal waste pyrolysis, the inhomogeneity causes problems of high ash and variable C.V.

8.1.3 Scrap Tyre

- Pyrolysis of tyre waste has shown significant recoveries of hydrocarbon liquid, solid char and gases. The liquid and gas yields increase with temperature and heating rate.

- The gases evolved were mainly hydrogen, carbon dioxide, carbon monoxide, methane, ethane and butadiene and with lower concentrations of other hydrocarbon gases.

- The liquids, gases and chars had a significant calorific value.

- The surface area of chars increased with the temperature and heating rate. It was also observed that further thermal treatments would improve the surface areas of chars.

8.2 Fluidised-Bed Pyrolysis

8.2.1 Fast Pyrolysis of Wood and Rice Husks

- The fast pyrolysis of wood and rice husks has shown that the gas yield increased and the liquid and char yield decreased as the temperature increased from 400°C to 550°C.

- The oils from the fluidised-bed showed an increase in calorific value compared to the static-batch reactor oils. The oils could be used directly as fuels although they are clearly highly oxygenated.

- The comparison of the distillation range by gas chromatography simulated distillation for the derived oils showed that the oil from the fixed-bed and fluidised-bed reactors were similar to the distillation range of kerosene.

8.2.2 Fast Pyrolysis of RDF

- Fast pyrolysis of RDF has shown that the char yield decreased and gas yield increased. The liquid yield did not show a significant change with the increased temperature.

- Increased temperature changed the properties of the oil which showed a lower viscosity compared to the oil from the fixed-bed pyrolyser.

- The calorific values of the oils increased with the increased temperature of pyrolysis.

8.2.3 Fast Pyrolysis of Scrap Tyre

- In the rapid pyrolysis of scrap tyres, it was found that the char and liquid yields decreased with the increased temperature. Conversely, gas yields increased with the increased temperature.

- The oil and char has quite a high calorific value.

8.3 Commercial Scale Pyrolysis

8.3.1 Scrap Tyre

- The commercial scale scrap tyre pyrolysis has shown that as the pyrolysis temperature is increased from 700°C to 950°C, the amount of char yield decreased from 59.4% to 46.8%. The oil yield also slightly decreased from a value of 27.3% at 950°C.

- The fuel properties tests of the oils have shown that the carbon residue of the oils increased in percentage with increased temperature of pyrolysis. The viscosity of the tyre oils was found between those of a diesel fuel and a light fuel oil. The API gravities and relative densities of oils were found between those of a light fuel oil and heavy fuel oil.

- The flash point of the tyre derived oils showed an increase with increasing pyrolysis temperature. The flash points are low when compared to petroleum refined fuels. The calorific values and sulphur contents of the oils were found to be similar to those of diesel fuel and light fuel oil. The economic feasibility report showed that the system, even for the worst case is still profitable. An economic appraisal for tyre pyrolysis depends entirely on the market for the products of the pyrolysis process.

- The work on the commercial scale pyrolysis of tyres showed broadly similar trends to those found in the bench scale

fixed-bed work reported in this thesis. Consequently, bench scale experiments to test a variety of pyrolysis parameters are applicable and can be scaled up to the commercial scale at much lower throughputs and consequently cost.

8.4 Thermogravimetric Analysis

8.4.1 Thermogravimetric Analysis of Biomass

- The TGA of rice husk and wood showed two main regimes of weight loss. The lower temperature regime could be correlated with the decomposition of hemicellulose and initial stages of cellulose decomposition. Lignin thermaldecomposition occurred throughout the temperature range of pyrolysis.

- TGA and DTG curves were used to estimate the amounts of major components of wood and rice husks. The hemicellulose, cellulose and lignin components of wood and rice husks were found to be 24.5%, 40.5%, 27.5% and 35%, 40.4% and 18.6% respectively.

- Activation energies for the decomposition of wood, rice husks, hemicellulose, lignin and cellulose were calculated assuming a first order rate of reaction and showed a decrease with increasing heating rate.

- As the heating rate was increased from 5°C min^{-1} to 80°C min^{-1} there was a shift to higher temperature values for the maximum rate of weight loss for the TGA.

- Comparison of the decomposition of cellulose in microcrystallise from and as Whatman No. 1 filter paper showed that different values of activation energy were produced, due mainly to the difference in crystalline form.

- The DTG traces for model compound saccharides typical of those found in or derived from pyrolysis of biomass has a similarity to wood and rice husks, showing two areas of weight loss, whilst cellulose and hemicellulose show a single DTG peak.

8.4.2 Thermogravimetric Analysis of RDF

- Thermogravimetric analysis of the components of RDF showed that the lower temperature thermaldegradation of RDF can be attributed to cellulosic waste and the higher temperature degradation to plastic waste.

- The individual components activation energies were found to be higher than RDF activation energies.

- RDF pyrolysis in the thermogravimetric pyrolyser is not affected greatly by the increased rate of heating and from this it can be concluded that for small particle size reaction is not heat transfer controlled.

8.4.3 Thermogravimetric Analysis of Scrap Tyre

- The TGA of scrap tyre, natural rubber (NR), butadiene rubber (BR) and styrene-butadiene rubber (SBR) has shown that the lower temperature thermaldegradation of scrap tyre can be attributed to NR and the higher temperature to butadiene

rubbers. It can be said that TGA is a very useful tool to estimate percentages of its components.

- The activation energies of scrap tyre, NR, BR, SBR and three different blend rubbers decreased with the increased heating rate.

The thermogravimetric analysis of biomass and waste materials showed that the thermal analysis can be used to determine the thermaldegradation pathways of the samples since the thermogravimetric analyser can provide the same experimental conditions to that of a fixed-bed reactor.

8.5 Characterisation of the Pyrolytic Oils

8.5.1 Functional Group Analysis by FT-ir

8.5.1.1 Pyrolytic Oils Derived from Fixed-Bed Reactor

8.5.1.1.1 Wood, Rice Husks and RDF Oils

- The FT-ir analysis of pyrolytic oils showed that biomass derived oils contain alcohols, acids, aldehydes, alkanes, alkenes and aromatics.

- The FT-ir spectra showed that the alkane and alkene compounds decrease and aromatic compounds increase as the temperature increased.

8.5.1.1.2 Scrap Tyre Oils

- The FT-ir spectra of scrap tyre oils showed the presence of alkanes, alkenes, aromatics, aldehydes, ketones, amids and amins.

- The alkane and alkene groups showed a decrease and aromatics showed an increase as the temperature increased as a result of Diels-Alder reactions.

8.5.1.2 Pyrolytic Oils Derived from Fluidised-Bed Reactor

- The pyrolytic oils derived from wood, rice husks, RDF and scrap tyre pyrolysis in the fluidised-bed reactor showed that the aromatic compounds increase and the alkenes and alkanes decrease as the temperature increased from 400°C to 500°C.

- When the formation of aromatics were compared with the fixed-bed derived oils for wood, rice husks and RDF, it was seen that the results were similar. The scrap tyre oils derived from the fluidised-bed reactor consist of very high concentrations of aromatic compounds.

8.5.2 Characterisation of Polycyclic Aromatic Hydrocarbons

8.5.2.1 Chemical Class Fractionation

8.5.2.1.1 Oil Derived from Biomass and RDF

- For wood, rice husks and RDF, chemical class fractionation showed that the aliphatic fraction decreased, light and heavy aromatics increased as the temperature increased.

- Similarly, for the oils derived from the fluidised-bed reactor, the aliphatic fraction decreased, light and heavy aromatic fractions increased as the temperature increased.

8.5.2.1.2 Oils Derived from Scrap Tyre

- The aliphatic fraction for the scrap tyre oil derived from both fixed-bed and fluidised-bed reactors, showed a decrease whilst light and heavy aromatic fractions increased as the temperature increased.

8.5.2.2 Characterisation of PAH Contents

8.5.2.2.1 Bio-Oils (From Wood, Rice Husks and RDF)

- The GC-MS and GC spectra of the wood, rice husks and RDF showed that PAH increased with the increased pyrolysis temperature. Acenophthylene has been detected as the most abundant compound in the wood oil. Also, 2-methylnaphthalene in the rice husks oil and phenanthrene in RDF oils were identified as the most abundant PAH's.

- The oils derived from the fluidised-bed reactor were found to contain higher concentrations of PAH compounds than the oils derived from the fixed-bed reactor.

- In the biomass and RDF derived oils, some mutagenic/carcinogenic PAH's such as phenanthrene, methylphenanthrene, chrysene, benzofuoranthene and benzopyrene have been identified.

8.5.2.2.2 Scrap Tyre Derived Oils

- As the reactor temperature for both the fixed-bed and the fluidised-bed pyrolyser was increased, the total concentration of PAH increased in the tyre derived pyrolytic oils.

- The alhylated naphthalenes, fluorenes and phenanthrenes were identified in tyre pyrolysis oils. Some of the PAH found in the oil have been shown to be carcinogenic and/or mutagenic.

- The formation of PAH was increased with increasing temperature and residence time and the mechanism of formation was attributed to a Diels-Alder type.

- The process conditions were found to significantly effect the PAH composition of the tyre oils.

- The results showed that the use of tyre pyrolysis oils may be limited without further improvements of the fuel properties of the oil.

8.6 Suggestions For Future Work

- After pyrolysis, the chars can be reactivated in order to improve their carbon black properties. And also, char/water, char/oil slurry systems can be tested as an alternative fuel source.

- The pyrolysis liquids can be upgraded with advanced catalytic cracking.

- A mathematical model should be developed for pyrolysis of waste materials in both fixed-bed and fluidised-bed systems.

- Thermaldecomposition characteristics of fast and flash pyrolysis should be investigated.

- Different chemical fractions of the pyrolytic oils such as pentane-1, pentane-2 and ethylacetate fractions should be characterised by using GC and GC/MS.

REFERENCES

1. Colombo, U. "Energy and the Future of Biomass" in "Biomass for Energy and Industry" 5th E.C. Conference 9-13th October 1989. Grassi, G., Gosse, G., Dos Santos, C., (eds) vol 1 21-37.

2. Clayton, P., Coleman, P., Leonard, A., Loader, A., Marlowe, I., Mitchell, D., Richardson, S. and Scott, D. Review of Municipal Solid Waste Incineration in the UK. Warren Spring Laboratory. Report No. LR 776, Department of Trade and Industry. H.M. Government HMSO, London, 1991.

3. Tillmann, D.A. Energy From Wastes: An Overview of Present Technology and Programs. "Fuels From Waste". Anderson, L.L. and Tilmann, D.A. (eds). 1977. 17-39.

4. Kruester, J.L. Thermal Systems for Conversion of MSW Pyrolytic Conversion: A Technology Status Report ANL/CNSV-TM-120 vol 5. DE 84 003664, 1983 5th June. 1-86.

5. Agrawal, R.K. "Compositional Analysis of Solid Waste and Refuse Derived Fuels by Thermogravimetry in "Compositional Analysis by Thermogravimetry" Earnst, C.M. (ed) 1987. 259-271.

6. Mallya, N., Helt, J.E. Effects of Feedstock Components on Municipal Solid Waste Pyrolysis in "Resaearch in Thermochemical Biomass Conversion" Bridgwater, A.V. and Kruester, J.C. (eds) 1988. 111-126.

7. Rampling, T.W., Hickey, T.J. "The Laboratory Characterisation of Refuse Derived Fuel". Report to United Kingdom Atomic Energy Authority acting on behalf of the Secretary of State for Energy. Report No. ETSU-B-1161 1988.

8. Grassi, G. "The Opening Speech" 6th European Conference in Biomass for Energy, Industry and Environment. 1990. 27-29.

9. Anderson, L.L. A Wealth of Waste; A Shortage of Energy in "Fuels from Waste" Anderson, L.L. and Tilmann, D.A. (eds). 1977. 1-16.

10. Strub, A. The Commission of the European Communities R & D Programme "Energy from Biomass" (Keynote paper) in "Thermochemical Processing of Biomass". Bridgwater, A.V. (ed). 1984. 1-10.

11. Roy, C. "Vacuum Pyrolysis of Scrap Tyres". United States Patent. Patent No. 4, 740, 270. Date of Patent April 26th 1988.

12. Roy, C., Labreque, B. and De Caumia, B. "Recycling of Scrap Tyres to Oil and Carbon Black by Vacuum Pyrolysis". Resources, Conservation and Recycling. 1990. 4, 203-213.

13. Reed, T.B. Survey of Pyroconversion Processes for Biomass. Biochemical Engineering: Renewable Sources of Energy and Chemical Feedstocks. AICHE Symp. Ser. 1988. 181, vol 74. 38-46.

14. Grassi, G. "Definition Din Programme Biomasse" in Biomass for Energy and Industry" Proc. 5th E.C. Conference. Grassi, G., Gosse, G., Dos Santos, G. (eds). 1989. Vol 1 39-48.

15. Beenackers, A.A., Bridgwater, A.V. "Gasification and Pyrolysis of Biomass in Europe" in "Pyrolysis and Gasification". Ferrero, G.C., Maniatis, K., Buekens, A., Bridgwater, A.V. 1989. 125-157.

16. Leben news. Edited by Coombs, D. Commission of the European Communities and CPL Scientific Ltd. October 1990. No. 1. 10-11.

17. Bridgwater, A.V. "Rapporteur's Report on Pyrolysis, Gasification and Liquefaction Techniques" in proc. "Pyrolysis and Gasification ". Ferrero, G.C., Maniatis, K., Buekens, A. and Bridgwater, A.V. (eds). 1989. 195-198.

18. Bridgwater, A.V. and Bridge, S.A. "A Review of Biomass Pyrolysis and Pyrolysis Techniques" in "Biomass Pyrolysis Liquids Upgrading and Utilisation". Bridgwater, A.V. and Grassi, G. (eds). 1991. 11-92.

19. Hiraoko, M. "Overview of Pyrolysis Thermal Gasification and Liquefaction Processes in Japan" in "Thermal Conversion of Solid Wastes and Biomass". Jones, J.L. and Radding, S.B. (eds). ACS symp ser. 130. 1980. 493-507.

20. Buekens, A.G. and Schoeters, D.G. "Basic Principles of Waste Pyrolysis and Review of European Processes" in "Thermal Conversion of Solid Wastes and Biomass". Jones, J.L. and Radding, S.B. (eds). ACS symp ser. 130. 1980. 397-421.

21. Stiles, H.N. "Secondary Reactions of Pyrolytic Tars". PhD Dissertation. Department of Chemical Engineering and Chemical Technology. Imperial College, London. 1986.

22. Soltes, J. "Of Biomass, Pyrolysis and Liquids These Form". ACS symp ser. "Pyrolysis Oil From Biomass Producing, Analysing and Upgrading". Edited by Soltes, J. and Milne, T.A. 1988. 1-7.

23. Capart, A., Elamin, A., Ammar, S. and Gelus, M. "A Survey of Biomass Liquefaction Processes" in "Pyrolysis and Gasification". Ferrero, G.C., Maniatis, K., Buekens, A.G. and Bridgwater, A.V. 1989. 158-168.

24. Zaror, C.A.Z. "Studies of the Pyrolysis of Wood at Low Temperatures". PhD Thesis Dissertation. Department of Chemical Engineering and Chemical Technology. Imperial College, London. 1982.

25. Graham, R.G., Bergougnou, N.A. and Overend, R.P. "Fast Pyrolysis of Biomass" (review) Journal of Analytical and Applied Pyrolysis 1986. 6. 95-135.

26. Elliott, D.C. Analysis and Comparison of Biomass Pyrolysis/Gasification Condensates Final Report. PNL 5943. Pacific Northwest Laboratory. Richland, W.A. 1986.

27. Elliott, D.C. "Relation of Reaction Time and Temperature of Chemical Composition of Pyrolysis Oils" in ACS sym ser proc "Pyrolysis Oils From Biomass". Soltes, J. and Milne, T.A. 1988. 55-65.

28. Diebold, J. In Proc. Specialists Workshop on Fast Pyrolysis of Biomass. SERI-CP-622-1096. Solar Energy Institute. Golden, C.O. 1980. P 3.

29. Evans, P.J., Milne, T.A. Fundamental Pyrolysis Studies: Final Report 1st October 1980. December 1985. SERI/PR-234-3026. Solar Energy Research Institute. Golden, C.O. 1986.

30. Shafizadeh, F. Journal of Analytical and Appl. Pyrolysis. 1982. 13, 283-305.

31. Lipinsky, E.S. "Pre-treatment of Biomass for Thermochemical Biomass Conversion" in "Fundamentals of Thermochemical Biomass Conversion". Overend, R.P., Milne, T.A. and Mudge, L.K. (eds). 1982. 77-87.

32. Deglise, X., Lede, J. Inst. Chem. Eng. 1982. 22-4 631-645.

33. Goldstein, I.S. AI Che. Symp. Ser. No. 177. 1978. 74-111.

34. Kanury, M.A. and Blackshear, Jr. P.L. Some Considerations Pertaining to the Problem of Wood Burning. "Combustion Science and Technology". 1970. 1, 339-355.

35. SJostrom, E. Wood Chemistry Fundamentals and Applications. 1981. Academic Press.

36. Young, R.A. and Davis, J.L. Thermochemical Fractionation and Liquefaction of Wood" in "Fundamentals of Thermochemical Biomass Conversion". Overend, R.P., Milne, T.A. and Mudge, L.K. 1985. 121-143.

37. Hills, W.E. Wood and Biomass Ultrastructure in "Fundamentals of Thermochemical Biomass Conversion". edited by Overend, R.P., Milne, T.A. and Mudge, L.K. 1985. 13-34.

38. Lipska-Quinn, A.E., Zeronian, S.H. and McGee, K.M. "Thermaldegradation of Rice Straw and Its Components" in "Fundamentals of Thermochemical Biomass Conversion". Overend, R.P., Milne, T.A. and Mudge, L.K. (eds). 1985. 453-471.

39. Ferrero, A.F. "Systems for Harvesting and Treatment of Rice Straw" in "Biomass for Energy, Industry and Environment". Grassi, G., Collina, A. and Zibetta, H. (eds). 6th European Conference. 1992. 329-335.

40. Grappi, F., Parrini, F. and Delbo, A. "Rice Straw and Co-generation Plant in Cascina Laura (Novara-Italy)" in "Biomass for Energy, Industry and Environment". 6th European Conference. Grassi, G., Collina, A. and Zibetta, H. (eds). Elsevier. App. Sci. 1992. 1222-1227.

41. Jenkins, B.M. and Goss, J.R. Performance of a Small Spark-Ignited Internal Combustion Engine on Producer Gas From Rice Hulls. "Biomass for Energy, Industry and Environment". 6th European Conference. 1992. 1057-1069.

42. Hartiniati, Soemardjo, A. and Youvial, M. "Performance of a Plot Scale Fuidised-bed Gasifier Fueled by Rice Husks" in "Pyrolysis and Gasification". Ferrero, G.L., Maniatis, K., Buekens, A. and Bridgwater, A.V. (eds). 1989. 257-263.

43. Susanto, H. and Reksowardojo, S. "A National Program on Implementation of Biomass Gasification Process in Indonesia. Progress and Economic Evolution" in "Pyrolysis and Gasification". Ferrero, G.L., Maniatis, K., Buekens, A. and Bridgwater, A.V. (eds). Elsevier App. Sci. (Publishers). 1989. 282-289.

44. Manurung, R. "A Reaction Engineering Model for Down Draft Rice Husk Gasification" in "Biomass for Energy, Industry and Evnvironment". 6th European Conference. Grassi, G., Collina, A., and Zibetta, H. (eds). Elsevier App. Sci. 1992. 816-821.

45. Maniatis, K. and Buekens, A. Fast Pyrolysis of Biomass in "Research in Thermochemical Biomass Conversion". Bridgwater, A.V. and Kuester, J.L. (eds). Elsevier Sci. Pub. 1988. 179-191.

46. Theander, O. Cellulose, Hemicellulose and Extractives in "Fundamentals of Thermochemical Biomass Conversion". Overend, R.P., Milne, T.A. and Mudge, L.K. (eds). 1985. 35-61.

47. Antal, M.J. Jr. Biomass Pyrolysis: A Review of the Literature Part 1. Carbohydrate Pyrolysis". Advance in Solar Energy. 1983. 61-111.

48. Shafizadeh, F. Chemistry of Pyrolysis and Combustion of Wood" in " Progress in Biomass Conversion". Vol 3. Sarkanen, K.V., Tillman, B.A. and Jahn, E.C. (eds). Academic Press. 1982. 51-76.

49. Shafizadeh, F. "Fuels From Wood Waste" in "Fuels From Waste". Anderson, L.L. and Tillman, D.D. (eds). Academic Press. 1977. 141-159.

50. Mitchell, C.P. and Pearce, M.L. "Feedstocks and Characteristics (Keynote Paper)" in "Thermochemical Processing of Biomass". Bridgwater, A.V. (ed). 1984. 53-67.

51. Train, P.M. and Klein, M.T. "Chemical Modelling of Lignin. A Monte Carlo Simulation of Its Structure and Catalytic Liquefaction in Pyrolysis Oils From Biomass Producing, Analysing and Upgrading". ACS Symposium Series. No. 376. Soltes, D. and Milne, T.A. (eds). 1988. 241-263.

52. Glasser, W.G. Lignin in "Fundamentals of Thermochemical Biomass Conversion". Overend, R.P., Milne, T.A. and Mudge, L.K. (eds). 1985. 61-76.

53. Powels, A.D., Tom, A., Eijkej, G.B. and Boon, J.J. Journal of Analy. and Appl. Pyrolysis. 1987. 11, 1417-1436.

54. Smith, E.L. Reactors: Some Design Perspectives (Keynote Paper) in "Thermochemical Processing of Biomass". Bridgwater, A.V. (ed). 1984. 255-266.

55. Schuchardt, U. and Goncalves, A.R. "Production of Chemical and Pharmeceutical Feedstocks From Hydrolytic Eucalyptus Lignin" in "Biomass For Energy and Industry" V.2. Grassi, G., Gosse, G. and Santos, G. 1990. 2897-2902.

56. Avni, E., Davoudzadeh, F. and Laughlin, W.R. "Flash Pyroysis of Lignin" in "Fundamentals of Thermochemical Biomass Conversion". Overend, R.P., Milne, T.A. and Mudge, L.K. (eds). 1985. 329-343.

57. Shafizadeh, F., Cochran, T.G. and Sakai, Y. "Application of Pyrolytic Methods for the Saccharification of Cellulose". AICHE Symp. Ser. "Advances in the Utilisation and Processing of Forest Products". No. 184. vol. 75. 1979. 24-34.

58. Basch, A. and Lewin, M. "The Influence of Fine Structure of the Pyrolysis of Cellulose. I-Vacuum Pyrolysis". Journal of Polymer Science. 1973. (11). 3071-3093.

59. Basch, A. and Lewin, M. The Influence of Fine Structure on the Pyrolysis of Cellulose. II-Pyrolysis in Air. Journal of Polymer Science. 1973. (11). 3095-3101.

60. Patai, S. and Halpern, Y. "Pyrolytic Reaction of Carbohydrates. Part ix. The Effect of Additives on the Thermal Behaviour of Cellulose Samples of Different Crystallinity". Israel Journal of Chemistry. 1970, 8, 655-662.

61. Weinstein, M. and Broido, A. Pyrolysis - Crystallinity Relationships in Cellulose. Combustion, Science and Technology. 1970. 1, 287-292.

62. Shafizadeh, F. Pyrolysis and Combustion of Cellulosic Materials in "Advances in Carbohydrate Chemistry". Korgram and Tippson (eds). Aca Press. 1968. 23, 419-474.

63. Ramiah, A.V. Journal of Applied Science. Vol 14. 1970. 1323-1337.

64. Kosiewicz, S.T. "Cellulose Thermally Decomposes at 70°C". Thermochimica Acta, 1980. 40, 319-326.

65. Bradbury, A.G.W., Sakai, Y. and Shafizadeh, F. "A Kinetic Model for Pyrolysis of Cellulose". Journal of Appl. Polymer Science. 1979. 23, 3271-3280.

66. Kilzer, F.J. and Broido, A. "Speculations on The Nature of Cellulose Pyrolysis". Pyrodynamics. 1965. 2, 151-163.

67. Broido, A. and Nelson, M.A. "Char Yield on Pyrolysis of Cellulose". Combustion and Flame. 1975. 24, 263-268.

68. Arsenau, D.F. "Competitive Reactions in The Thermaldecomposition of Cellulose"F. Canadian Journal of Chemistry. 1971. 49, 632-638.

69. Antal, M.F. Jr., Friedman, H.L. and Rogers, F.E. "Kinetics of Cellulose Pyrolysis in Nitrogen and Steam". Combustion and Science and Technology. 1980. 21, 141-152.

70. Agrawal, R.K. Kinetics of Reactions Involved in Pyrolysis of Cellulose. I, The Three Reaction Model". The Canadian Journal of Chem. Eng. 1988. 66, June, 403-412.

71. Agrawal, R.K. Kinetics of Reactions Involved in Pyrolysis of Cellulose. II, The Modified Kilzer-Broido Model. The Canadian Journal of Chem. Eng. 1988. 66, 413-448.

72. Shafizadeh, F., Furneaux, R.H., Cochran, T.G., Scholl, J.P. and Sakai, Y. "Production of Levoglucosan and Glucose from Pyrolysis of Cellulosic Materials". Journal of App. Polymer Sci. 1979. 23, 3525-3539.

73. Alves, S.S. and Figueiredo, J.L. Interpreting Isothermal Thermogravimetric Data of Complex Reactions: Application to Cellulose Pyrolysis at Low Temperatures. Journal of Analytical and Applied Pyrolysis. 1989. 347-355.

74. Alves, S.S. and Figueiredo, J.L. Kinetics of Cellulose Pyrolysis Modelled by Three Consecutive First-Order Reactions. Journal of Analytical and Applied Pyrolysis. 1989. 17, 37-46.

75. Liden, A.G., Berruti, F. and Scott, D.S. A Kinetic Model For The Production of Liquids From the Flash Pyrolysis of Biomass. Chem. Eng. Comm. 1988. 65, 207-221.

76. Piskorz, J., Radlein, D. and Scott, D.S. Journal of Analytical and Applied Pyrolysis. 1986. 9, 121-137.

77. Piskorz, J., Radlein, D., Scott, D.S. and Czernik, S. Pre-Treatment of Wood and Cellulose for Production of Sugars by Fast Pyrolysis. Journal of Analytical and Applied Pyrolysis. 1989. 16, 127-142.

78. Piskorz, J., Radlein, D., Scott, D.S. and Czernik, S. Liquid Products From the Fast Pyrolysis of Wood and Cellulose in "Research in Thermochemical Biomass Conversion". Bridgwater, A.V. and Kuester, J.L. (eds). 1988. 557-571.

79. Radlein, D., Piskorz, J. and Scott, D.S. Control of Selectivity in The Fast Pyrolysis of Cellulose in "Biomass for Energy, Industry and Environment". 6th European Conference. Grassi, G., Collina, H. and Zibetta, H. (eds). Elsevier App. Science. 1992 643-649.

80. Maa, P.S. and Bailie, R.C. Influence of Particle Sizes and Environmental Conditions on High Temperature Pyrolysis of Cellulosic Material I. Combustion, Science and Technology. 1973. 7, 257-269.

81. Connor, N.A. and Salazar, C.M. "Factors Influencing the Decomposition Processes in Wood Particles During Low Temperature Pyrolysis" in "Research in Thermochemical Biomass Conversion". Bridgwater, A.V. and Kuester, J.L. (eds). 1988. 164-178.

82. Jonsson, O. "Thermal Cracking of Tar Sand Hydrocarbons by Addition of Steam and Oxygen in The Cracking Zone" in "Fundamentals of Thermochemical Biomass Conversion". Overend, R.P., Milne, J.A. and Mudge, L.K. (eds). 1985. 733-746.

83. Soltes, E.J. and Elder, T.J. Organic Chemicals from Biomass. 1981. 85-97. CRC Press, Florida.

84. Avni, E., Laughlin, R.W., Solomon, P.R. and King, H.K. Mathematical Modelling of Lignin Pyrolysis Fuel. 1985. 64, 1495-1501.

85. Shafizadeh, F. Pyrolytic Reactions and Products of Biomass in "Fundamentals of Thermochemical Biomass Conversion". Overend, R.P., Milne, T.A. and Mudge, L.K. (eds). 1985. 183-217.

86. Hurff, S.J. and Klein, M.T. Reaction Pathway Analysis of Thermal and Catalytic Lignin Fragmentation by Use of Model Compounds. Ind. Eng. Chem. Fundam. 1983. 22, 426-430.

87. Sada, E., Kumazawa, H. and Kudsy, M. Pyrolysis of Lingnins in Molten Salt Media. Ind. Eng. Chem. Res. 1992. 31, 612-616.

88. Pakdel, H., De Caumia, B. and Roy, C. Vacuum Pyrolysis of Lignin Derived From Steam-Exploded Wood. Biomass and Bioenergy. Vol 3. No. 1. 1992. 31-40.

89. Vasalos, I.A., Samolada, M.C. and Achlados, G.E. "Biomass Pyrolysis for Maximising Phenolic Liquids" in "Research in Thermochemical Biomass Conversion". Bridgwater, A.V. and Kuester, J.L. (eds). 1988. 251-263.

90. Chua, M.G.S. and Wayman, M. "Characterisation of Autohydrolysis of Aspen (P. Tremuloides) Lignin. Part 1. Combustion and Molecular Weight Distribution of Extracted Autohydrolysis Lignin. Can. J. of Chemistry. Vol 57. 1979. 1141-1149.

91. Jaradat, Q.M., Saleh, F.Y., Lewis, R.W. and Daugherty, K.E. Characterisation of Refuse Derived Fuel by Pyrolysis, Gas Chromatography and Gas Chromatography/Mass Spectrometry. Journal of Analytical and Applied Pyrolysis 1990. 17, 169-180.

92. Evans, R.J. and Milne, T.A. Liquid Fuels From the Pyrolysis of Municipal Solid Waste and its Components. Rapid Product Characterisation and Process Parameter Screening by Molecular Beam-Mass Spectrometry. Energy, Biomass and Wastes. 1988. Vol. 11. 807-838.

93. Levie, B., Diebold, J.P. and West, R. Pyrolysis of Single Pellets of Refuse Derived Fuel. in "Research in Thermochemical Biomass Conversion". Bridgwater, A.V. and Kuester, J.L. (eds). 1988. 312-326.

94. Sueyoshi, H. and Kitaoka, Y. "Make Fuel From Plastic Wastes". Hydrocarbon Processing. Oct. 1992. 161-163.

95. Brydson, J.A. "Plastic Materials". 5th ed. Butterworths (publishers). 1989. ISBN 0-408-00721-4.

96. Dubois, J.H. and John, F.W. "Plastics". 6th Edition. 1981. VNB. ISBN 0-442-26263-9.

97. Billmeyer, Jr. F.W. Textbook of Polymer Science. 1962. Interscience Pub.

98. Daborn, G.R. and Rampling, T.W. A Literature Survey of Published Research on Refuse Derived Fuel and its Components in the Laboratory. Characterisation of Refuse Derived Fuel by Rampling, T.W. and Hickey, T.J. Report No. ETSU-B-1161. ISBN 0-85624-502-X.

99. Wilkins, E.S. and Wilkins, M.G. Review of Pyrolysis and Combustion Products of Municipal and Industrial Wastes. J. Environ. Sci. Health. A18 (6) 747-772.

100. Tsuchiya, Y. and Sumi, K. Thermal Decomposition Products of Polyethylene. Journal of Polymer Science. Part A-1. Vol 6. 1968. 415-424.

101. Kiran, E. and Gillham, J.K. Pyrolysis-Molecular Weight Chromatography: A New On-Line System for Analysis of Polymers. II. Thermaldecomposition of Polyolefins, Polyethylene, Polypropylene and Polyisobutylene. J. App. Poly. Sci. 1976. 70, 2045-2068.

102. Daust, D. Bormann, S. Legras, R and Mercier, J.P. Thermaldegradation of Polystyrene: Changes in Molecular Composition. Polymer Eng. and Science. August 1981. 21-11 721-726.

103. Kaminsky, W., Menzel, J. and Sinn, H. Some Remarks About Recycling Thermoplastics by Pyrolysis Plastic and Rubber Processing. June 1976. 69-76.

104. Schoeters, J.G. and Buekens, A.G. Pyrolysis of Plastics in a Steam Fluidised-Bed.

105. Buekens, A.G. and Schoeters, J.G. "Basic Principles of Waste Pyrolysis and Review of Europe on Processes" in "Thermal Conversion of Solid Wases and Biomass" Am. Chem. Soc. Jones, J.L. and Rodding, S.B. (eds). 1980. 397-421.

106. Nishizaki, H., Yoshida, K. and Endoh, K. Material Recovery from Plastic Waste by Fluidised-Bed Pyrolysis in Moo-Young, M. and Farquhar, G.J. (eds). Int. Symp. on Waste Treatment Utilisation and Processing. Pergamon Press, Oxford. 1979. 173-183.

107. Koo, J.K., Kim, S.W. and Seo, Y.H. Characterisation of Aromatic Hydrocarbon Formation from Pyrolysis of Polyethylene-Polystyrene Mixtures. Resources, Conservation and Recycling. 1991. 5, 365-382.

108. Diebold, J. Evans, R. and Schahill, J. Fast Pyrolysis of RDF to Produce Oils, Char and a Metal-Rich By-Product. Energy, Biomass, Wastes. 1990. 13, 851-878.

109. Roy, C., De Caumio, B., Pakdel, H., Couture, G. and Labreque, B. Treatment of Biomass and Municipal Solid Wastes by Vacuum Pyrolysis in "Biomass for Energy, Industry and Environment" 6th E.C. Cong. Grassi, G. (ed). 1992. 979-985.

110. Pober, K.W. and Bauer, F.H. The Nature of Pyrolytic Oil from Municipal Solid Waste in "Fuels From Waste". Anderson, L.L. and Tillman, A.A. (eds). 1977. 73-85.

111. Beckman, J.A., Crane, G., Kay, E.C. and Laman, J.R. Scrap Tyre Disposal. Rubber Chem. Technology. 1974. 47, 597-624.

112. Kaminsky, W. and Sinn, H. "Pyrolysis of Plastic Waste and Scrap Tyres Using a Fluidised-Bed Process" in "Thermal Conversion of Solid Wastes". Jones, J.L. and Rodding, S.B. Am. Chem. Soc. 1980. 423-439.

113. Roy, C. and Unsworth, J. "Pilot Plant Demonstration of Used Tyres Vacuum Pyrolysis" in "Pyrolysis and Gasification". Ferrero, G.L., Maniatis, K., Buekens, A. and Bridgwater, A.V. (eds). 1989. 205-215.

114. Mirmiran, S., Pakdel, H. and Roy, C. Characterisation of Used Tyre Vacuum Pyrolysis Oil: Nitrogenous Compounds From the Naphta Fraction. Journal of Analy. and Appl. Pyrolysis. 1992. 22, 205-215.

115. Bouvier, J.M., Charbell, F. and Gelus, M. Gas-Solid Pyrolysis of Tyre Wastes, Kinetics and Material Balances of Batch Pyrolysis of Used Tyres. Resources and Conservation. 1987. 15, 205-214.

116. Nag, D.P., Nath, K.C., Mitra, D.C. and Raja, K. A Laboratory Study on the Utilisation of Waste Tyre for the Production of Fuel Oil and Gas of High Calorific Value. Journal of Mines, Metals and Fuels. October 1983. 473-476.

117. Bouvier, J.M., Forhadi, F. and Gelus, M. A New Method For Upgrading Rubber Wastes. Int. Chem. Eng. 23-4. 1984. 645-650.

118. Dodds, J., Domenico, W.F., Evans, D.R., Fish, L.W. and Toth, W.J. Scrap Tyres: A Resource and Technology Evolution of Tyre Pyrolysis and Other Selected Alternate Technologies. Report No. DE-AC07-761D0-1570. 1983.

119. Roy, C., Labrecque, B. and De Caumia, B. Recycling of Scrap Tyres to Oil and Carbon Black by Vacuum Pyrolysis. Resources, Conservation and Recycling. 1990. 4, 203-213.

120. Macaione, D.P., Sacher, R.E. and Singler, R.E. Thermogravimetric Characterisation of Elastomer and Carbon-Filled Rubber Composites For Military Applications in "Compositional Analysis by Thermogravimetry". Earnst, C.M. (ed). 1988. 59-69.

121. Bililewski, B., Hardtle, G. and Morek, K. Usage of Carbon Black and Activated Carbon in Relation to Input and Technical Aspects of the Pyrolysis Process" in "Pyrolysis and Gasification". Ferrero, G.C., Maniatis, K., Buekens, A. and Bridgwater, A.V. (eds). 1989. 98-105.

122. Lucchesi, A. and Maschio, G. "Semi-Active Carbon and Aromatics Produced by Pyrolysis of Scrap Tyres" Conservation and Recycling. Vol. 6 No. 3. 1983. 85-90.

123. Cypres, R. and Bettens, B. "Production of Benzoles and Active Carbon From Waste Rubber and Plastic Materials by Means of Pyrolysis With Simultaneous Post-Cracking" in "Pyrolysis and Gasification". Ferrero, G.L., Maniatis, K., Buekens, A. and Bridgwater, A.V. 1989. 209-229.

124. Roy, C. Vacuum Pyrolysis of Scrap Tyres. Presented at the Conference "Waste and Scrap in the Rubber Industry: Treatment and Lepistlation". The Plastic and Rubber Institute. Belgian Section. September 23, 1992.

125. Kawakami, S., Inoue, K. Tanaka, H. and Sakai, T. Pyrolysis Process for Scrap Tyres. "Thermal Conversion of Solid Wastes and Biomass". Jones, J.L. and Radding, S.B. (eds). ACS Symp. Ser. 1980. 557-572.

126. Pakdel, H., Roy, C., Aubin, H., Jean, G. and Coulombe, S. Formation of Di-Limonene in Used Tyre Vacuum Pyrolysis Oils. Environ. Sci. Tchnol. 1991. 25, 1696-1699.

127. Roberts, A.F. "A Review of Kinetics Data for the Pyrolysis of Wood and Related Substances". Combustion and Flame. 1990. 14, 261-272.

128. Roy, C., De Caumia, B., Brauillard, D. and Menard, H. "The Pyrolysis Under Vacuum of Aspen Poplar" in "Fundamentals of Thermochemical Biomass Conversion". Overend, R.P., Milne, T.A. and Mudge, L.K. (eds). 1985. 237-255.

129. Nunn, T.R., Howard, J.B., Longwell, J.P. and Peters, W.A. "Studies of the Rapid Pyrolysis of Sweet Gum Hardwood" in "Fundamentals of Thermochemical Biomass Conversion". Overend, R.P., Milne, T.A. and Mudge, L.K. (eds). 1982. 293-314.

130. Graham, R.G., Bergougnou, M.A., Mok, L.K.S. and De Lasa, H.I. "Fast Pyrolysis (Ultra Pyrolysis) of Biomass Using Solid Heat Carriers" in "Fundamentals of Thermochemical Biomass Conversion". Overend, R.P., Milne, T.A. and Mudge, L.K. (eds). 1982. 397-410.

131. Mezerette, C. and Girard, P. "Environmental Aspects of Gaseous Emissions From Wood Carbonisation and Pyrolysis Process" in "Upgrading of Pyrolysis Liquids". Bridgwater, A.V. (ed). 1991. 263-287.

132. Roy, C., Lemieux, R., De Caumia, B. and Blanchette, D. "Processing of Wood Chips in a Semi-Continuous Multiple-Hearth Vacuum Pyrolysis Reactor" in Pyrolysis Oils From Biomass Producing, Analysing and Upgrading". Soltes, J. and Milne, A. (eds). ACS Symp. Ser. 1988. 16-30.

133. Stiles, H.N. and Kondiyoti, R. "Secondary Reactions of Flash Pyrolysis Tars Measured in a Fluidised-Bed Pyrolysis Reactor With Some Novel Design Features". Fuel, 1989. 68, 275-282.

134. Figueiredo, J.L., Valenzuela, C., Bernalte, A. and Encinar, J.M. "Pyrolysis of Holm Oak Wood: Influence of Temperature and Particle Size". Fuel, 1989. Vol. 68. 1012-1016.

135. Eklund, H. and Wanzl, W. "Pyrolysis and Hydropyrolysis of Peat at High Heating RAtes" in "Fundamentals of Thermochemical Biomass Conversion". Overend, R.P., Milne, T.A. and Mudge, L.K. (eds). 1985. 315-327.

136. Boateng, A.A., Fan, L.T. Walawender, W.P. and Chee, C.S. Morphological Development of Rice-Hull Derived Charcoal in a Fluidised-Bed Reactor. Fuel, 1991. Vol. 70. 995-1000.

137. Ganesh, A., Grover, P.D. and Lyer, P.V.R. "Combustion and Gasification Characteristics of Rice Husks". Fuel, 1992. Vol. 71. 889-894.

138. Jiang, W.D., In-Chul, L. and Yang, R.Y.K. J. Fuel. Proc. Technal. 1988. 18-11.

139. Beaumont, O. and Schwob, Y. "Influence of Physical and Chemical Parameters on Wood Pyrolysis". Ind. Eng. Chem. Process. Des. Dev. 1984. 23, 637-641.

140. Barton, J.R. "Processing of Urban Waste to Provide Feedstock For Fuel/Energy Recovery" in "Pyrolysis and Gasification". Ferrero, G.L., Maniatis, K., Buekens, A. and Bridgwater, A.V. (eds). Elsevier App. Sci. 1989. 57-71.

141. Helt, J.E. and Agrawal, R.K. "Liquids From Municipal Solid Waste" in "Pyrolysis Oils From Biomass, Producing, Analysing and Upgrading". Soltes, D. and Milne, T.A. (eds). ACS Symp. Series 376. ACS Symp. Ser. 1988. 79-91.

142. Bouvier, J.M. and Gelus, M. "Pyrolysis of Rubber Wastes in Heavy Oils and Use of the Products". Resources and Conversation. 1986. 12, 77-93.

143. Zanzi, R., Sjostrom, K. and Bjornbom, E. "Properties of Wood Char". 7th European Conference on Biomass for Energy and Environment, Agriculture and Industry. Florence, Italy, 5th - 9th October 1992.

144. Collin, G. in "Thermal Conversion of Solid Wastes and Biomass". Jones, J.L. and Rodding, S.B. (eds). ACS Sym. Series. 1980. 130.

145. Douglas, E., Webb, M. and Daborn, G.R. "Symposium on Treatment and Recycling of Solid Wastes". Institute of Solid Wastes Management. Manchester, UK. 1974.

146. Wolfson, D.E., Bechman, J.A. Walters, J.G. and Bennett, D.J. "Destructive Distillation of Scrap Tyres". U.S. Dept. of Interior. Bureau of Mines. Report of Investigations. 1969. 1302.

147. American Society for Testing and Materials. As T.M. D- 1765-1886. Vol. 9. 01-1988.

148. Roy, C., De Caumia, B., Pakdel, H., Plante, P,. Blanchette, D. and Labreque, B. "Vacuum Pyrolysis of Used Tyres, Petroleum Sludges and Forestry Wastes: Technological Development and Implementation Perspectives" in "Biomass Thermal Processing". Proceedings of the first Canada/European Community. R and D Contractors Meeting. October 1990. Canada, 1992. 109-125.

149. Blunauer, S., Emmett, P.H. and Teller, E.J. Am. Chem. Soc. 1938. 60, 309.

150. Nelson, F.M. and Eggertson, F.T. Anal. Chem. 1958. 30, 1387.

151. ASTM. D. 1106-84. American Society for Testing Materials Method. D. 1106-84. Annual book of ASTM Standards 1984.

152. Methods for Analysis and Testing Institute of Petroleum. IP Standards for Petroleum and its Products. Part 1. Volume 1. 1977. London. Heyden and Son Ltd. (publishers).

153. Green, D.W. and Reedy, G.T. "Matrix-Isolation Studies With Fourier Transform Infrared" in " Fourier Transform Infrared Spectoscopy Applications to Chemical Systems". Volume 1. Ferrero, J.R. and Basile, L.J. (eds). 1978. 1-55.

154. Powder Surface Area and Porosity. Lowell, S. and Shields, J.E. 3rd. Edition 1984. Chapman and Hall (Pub).

155. Bartle, K.D., Mulligan, M.J. Taylor, N. et al. Fuel 1984. 63, 1556.

156. Williams, P.T. and Taylor, D.T. "The Fuel Properties of Hydrocarbon Liquids Derived From Pyrolysis of Waste" in "Pyrolysis and Gasification". Ferrero, G.C., Maniatis, K., Buekens, A. and Bridgwater, A.V. 1989. 486-491.

157. Esnouf, C. Charcoal-Water Slurries: State of the Art and Future Prospects in "Biomass Pyrolysis Liquids Upgrading and Utilisation". Bridgwater, A.V. and Grassi, G. (eds). 1991. 119-153.

158. Boateng, A.A., Walawender, W.P. and Fan, L.T. Devolatilisation Studies of Rice Husks in a TGA and a Fluidised-Bed Reactor.

159. Harber, J.H. and Backhurst, J.R. Fuel and Energy. 1981. Academic Press, London.

160. Churin, E., Maggi, R. and Delmon, B. Characterisation and Composition of Bio-Oils Obtained by Pyrolysis in "Biomass for Energy and Industry". 5th. E.C. Conference. Vol. 2. Grassi, G., Gosse, G. and Santos, G. (eds). Elsevier. App. Sci. 1989. 2621-2626.

161. Williams, D.H. and Fleming, I. Spectroscopic Methods in Organic Chemistry. 3rd. Edition. McGraw Hill Company, UK. 1980.

162. Pakdel, H., Zhong, H.G. and Roy, C. "Detailed Chemical Characterisation of Biomass Pyrolysis Oils, Polar Fractions" in "Advances in Thermochemical Biomass Conversion". Interlaken, Switzerland. May 11-15. 1992.

163. Norman, R.D.C. and Waddington, D.J. Modern Organic Chemistry. 3rd, Ed. 1981. "Bell and Hyman" (pub). London.

164. Bhowmick, A.K., Rampalli, S. and Gallagher, K. The Degradation of Guagule Rubber and the Effect of Resin Components on Degradation at High Temperature. Jour. of Appl. Polymer Science. Vol. 33. 1987. 1125-1139.

165. Midgley, Jr. T. and Henne, A.L. Natural and Synthetic Rubber I. Products of The Destructive Distillation of Natural Rubber. J. Am. Chem. Soc. 1929. 51, 1215-1226.

166. Tamura, S., Murakami, K. and Kuwozoe, H. Isothermal Degradation of Cis-1,4-Polyisoprene vulcanirates. J. of Appl. Polymer Science. 1983. Vol. 28. 3467-3484.

167. Brazier, D.W. "Thermal Analysis". Rubber Chemistry and Technology 1980. Vol. 3. No. 3. 437-511.

168. Maurer, J.J. "Elastomers in Thermal Characterisation of Polymeric Materials" Turi, E. (ed). Academic Press, New York. 1981. 571-708.

169. Davlath, A.E. and Gregorski, K.S. Carbohydrate Pyrolysis II Formation of Furfurol and Furfuryl Alcohol During the Pyrolysis of Selected Carbohydrates with Acidic and Basic Catalysts. in "Research in Thermochemical Biomass Conversion". Bridgwater, A.V. and Kuester, J.L. (eds). 1988. 155-163.

170. Pavlath, A.E. and Gregorski, K.S. in "Fundamentals of Thermochemical Biomass Conversion". Overend, R.P., Milne, T.A. and Mudge, L.K. 1985. 437-452.

171. Shafijadeh, F. and McGinnis, G.D. Carbohydrate Research. 1971. 16, 273-277.

172. Grandmaison, J.L., Ahmet, S. and Kaliaguine, S. Analysis of Partially Converted Lignocellulosic Materials. Am. Chem. Soc. Div. Fuel. Chem. 1987. 32, 157-163.

173. Thurner and Mann. Ind. Eng. Chem. Proc. Des. Dev. 1981. 20, 482.

174. Cordero, T., Garcia, F. and Rodrigues, J.J. A Kinetic Study of Holm Oak Wood Pyrolysis from Dynamic and Isothermal TG Experiments. Thermochimica Acta. 1989. 149, 225-237.

175. Chan, M., Kelbon, M. and Krieger, B. Fuel. 1985. 64, 1505.

176. Zaror, C.A., Hutchings, I.S., Pyle, D.L. Stiles, H.N. and Kandiyoti, R. Fuel. 1985. 64, 990-994.

177. Shafizadeh, F. Jour. of Analy. and Appl. Pyrolysis. 1982. 3, 283-305.

178. Barooh and Long. Fuel. 1976. 55, 116-120.

179. Font, R., Marcilla, V. and Deveso, E. Jour. of Ind. Eng. Chem. Res. 1988. 29, 1846-1855.

180. Browne and Tang. Fire Res. Abst. Rev. 1963(-) 76-86.

181. Figueiredo. Alves. Journal of Analy. Appl. Pyrolysis. 1988. 13, 123-134

182. Boateng, A.A. Walawender, W.P. and Fan, L.T. "Devolatilisation Studies of Rice Husks in TGA and Fluidised-bed Reactor" in "Biomass for Energy and Industry" 5th E.C Conference. Grassi. G., Gosse, G. and Dos Santos. G. (eds) 1990. 2536-2540.

183. Raman, P., Walawender, W.P., Fan, L.T. and Howel, S.A. Ind. Eng. Chem. Process Des. Dev. 1981. 20. 630-636.

184. Chornet, E. and Roy, C. "Compensation Effect in the Thermal Decomposition of Cellulosic Materials". Thermochimica Acta. 1980. 35. 389-393.

185. Lewellen, P.C., Peters, W.A. and Howell, J.B. "16th Int. Sym. on Comb. Tec". Comb. Inst. 1977. 1471-1480.

186. Shafizadeh, F. and Bradbury, A.G.W. "Journal of App. Poly. Science". 1979. 23. 1431-1442.

187. Heyns, K. and Klier, M. Carbohydrate Research, 1968. 436-448.

188. Essig, M.G. adn Richards, G.N. Carbohydrate Research.

189. Shafizadeh, F. and Yu, F.L. Pyrolysis of Cellulose. Carbohydrate Research. 1973. 29. 113-122.

190. Agrawal, R.K. "On the Use of the Arrhenius Equation to Describe Cellulose and Wood Pyrolysis". Thermochimica Acta. 1985. 91. 343-349.

191. Agrawal, R. Compensation Effect in the Pyrolysis of Cellulosic Materials. Thermochimica Acta. 1985. 90. 347-351.

192. Lee, M.L., Novotny, M. and Bartle, K.D. "Analytical Chemistry of Polycyclic Aromatic Compounds". Academic Press. New York. USA. 1981.

193. Longwell, J.P. in "Soot in Combustion Systems and its Tonic Properties". La haye. J. and Prado, G. (eds). Plenum Press. New York. USA. 1983.

194. Keirsse, H., Hartoyo. W., Buekens, A., Schoeters, J. and Janssens, J. in "Research in Thermochemical Biomass Conversion". Bridgwater, A.V. and Kuester, J.L. (eds). Elsevier App. Sci. 1988. 531-541.

195. Nimmo, W. "Gasification and Pyrolysis of Solid Fuels and Waste in a Fluidised-Bed Reactor". PhD Thesis 1984. Leeds University.

196. Corella, J., Herguido, J. and Alday, F.J. "Pyrolysis and Steam Gasification of Biomass in Fluidised-Beds: Influence of the Type and Location of the Biomass Feeding Point on the Product Distribution" in "Research in Thermochemical Biomass Conversion". Bridgwater, A.V. and Kuester, J.L. (eds). Elsevier Sci. Pub. 1988. 384-398.

197. Scott, D.S. and Piskorz, J. "The Flash Pyrolysis of Aspen-Poplar Wood". The Canadian Journal of Chem. Eng. Vol. 60. 1982. 666-674.

198. Hastaoglu, M.A. and Berruti, F. "A Gas Solid Reaction Model for Flash Wood Pyrolysis". Fuel. 1989. 68. 1408.

199. Peel, R.B. "Fluidised-Bed Combustion and Gasification of Biomass" in "Biomass for Energy and Industry". Gross, G., Gosse, G. and Dos Santos, G. (eds). 5th. E.C. Conference. 1989. Vol. 2. 541-545.

200. Nishizaki, H., Yoshido, K. and Endoh, K. in "International Symposium on Waste Treatment: Utilisation and Processing". Moo-Young, M. and Farquhar, G.J. (eds). Perganon Press. 1979. 173-187.

201. Lowell, S. and Shields, J.E. "Powder Surface Area and Porosity". 3rd. Ed. Chapman and Hall. 1991.

202. Cameron, G.C. National Bureau of Standards Special Publication. June 1972. 61-72.

203. Cameron, G.G. and MacCallum, J.R. "Mechanism of Volatile Production During Pyrolysis of Polystyrene". J. Macromol. Sci., Rev. Macromol. Chem. 1967. 1. 327-335.

204. Pakdel, H. and Roy, C. "Characterisation of Vacuum Pyrolysis Oils of Diverse Origins" in " Biomass Thermal Processing". Proceeding of the First Canada/European Community. R & D Contractors Meeting. 1990. Canada. Hogan, E., Robert, D., Grossi, G. and Bridgwater, A.V. (eds). 1992. 144-156.

205. Scott, D.S., Radlein, D., Piskorz, J. and Majerski, P. "Potential of Fast Pyrolysis for the Production of Chemicals" in "Biomass Thermal Processing". Proceedings of the first Canada/European Community R & D Contractors Meeting. 1990. Canada. Hogan, E., Robert, D., Grassi, G. and Bridgwater, A.V. (eds). 1992. 171-178.

206. Desbene, P.L., Essayegh, M., Desmazieres, B. and Bosselier, J.J. "Contributions to the Analytical Study of Biomass Pyrolysis Oils" in "Biomass Pyrolysis Liquids Upgrading and Utilisation". Bridgwater, A.V. and Grassi, G. (eds). 1991. 155-176.

207. Elliott, D.C., Sealock, J.Jr. and Butner, S.R. "Product Analysis From Direct Liquefaction of Several High-Moisture Biomass Feedstocks" in "Production Analysis and Upgrading of Oils From Biomass". Am. Chem. Soc. Div. Fuel. Chemistry. Argonne Not Labs. 1987. Vo.32. 1-2. 179.

208. Williams, P.T. Journal of Institute of Energy. 1990. 63-454. 22-30.

209. Williams, P.T., Horne, P.A. and Taylor, D.T. "Polycyclic Aromatic Hydrocarbons in Polystyrene Derived Pyrolysis Oil" in "The 10th Int. Conf. of Fundamental Aspects, Processes and Applications on Pyrolysis" (In Press).

210. Williams, P.T. and Taylor, D.T. "Aromatisation of Tyre Pyrolysis Oil to Yield Polycyclic Aromatic Hydrocarbons" Fuel (In Press).

211. Sharma, R.K. and Bakhshi, N.N. "Catalytic Upgrading of Pyrolytic Oils Over H2SM-5 in Biomass Thermal Processing". Proceeding of the First Canada/European Community R & D Contractors Meeting. October 1990. Ottowa Canada. Hogan, E., Robert, D., Grossi, G. and Bridgwater, A.V. (eds). 1992. 157-170.

212. Pakdel, H. and Roy, C. "Hydrocarbon Content of Liquid Products and Tar From Pyrolysis and Gasification of Wood". Energy and Fuels. 1991. 5. 427-435.

213. Breadel, P. Mechanisms of Aromatisation of n-decane Ann. Mine de Belgique. 1945. 11. 1046-1052.

214. Cypres, R. "Aromatic Hydrocarbons Formations During Coal Pyrolysis". Fuel Processing Technology. 1987. 15. 1-15.

215. Diebold, J.P. "Gasoline From Solid Wastes by a Non-Catalytic Thermal Process" in "Thermal Conversion of Solid Wastes and Biomass". Jones, J.L. and Rodding, S. (eds). 1980. 209-226.

216. Menard, H., Belanger, D., Chauvette, G., Gaboury, A., Khorami, N., Grise, M., Martel, A., Potvin, E., Roy, C. and Langlais, R. in Fifth Canadian Bioenergy R & D Seminar. Hasnain, S. (ed). Elsevier Applied Science Publishers. New York. 1984. 418-434.

217. Depeyre, D., Flicoteaux, C. and Chardoire, C. Ind. Eng. Chem. Process. Des. Dev. 1985. 24. 1251-1258.

218. Guerin, M.R. PAH and Cancer. Academic Press. New York. USA. 1978.

219. Herlan, A. Combustion and Flame. 1978. 31. 297.

220. Williams, P.T., Bartle, K.D. and Andrews, G.E. Fuel. 1986. 65. 1150.

221. Williams, P.T., Abbass, M.K., Andrews, G.E. and Bartle, K.D. Combustion and Flame. 1989. 75.1.

222. Vassilatos, V., Brage, C., Taralas, G. and Sjostrom, K. "The Effects of Temperature and Additives on Product Composition in Thermal Cracking of Biomass" in "Biomass for Energy, Industry and Environment". 6th E.C. Conference. Grassi, G., Collina, A. and Zibetta, H. (eds). Elsevier Appl. Sci. 1992. 762-765.

223. Fairburn, J.A., Behie, L.A. and Svrcek, W.Y. "Ultra Pyrolysis of n-hexadecane in a Novel Micro-Reactor". Fuel. 1990. Vol.69. Dec. 1537-1545.

224. Ren, R.L., Itoh, H. and Ouchi, K. "Dealhylation of Coal Derived Oil by the Hydrogen Generated From Methanol Decomposition". Fuel. 1989. Vol.68. 58-65.

225. Fraga, A.R., Gaines, A.F. and Kendiyati, R. "Characterisation of Biomass Pyrolysis Tars Produced in the Relative Absence of Extra Particle Secondary Reactions. Fuel. 1991. Vol.70. July. 803-809.

226. Nunn, T.R., Howard, J.B., Longwell, J.P. and Peters, W.A. "Product Compositions and Kinetics in the Rapid Pyrolysis of Sweet Gum Hardwood" Ind. Eng. Chem. Process. Des. Dev. 1985. 24. 836-844.

227. Beaumont, O. Flash Pyrolysis Products from Beechwood. Wood and Fiber Science. 1985. 17 (2) 228-239.

228. Scott, D.S., Piskorz, S. and Radlein, D. Liquid Products from the Continuous Flash Pyrolysis of Biomass. Inds. Eng. Chem. Process. Des. Dev. 1985. 24. 581-588.

229. Font, R., Marcillo, A., Verdù, E. and Deveso, J. "Chemicals From Almond Shells by Pyrolysis in Fluidised-Bed" in "Pyrolysis and Gasification". Ferrera, B.L., Maniatis, K., Buekens, A. and Bridgwater, A.V. (eds). 1989. 230-237.

230. Pakdel, H., Couture, G. and Roy, C. Unpublished Work.

231. Ames, B.N., Sims, P. and Grover, P.L. Science. 1972. 176. 47.

232. Ames, B.N., Durston, W.E. Yomasaki, E. and Lee, F.D. Proc. Natl. Acod. Sci. USA. 70. 1973. 2281.

233. Biological Effects of Atmospheric Pollutants: Particulate Polycyclic Organic Matter. National Academy of Science. Washington D.C. 1972.

234. Blumer, M. and Youngblood, W.W. "Polycyclic Aromatic Hydrocarbons in Soils and Recent Sediments". Science. 1975. 188. 53-55.

235. Grimmer, G. "Distribution of Polycyclic Aromatic Hydrocarbons in Environmental Samples" in Environmental Carcinogens - Selected Methods of Analysis. Analysis of PAH in Environmental Samples. Egan, H. (ed). 1979. Vol.3.

236. Mills, G.A. PhD Thesis. University of Southampton. 1983.

237. Katz, M., Sakumo, T. and Ho, A. "Chromatographic and Spectral Analysis of Polynuclear Aromatic Hydrocarbons - Quantitative Distribution in Air of Ontario Cities". Env. Sci. Tech. 1978. Vol.12. 905-914.

238. Colwill, D., Butler, J.D. and Crossley, P. "Polynuclear Aromatic Hydrocarbons in the Atmosphere in Birmingham". TRRL Suppl. Report. Dept. of Environ. and Dept. of Transport. No.656. 1981.

239. Doll, R. "Br J. Cancer (Quotation from Chirugical Observations - A Short Treatise The Chimney Sweeps Cancer). Pott. P. London. 1775. Br. J. Cancer. 1975. Vol.32. 263-269.

240. Yamagiwa, K. and Ichikawa, K. "Experimental Study of the Photogenesis of Carcinoma". J. Cancer Research. 1918. Vol.3. 1-29.

241. Kenneway, E.L. "Further Experiments on Cancer Producing Substance". Biochemical J. 1930. Vol.24. 497-504.

242. Cook, J.W., Hewett, C.L. and Hieger, I. "The Isolation of a Cancer Producing Hydrocarbon From Coal Tar". Journal of Chem. Sci. 1933. Parts I, II, III. 395-407.

243. Hartwell, J.L. "Survey of Compounds Which Have Been Tested for Carcinogenic Activity". Public Health Services Publication. 1951. No.149. 2nd. Edition.

244. Hoffman, D. and Wynder, E.I. "Chemical Analysis on Carcinogenic Bioassay of Organic Particulate Pollutants". In Air Pollution - Analysis, Monitoring and Surviving. Stern, A.C. (Aco. Press). 1968. Vol.2.

PUBLICATIONS

1. Williams, P.T., Besler, S., Taylor, D.T. "The Pyrolysis of Scrap Automotive Tyres", Fuel, 990-69, 1474-1482.

2. Williams, P.T., Besler, S. "The Pyrolysis of Rice Husks The Influence of Temperature and Heating Rate on Product Composition" in 6th. European Conference on Biomass, Athens, Greece. 1991.

3. Williams, P.T., Besler, S. "The pyrolysis of Rice Husks in Thermogravimetric Analysis and Static Batch Reactor", Fuel. February 93, Vol. 72, No. 2. 1993.

4. Williams, P.T., Besler, S. "Thermogravimetric Analysis of the Compounds of Biomass". Advances in Thermochemical Biomass Conversion Conference. 11-15 May 1992, Interlaken, Switzerland (in press).

5. Garcia, A., Besler, S., Williams, P.T., Font, M. "Slow Pyrolysis of Municipal Wastes". Advances in Thermochemical Biomass Conversion Conference 11-15 May 1992, Interlaken, Switzerland (in press).

6. Besler, S., Horne, P.A. and Williams, P.T. "The Fuel Properties of Biomass Derived Pyrolytic Oils And Analytically Upgraded Products". 2nd World Renewable Energy Conference, September 1992. Sayigh, A.A.M. (ed) 1992. Vol. 3 1341-1345.

7. Besler, S., Taylor, D.T., Williams, P.T., Allen, R., Bevan, H.D., Jervis, A. and McKenzie, K.A. "The Fuel Properties of Pyrolytic Oil Derived From the Batch Pyrolysis of Tyre Waste". Submitted to Inst. Mech. Eng. Conference. Waste, Handling, Processing and Recycling. April 27th. 1993. London.

8. Williams, P.T. and Besler, S. "The Pyrolysis of Municipal Solid Waste". Journal of Instituted of Energy. December 1992, Vol. LXV, No. 465, 192-200.